Granular activated carbon sparking anaerobic digestion: the path to municipal sewage resource recovery

by

Yingdi Zhang

A thesis submitted in partial fulfillment of the requirements for the degree of

Doctor of Philosophy

in

Environmental Engineering

Department of Civil and Environmental Engineering

University of Alberta

Abstract

Anaerobic digestion (AD) is an effective and economical technology that can convert organic pollutants to biomethane, playing a pivotal role in resource recovery and greenhouse gas emission control. However, the anaerobic treatment of municipal sewage under psychrophilic conditions faces significant challenges. The overall goal of this research is to investigate, develop, and optimize carbon-based materials (CBMs) amended AD of municipal sewage under psychrophilic conditions for biomethane recovery. This research deepens understanding of fundamental anaerobic processes, improves AD technology effectiveness, and contributes to implementing a circular economy.

CBMs, such as granular activated carbon (GAC), have been shown to promote direct interspecies electron transfer (DIET) in anaerobic co-culture experiments; however, their roles in continuous feeding AD with mixed cultures remain unknown. This Ph.D. research thoroughly explored the roles of GAC in laboratory-scale up-flow anaerobic sludge blankets (UASBs) treating municipal sewage, focusing on alteration of electron transfer, biosynthesis of growth factors (e.g., amino acids and vitamins), impacts of sulfate concentrations, as well as microbiome developments and physiological changes. Over the past four and a half years, 14 bioreactors were operated. Experiments were performed at both University of Alberta laboratories and in the field of a full-scale municipal wastewater treatment plant. Under all operation conditions, it was observed that GAC addition could significantly enhance AD reactor performance, methanogenic activities and effectiveness in vital syntrophic partnerships.

This thesis led to several innovations. In particular, this study is the first to operate

continuous GAC-amended UASB for municipal sewage treatment under psychrophilic conditions, focusing on the development of an electro-active microbiome. More importantly, this study fully demonstrates (i) the shift of electron transfer pathway with GAC addition in continuous feeding AD by a range of methods, (ii) the roles of GAC in stimulating the biosynthesis of growth factors and their positive impacts on microbiome development and reactor performance, (iii) the impacts of GAC addition on microbiome resistance to H_2S toxicity and sulfate reduction activities.

The results of this thesis provide insights into the changes in microbial communities, physiologies, and metabolites with GAC addition, and demonstrate that GAC addition is a feasible approach to enhance the AD performance of municipal sewage under psychrophilic conditions. This research deepens our understanding of the roles of CBMs in AD and provides significant guidance both in theory and practice.

Preface

The contents of this thesis are my original work under the supervision of Prof. Dr. Yang Liu at the University of Alberta, who has made significant contributions to all areas of this research, including conceptualization, methodology, supervision, writing-review & editing, project administration, resources, and funding acquisition. Some colleagues also contributed to the manuscript, and their contributions are listed as follows:

Chapter 3:

A version of this chapter has been published: Zhang, Y., Zhang, L., Guo, B., Zhou, Y., Gao, M., Sharaf, A. and Liu, Y. (2020). Granular activated carbon stimulated microbial physiological changes for enhanced anaerobic digestion of municipal sewage. *Chemical Engineering Journal*, 400, 125838.

https://doi.org/10.1016/j.cej.2020.125838

Dr. Lei Zhang contributed to the methodology and writing of the manuscript. Dr. Guo Bing contributed to the data analysis, methodology, and writing of the manuscript. Dr. Yun Zhou contributed to the review and editing of the manuscript. Dr. Mengjiao Gao and Dr. Ahmed Sharaf contributed to the methodology and investigation.

Chapter 4:

A version of this chapter has been submitted to *Chemical Engineering Journal* in July 2022.

Dr. Lei Zhang contributed to the methodology and conceptualization. Dr. Huijuan Sun and Yiyang Yuan contributed to the methodology.

Chapter 5:

A version of this chapter has been published: Zhang, Y., Zhang, L., Yu, N., Guo, B. and Liu, Y. (2022). Enhancing the resistance to H_2S toxicity during anaerobic digestion of low-strength wastewater through granular activated carbon (GAC) addition. *Journal of Hazardous Materials*, 430, 128473.

https://doi.org/10.1016/j.jhazmat.2022.128473

Dr. Lei Zhang contributed to the conceptualization, methodology, and investigation. Najiaowa Yu contributed to the methodology and investigation. Dr. Guo Bing contributed to the methodology, conceptualization and software.

Chapter 6:

A version of this chapter has been published: Zhang, Y., Guo, B., Zhang, L. and Liu, Y. (2020). Key syntrophic partnerships identified in a granular activated carbon amended UASB treating municipal sewage under low temperature conditions. *Bioresource Technology*, 312, 123556.

https://doi.org/10.1016/j.biortech.2020.123556

Dr. Guo Bing contributed to the data analysis, methodology, investigation, software and writing of the manuscript. Dr. Lei Zhang contributed to the methodology, validation, and review.

Chapter 7:

A version of this chapter has been published: Zhang, Y., Guo, B., Zhang, L., Zhang, H. and Liu, Y. (2021). Microbial community dynamics in granular activated carbon enhanced up-

flow anaerobic sludge blanket (UASB) treating municipal sewage under sulfate reducing and psychrophilic conditions. *Chemical Engineering Journal*, 405, 126957.

https://doi.org/10.1016/j.cej.2020.126957

Dr. Guo Bing contributed to the data analysis, methodology, and review. Dr. Lei Zhang contributed to the methodology and review. Dr. Huixin Zhang contributed to the methodology.

Chapter 8:

A version of this chapter has been published: Zhang, Y., Guo, B., Dang, H., Zhang, L., Sun, H., Yu, N., Tang, Y. and Liu, Y. (2022). Roles of granular activated carbon (GAC) and operational factors on active microbiome development in anaerobic reactors. *Bioresource Technology*, 343, 126104.

https://doi.org/10.1016/j.biortech.2021.126104

Dr. Guo Bing contributed to the conceptualization, data analysis, methodology, investigation, and review. Dr. Hongyu Dang contributed to the methodology, visualization, and writing. Dr. Lei Zhang contributed to the methodology, conceptualization, investigation, and review. Dr. Huijuan Sun contributed to the methodology and data analysis. Najiaowa Yu contributed to the methodology and investigation. Yao Tang contributed to the investigation.

Chapter 9:

A version of this chapter has been published: Zhang, Y., Yu, N., Guo, B., Mohammed, A., Zhang, L., & Liu, Y. (2022). Conductive biofilms in up-flow anaerobic sludge blanket

enhanced biomethane recovery from municipal sewage under ambient temperatures. *Bioresource Technology*, 361, 127658.

https://doi.org/10.1016/j.biortech.2022.127658

Najiaowa Yu contributed to the conceptualization and methodology. Dr. Guo Bing contributed to the methodology. Abdul Mohammed contributed to the investigation. Dr. Lei Zhang contributed to the methodology.

Chapter 2 and Chapter 10:

A version of these two chapters has been submitted for journal publication in August 2022.

Acknowledgement

First and foremost, I would like to express my deep gratitude and sincere appreciation to my supervisor, Dr. Yang Liu, for her excellent guidance, dedication, and encouragement throughout my program. When I started my program five years ago, I did not prepare well for working as a Ph.D., even though I had years of experience working in the anaerobic digestion field. Hard as it was, Dr. Liu trusted me. We worked together and found solutions to overcome many challenges. After two and a half years, everything went on the right track. However, the pandemic started and interrupted the program. Dr. Liu tried everything possible to keep the program going. This work could not have been done without her continuous support. In addition, Dr. Liu has shown me what a great scientist should be. Working under the supervision of Dr. Liu is the treasure of my life.

I would like to thank my colleagues and technicians in the department of Civil and Environmental Engineering at the University of Alberta: Dr. Lei Zhang, Dr. Bing Guo, Dr. Huixin Zhang, Dr. Yun Zhou, Abdul Nayeem Mohammed, Dr. Mian Nabeel Anwar, Dr. Huijuan Sun, Dr. Mengjiao Gao, Dr. Ahmed Sharaf, Najiaowa Yu, Yao Tang, Dr. Rui Xu, Dr. Hongyu Dang, Yiyang Yuan, Dr. Qianyi Zhang, Xin Zou, Lu Liu, Qi Huang, David Zhao, Liang Chen, and all my other colleagues, who provided me with immediate help, guidance and suggestions along the way.

Thanks to the financial support for this project provided by research grants from the Natural Sciences and Engineering Research Council of Canada (NSERC) Strategic Partnership Grants for Projects (SPG-P), the University of Alberta PILOT Seed Grant Program, an NSERC Industrial Research Chair (IRC) Program in Sustainable Urban Water

Development (Liu, Y.) through the support by EPCOR Water Services, EPCOR Drainage Operation, Alberta Innovates, and WaterWerx, an NSERC Discovery project, the Canada Research Chair (CRC) in Future Water Services (Liu, Y.).

Finally, I would like to express my gratitude to my parents, families, and close friends for their support, encouragement, and help in my life and career.

Table of Contents

List of Tables

List of Figures

Abbreviations

AC: activated carbon

AD: anaerobic digestion

ASBR: anaerobic sequencing batch reactor

ASV: amplicon sequence variant

BC: biochar

BMP: biochemical methane production

CM: conductive material

COD: chemical oxygen demand

CSTR: continuous stirred tank reactor

DI: deionized

DIET: direct interspecies electron transfer

EET: extracellular electron transfer

EPS: extracellular polymeric substance

GAC: granular activated carbon

GC: gas chromatography

HRT: hydraulic retention time

IET: interspecies electron transfer

IFT: interspecies formate transfer

IHT: interspecies hydrogen transfer

OLR: organic loading rate

PAC: powdered activated carbon

PCR: polymerase chain reaction

SCOD: soluble COD

SMA: specific methanogenic activity

SMP: soluble microbial product

SRB: sulfate-reducing bacteria

SRT: sludge retention time

TCOD: total COD

TS: total solids

TSS: total suspended solids

UASB: up-flow anaerobic sludge blanket

VFA: volatile fatty acid

VS: volatile solids

VSS: volatile suspended solids

WWTP: wastewater treatment plant

Chapter 1. Introduction

1.1. Background

Human beings have a long history of municipal sewage treatment and reuse. Modern sewer pipes and sewage treatment systems were conceptualized in the mid-19th century along with industrialization and urbanization (Angelakis & Snyder, 2015). Municipal sewage treatment and reuse are becoming more critical to human health, social development, ecosystem, and the natural environment.

Modern sewage systems are complex. Various technologies and multi-stage processes are typically needed to meet the requirements of discharge or reuse. The gradually increased application of the activated sludge process (AS) worldwide has shown a compelling association with the increase in average life expectancy in the 20th century (van Loosdrecht & Brdjanovic, 2014). However, with an increase in global population and environmental pressure (e.g., water pollution), the demand for reducing energy consumption and resource recovery (e.g., water, energy, and chemicals) from municipal sewage treatment has become more critical than ever. Wastewater treatment plants (WWTPs) are among the most energy-intensive industries (Ji et al., 2020; Lu et al., 2019b; Wang et al., 2018b). For instance, with the rapid progress in the construction of WWTPs and related infrastructures, the average energy consumption intensity by WWTPs further increased by 30% over the past 10 years (Lu et al., 2019b). Aeration in AS systems is one of the most energy-consuming processes, which may consume more than half of the electricity used by a plant (Drewnowski et al., 2019). Moreover, WWTPs are among the largest greenhouse gas emitters (Ji et al., 2020). Thus, the current design and operation of

WWTPs based on the conventional AS systems appear to be against the sustainable development goals in the 21st century. Sustainable technologies for municipal sewage treatment and reuse have become an urgent necessity.

Anaerobic digestion (AD) has attracted global attention owing to the advantages of carbon resource recovery, low operational cost, and low residual sludge production (Zhang et al., 2018). AD is considered an essential and sustainable technology to achieve net energy production and carbon neutrality (McCarty et al., 2011). Hundreds of full-scale AD of municipal sewage have been applied in tropical areas, such as Latin America and India (Gali et al., 2018; Noyola et al., 2012). However, this technology has been restricted to (sub)tropical areas (Chernicharo et al., 2015). Low temperatures in temperate areas and low organic concentrations in municipal sewage are often considered barriers to the anaerobic treatment of municipal sewage (McCarty et al., 2011). In the AD process, multiple biochemical processes are required for complex organic macromolecule degradation. Microorganisms work in a consortium to convert organic macromolecules into biogas (McKeown et al., 2012). Various intermediates are oxidized or reduced, and electrons are transferred between different microorganisms and chemicals during these processes. Electron transfer enhancement might be one of the keys to overcoming barriers in the anaerobic treatment of municipal sewage under psychrophilic conditions, which has not been studied systematically.

Recent studies demonstrated that anaerobic microbial activities can be enhanced by adding conductive materials (CMs), such as granular activated carbon (GAC), possibly by enhancing a recently discovered metabolic pathway for methane production, known as

direct interspecies electron transfer (DIET) (Lovley, 2017; Lu et al., 2019a; Martins et al., 2018). DIET enables cell-to-cell electron transport between bacterial and archaeal members in AD and creates a thermodynamically and metabolically favorable condition for the rapid conversion of organics to biomethane (Lovley, 2017). Therefore, electron transfer enhancement through GAC addition might be a suitable approach to enhance the anaerobic treatment of municipal sewage under psychrophilic conditions, which has not been well studied.

Laboratory studies focused on CMs addition in AD are preliminary, while the understandings of mechanisms for the effects of CMs addition to AD are poor. First, only several microorganisms have been proven to participate in DIET (e.g., *Methanosarcina* and *Methanosaeta*) (Rotaru et al., 2014a; Rotaru et al., 2014b). These DIET-indicator microbiomes accounted for only a small proportion of the total microbial community in continuous-fed AD (Dang et al., 2017; Zhao et al., 2017; Zhao et al., 2016c). However, the enhancement in methane production could be more than a hundred percent high (Lu et al., 2019a). Inconsistent results of essential DIET functional genes, such as *pilA* and *omcS* genes, were found (Lei et al., 2019; Park et al., 2018; Zhao et al., 2020b). Previous studies on CMs mainly focused on the identification of the key DIET microorganisms/functional genes with DNA-based analysis (Dang et al., 2017; Zhao et al., 2017). RNA reverse transcription, implying the gene expression, should be considered. Second, it should be noted that in CMs-based AD studies, the amounts of CMs and biofilms formed on the CMs were often low compared to the suspended sludge in the whole AD system. As a result, direct interactions between CMs and AD suspended sludge might not be as significant as envisioned. These results suggest mechanisms other than direct contact of CMs and reactor

biomass may play a significant role in GAC-amended reactors (Zhang et al., 2020a), which has not been well studied. Last, sulfate-reducing bacteria (SRB) are common in AD bioreactors, participating in the conversion of sulfate to sulfide (Lens et al., 1998). Sulfide is toxic to anaerobic microorganisms (Lens et al., 1998). The understanding of CMs addition on the resistance to H_2S inhibition is poor. In addition, SRB have the potential to participate in the DIET process (Krukenberg et al., 2018). The competition and cooperation relationship between SRB and methanogens under CMs-amended conditions is unclear.

In practice, previous studies were conducted at temperatures higher than 20 °C (typically 35 °C–37°C or 55 °C) (Dang et al., 2017; Florentino et al., 2019a; Yan et al., 2017). The impacts of CMs additions to AD systems treating municipal sewage under psychrophilic conditions have not yet been investigated. Similar to other treatment options, CMs addition cannot guarantee enhanced methane recovery under various inflow conditions (Dang et al., 2016; Florentino et al., 2019b); understanding the limitations of CMs-amended AD is critical for future process design and control. Furthermore, GAC settled at the bottom of the reactor owing to the gravity (Yu et al., 2020), which may limit the contact between GAC and suspended sludge and result in clogging when treating wastewater with high suspended solids. New designs of CMs-amended reactors are required to overcome these drawbacks for practical applications.

In the past four and a half years, 14 bioreactors were operated to explore the influences of GAC addition in AD treatment of municipal sewage under psychrophilic conditions, focusing on the shift of electron transfer, biosynthesis of growth factors (e.g., vitamins and amino acids), microbial community dynamics, and the practical application.

Multiple bioinformatics analysis tools were used to analyze functional microorganisms under various conditions. This thesis demonstrates that the shift of electron transfer pathways and the stimulation of biosynthesis of growth factors are the two important mechanisms in CMs-amended AD. GAC addition to AD is an effective way for biomethane recovery from municipal sewage under psychrophilic conditions. This thesis provides important theoretical and practical guidance for the future anaerobic biological treatment of municipal sewage under psychrophilic conditions.

1.2. Research objectives

The main objective of this thesis is to investigate the impacts of GAC addition on anaerobic microbial community functions, and then develop and optimize an engineered GAC-amended AD of municipal sewage under psychrophilic conditions for biomethane recovery. This main objective was achieved through two specific phases:

(1) to elucidate the roles of GAC addition on anaerobic digestion, with focuses on the GAC impacts on microbial community dynamics, activities, physiological changes, as well as DIET among anaerobic microbes, biosynthesis of growth factors (e.g., vitamins and amino acids), and microbiome resistance to H_2S toxicity,

(2) to develop and optimize the application of GAC-based anaerobic treatment of municipal sewage under psychrophilic conditions.

1.3. Thesis outline

This thesis consists of ten chapters.

Chapter 1 introduces the general background, research objectives, and the outline of this research.

Chapter 2 provides a detailed literature review on the anaerobic process and related microorganisms, the status of AD treating municipal sewage, as well as the roles of carbon-based materials in AD.

Chapters 3-5 mainly address specific objective 1 to investigate the roles of GAC in AD. Specifically, Chapter 3 investigates the effects of GAC addition on treating low-strength wastewater at ambient temperatures. The key mechanism for electron transfer with GAC addition in continuous AD was illustrated. H_2 inhibition tests were performed to verify electron transfer pathway, and microbial physiological changes were determined through the measurements of sludge conductivity and the expression of related genes.

Chapter 4 explores the impacts of GAC on the biosynthesis of growth factors (e.g., vitamins and amino acids) and the effects of these products on anaerobic sludge, which does not contact GAC directly, revealing a vital mechanism beyond DIET of GAC addition in AD. Growth factors in up-flow anaerobic sludge blanket (UASB) effluents were analyzed and compared between the non-GAC and the GAC-amended UASB. The effluents of the two UASBs were used to stimulate anaerobic sludge. Microbial communities and kinetics were determined between two anaerobic sludges stimulated by UASB effluents.

Chapter 5 studies the effects of COD/SO_4^{2-} ratios in the non-GAC and GAC-amended UASBs treating low-strength wastewater. H_2S inhibition test was performed to test the effects of GAC addition on H_2S inhibition. Changes in microbial communities were

determined, and the relationship between methanogens and SRB under GAC addition conditions was discussed.

Chapters 6-9 further reveal the roles of GAC in the anaerobic treatment of municipal sewage and address specific objective 2 to develop and optimize the application of GAC-based anaerobic treatment of municipal sewage under psychrophilic conditions. Chapters 6 and 7 investigate the effects of GAC addition in UASB treating actual municipal sewage at ambient temperatures. Different operational factors, such as hydraulic retention time (HRT), were tested. Microbial communities and key microbes were analyzed and identified.

Chapter 8 explores active microbes during the treatment of actual municipal sewage using the mass balance model. Multiple bioinformatic and statistical tools were applied to evaluate the dynamics of the active microbes and the key operational factors controlling the bioreactor microbial community and affecting reactor performance.

Chapter 9 investigates the effects of a new design of GAC addition to UASB treating municipal sewage. Unlike in previous chapters, GAC or sponge was added to hollow plastic balls and was suspended in the upper layer of the UASBs in this chapter. The contribution to methane production of biofilms and suspended sludge was discussed. Microbial communities in biofilms and suspended sludges in sludge beds were compared.

Chapter 10 gives the main conclusion of the research findings and achievements. Recommendations are presented in this chapter.

Chapter 2. Literature review[1]

2.1. The steps of anaerobic digestion treating complex substrates

AD is a complex process and includes four steps: hydrolysis, acidogenesis, acetogenesis and methanogenesis (Figure 2.1) (McKeown et al., 2012). Hydrolysis is the first step in which disintegration happens from homogeneous particulates to carbohydrates, proteins and lipids, and further to basic monomers (sugars, amino acids, and long-chain fatty acids [LCFA]) (Batstone et al., 2002). In this step, hydrolytic microorganisms could secrete various extracellular enzymes (e.g., lipases and proteases), either bound to the cell surface or released into the medium (Cadoret et al., 2002; Facchin et al., 2013). These enzymes can be coupled to the polymers and then convert polymers into monomers. Acidogenesis is the second step, in which acidogenic microorganisms could ferment the basic monomers into volatile fatty acids (VFAs) and alcohols, such as propionic acid and butyric acid. H_2 and CO_2 can also be generated in this step (Van et al., 2020). The third step is acetogenesis, in which acetogenic microorganisms convert the mixture of VFAs and alcohols to acetate, accompanied by more CO_2 and H_2 gases. The last step is called methanogenesis, in which methanogens take responsibility for methane production (Van et al., 2020).

[1] A version of this chapter has been submitted for journal publication in August 2022.

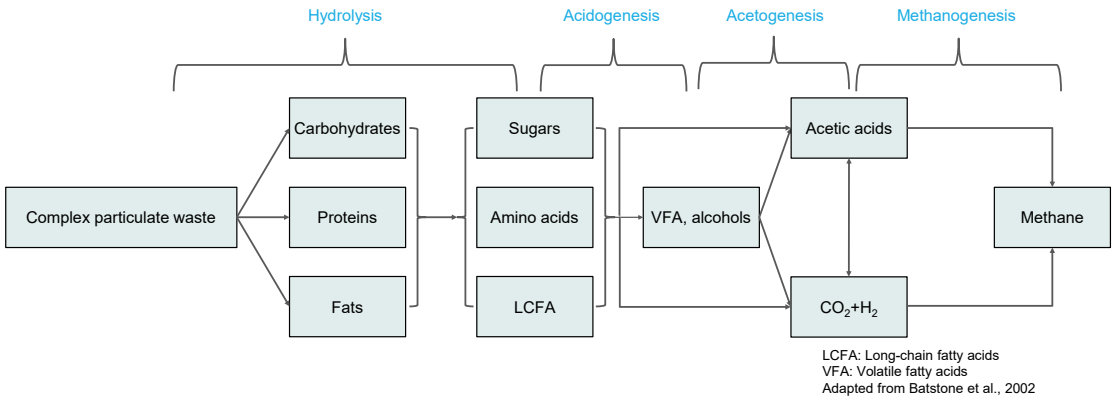

Figure 2.1 The steps of anaerobic digestion of complex substrates.

2.2. Methanogens and sulfate-reducing bacteria

Methanogens are a very diverse archaeal group characterized by the ability to produce methane (Balch et al., 1979). They are unique in terms of metabolism and are widespread in different habitats, including extensive natural habitats (e.g., lakes and soils), artificial habitats (e.g., landfills and anaerobic digesters), and also in animals and human bodies (Enzmann et al., 2018). Methanogens are highly diverse in terms of morphology. For instance, various shapes (e.g., coccoid, rod, plate, spiral) of methanogens have been identified. The growth conditions of methanogens are also diverse. Many methanogens grow under mesophilic conditions and are widely used in anaerobic digesters (Enzmann et al., 2018). Meanwhile, thermophilic and hyperthermophilic methanogens are identified, e.g., *Methanothermobacter thermautotrophicus* (Wasserfallen et al., 2000). In addition, cold-loving methanogens have been found in cold areas, such as on the Tibetan plateau (Zhang et al., 2008). The optimal pH for most methanogens is around neutral. Several methanogens can adapt to weak acidic or alkalic conditions (Enzmann et al., 2018).

Methanogens could use limited types of substrates: CO_2 and H_2 or formic acid

(hydrogenotrophic methanogens), acetic acid (acetoclastic methanogens), and methyl compounds (methylotrophic methanogens) (Zabranska & Pokorna, 2018). In hydrogenotrophic methanogenesis, CO_2 is reduced to a formyl group of methanofuran (formyl-MFR). Subsequently, formyl-MFR is transferred to tetrahydromethanopterin (H_4MPT) and further dehydrated to methenyl-H_4MPT. Next, methenyl-H_4MPT can get electrons from reduced cofactor F_{420} and further reduced to methylene-H_4MPT and then to methyl-H_4MPT. Finally, the methyl group is transported to sulfhydryl-containing coenzyme M (HS-CoM) and reduced to CH_4. In methylotrophic methanogenesis, methyl groups are transferred to a protein and then to HS-CoM, forming methyl-S-CoM and CH_4. In acetoclastic methanogenesis, acetate is first converted with ATP and coenzyme A (CoA) to acetyl-CoA. Then, the methyl group is transported to H_4MPT as methyl-H_4MPT and further converted to CH_4 like in the CO_2 pathway (Costa & Leigh, 2014; Enzmann et al., 2018; Zabranska & Pokorna, 2018). Acetoclastic and hydrogenotrophic methanogens are postulated to be dominant pathways, while methylotrophic pathway is the secondary process in anaerobic processes (Zhu et al., 2020). More contributions of the methylotrophic pathway in AD have been reported in a recent study (Zhu et al., 2020).

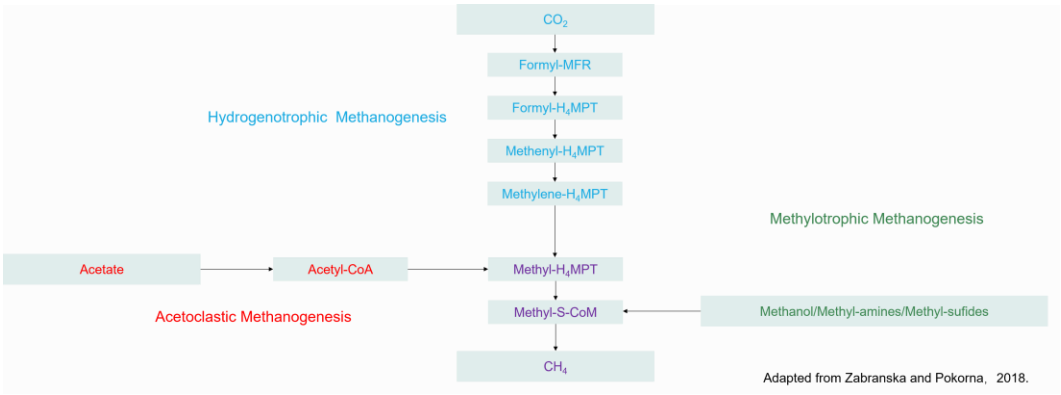

Figure 2.2 Pathways of methanogenesis.

Microbial electroactivity has been considered one of the critical mechanisms of electron transfer in the microbial world (Zhao et al., 2021). Electrochemical anaerobic technologies based on microbial electroactivity could overcome challenges associated with conventional anaerobic digestion (Huang et al., 2022). Methanogens have been shown the capacity for electroactivity in the uptake of electrons directly from electrodes and electroactive bacteria (Cheng et al., 2009; Rotaru et al., 2014a; Rotaru et al., 2014b; Zhen et al., 2015).

Biomethane generation is often impacted by sulfate-reducing bacteria (SRB), a type of widespread microorganism in AD. Different from methanogens, SRB can utilize a wide range of electron donors (e.g., H_2, acetate, propionate, butyrate, ethanol, molasses) to reduce sulfate and produce H_2S (Xu et al., 2020a; Zhang et al., 2021b). In the absence of sulfate, SRB can form a syntrophic relationship with methanogens (Gao et al., 2020), and act as fermenters (Scholten et al., 2007); in the presence of sulfate, SRB may outcompete methanogens through at least two mechanisms (Dar et al., 2008; Gao et al., 2020; Gavala et al., 2003). Firstly, SRB have more advantageous kinetic properties (lower K_s and higher μ_{max}), and sulfate reduction is thermodynamically more favorable than methanogenesis (Dar et al., 2008; Gavala et al., 2003). Secondly, sulfides, the end products of sulfate reduction, are toxic to methanogens and other AD microorganisms (Gao et al., 2020). Sulfides can form cross-links among polypeptide chains to denature proteins and interfere with key microbial enzymes (Chen et al., 2014). Methanogens have been shown to be sensitive to sulfide concentrations of 50 mg/L. The half-maximal inhibitory concentrations (IC_{50}) of H_2S for acetoclastic and hydrogenotrophic methanogens are 160 and 220 mg/L, respectively (Chen et al., 2014; Yamaguchi et al., 1999). Further, similar to

methanogens, some SRB are also electroactive (Lovley & Holmes, 2022).

2.3. Anaerobic digestion of municipal sewage

Anaerobic technologies, such as up-flow anaerobic sludge blanket (UASB), have been widespread for treating municipal sewage in trophic counties (Chernicharo et al., 2015). Compared to a conventional activated sludge plant, a sewage treatment plant using a UASB reactor followed by an aerobic process could save capital expenditures (CAPEX) by 20-50% and operational expenditures (OPEX) by above 50% (Chernicharo et al., 2015; Chernicharo, 2006). However, in temperate climates, such as Canada, the anaerobic system is still considered a challenge since low temperatures lead to low microbial activities and AD efficiency (Lettinga et al., 2001b; Xu et al., 2018).

Anaerobic treatment of municipal sewage at low temperatures has been intensively studied in the last two decades, and multiple operational conditions have been tested, as shown in Table 2.1. The HRTs have been tested from 24 h to 2 h. Temperatures were from more than 30 °C in the summer and below 10 °C in the winter. The CODs of most municipal sewage were below 1000 mg/L. The higher COD (2400 mg/L) was due to extra COD added to avoid low COD concentrations (Farajzadehha et al., 2012). The COD removal efficiencies ranged from ~ 10% to > 80%, depending on temperatures. Methane yields were below 10% of the COD input to above 50%. The high solubility of methane at low temperatures means that more methane is dissolved in the liquid part and is difficult to recover (Zhang et al., 2013). Meanwhile, considerable sulfate is commonly present in municipal sewage (Van Den Brand et al., 2015), leading to H_2S production and low methane production. The effluent contained volatile fatty acids (VFAs) in single UASBs

at low temperatures, indicating that methanogenesis was the limiting step (Bandara et al., 2012; Mahmoud et al., 2004).

Table 2.1 Anaerobic treatment of municipal sewage at low temperatures

Reactor type	HRT (h)	Temperature (℃)	Influent COD (mg/L)	Effluent COD (mg/L)	Removal efficiency (%)	Methane yield (%)	References
UASB	4.7	25-13	312±73	89±26	69	32-54	(Uemura & Harada, 2000)
UASB	5±0.5	16.5	153±6	69±4	55±2	-	(Seghezzo et al., 2002)
UASB/UASB-Filter	24-3	28-10	200-1300	102±43	38-82	5-31	(Lew et al., 2004)
UASB-Digester	6	15	460±122	151±34	66±6	47±15	(Mahmoud et al., 2004)
UASB-Digester	6	15	-	-	37.1±9.8	30	(Zhang et al., 2012b)
UASB-Filter	8-2	31-6	70-310	-	8-71	-	(Bandara et al., 2012)
UASB	4	20	600-2400	-	73	-	(Farajzadehha et al., 2012)
UASB	9	20	474.4±36.5	-	77-82	-	(Rizvi et al., 2015)
UASB-Digester	6	20-10	616±140	242±49	60±4.6	39.7±4.4	(Zhang et al., 2018)
UASB	7.7	15	-	84±8	79±2	17	(Petropoulos et al., 2019)

2.4. Carbon-based materials in anaerobic digestion

Carbon-based materials (CBMs), such as granular activated carbon (GAC), are commonly used in environmental protection for contaminant removal (Hagemann et al., 2018). GAC is a commercialized product and has become one of the most widely used CBMs in the water and wastewater treatment processes. Biochar (BC), another representative of CBMs, originated mainly from researching fertile anthropogenic soils and was defined as carbonized biomass for agricultural purposes in soils (Hagemann et al., 2018). Currently, the applications of BC are expanded widely, and the overlap of applications between BC and GAC has increased significantly. The use of other CBMs, such as hydrochar and graphene, is also increasing (Lin et al., 2018; Ren et al., 2020).

Fabrication methods (e.g., gasification, pyrolysis, and activation) may be different for different CBMs, but common properties include high porosity, large specific surface area, good electrical conductivity, and abundant surface functional groups (Aller, 2016; Naeem et al., 2017; Tobi et al., 2019). CBMs can act as carriers for microbial colonization, buffer pH, and are good adsorbents for organic compounds. During AD, CBMs can also provide electron conduits and mediators for extracellular electron transfer (EET) and affect microbial secretions. This thesis focuses on working as electron conduits and shifting microbial secretions.

2.4.1. Electron conduits and mediators of extracellular electron transfer

Extracellular electron transfer (EET) represents the biocapacity to transfer electrons between microbial cells and/or solid materials (e.g., electrodes and minerals) and is

widespread in nature (Kato, 2015; Schröder et al., 2015; Tremblay et al., 2017). In AD reactors, microorganisms can use indirect and direct EET to achieve electron transfer. Indirect EET is mediated by mobile or spatially fixed molecular redox mediators or by electron shuttles; microorganisms oxidize or reduce electron mediators/shuttles to achieve electron transfer (Kato, 2015). In direct EET, microorganisms stick to solid material surfaces or connect with each other, transferring electrons directly (Kato, 2015). Direct interspecies electron transfer (DIET) is one of the hotspots of current research on direct EET. In this process, c-type cytochromes and conductive nanowires play a crucial role, involving the electrons transfer through cell membranes or extending the transfer distance to maximize transmission efficiency, respectively (El-Naggar et al., 2010; Summers et al., 2010). EET plays a crucial role in degrading complex organic matter by anaerobic microbial communities. The bioprocess involves the disintegration of homogeneous particulates, extracellular hydrolysis, acidogenesis, acetogenesis, and methanogenesis (Batstone et al., 2002). Various microorganisms participate and cooperate to convert organic matter to methane. At the same time, electrons are transferred during these processes. For instance, interspecies hydrogen transfer (IHT) and interspecies formate transfer (IFT) between methanogenic archaea and syntrophic bacteria are essential EET mechanisms that are well understood (De Bok et al., 2004; Stams et al., 2006). The presence of carbon-based materials (CBMs) can accelerate direct and indirect EET in anaerobic digestion.

2.4.1.1. Electron mediator for indirect EET

Various functional groups or organic compounds can work as redox mediators and

facilitate electron transfer from cells to electron acceptors. In AD, the oxidized mediator can be used by one species as the electron acceptor and be reduced. Then, other species can use the reduced mediator as the electron donor (Hassan, 2018). In addition, electrons from functional groups can be used to reduce a variety of compounds (e.g., azo dye and halogenated organics) (Watanabe et al., 2009). Thus, functional groups can be used to remove recalcitrant compounds (Alvarez et al., 2017). Quinines (e.g., anthraquinone-2, 6-disulfonate [AQDS]), flavins, phenazines and their derivatives can work as molecular redox mediators in AD.

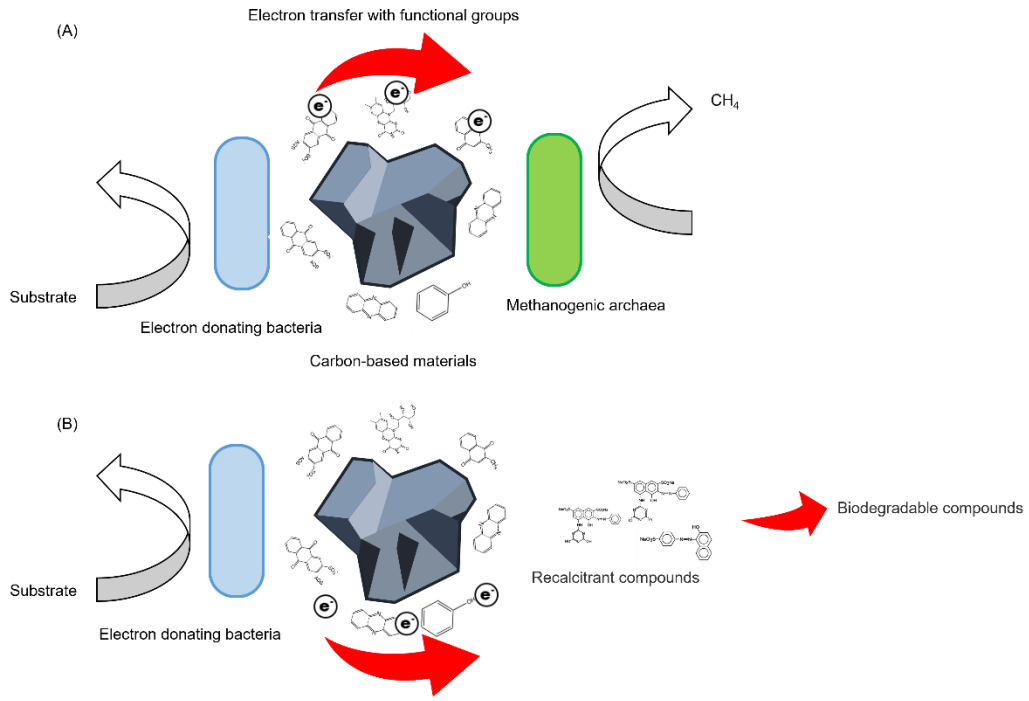

Figure 2.3 Mechanisms of indirect EET, (A) between electron-donating bacteria and methanogenic archaea, and (B) between electron-donating bacteria and recalcitrant compounds.

CBMs contain various functional groups, such as carboxyl, carbonyl, phenol, lactone, and quinone, derived from the activation process, precursor, thermal treatment, and post chemical treatment (Bhatnagar et al., 2013). These functional groups adsorb pollutants, mediate redox reactions, and convert pollutants in AD (Bhatnagar et al., 2013; Van Der Zee et al., 2003). CBMs with more surface functional groups produce more methane than CBMs with fewer surface functional groups. In an anaerobic treatment of kitchen waste, Wang et al. (2021a) found that biochar with more redox-active organic functional groups and a lower electrical conductance led to a better performance than biochar with fewer redox-active organic functional groups and a higher electrical conductance. Alvarez et al. (2017) found that the addition of AQDS modified GAC to a UASB treating wastewater containing Congo red, resulted in a 14.9-22.8% higher decolorization efficiency than a UASB treating wastewater containing Congo red treated with unmodified GAC. Deng et al. (2021) suggested that abundant active surface functional groups, such as -C=O, pyridinic-N, and graphitic-N, were correlated with a higher interspecies electron transfer. These results indicate that functional groups on the surface of CBMs can stimulate indirect EET in AD.

2.4.1.2. The DIET electron conduit

The methanogen capacity for direct interspecies electron transfer (DIET) has been studied in co-culture experiments between *Geobacter* and *Methanosarcina*, *Geobacter* and *Methanosaeta* (Rotaru et al., 2014a; Rotaru et al., 2014b). Compared to IHT/IFT, DIET is an energy-saving and more efficient electron transfer pathway among microorganisms (Lovley, 2017) because there is no guarantee that the metabolites released from syntrophic

bacteria using IHT/IFT will reach cooperative methanogens. Extracellular enzymes, unwanted competitors, and diffusions can affect IHT/IFT (Lovley, 2011). DIET is a point-to-point process with fewer impacts from extracellular activities. In addition, DIET is considered thermodynamically more favorable, and microorganisms growing with the DIET pathway could be faster than traditional pathways (Holmes et al., 2017; Zhang et al., 2022a). DIET can occur via (1) bioelectric connections (e.g., conductive pili and c-type cytochrome); (2) abiotic conductive connections (e.g., carbon-based materials) (Figure 2.4) (Rotaru et al., 2014a).

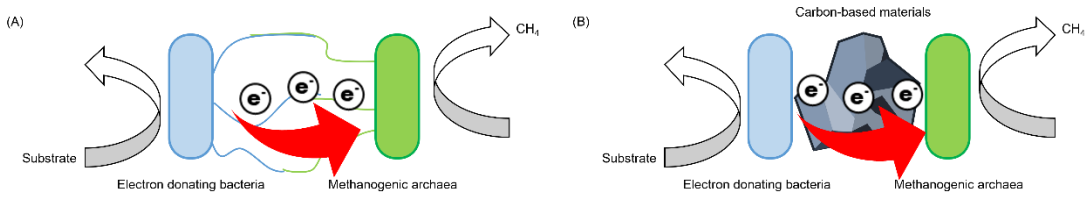

Figure 2.4 Mechanisms of DIET between electron-donating bacteria and methanogenic archaea, (A) DIET via bioelectric connections, and (B) DIET via abiotic conductive connections.

Enhanced AD processes by CBMs have been demonstrated in treating high-strength wastewater with simple and complex substrates under either mesophilic conditions (30-37 °C) or thermophilic conditions (55 °C) (Dang et al., 2016; Florentino et al., 2019a; Lei et al., 2016; Yan et al., 2017; Zhao et al., 2016a). DIET and electroactive microorganism enrichment induced by CBMs addition in AD have been considered the primary mechanism for enhancing reactor performance. However, whether DIET exists or not in mixed cultures is still a question. *Geobacter*, *Mathanosarcina*, and *Mathanosaeta* have been confirmed with DIET function in co-culture experiments and are considered the key

DIET-indicator microorganisms in AD bioreactors, but these DIET-indicator microorganisms accounted for only a small proportion of the total microbial community in continuous feeding AD (Dang et al., 2016; Dang et al., 2017; Lei et al., 2016; Rotaru et al., 2014a; Rotaru et al., 2014b; Tian et al., 2017; Yan et al., 2017; Zhao et al., 2016a; Zhao et al., 2017; Zhao et al., 2016c). Meanwhile, inconsistent results of the key DIET functional genes (e.g., *pilA* and *omcS* genes) have been found (Lei et al., 2019; Park et al., 2018; Van Steendam et al., 2019). Park et al. (2018) found that GAC amendment led to the significantly decreased relative abundance of *pilA* and *omcS* genes in a batch test treating acetic acid and ethanol, whereas GAC amendments led to an increase in the *pilA* and *omcS* gene copies of *Geobacter* in a continuous UASB treating leachate (Lei et al., 2019). In another semi-continuous-flow digester treating volatile fatty acids and alcohols, *Geobacter* was not enriched. The gene for *pliA* was primarily derived from *Sphaerochaeta*, *Sedimentibacter* and *Pseudomonas* species while *omcS* was not detected (Zhao et al., 2020b). Thus, the impact of CMs on DIET-related functional genes remains unclear (Van Steendam et al., 2019). Further, only limited DIET-related studies were performed in a continuous AD bioreactor treating low-strength wastewater under psychrophilic conditions (Tian et al., 2017). The effects of CBMs on anaerobic treatment of municipal sewage have not been studied.

2.4.2. Shifting microbial secretions

Extracellular functional secretions are the key to tuning the dynamics and behavior of the microbial community. CBMs addition might affect extracellular secretions. Signal molecules and extracellular polymeric substances (EPS) are the two widely discussed

extracellular secretions in carbon-amended AD. Growth factors (e.g., vitamins and amino acids) are common secretions, which have not been studied.

2.4.2.1. Signal molecules

Archaea and bacteria use quorum sensing (QS), i.e., signal molecules, to regulate gene expression and social behaviors. Microbial QS enables cell-cell communication when the concentration of extracellular signal molecules reaches a threshold density (Hao et al., 2010). QS signal molecules include acyl-homoserine lactone (AHL), autoinducer-2 (AI-2), diffusible signal factor (DSF), and diguanosine monophosphate (c-di-GMP) (Dang et al., 2022; Yin et al., 2020a). QS affects multiple microbial behaviors, such as biofilm formation, antibiotic resistance, extracellular secretions, and metabolic flux (Zhang et al., 2012a). Further, QS molecules can affect syntrophic partnerships and type IV pili; this suggests that QS can influence interspecies electron transfer (Yin et al., 2020a).

Studies of QS molecules in anaerobic digestions containing CBMs are limited. GAC addition to an AD in which glucose was used as the carbon source promoted secretions of medium-chain AHLs (e.g., 3O-C8-HSL and C8-HSL) in the sludge phase. Medium-chain AHLs have been positively correlated with methane production (Yu et al., 2020). Similar results were found in ADs treating blackwater, where GAC addition resulted in higher concentrations of AHLs, and the related genes were enriched in GAC biofilms (Dang et al., 2022). Dang et al. (2022) found that although suspended sludge in a GAC-amended reactor was not in direct contact with GAC particles, it developed more functional partners and genes than the non-GAC suspended sludge. It was likely that QS signal molecules from microorganisms in the GAC-biofilm activated electroactive

microorganisms in the GAC suspended sludge.

2.4.2.2. Extracellular polymeric substances

Extracellular polymeric substances (EPS) are complex mixtures of high molecular weight polymers, comprising carbohydrates, protein, humic substances, lipids, and some inorganic components (Sheng et al., 2010). EPS cover the surface of microbial aggregates and influence the effective diffusion of substrates (Sheng et al., 2010). Redundant EPS might reduce nutrient diffusion into cells and resist harmful exogenous materials (Xiao & Zheng, 2016). The redox properties of EPS can affect indirect EET (Li et al., 2016). In AD, EPS was also linked to anaerobic granulation. Anaerobic cells could be connected with EPS through ion bridging interactions, hydrophobic interactions, and polymer entanglement (Sheng et al., 2010).

CBMs can induce EPS excretion in AD (He et al., 2021; Li et al., 2015a; Zhuang et al., 2018). The addition of CBMs increased the concentrations of proteins/protein-like substances and polysaccharides (He et al., 2021; Xu et al., 2020b). Further, an enhanced electron transfer capacity in EPS was observed in carbon-amended reactors (Xu et al., 2020b), indicating more active redox components inside. Enhanced electron transfer can drive multistep electron hopping to compensate for the gap in electron transfer from cells to CBMs, and can enhance indirect EET (Liu et al., 2021a). EPS secreted from biofilm might enhance long-distance indirect EET (Yan et al., 2018), which might be one of the most important mechanisms in AD.

2.4.2.3. Growth factors

The biosynthesis of growth factors (e.g., vitamins and amino acids) is costly in energy and

requires a number of genes (Heizer Jr et al., 2006; Hubalek et al., 2017). The loss of some functions with high energy demand is an adaptation under nutrient and energy limitation conditions (Hubalek et al., 2017; Morris et al., 2012). Auxotrophy might reduce the burden of biosynthesis and promote cooperative interactions in the microbiome (Mee et al., 2014). In the AD, genes for the biosynthesis of crucial amino acids and vitamins were absent in the most abundant metagenome-assembled genomes, indicating that rather than synthesizing, some bacterial and archaeal members might borrow amino acids and vitamins from other microbes (Hubalek et al., 2017; Zhu et al., 2020). Some methanogens need vitamin B for their growth or activity (Patel & Sprott, 1990; Widdel, 1986). Previous studies reported that some bacteria (e.g., *Shewanella*, *Geothrix* and *Selenomonas*) could release vitamin B (Dryden et al., 1962; Marsili et al., 2008; Mehta-Kolte & Bond, 2012). These bacteria might work together with methanogenic archaea, which do not encode genes to biosynthesize required vitamins (Zhu et al., 2020). Although the biosynthesis of growth factors is an essential mechanism, the impacts of CBMs on biosynthesis have not been studied.

2.5. Summary

The impacts of CBMs addition (e.g., GAC) on enhancing anaerobic digestion have been reported widely. Various types of substrates (e.g. food waste and blackwater) and anaerobic reactors (e.g. batch test, UASB, anaerobic dynamic membrane bioreactor) have been tested (Florentino et al., 2019a; Jia et al., 2020; Tsui et al., 2020). However, the impacts of CMs addition to AD systems treating municipal sewage under psychrophilic conditions have not yet been investigated systematically. Meanwhile, the enhancement with CBMs addition in

AD has been largely attributed to DIET or microbial community shifting to perform DIET. The DIET pathway identification in continuous feeding AD with mixed cultures has not been systematically examined. Other mechanisms, such as the effects of changes in extracellular appendages and microbial extracellular compounds, draw less attention. Although previous studies have demonstrated that both SRB and methanogens have the capacity for EET (Shi et al., 2016), the relationships between SRB and methanogens under CMs addition conditions and the effects of CMs addition on resistance to H_2S toxicity have not been well assessed. Thus, comprehensively exploring the mechanisms of how CBMs affect AD is necessary to promote AD of municipal sewage under psychrophilic conditions.

Chapter 3. Granular activated carbon stimulated microbial physiological changes for enhanced anaerobic digestion[2]

3.1. Introduction

Methanogenesis activities can be enhanced by adding conductive materials (CMs), such as granular activated carbon (GAC), possibly by enhancing a recently discovered metabolic pathway, known as direct interspecies electron transfer (DIET) (Lovley, 2017; Lu et al., 2019a; Martins et al., 2018). However, the impact of CMs on anaerobic digestion (AD) microbial processes is not well understood (Martins et al., 2018; Raskin & Nielsen, 2019). Recent metagenomics studies provided insights into the key DIET functional genes, such as *pilA* and *omcS* genes, but inconsistent results have been found (Lei et al., 2019; Park et al., 2018; Van Steendam et al., 2019). Furthermore, previous studies on CMs mainly focused on the identification of the key DIET microorganisms/functional genes with DNA-based analysis (Lei et al., 2019; Park et al., 2018; Zhao et al., 2020b). Whether the expression levels of functional genes are affected by CMs and related to reactor performance has not been examined in continuously operated AD reactors. RNA reverse transcription, implying the gene expression, should be taken into consideration (Guo et al., 2020b; Ziels et al., 2018). In addition, studies demonstrated that the addition of CMs to AD

[2] A version of this chapter has been published: Zhang, Y., Zhang, L., Guo, B., Zhou, Y., Gao, M., Sharaf, A. and Liu, Y. (2020). Granular activated carbon stimulated microbial physiological changes for enhanced anaerobic digestion of municipal sewage. *Chemical Engineering Journal*, 400, 125838. https://doi.org/10.1016/j.cej.2020.125838

reactors led to an increase in AD sludge conductivity (Florentino et al., 2019a; Lei et al., 2016), which was accompanied by an increase in pili-like appendage development and may contribute to the enhanced AD performance. Such physiological changes in microorganisms may play a significant role in influencing microbial activities; however, the linkage between the microbial community/activity and physiological changes in the presence of CMs has not been evaluated.

The current chapter focuses on exploring the underlying mechanisms of GAC affecting microbial community/activity and physiological changes, which have never been evaluated under psychrophilic conditions treating low-strength wastewater. This chapter provides insights into the significance of microbial physiological developments in AD processes through the DIET-related functional gene expression and demonstrates that GAC addition is a feasible method to enhance methanogenesis for full-scale application under psychrophilic conditions.

3.2. Materials and methods

3.2.1. Reactor operation

Two laboratory-scale plexiglass UASB reactors (height 78 cm, diameter 10 cm) with working volumes of 4.7 L were operated at ambient temperature (20.0 ± 0.5 °C). Influent was pumped by a peristaltic pump (LongerPump®, BT100-2J, Baoding, China) from a feeding tank with a volume of 22 L. Biogas was collected by a 2 L gas bag (CHROMSPEC™, Brockville, Canada). Both UASB reactors were seeded with 3 L inoculum sludge collected from an anaerobic digester operated at 37 °C in a full-scale

wastewater treatment plant (WWTP) in Edmonton, Alberta, Canada. GAC (4-12 mesh, Sigma-Aldrich, St. Louis, USA) was added to one of the reactors at a concentration of 25 g/L and settled at the bottom of the reactor, resulting in a GAC packing ratio of 7%. The properties of GAC used in this thesis are shown in Table 3.1. The detailed reactor configuration is shown in Figure 3.1.

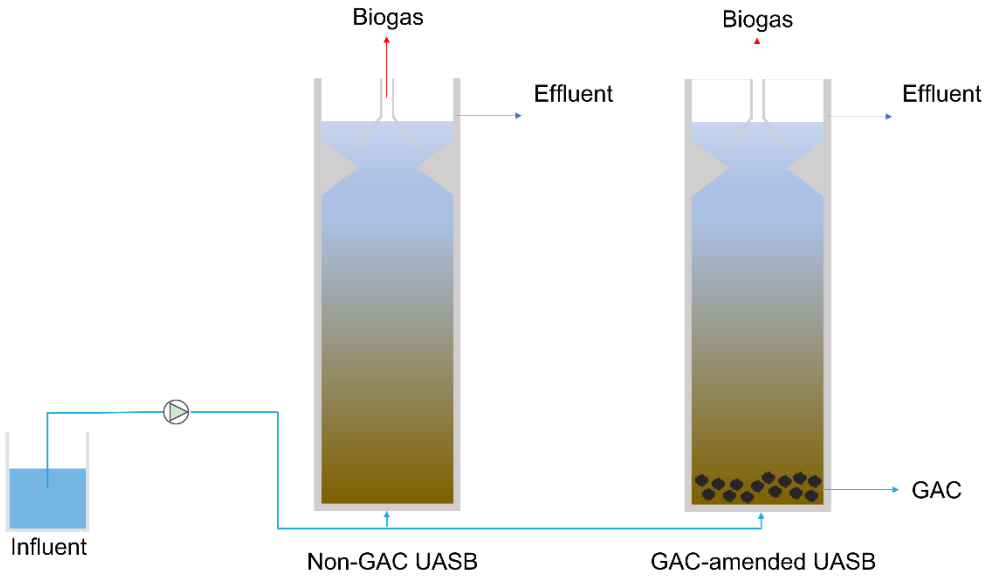

Figure 3.1 The schematic layout of the UASB system with or without GAC particles.

Table 3.1 Properties of granular activated carbon

Properties	Values
Vapor pressure	<0.1 mmHg (20 °C)
Autoignition temp.	842 °F
Particle size	4-12 mesh
Specific surface area	600-675 m^2/g
Resistivity	1375 μΩ-cm, 20°C (graphite)

The UASBs were fed with synthetic municipal sewage prepared following the recipe reported previously (Sheng et al., 2018), shown in Table 3.2. Wastewater influent contained COD of 500 mg/L, 40 mg/L of ammonia, and 10 mg/L of phosphate. The UASBs were operated for 120 days, with an initial hydraulic retention time (HRT) of 2 days during the start-up phase; after which, the HRT of the GAC-amended UASB was gradually reduced to 1.5 d, 1 d, 0.67 d, 0.5 d, and finally to 0.25 d. However, the lowest HRT achieved in the non-GAC UASB was 1 d.

Table 3.2 Synthetic municipal sewage recipe

Macro nutrient	
Chemicals	Concentrations (g/L)
Glucose	0.53
$MgCl_2 \cdot 7H_2O$	0.05
$CaCl_2 \cdot 2H_2O$	0.026
NH_4Cl	0.165
KH_2PO_4	0.027
K_2HPO_4	0.031
Trace nutrient stock solution[a]	
Chemicals	Concentrations (g/L)
$FeCl_3 \cdot 6H_2O$	1.5
H_3BO_3	0.15
$CuSO_4 \cdot 5H_2O$	0.03
HI_2KO_6	0.21
$MnCl_2 \cdot 4H_2O$	0.12
$Na_2MoO_4 \cdot 2H_2O$	0.06
$ZnCl_2$	0.056
$CoCl_2 \cdot 6H_2O$	0.15
Ethylenediaminetetraacetic acid (EDTA)	10

[a] The trace nutrient stock solution was used as 0.3 mL/L influent.

3.2.2. Analytical methods

Total COD (TCOD), soluble COD (SCOD), total suspended solids (TSS), and volatile suspended solids (VSS) were analyzed according to the Standard Methods of American Public Health Association (2012). Ammonia nitrogen (NH_4-N) concentrations were determined via the Nessler method (Hach, Loveland, USA, method 8038). Phosphate concentrations were determined using cuvette tests (Hach, Loveland, USA, method 10209). pH was measured using a sympHony pH probe (VWR, Radnor, USA). Gas pressures were measured using a hand-held pressure meter (GMH 3151, Regenstauf, Germany). Biogas concentrations of nitrogen, methane, oxygen, and carbon dioxide in the headspace of batch bottles and gasbags produced by the UASB reactors were determined using a gas chromatograph GC-7890B (Agilent Technologies, Santa Clara, USA). The oven and detector were operated at 100 ºC and 200 ºC, respectively. Helium (99.999% purity) was used as the carrier gas in the system.

The dissolved methane concentration in the effluent was determined once per week in duplicate. UASB effluent of 30 mL was injected into sealed glass serum bottles (60 mL) filled with 10.6 g NaCl. After shaking and settling, the final pressure was measured and the gas composition in the headspace was determined by the gas chromatograph. The dissolved methane concentration (mg COD/L) was calculated using the following formula:

$$CH_{4\,dissolved} = \frac{PVC}{RT} * \frac{64\frac{\text{g } CH_4-COD}{\text{mol } CH_4} * 1000\frac{ml}{L}}{30\,ml} \qquad \text{(Equation 3.1)}$$

where P is the final pressure of headspace in the glass bottle (Pa); V is the volume of the headspace of the bottle (m^3); C is the percentage of methane in the headspace; R = 8.314

J/ (mol K); and T = 293 K.

3.2.3. Specific methanogenic activity

UASB sludge was tested for specific methanogenic activity (SMA) once per week in duplicate. Sludge samples of 10 mL were collected from each UASB reactor, mixed with 20 mL glucose solution to a concentration of 1 g COD/L, then transferred into a serum bottle (60 ml). To achieve anaerobic conditions, the bottles were flushed with nitrogen gas, sealed, and placed in a shaker at 120 rpm and 20.0 ± 0.5 °C in the dark. Gas pressures were measured using the pressure meter as mentioned above (GMH 3151, Regenstauf, Germany). A 5 mL syringe was used to take biogas samples from the bottles. Then, methane concentrations were determined through the gas chromatograph. SMA was calculated according to the methane produced.

3.2.4. Batch test for H_2 inhibition

To examine the DIET activities in UASB sludge, batch experiments were performed using propionate as the sole carbon source, and high H_2 partial pressure was maintained in the reactor headspace (0.17 atm, 293 K). Under such conditions, propionate degradation and subsequent methane production can only be facilitated through DIET, as high H_2 partial pressure inhibits propionate degradation and eliminates syntrophic metabolism of propionate for methane production (Cruz Viggi et al., 2014; Zhao et al., 2016c). Batch reactors were seeded with suspended sludge samples from the non-GAC and GAC-amended UASB reactors for comparison. Each test bottle contained 5 mL sludge and 45 mL propionate solution (1 g COD/L). The COD/VSS ratio was ~ 0.6. The headspace of the

bottles was first flushed with N_2, then injected with H_2 to reach a H_2 partial pressure of 0.17 atm (293 K). Bottles were placed in a shaker at 120 rpm and 20.0 ± 0.5 °C in the dark and were monitored for methane production. This test was performed in two cycles. The second cycle of H_2 inhibition test was conducted under the same initial H_2 partial pressure (0.17 atm) and propionate concentration conditions, without further GAC addition. This test was performed in duplicate.

3.2.5. Sludge conductivity

Sludge conductivity was measured after 120 days reactor operation according to the method described by Florentino et al. (2019a). Suspended sludge was collected from each reactor by centrifuging samples at 800 × g for 5 minutes. Gold spiral electrodes (A-AD-GG-103-N Bare Gold Electrode, Zimmer and Peacock, Horten, Norway) were used to place the biomass. A voltage ramp from 0.0 V to 0.3 V was applied by a Keithley 2400 SourceMeter (Keithley, Cleveland, OH). LabTracer 2.0 (Keithley, Cleveland, OH) software was used to record the measurement. The measurements were performed for 11 times.

The following equations were used to evaluate the conductivity (σ, S/m) of the suspended sludge:

$$\sigma = \frac{1}{\rho} \qquad \text{(Equation 3.2)}$$

where ρ is the resistivity of the suspended sludge (Ωm).

$$\rho = \frac{RS}{L} \qquad \text{(Equation 3.3)}$$

where R is the reciprocal of the slope in the current-voltage curve (Ω), S is the side area of the spiral conductive print (length of 2.09 x 10^{-2} m and thickness of 13.50 x 10^{-9} m, m^2) and L is the width of the gap between working and counter electrodes (3.00 x 10^{-4} m).

3.2.6. Microbial community analysis

Microbial community analysis was performed at the end of the reactor operations on day 120. Biomass samples (2 ml) were collected from each UASB reactor, using DNeasy PowerSoil Kit (QIAGEN, Germany) for DNA extraction. Purity and concentration of the extracted DNA were analyzed using a NanoDrop One (ThermoFisher, USA). DNA samples were sent to RTL Genomics (Texas, USA) to perform polymerase chain reaction (PCR) and sequencing on the Illumina MiSeq pair-end 300 platform using primer pair 357F/785R for bacteria and primer pair 517F/909R for archaea.

3.2.7. Sequence data analysis

The forward and reverse sequence reads were paired, quality-filtered, and chimera removed using the QIIME2 pipeline DADA2 algorithm (Callahan et al., 2016). Taxonomy was assigned using 99% similarity in GreenGenes (version 13_8) reference database (McDonald et al., 2012a; Werner et al., 2012a). Shannon diversity was analyzed using the "vegan" package (Jari Oksanen et al., 2017) in RStudio version 3.4.1.

3.2.8. RNA extraction, reverse transcription and qPCR

Biomass samples stored in RNA*later* solution on day 120 were used for RNA extraction using TRIzol™ Reagent (Thermo Fisher Scientific, Mississauga, ON, Canada) following

the manufacturer's protocol. The extracted RNA was purified using an Aurum™ Total RNA Mini Kit with DNase I (BIO-RAD, Mississauga, ON, Canada). cDNA was obtained by reverse transcription of total RNA using iScript™ cDNA Synthesis Kit (BIO-RAD) following the manufacturer's protocol.

DNA and cDNA samples were used for quantitative PCR (qPCR) of the *pilA* gene and a reference gene *recC* (Hernández-Eligio et al., 2020). The qPCR reactions were performed in triplicate using the SsoFastTM EvaGreen® Supermix and BioRad CFX96 system (BIO-RAD) following the manufacturer's protocol. The *pilA* gene was amplified using forward primer 5'-AAT TAC CCC CAT ACC CCA AC-3' and reverse primer 5'-AGC AGC TCG ATA AGG GTG AA-3' (Hernández-Eligio et al., 2020) with the steps of 3' at 95 °C, 55 cycles of 10" at 95 °C, and 20" at 55 °C, followed by plate reads. The *recC* gene was amplified using forward primer 5'- CTG TCG TCA CCC TTT GTT CC-3' and reverse primer 5'- GAA AGG GAT AGG AGC CGT TC-3' with the steps of 3' at 95 °C, 55 cycles of 10" at 95 °C, and 20" at 55 °C, followed by plate reads. The relative abundance and expression were quantified by the $2^{-\Delta\Delta CT}$ method following the qPCR guide from BIO-RAD.

3.3. Results

3.3.1. Reactor performance

COD removal, methane production, and SMA results of non-GAC and GAC-amended UASBs are shown in Figure 3.2. The organic loading rate (OLR) gradually increased by decreasing the HRT. The methane production of the non-GAC UASB and GAC-amended

UASB took into account the dissolved methane in the liquid phase (Figure 3.3). At HRTs of 2 and 1.5 d, the effluent COD and methane production rates were comparable between the non-GAC reactor (Figure 3.2A) and GAC-amended reactor (Figure 3.2B). At the beginning of the start-up period (HRT 2 d), COD removal efficiencies of both UASB reactors fluctuated before reaching stable performance after 10 days, with COD removal efficiencies varied between 75 and 93%. When the HRT was reduced to 1.5 d, the COD removal efficiency of the non-GAC and GAC-amended reactors was 77 ± 6% and 82 ± 9%, respectively. The daily methane production in both reactors increased from 102 ± 17 to 192 ± 16 mL CH_4/g feed-COD in the non-GAC reactor (Figure 3.2C), and 94 ± 11 to 195 ± 27 mL CH_4/g feed-COD in the GAC-amended reactor (Figure 3.2D) compared to the HRT of 2 d.

When the HRT was further reduced to 1 d, notable differences were observed between the two reactors. The average daily COD removal efficiency and methane production in the non-GAC reactor decreased dramatically to 58 ± 17% and 128 ± 13 mL CH_4/g feed-COD, respectively; however, in the GAC-amended reactor, these values increased to 93 ± 4% and 230 ± 19 mL CH_4/g feed-COD, respectively.

Due to the poor performance of the non-GAC reactor with regards to COD removal efficiency and methane production, the HRT of the non-GAC reactor was increased back to 1.2 d to allow for recovery. Then, increases in average COD removal efficiency (74 ± 11%) and methane production (155 ± 17 mL CH_4/g feed-COD) were observed. After stabilization (on day 95), the reactor HRT was reduced to 1 d, again leading to a reduced COD removal efficiency (56 ± 6%) and methane production (132 ± 6 mL CH_4 /g feed-

COD).

For the GAC-amended reactor, HRT was further decreased to 0.67 d, and then to 0.5 d. Under these conditions, the average COD removal efficiency remained relatively stable (93 ± 4%), and the methane production further increased to 283 ± 28 mL CH_4/g feed-COD for 0.67 d HRT, and 309 ± 17 mL CH_4/g feed-COD for 0.5 d HRT. When the HRT was further reduced to 0.25 d, effluent COD first increased to 100-118 mg/L before decreasing and stabilizing at 75-80 mg/L after 4 days. The average COD removal efficiency decreased to 82 ± 4% and the methane production decreased to 264 ± 15 mL CH_4/g feed-COD. This suggests that the GAC-amended reactor reached its capacity at an HRT of 0.25 d.

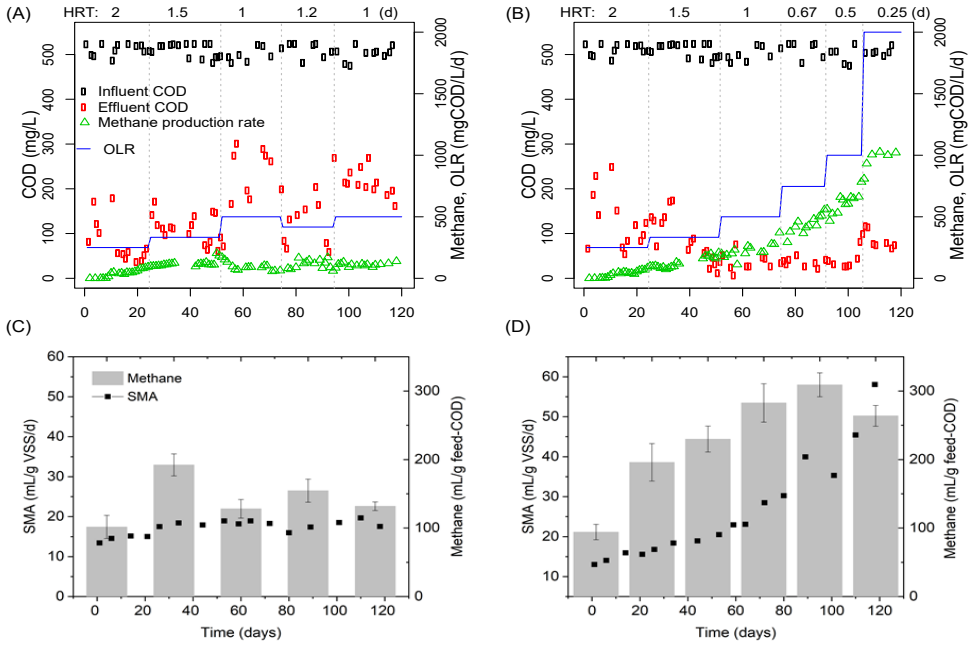

Figure 3.2 Performances of (A) non-GAC and (B) GAC-amended UASBs, and the methane production and specific methanogenic activity (SMA) in (C) non-GAC and (D) GAC-amended UASBs. Error bar represents standard deviations.

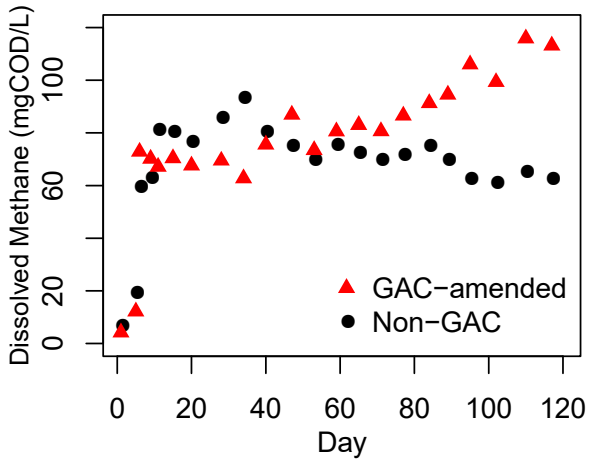

Figure 3.3 Dissolved CH_4 in the GAC-amended and non-GAC UASBs.

3.3.2. Biomass concentration

The total VSS at the end of the experiments (Day 120) in the non-GAC (sludge only) and GAC-amended (sludge and biofilm) reactors were 20.0 g and 26.6 g, respectively. The total biomass content in the GAC-amended reactor was 33% higher than the non-GAC reactor in comparison to the GAC-amended reactor. The VSS of GAC attached biofilm was 0.66 ± 0.16 g, which only accounted for 2.5 ± 0.6% of the total VSS in the GAC-amended reactor. Considering the 100% increase in methane production rate (132 mL CH_4/g feed-COD for non-GAC under 1 d HRT and 264 mL CH_4/g feed-COD for GAC-amended reactor under 0.25 d HRT, Figure 3.2 C and D), it can be concluded that the increased total biomass content in the GAC-amended reactor only contributed partially to the enhanced methane production.

3.3.3. Microbial community analysis

Archaeal and bacterial community diversities and compositions are shown in Figure 3.4. The GAC-amended reactor had higher Shannon diversity than the non-GAC reactor for both archaea and bacteria, and the microbial communities shared high similarity: 0.67 for archaea and 0.77 for bacteria based on Bray-Curtis distance. Compared with the seed sludge, microbial community in both UASBs shifted and developed similarly as shown in the cluster analysis (Figure 3.4).

The non-GAC and GAC-amended reactors shared dominant genera in both archaeal and bacterial communities. In the archaeal community (Figure 3.4A), *Methanosaeta* was the most abundant genus in the GAC-amended reactor (38% relative abundance) and the second abundant genus in the non-GAC reactor (22%). One unidentified genus in the family WSA2 (class *Methanobacteria*) was the most abundant genus in the non-GAC community (42%) and second in the GAC-amended reactor (21%). *Methanobacterium*, *Methanolinea*, and *Methanomassiliicoccus* were slightly higher in the GAC-amended reactor than in the non-GAC reactor.

In the bacterial community (Figure 3.4B), *Geobacter* (12%), *Paludibacter* (10%), one unidentified genus in the order *Bacteroidales* (9%), T78 (phylum *Chloroflexi*, 7%), and one unidentified genus in the family *Enterobacteriaceae* (6%) dominated the GAC-amended reactor. The non-GAC community was dominated by one unidentified genus in the order *Bacteroidales* (15%), T78 (15%), *Geobacter* (9%), and *Trichococcus* (9%).

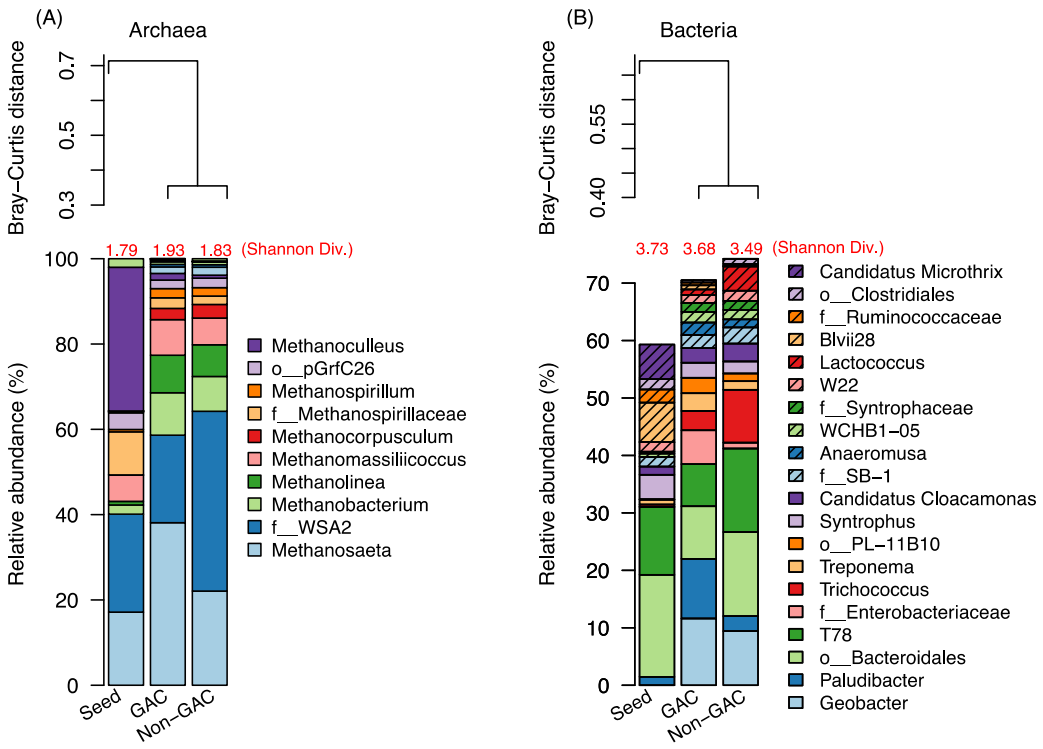

Figure 3.4 Bray-Curtis distance and relative abundances of archaeal genera (A) and bacterial genera (B) with average abundance > 1% in the seed, non-GAC and GAC-amended UASBs. Shannon diversity is labeled on top of bars. Unidentified genera were named at family (f__) or order level (o__).

3.3.4. Suspended sludge activities

3.3.4.1. Sludge methanogenesis activities (SMA)

The temporal changes of suspended sludge SMA are shown in Figure 3.2 C and D. Under HRTs of 2 d and 1.5 d, the SMAs were similar in the two reactors. With further reduced HRTs, the SMA in the GAC-amended reactor increased, whereas the SMA in the non-GAC reactor reduced. At the end of the experiment, the sludge SMA of the GAC-amended

reactor reached 58.0 ± 2.5 mL CH_4/g VSS/d with an HRT of 0.25 d, which was significantly higher than the SMA of the non-GAC reactor (19.7 ± 0.5 mL CH_4/g VSS /d with an HRT of 1.2 d).

3.3.4.2. Sludge activities in the presence of H_2 inhibition

As shown in Figure 3.5, in the absence of H_2 (headspace filled with N_2), suspended sludge from both reactors was able to use propionate as substrate to produce methane. Addition of fresh GAC particles (pristine GAC without biofilm) in the batch reactors did not further enhance methane production from these reactors. However, under high H_2 partial pressure conditions, methane production was significantly inhibited in reactors seeded with sludge collected from both reactors. Further, adding fresh GAC particles in reactors seeded with non-GAC reactor sludge did not result in any improvement in methane production during the incubation period of 35 days. Interestingly, when fresh GAC particles were added to the reactors seeded with GAC-amended UASB suspended sludge (Figure 3.5B), enhanced methane production was observed after 10 days of incubation, and high methane production was achieved after 30 days of incubation. These results indicate that suspended sludge from the GAC-amended UASB was able to overcome H_2 inhibition in the presence of fresh GAC. The resistance of GAC amended culture towards H_2 inhibition has been previously demonstrated in batch experiments at 37 °C and 55 °C (Li et al., 2017; Yan et al., 2017; Zhao et al., 2017; Zhao et al., 2016c); the present study is the first to demonstrate this capacity for sludge collected from continuous operating reactors treating low-strength wastewater under low-temperature conditions.

As shown in Figure 3.5B, no inhibition was observed in the second test cycle,

inferring that the suspended sludge from the GAC-amended reactor developed functions to convert propionate to methane under a high H_2 pressure condition, suggesting the existence of DIET where GAC serves as an electron conduit, allowing for electron transfer directly from bacteria to methanogens without H_2 as electron carriers (Cruz Viggi et al., 2014; Zhao et al., 2016c).

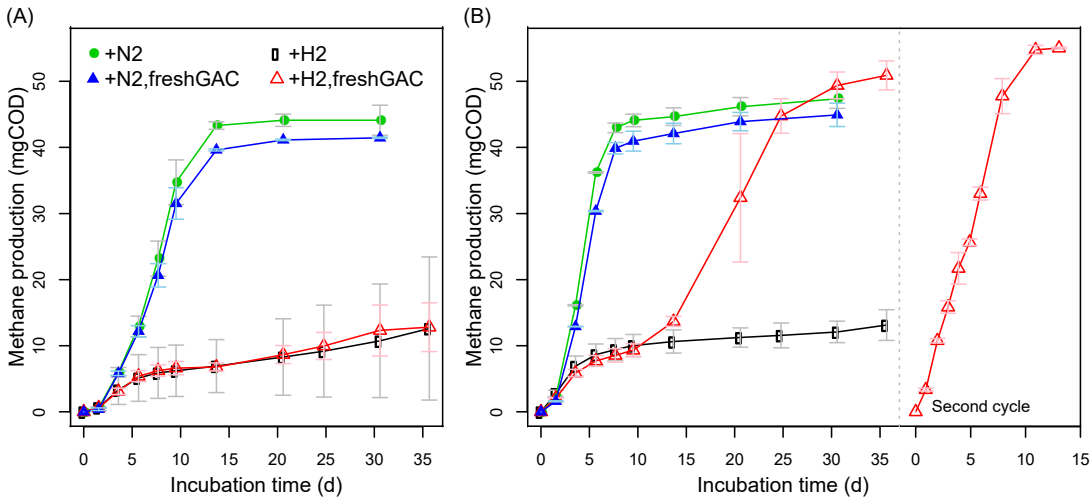

Figure 3.5 Batch experiments using propionate as the carbon source under high H_2 partial pressure. Suspended sludge from (A) the non-GAC reactor and (B) the GAC-amended reactor.

3.3.5. Sludge physiological properties

3.3.5.1. Sludge conductivities

To explain the GAC-induced microbial activity enhancement and DIET function, the physiological changes of suspended sludge were tested. Figure 3.6 shows the current-voltage responses of the sludge samples and the linear regression coefficients. The GAC-amended UASB sludge showed a significantly higher regression coefficient (7.27 e-07)

than the non-GAC UASB sludge (1.72 e-07) ($p < 0.05$). Based on this result, the calculated conductivities for suspended sludge from the non-GAC and GAC-amended UASBs were 1.52 ± 0.12 and 8.37 ± 0.32 µS/cm, respectively, indicating that the microorganisms in the GAC-amended UASB developed high electric conductivity. Enhanced biomass conductivity (4.87~16.5 µS/cm) has also been reported previously for DIET-relative bioreactors (Florentino et al., 2019a; Zhao et al., 2016c).

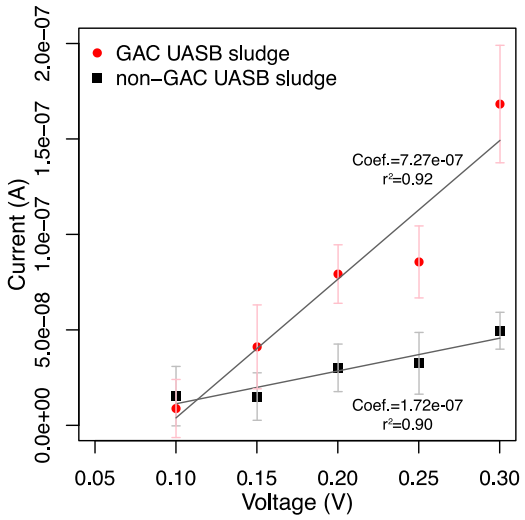

Figure 3.6 Current-voltage response of suspended sludge from the non-GAC and GAC-amended UASBs with linear regression coefficients (Coef.) and coefficient of determination (r^2). Error bar represents standard deviation of 11 measurements.

3.3.5.2. Gene abundance and expression of conductive pili

The functional cellular structures for DIET involve conductive e-pili and c-type cytochromes, which could be evaluated by targeting *pilA* and *omcS* genes using qPCR (Lovley, 2017; Rotaru et al., 2014b). Figure 3.7 shows the *pilA* gene abundances and expression levels using *recC* as a reference gene. Based on the DNA qPCR analysis, the

pilA gene abundances were found to be at the same level in the two reactor communities (p = 0.10, student t-test), correlating to the similar suspended sludge microbial communities in two reactors (Figure 3.4). However, the qPCR of cDNA (RNA reverse transcription) showed that the expression level of *pilA* in the GAC-amended UASB suspended sludge community was significantly higher than that in the non-GAC UASB suspended sludge community (p = 0.03). These results underline the significance in targeting RNA when evaluating the DIET associated microbial functions in bioreactors. The *omcS* gene was below the detection limits in our samples, thus results are not shown. Similar to the reported bioreactor studies, the c-type cytochrome gene *omcS* abundance was much less than the *pilA* gene abundance (Park et al., 2018). Further studies using metagenomic and metatranscriptomic analysis are needed to comprehensively elucidate abundance and expression of c-type cytochrome in GAC-amended reactors (Park et al., 2018).

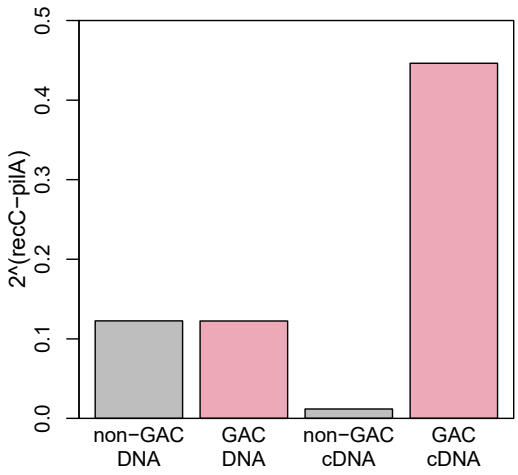

Figure 3.7 Relative *pilA* abundances in DNA and expression levels in RNA reverse transcribed cDNA using *recC* as the reference gene in suspended sludge samples from non-

GAC UASB and GAC-amended UASB.

3.4. Discussion

3.4.1. GAC addition facilitated a DIET pathway

The batch study (Figure 3.5) showed that under H_2 inhibition conditions, sludge from GAC-amended UASB was able to resist the H_2 inhibition, a feature of DIET-functioning microbial community (Li et al., 2017; Yan et al., 2017; Zhao et al., 2016c). The increased biomass conductivity (Figure 3.6) and *pilA* gene expression (Figure 3.7) further reinforced that GAC induced the development of DIET pathway. These results correlated well with the improved reactor performance in the GAC-amended UASB; GAC amendment reduced allowable HRT (from 1 d to 0.25 d) and increased OLR (from 500 to 2000 mg COD/L/d). The changes in operational parameters further led to the increased CH_4 production rate (from 36 mL CH_4/L reactor/d to 328 ml CH_4/L reactor/d) and COD removal efficiency (from 56% to 82%) (Figure 3.2).

Improvement in reactor performance with CMs addition has been previously demonstrated in continuous reactor operation studies (using UASB and other reactor types), as summarized in Table 3.3. For instance, Lei et al. (2016) found that with carbon cloth addition, OLR and COD removal increased by 34% and 160%, respectively. All of these studies attributed the enhanced AD performance to the DIET mechanism, although none has systematically examined the sludge activity, physiological properties, and DIET pathway as demonstrated in the current study.

Table 3.3 Summary of studies using different carbon-based materials in continuous AD systems

Reactor type	Temperature	Carbon-based Material	Substrate type	OLR[1] (g COD/ L/d)	COD removal (%, CM vs non-CM)	Methane production[2]	SMA[3]	Study
UASB	20 °C	GAC	Glucose	0.5 2 vs 0.5	93 vs 56 82 vs 56	75 vs 36 328 vs 36	24 vs 18 58 vs 20	Present study
CSTR	35 °C	GAC	Acetate	NA	NA	71 vs 40	NA	Lee et al. (2016)
SBR	37 °C	GAC	Dog food	6.7 8.5	NA	1272 vs 1200 1560 vs failure	NA	Dang et al. (2016)
UASB	37 °C	Biochar	Butyrate Propionate	10.3 10.3	99.7 vs 85.3 98.0 vs 87.8	3439 vs 2760 3048 vs 2644	NA NA	Zhao et al. (2016a)
UASB	33 °C	Carbon cloth	Incineration leachate	49.4	80 vs 30	13684 vs 2683	NA	Lei et al. (2016)
UASB	10-20 °C	Graphene	Glucose	1.6	50 vs 50	15.36 vs 13.44	NA	Tian et al. (2017)

[1] Organic loading rate.
[2] Methane production, gas phase, CM vs non-CM, mL CH_4/L reactor/d
[3] Specific methanogenetic activity, mL CH_4/g VSS /d.

3.4.2. Importance of microbial community structure and biomass density

The results show that with continuous reactor operation of 120 days with and without GAC addition and under different HRT conditions, similar microbial communities and dominant microorganisms develop (Figure 3.4), indicating that factors other than HRT/OLR and GAC addition play significant roles in controlling the microbial community in bioreactors. Note that the complex microbial community structure can be shaped by various deterministic factors such as substrate composition, temperature, pH, and reactor configuration (Cydzik-Kwiatkowska & Zielińska, 2016; Raskin & Nielsen, 2019). Further, when considering key DIET indicator microorganisms (*Geobacter and Mathanosarcina* or *Mathanosaeta*), the results (Figure 3.4) only showed a slight increase in *Geobacter* (3% increase) and *Methanosaeta* (16% increase) in the GAC-amended reactor. These results are

in agreement with previous studies, as the reported increases in the abundance of *Geobacter* (0-8%) and *Methanosaeta* (0-19%) are often limited (Dang et al., 2017; Zhao et al., 2017; Zhao et al., 2016c). In addition, the observed simultaneous increases of *Geobacter* and *Methanosaeta* in this study may be associated with their syntrophic relationship during DIET, which has been verified previously (Liu et al., 2012; Rotaru et al., 2014b; Zhao et al., 2016a; Zhao et al., 2016c). It was also noted that the biomass density did not significantly increase in the presence of GAC (33% in the present study, and 5% in a previous study) (Lee et al., 2016), indicating that the impact of biomass quantity on reactor performance was limited.

To summarize, while the changes in the microbial community structure and biomass density are often discussed in the literature as (i) the evidence for a shift of interspecies hydrogen transfer to DIET, and (ii) an explanation for the improved methane production, caution should be taken to analyze the contribution of these factors to the reactor performance. We propose that neither the level of increase in biomass density nor the extent of changes in microbial community is sufficient to explain the significantly enhanced biomethane production in the presence of conductive materials; rather, the sludge activity and functionality should be taken into evaluation for understanding CM effects.

3.4.3. Importance of microbial physiological changes

Biomass conductivity and e-pili are the two important physiological parameters linked to the establishment of DIET (Florentino et al., 2019a; Zhao et al., 2016c). In particular, enhanced conductivity of microbial cultures in the presence of CMs has been observed in previous studies (Florentino et al., 2019a; Lei et al., 2016; Li et al., 2017; Yan et al., 2017;

Zhao et al., 2016c) and demonstrated in the present study, which has been suggested as evidence of DIET between microbial syntrophic partners.

Although the development of electrically conductive pili (e-pili) is known to be important for facilitating DIET in anaerobic systems (Lovley, 2017; Walker et al., 2020) and directly correlates with biomass conductivity (Leang et al., 2013; Malvankar & Lovley, 2014; Storck et al., 2016), controversial results have been demonstrated previously. Recently, one batch study reported a reduced *pilA* gene abundance (by 69.4%) based on metagenomic analysis in GAC-amended batch reactor (Park et al., 2018); the authors concluded that GAC could transfer electrons, which reduced the needs for conductive pili structure. This conclusion was linked to pure or co-culture studies (Liu et al., 2012; Salvador et al., 2017), which demonstrated that e-pili deficient mutant strains could use conductive materials for DIET. However, direct evidence is not available to support this conclusion that microorganisms reduce their e-pili production in the presence of conductive materials.

On the other hand, another two studies based on metagenomic analysis showed the abundances of *pilA* gene significantly increasing (Lei et al., 2019; Zhao et al., 2020b). Further, a recent study has shown an increased density in pili structure (observed with SEM) in GAC-amended AD reactors (Florentino et al., 2019a). Results from the present study showed similar *pilA* gene abundance in the non-GAC and GAC-amended reactor sludge, but a significantly higher gene relative expression level (36 folds increase) in GAC-amended reactor (Figure 3.7). It is hypothesized that GAC stimulates the e-pili gene expression in the AD reactor, resulting in more pili production, which improves the electron

transfer efficiency and syntrophic methanogenesis. This is in accordance with the increased biomass conductivity (Figure 3.6) and higher SMA (Figure 3.2 C and D). Overall, the presented study suggests the significance of e-pili secretion in mediating DIET, and gene expression studies based on RNA are needed when evaluating DIET in AD amended by CMs.

3.5. Conclusion

This chapter demonstrated that GAC enhanced methane recovery from low-strength wastewater at 20 °C. The organic loading rate could be increased to 2000 mg COD/L/d with GAC amendments, compared to 500 mg COD/L/d without GAC. The mechanisms to achieve this enhancement were multi-fold. Firstly, total biomass content was increased by 33% with GAC amendments, not comparable to the 300% increase in COD loading. Secondly, similar microbial communities were observed in the suspended sludge between two reactors, with slight increases in *Geobacter* and *Methanosaeta*, but the specific methanogenic activity was 1.9 times higher in GAC-amended reactor. Thirdly, the DIET function was verified using batch tests under high H_2 partial pressure. The enriched microorganisms within the GAC-amended reactor were able to resist H_2 inhibition in the presence of GAC particles. In addition, the conductivity of the sludge, and the gene expression of *pilA* were much higher in the GAC-amended reactor sludge than in the non-GAC reactor sludge, implying that the microbial physiological changes were stimulated by GAC addition. Comprehensively, the microbial physiological changes played a significant role in the GAC-amended AD process. These results provide evidence of the DIET function and microbial physiological changes for AD enhancement and suggest the feasibility of

wide application of low-cost GAC for AD processes, especially for low-strength wastewater anaerobic digestion.

Chapter 4. Granular activated carbon stimulated microbial extracellular secretions in anaerobic digestion: An egalitarian act and beyond[3]

4.1. Introduction

In Chapter 3, the amounts of granular activated carbon (GAC) and biofilms formed on the GAC were low compared to the suspended sludge in the whole AD system. As a result, direct interactions between GAC and AD suspended sludge might not be as significant as we envisioned. Meanwhile, high specific methanogenic activities were not only observed for GAC-attached biofilms, but also for suspended sludge in the GAC-amended reactors, suggesting a mechanism that does not rely on direct contact of CMs and reactor biomass plays significant roles in GAC-amended reactors.

So far, only limited studies have explored the role of microbial extracellular products (e.g., extracellular polymeric substances [EPS]) in CMs-amended AD reactors (Liu et al., 2021a). Yin et al. (2018) found that CMs addition could increase the distribution of potential electron shuttles (e.g., quinone-like substances and flavins) in the soluble microbial products (SMP) and EPS. The various redox-active components in EPS developed with CMs addition can drive multistep electron hopping to compensate for the gap in electron transfer from cells to CMs, and may enhance the electron transfer capacity between the cell surface and CMs surface (Liu et al., 2021a; Xu et al., 2020b). However, the effects of CMs addition on extracellular secretions have not been well evaluated. In

[3] A version of this chapter has been submitted to *Chemical Engineering Journal* in July 2022.

particular, in order to better design and operate CMs-amended AD reactors, it is important to explore the impacts of CMs stimulated extracellular secretions on the activities of suspended sludge that is not in direct contact with CMs.

This chapter explores the effects of GAC addition on the biosynthesis of extracellular secretions in an up-flow anaerobic sludge blanket (UASB) reactor; the microbial syntheses of amino acids and vitamins are a focus. The impact of extracellular secretions in UASB reactors with and without CAC addition was studied by feeding UASB effluents to different downstream anaerobic sequencing batch reactors (ASBRs). Enhanced performance in the downstream ASBR that fed with effluent from the GAC-amended UASB was attributed to the impact of extracellular bioproducts.

4.2. Materials and methods

4.2.1. Experimental setup and reactor operation

UASB1 and UASB2, each with a working volume of 2.3 L, were operated continuously at ambient temperature (20 ± 0.5 °C) for more than 200 days. Inoculum sludge was obtained from a full-scale anaerobic digester treating waste-activated sludge in a local wastewater treatment plant (WWTP) (Edmonton, Alberta, Canada). UASB1 was not amended with GAC; UASB2 was amended with 60 g GAC (4-12 mesh, Sigma-Aldrich, St. Louis, USA), occupying ~ 7% working volume of the UASB. The hydraulic retention time (HRT) was controlled at ~ 1 day, and the chemical oxygen demand (COD) loading rate was ~ 2.5 kg COD/L reactor/d. Glucose was used to provide influent COD. The concentrations of other nutrients are shown in Table 3.2. Effluents from UASB1 and UASB2 were collected daily,

centrifuged at 3000 rpm for 15 min (to remove any suspended biomass or GAC in UASB effluents), and the supernatants were used as influents for the downstream anaerobic sequencing batch reactors ASBR1 and ASBR2, respectively.

ASBR1 and ASBR2, each with a working volume of 0.9 L, were operated at ambient temperature (20 ± 0.5 °C) for 80 days divided into three stages: start-up, stage I, and stage II, varying in influent COD concentrations and the feeding time intervals (Table 4.1). Effluent of UASB1 without GAC-amended was used as the influent to ASBR1; effluent of UASB2 with GAC-amended was used as the influent to ASBR2. Glucose was added to equalize the influent COD in each ASBR. The ASBRs were shaken at 120 rpm in the dark for 3 days (start-up phase and stage I phase) or 2 days (stage II phase), then 30 minutes of settling time was applied to settle the sludge. After sludge settling, 0.4 L effluent (or 44% of total working volume) was removed from each ASBR, and 0.4 L of influent was added. The procedure is shown in Figure 4.1 and Table 4.1.

Table 4.1 ASBR operational conditions

	Influent COD (mg COD/L)	Interval for influent (days)	Settling time (min)	Influent exchange ratio (%)
Start-up	Steps to 2000	3	30	44
Stage I	2000	3	30	44
Stage II	4000	2	30	44

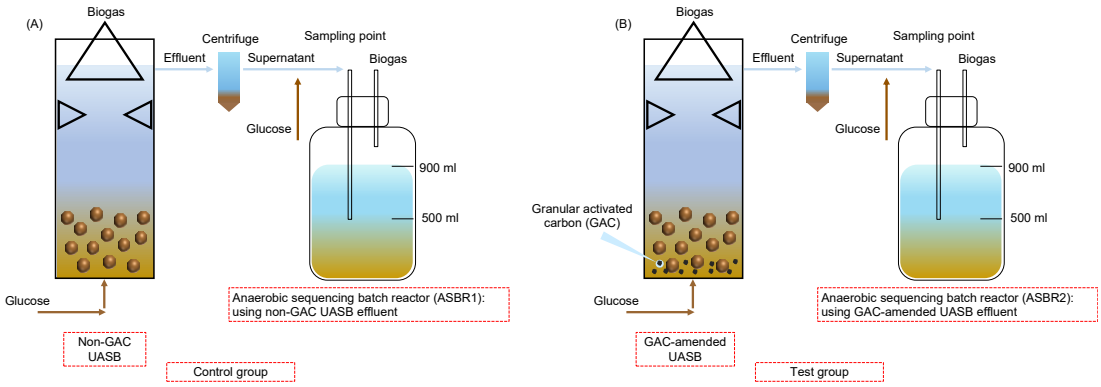

Figure 4.1 Experimental flowchart.

4.2.2. Microbial kinetics in ASBR sludge

Microbial kinetics in the ASBRs were determined: 5 mL of sludge from each ASBR was mixed with 10 mL of deionized water. Glucose was added to obtain 0.1, 0.25, 0.5, 1, 2, and 4 g COD/L. The 15 mL mixture was transferred to a 38 mL serum bottle, and the headspace was flushed with N_2 gas to obtain anaerobic conditions. The bottles were sealed with rubber stoppers and aluminum caps and placed on a shaker (120 rpm) at 20.0 ± 0.5 °C in the dark. The biogas composition in the bottles was determined with a gas chromatograph (GC-7890B, Agilent Technologies, Santa Clara, USA) over the same time interval. The methane production rate was determined and fitted using the Monod equation (Gonzalez-Estrella et al., 2017), as defined in Equation 4.1:

$$m = M_{max}\frac{S}{S+K_S} \qquad \text{(Equation 4.1)}$$

where M_{max} is the maximum methane production rate achieved, in units of mg CH_4-COD/g VSS/d, S is the substrate concentration in units of g COD/L, and K_s is the half-saturation constant in units of g COD/L. Kinetic parameters were calculated using nonlinear

regression using Origin® (OriginLab Corporation; Northampton, MA).

4.2.3. Analytical methods

Chemical oxygen demand (COD), total suspended solids (TSS), and volatile suspended solids (VSS) were determined based on protocols from Standard Methods of the American Public Health Association (APHA, 2012). The pH was measured with a benchtop meter (VWR, USA). The biogas produced by the reactors was collected in a 1 L foil gas bag (CHROMSPEC™, Brockville, Canada). Gas volumes were sampled with a 140 mL syringe. The biogas composition was determined using a gas chromatograph (GC-7890B, Agilent Technologies, USA) equipped with Molsieve 5A 2.44 m 2 mm and Hayesep N 1.83 m 2 mm columns. The operational temperatures of the oven and the detector were 100 °C and 200 °C, respectively.

Soluble microbial products were characterized with an excitation-emission matrix (EEM) fluorescence spectrophotometer (Varian Cary Eclipse, Agilent, Australia); ultrapure water was used as the blank. The samples were filtered with 0.45-µm membranes and diluted with ultrapure water to reduce inner filtering effects (Baghoth et al., 2011). Fluorescence regional integration (FRI) was used to quantify EEM fluorescence (Chen et al., 2003; Zhou et al., 2022).

The amino acids in the effluents of UASBs were measured through a high-performance liquid chromatography equipped with Supelcosil LC-18 150mm x 4.6mm, 3µm column and fluorescence detector (HPLC 1200, Agilent Technologies, USA). 0.1 M sodium acetate buffer and methanol were used as solvents. Vitamins B in the effluents of UASBs were measured through HPLC equipped with a C18 column, 150*4.6mm, 3 µm.

0.05 M KH_2PO_4 and ACN/H_2O (ratio 80:20) were used as solvents.

4.2.4. Microbial community analysis

Inoculum sludge and sludge samples from the ASBRs were collected at the end of stages I and II. DNA extraction was performed using DNeasy PowerSoil Kit (QIAGEN, Hilden, Germany) following the manufacturer's protocol. The concentration and purity of the extracted DNA were checked by NanoDrop One (ThermoFisher, Waltham, MA). The universal primer pair 515F and 806R were used to amplify 16S rRNA genes. Sequencing was performed on the Illumina Miseq platform in Génome Québec (Montréal, Canada). Qiime2 DADA pipeline and the Silva 138 database were used to analyze raw data (Bolyen et al., 2019; Callahan et al., 2016; Yilmaz et al., 2014). R version 4.0.3 was used for data analysis.

4.2.5. Statistical analysis

A paired student's t-test was used to determine the level of significance between means of reactor performance. A p-value of less than 0.05 was considered to be a significant difference.

4.3. Results and discussion

4.3.1. UASB performance

UASB performance is shown in Table 4.2. The average effluent COD in the non-GAC UASB was 828 ± 86 mg/L, much higher than the average effluent COD in the GAC-amended UASB (183 ± 39 mg/L). The average COD removal efficiency (68 ± 5%) in the

non-GAC UASB was lower than the average COD removal efficiency (92 ± 1%) in the GAC-amended UASB. Methane production was 3.1 ± 0.4 g CH_4-COD/d in the non-GAC UASB and 4.6 ± 0.6 g CH_4-COD/d in the GAC-amended UASB. The methane yield was 81 ± 10% of the influent COD in the GAC-amended UASB, and 55 ± 7% in the non-GAC UASB. The enhancement in methane production with GAC addition in UASB was consistent with the results in previous studies (Yu et al., 2020; Zhang et al., 2020b).

Table 4.2 UASB performance

	Effluent COD (mg/L)	COD removal efficiency (%)	Methane production (g COD/d)	Methane yield (%)
Non-GAC UASB	828 ± 86	68 ± 5	3.1 ± 0.4	55 ± 7
GAC-amended UASB	183 ± 39	92 ± 1	4.6 ± 0.6	81 ± 10

4.3.2. Soluble microbial products (SMP) in UASB effluents

3D-EEM fluorescence spectra were used to characterize organic substances in UASB effluents. The two effluents had similar compositions, but the spectral intensities of the GAC-amended UASB effluent were higher than the spectral intensities of the non-GAC UASB effluent (Figure 4.2 A and B). Normalized excitation-emission-area volumes (Φ_i) indicate that effluent from the GAC-amended UASB increased the volumes in all five regions by 25%, 16%, 16%, 44%, and 22%, respectively, compared to effluent from the non-GAC UASB (Figure 4.2C). The percent fluorescence responses in the five specific fluorescence regions were similar for both effluents (Figure 4.2D).

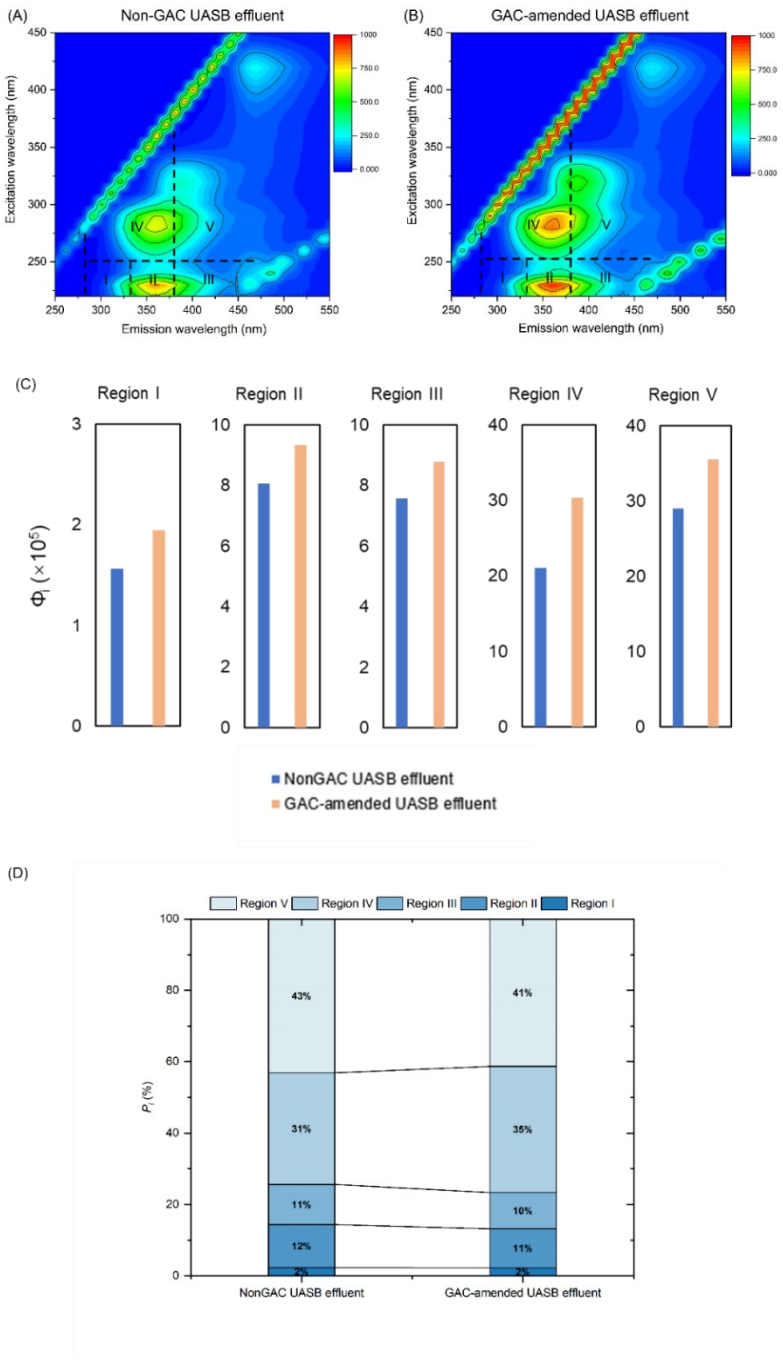

Figure 4.2 (A) EEM fluorescence spectra of non-GAC UASB effluent, (B) EEM fluorescence spectra of GAC-amended UASB effluent, (C) normalized excitation-emission area volumes ($\Phi_{i,n}$) of the five fluorescence regions in the fluorescence spectrum, and (D) FRI distribution in the non-GAC UASB effluent and the GAC-amended UASB effluent.

The five regions represent tyrosine-like substances (region I), tryptophan-like substances (region II), fulvic acid-like substances (region III), soluble microbial by-products and aromatic protein-like substances (region IV), and humic acid-like substances (region V) (Chen et al., 2003; Yin et al., 2018). Tyrosine and tryptophan would participate in multiple biochemical reactions in AD and play an important role in electron transport (Tan et al., 2016). Humic and fulvic substances were correlated with electron-accepting and electron-donating capacities. These substances could enhance methane production at a suitable concentration (Huang et al., 2021). Previous studies have reported that the addition of CMs to AD changed the synthesized bioproducts that were produced (Xu et al., 2020b; Yang et al., 2020; Yin et al., 2018). For instance, Yin et al. (2018) found that Fe_3O_4 promoted the production of extracellular polymeric substances (EPS) and increased the concentrations of humic-like substances and flavins in EPS and soluble microbial products (SMPs). When Yang et al. (2020) put GAC-MnO_2 nanocomposites into an anaerobic system, EPS and humic-like substances were stimulated. Xu et al. (2020b) found that Fe_2O_3 modified on conductive carbon cloth induced microorganisms to secret electron shuttle components of EPS. This enlarged the electronic exchange capacity of EPS and benefited the DIET mode of methane production in CM-amended reactors. In this study, all the regions were enhanced with GAC addition, indicating that GAC stimulated secretions (Figure 4.2). Different experiment conditions in these studies could be the reason for the different changes in secretions in the CMs-amended reactors.

Table 4.3 shows the concentrations of 15 amino acids and five vitamins in effluents of UASBs. In total, eight amino acid and vitamin concentrations (e.g., tryptophan and B2) were significantly higher in the GAC-amended UASB effluent than those in the non-GAC

UASB effluent. The high concentration of tryptophan in the GAC-amended UASB effluent was consistent with results from 3D-EEM, in which the intensity of region II was high in the GAC-amended UASB effluent. Tryptophan has been reported to promote electron transport in *Geobacter* (Tan et al., 2016). The concentrations of three detected vitamins in the GAC-amended UASB effluent were higher than those in the non-GAC UASB effluent. Similarly, Song et al. (2019) determined riboflavin (vitamin B2) concentration in a batch anaerobic system and found that GAC addition could increase the concentration of vitamin B2 by 31%. These results indicate that GAC stimulated the biosynthesis of certain amino acids and vitamins.

Table 4.3 Amino acids and vitamins in effluents of UASBs

μmol/L	Non-GAC UASB effluent	GAC-amended UASB effluent	*p*
Aspartate	4.4 ± 0.6	8.3 ± 0.5	<0.05
Glutamate	18.5 ± 1.4	29.2 ± 0.9	<0.05
Alanine	2.8 ± 0.1	3.6 ± 0.1	<0.05
Tryptophan	1.9 ± 0.1	2.5 ± 0.0	<0.05
Lysine	28.7 ± 1.2	34.3 ± 0.7	<0.05
Vitamin B2	0.4 ± 0.0	0.8 ± 0.1	<0.05
Vitamin B3	2.1 ± 0.1	3.0 ± 0.1	<0.05
Vitamin B9	0.2 ± 0.1	0.7 ± 0.1	<0.05
Serine	0.7 ± 0.4	0.9 ± 0.4	>0.05
Glycine	6.5 ± 0.7	7.2 ± 0.5	>0.05
Tyrosine	0.5 ± 0.1	0.7 ± 0.2	>0.05
Methionine/Valine	0.2 ± 0.0	0.2 ± 0.0	>0.05
Phenylalanine	0.1 ± 0.0	0.3 ± 0.1	>0.05
Isoleucine	0.1 ± 0.0	0.1 ± 0.0	>0.05
Leucine	0.3 ± 0.0	0.4 ± 0.0	>0.05
Histidine	Not detected	Not detected	
Threonine	Not detected	Not detected	
Arginine	Not detected	Not detected	
Vitamin B1	Not detected	Not detected	
Vitamin B5	Not detected	Not detected	

4.3.3. ASBR performance

Figure 4.3 shows that in stage I, the COD effluent fluctuated between 430 and 725 mg/L in ASBR1 (fed with non-GAC UASB effluent) and between 260 and 637 mg/L in ASBR2 (fed with GAC UASB effluent). In stage I, the average COD in ASBR1 was 546 ± 90 mg/L and the average COD in ASBR2 was 365 ± 93 mg/L. The difference was significant ($p < 0.01$). The average removal efficiency of COD in stage I was 74 ± 4% in ASBR1 and 82 ± 4% in ASBR2. In stage II, the difference in effluent COD between the two reactors increased. At the steady state, the average effluent COD in ASBR1 was 2023 ± 74 mg/L, whereas the average effluent COD was 1531 ± 80 mg/L in ASBR2 ($p < 0.001$). The COD removal efficiency decreased to 48 ± 3% in ASBR1. In ASBR2, the COD removal efficiency was 60 ± 1%.

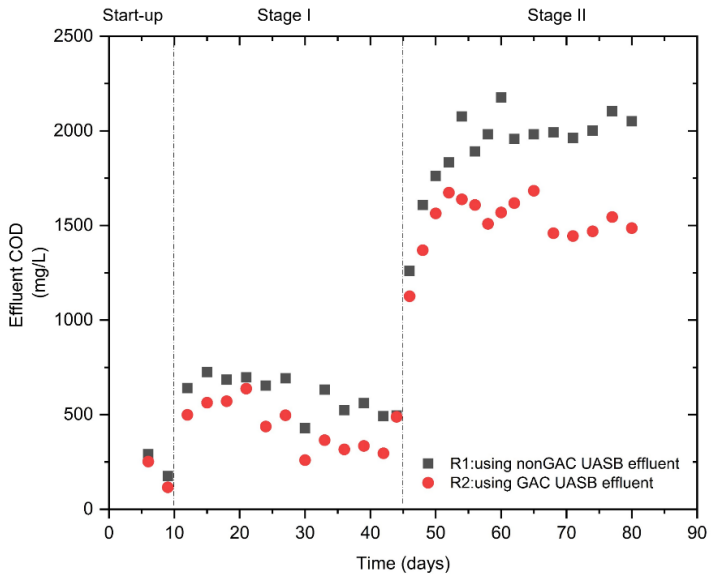

Figure 4.3 Temporal changes in effluent COD in the ASBR1 and ASBR2 during the treatment.

Methane production (gas phase) is shown in Figure 4.4. In stage I, the methane production increased during reactor operation in ASBR1 and ASBR2. At the steady state, the average methane production was 48 ± 7% of total COD input in ASBR1 and 53 ± 6% of total COD input in ASBR2. The difference was significant ($p < 0.05$). In stage II, the methane production decreased to 31 ± 3% in ASBR1 and to 47 ± 5% in ASBR2. The dissolved methane in the reactors accounted for 4%-18% of the total COD input during reactor operation in both reactors. The dissolved methane in ASBR2 was slightly higher (~ 1% of the total COD input) than the dissolved methane in ASBR1.

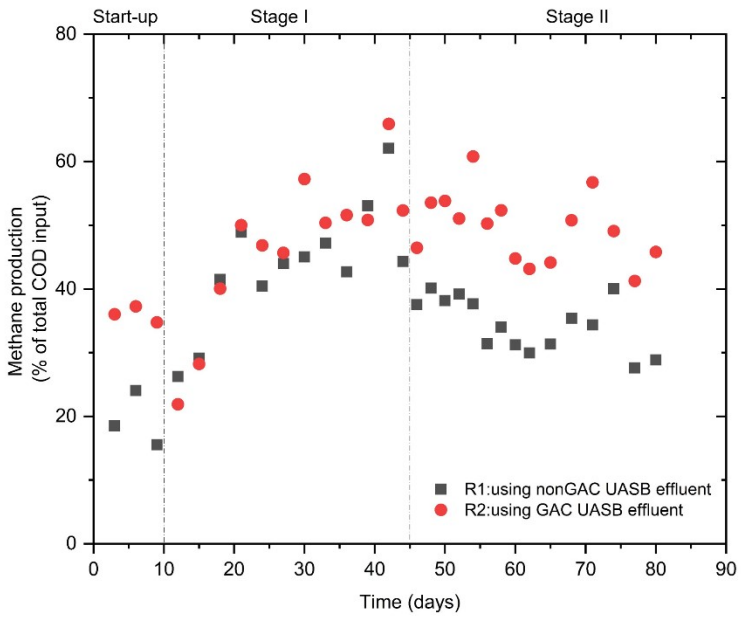

Figure 4.4 Methane production (gas phase) in ASBR1 and ASBR2 during the treatment.

The enhanced COD removal and methane production observed in ASBR2 (fed with GAC-amended UASB effluent) indicated that the microbial secretions in the GAC-amended UASB effluent may have activated anaerobic sludge in ASBR. Note that UASB

effluents were centrifuged to remove suspended solids/cells/GACs before feeding into ASBR reactors.

4.3.4. Microbial kinetics of sludge in ASBRs

Figure 4.5 shows the kinetic parameters of sludge in the ASBRs. The maximum methane production rate of the ASBR1 sludge was 72.5 ± 1.5 mg CH_4-COD/g VSS/d. The maximum methane production rate of the ASBR2 sludge was 105.6 ± 1.2 mg CH_4-COD/g VSS/d. The half-saturation constants (K_s) of ASBR1 and ASBR2 sludge were 0.035 ± 0.007 and 0.013 ± 0.003 g COD/L, respectively. The K_s values observed were similar to K_s values in previous studies of psychrophilic anaerobic digestion (King et al., 2012; Zhang, 2016). The different kinetic parameters reflected ASBR microbial growth kinetics were significantly impacted by the different ASBR feeding from UASB reactors with and without GAC amendment.

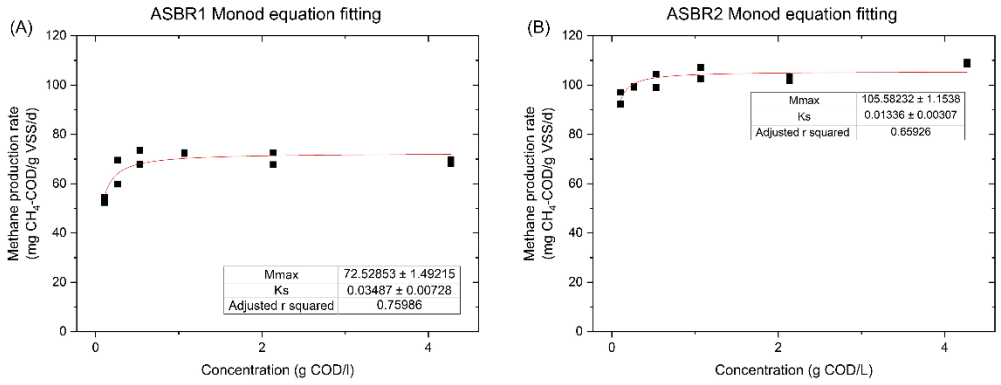

Figure 4.5 Kinetic parameters of (A) sludge from ASBR1, (B) sludge from ASBR2.

4.3.5. Microbial community analysis in ASBRs

4.3.5.1. Microbial community diversity

Bray-Curtis dissimilarities between different samples collected from ASBRs were analyzed (BC index, Figure 4.6). During ASBR reactor operation, archaeal communities in both ASBR1 and ASBR2 (Figure 4.6A) changed slightly from the archaeal communities in the inoculum. At the end of stage II, both ASBRs had archaeal communities similar to the archaeal communities in the inoculum (BC index ~ 0.3). The BC index between the two ASBRs was 0.12 in stage I and decreased to 0.08 in stage II. These results indicated that the archaeal communities in the two ASBRs were similar. Bray-Curtis dissimilarities in the bacterial communities are shown in Figure 4.6B. During reactor operation, bacterial communities changed significantly from the bacterial communities in the inoculum. At the end of stage II, the BC index increased to ~ 0.6 between the bacterial communities in the ASBRs and the bacterial communities in the inoculum. Similar to the archaeal community, the bacterial communities in the two ASBRs were similar (BC index 0.07 in stage I and 0.11 in stage II). Although the bacterial communities in both ASBRs shifted from the inoculum, the two ASBRs had similar microbial changes. These results indicate that the difference in the ASBR feeding originated from different UASB reactor effluents did not significantly impact the dominant microbial communities in ASBRs.

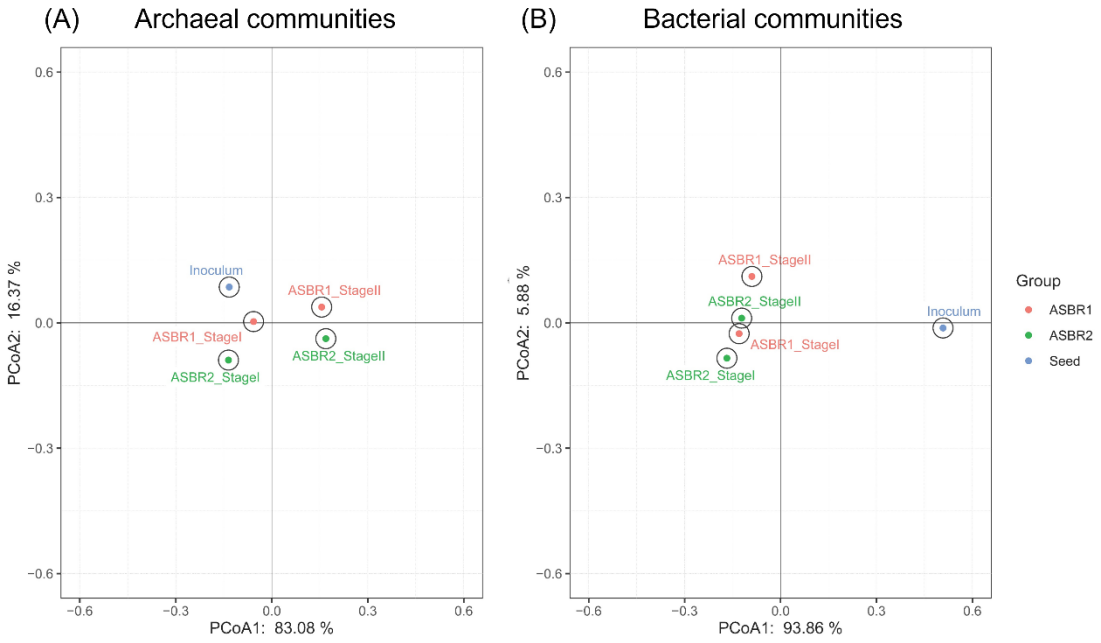

Figure 4.6 Bray-Curtis dissimilarity: (A) archaeal communities, (B) bacterial communities.

4.3.5.2. Archaeal communities

Figure 4.7 shows the archaeal communities at the genus level in the inoculum and in ASBR1 and ASBR2. *Methanosaeta*, an acetoclastic methanogen (Patel, 2015), dominated the inoculum, ASBR1 and ASBR2 in stage I, with relative abundances of 51%, 50%, and 54%, respectively. In stage II, the relative abundances of *Methanosaeta* decreased to 33% in ASBR1 and 29% in ASBR2. *Methanobacterium*, a hydrogenotrophic methanogen (Boone, 2015), was the second most dominant genus (31%) in the inoculum and in the two reactors (34% in ASBR1 and 25% in ASBR2) in stage I. The relative abundance of *Methanobacterium* increased, and it became the dominant genus in stage II (47% in ASBR1 and 46% in ASBR2). *Methanobacterium* enrichment suggested that the hydrogenotrophic pathway was dominant in the two reactors at high COD loading conditions. In stage II, *Methanosphaerula* was the third dominant genus, with relative

abundances of 10% and 15% in ASBR1 and ASBR2, respectively. Dominant archaea were similar in the two reactors, and slightly different in relative abundances.

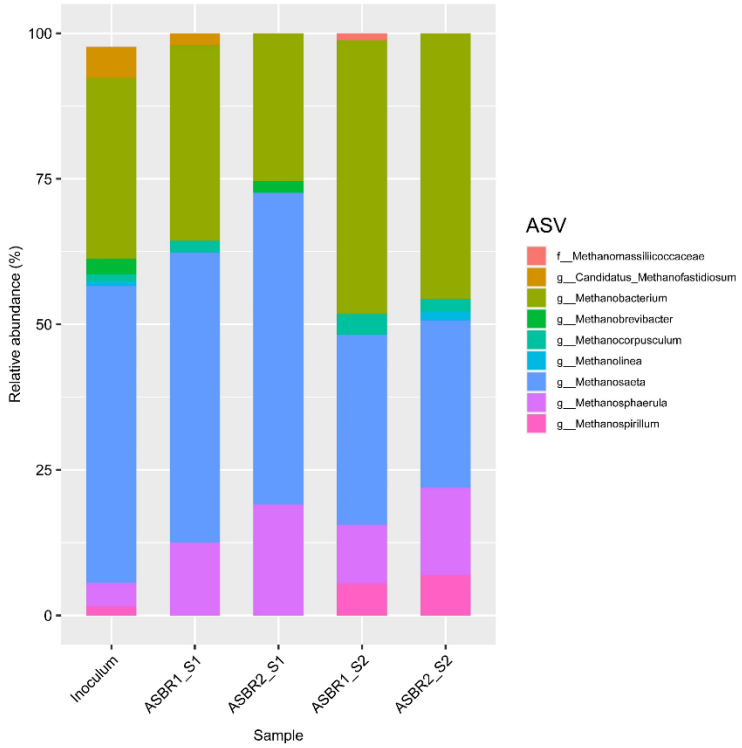

Figure 4.7 Archaeal genera in the inoculum, ASBR1, and ASBR2 in stages I and II. Taxonomic names are shown for genus level (g__) or higher level (family: f__) if not identified at the genus level. A relative abundance of > 1% in any samples is shown in this figure.

4.3.5.3. Bacterial communities

The most abundant (> 2% in any samples) bacterial genera are shown in Figure 4.8. *Trichococcus*, *Clostridium_sensu_stricto_6*, and *Anaeromusa-Anaeroarcus* were the three most dominant genera in the inoculum, with relative abundances of 27%, 15%, and 5%, respectively. During reactor operation, *Trichococcus* became the dominant genus in

ASBR1 and ASBR2 in stage I, with a relative abundance of 87% in ASBR1 and 95% in ASBR2. In stage II, the relative abundance of *Trichococcus* decreased to 74% in ASBR1 and to 84% in ASBR2. *f_Eubacteriaceae* became the second dominant genus with relative abundances of 18% in ASBR1 and 10% in ASBR2 in stage II. *Trichococcus* converts glucose to lactate, formate, acetate, and ethanol (Vos et al., 2011) and played a leading role in glucose fermentation in the two ASBRs.

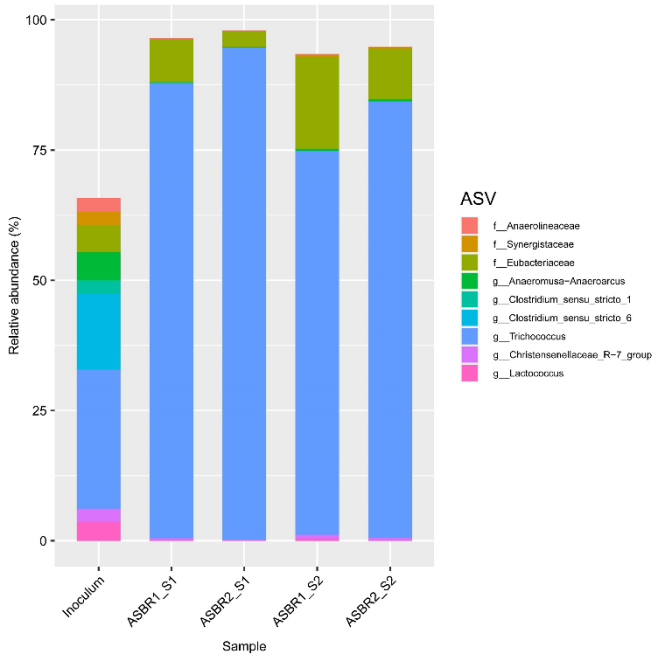

Figure 4.8 Bacterial genera in the inoculum, ASBR1 and ASBR2 in stages I and II. Taxonomic names refer to genus level (g__) or higher level (family: f__) if not identified at the genus level. A relative abundance of > 2% in any samples is shown in this figure.

4.3.6. Proposed mechanism of anaerobic digestion in the GAC-amended UASB

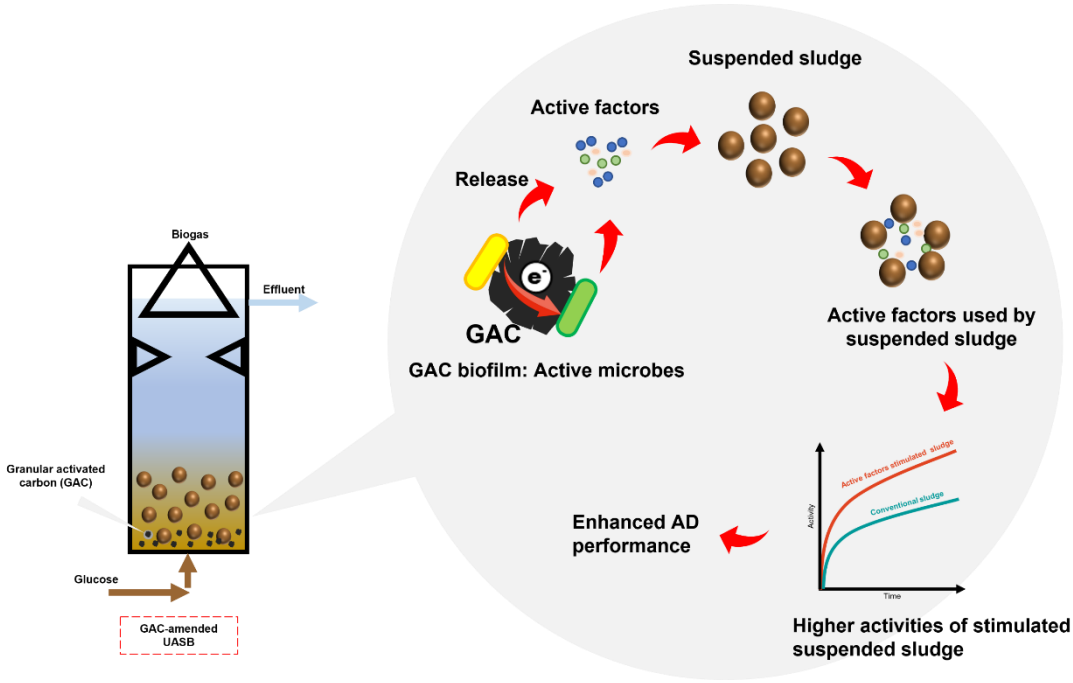

Figure 4.9 Proposed mechanism of anaerobic digestion in the GAC-amended UASB.

DIET, functional groups participating in redox reactions, and exerting protein functions to enhance acetate cleave are the main mechanisms for CMs to improve AD in the previous studies, all requiring direct contact of CMs and AD microorganisms (Shen et al., 2021; Xiao et al., 2020; Zhang et al., 2022b). In this study, indirect contact with GAC could stimulate anaerobic sludge, indicating a mechanism that does not rely on the direct contact of CMs. The results of amino acids, vitamins, and 3D-EEM in UASB effluents demonstrated that GAC addition stimulated extracellular "public goods" (e.g., amino acids, vitamins, and electron shuttles) in anaerobic digestion. Considering that biosynthesis is an energy-consuming process, GAC addition might have enhanced energy production, resulting in more biosynthesis of public goods in microbial communities.

More importantly, auxotrophy (inability of an organism to synthesize a particular organic compound required for its growth) is widespread in anaerobic consortia, and exchanging extracellular public goods is essential (Hubalek et al., 2017; Yao et al., 2021). For instance, methanogens (e.g., *Methanosaeta* and *Methanobacterium*) do not contain a complete gene set for the synthesis of several energy-costly amino acids (e.g., tyrosine and tryptophan) and vitamins, indicating that methanogens rely on the exchange of public goods (Hubalek et al., 2017; Yao et al., 2021). The enhanced production of extracellular public goods in the GAC-amended UASB could have further enhanced the activities of anaerobic sludge, as observed in the present study that GAC-amended UASB effluent stimulated anaerobic sludge and improved its growth kinetics and microbial activities in the downstream ASBR2. These results underline the importance of the soluble compounds in GAC-amended UASB effluents in influencing ASBR performance in terms of COD reduction and methane production. Further, microbial communities in ASBR1 and ASBR2 were similar (BC index < 0.1), but their activities were significantly different. Zhang et al. (2020b) described that physiological changes in a GAC-amended UASB led to high microbial activity in suspended sludge. All these results indicate that, rather than changing the microbes in the microbial community, the presence of GAC can actively promote microbial activity indirectly.

As shown in Figure 4.9, we propose a new mechanism for the anaerobic digestion of organic substances amended with CMs. The sludge attached to CMs could secret more active factors. Suspended sludge could uptake these active factors and be stimulated, thus enhance AD performance. This mechanism is supported by the finding that the suspended sludge in the reactors containing CMs had a higher specific methanogenic activity than the

suspended sludge in the reactors that lacked CMs. Such findings have been reported in previous studies (Zhang et al., 2020a; Zhang et al., 2021b). This study increased our knowledge of the extracellular microbial bioproducts produced in anaerobic reactors amended with conductive materials to enhance performance.

4.4. Conclusion

This chapter determined extracellular microbial secretions in the effluents of UASBs with/without GAC addition and explored the effects of microbial secretions on anaerobic sludge. GAC addition stimulated extracellular microbial secretions (i.e., amino acids, vitamins, and electron shuttles), and these secretions enhanced COD removal and methane production in the downstream ASBR. Further, the two ASBRs produced similar microbial communities, but these microbial communities evinced different microbial kinetics. Extracellular microbial secretions from the GAC-amended UASB improved microbial activity, rather than simply changing the microbial community. This study provides further evidence for the functions of conductive materials in anaerobic digestion.

Chapter 5. Granular activated carbon enhanced the resistance to H_2S toxicity in anaerobic digestion[4]

5.1. Introduction

Both sulfate-reducing bacteria (SRB) and methanogens have the capacity for extracellular electron transfer (EET) (Stams et al., 2006; Stams & Plugge, 2009), indicating that they might be affected by conductive materials (CMs) addition. However, the relationships between SRB and methanogens under CMs addition conditions have not been well assessed. Only limited studies have evaluated the effects of adding CMs to AD under sulfate-reducing conditions (Yin et al., 2020b). Li et al. (2017) reported that stainless steel addition might enable active methanogens to outcompete SRB in an up-flow anaerobic sludge blanket (UASB). In a magnetite (Fe_3O_4)-amended anaerobic sequencing batch reactor (ASBR), magnetite enhanced the methanogens by re-enriching their syntrophic partners and thus recovering their syntrophic interactions (Liu et al., 2019). In a magnetite-amended UASB, Jin et al. (2019) found that methanogens and SRB (or iron-reducing bacteria, which also have a capacity to reduce sulfate to sulfide) were stimulated simultaneously. SRB and methanogens can be enriched on the biofilm formed on granular activated carbon (GAC) (Zhang et al., 2021b), but the effects of CMs on sulfate-reducing

[4] A version of this chapter has been published: Zhang, Y., Zhang, L., Yu, N., Guo, B. and Liu, Y. (2022). Enhancing the resistance to H_2S toxicity during anaerobic digestion of low-strength wastewater through granular activated carbon (GAC) addition. *Journal of Hazardous Materials*, 430, 128473. https://doi.org/10.1016/j.jhazmat.2022.128473

conditions and the interactions between SRB, methanogens, and syntrophic bacteria remain unclear.

This chapter evaluates the effects of GAC addition to an anaerobic reactor treating low-strength wastewater under sulfate-reducing and ambient (20.0 ± 0.5 °C) conditions. Chemical oxygen demand (COD), sulfate concentrations, methane production, and specific methanogenic activities were determined. The COD balance was analyzed to identify the electron competition between methanogens and SRB. The H_2S toxicity test was performed to verify if the GAC addition can enhance the resistance to H_2S toxicity. The dynamics of microbial communities and their syntrophic relationships with and without the GAC addition are discussed. These findings provide significant insights into microbial communities, especially SRB and methanogens, in a GAC-amended AD process under sulfate-reducing conditions.

5.2. Materials and methods

5.2.1. Reactor setup and operation

Two laboratory-scale plexiglass UASB reactors (4.2 L working volume each) were operated at ambient temperature (20.0 ± 0.5 °C) for 130 days (Figure 5.1). Each UASB was inoculated with 2 L of anaerobic sludge from a local full-scale anaerobic digester treating waste activated sludge. Synthetic wastewater was pumped continuously into the reactors by peristaltic pumps (LongerPump®, BT100-2J, Baoding, China). A 2 L gas bag (CHROMSPEC™, Brockville, Canada) was used to collect the biogas in each reactor. 100 g of GAC (4-12 mesh, Sigma-Aldrich, St. Louis, USA) was added into one of the UASBs,

and it settled at the bottom of the reactor after a few days. Detailed characteristics of the GAC used in this study can be found in Table 3.1. The volume occupied by the GAC was around 6.7% of the total working volume of the reactor. Synthetic wastewater was prepared according to Table 3.2. The carbon source was 1 g COD/L glucose. The hydraulic retention time (HRT) was fixed at around 1.5 days. The operation can be divided into four stages (I-IV) with varying COD/SO_4^{2-} ratios, which were 0 (stage I), 10 (stage II), 6.7 (stage III), and 5 (stage IV). The corresponding sulfate concentrations were 0, 100, 150, and 200 mg Na_2SO_4/L-SO_4^{2-} in stages I-IV, respectively. Reactor start-up phase lasted for 40 days, with unstable effluent COD concentration and methane production. Performance of the start-up phase is shown in Table 5.1.

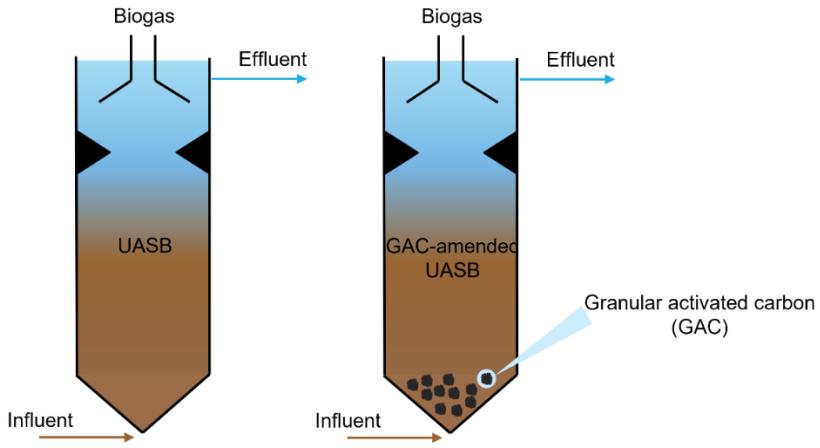

Figure 5.1 The schematic layout of the UASB system with or without GAC particles.

Table 5.1 The performance of the two reactors in the start-up phase

	Effluent COD (mg/L)	Methane production (gas, mg COD/d)
Non-GAC reactor	353±25	1107±267
GAC-amended reactor	327±16	1215±249

5.2.2. Specific methanogenic activity

Quantification of the specific biological activity of key microbial groups (e.g., methanogens) in AD is essential to monitor both the routine operation of AD and the development of microorganisms (Colleran et al., 1992). In this study, specific methanogenic activity (SMA) tests were performed at the end of each stage using the suspended sludge from the UASBs to evaluate the capability of sludge to convert substrate into methane. Hydrogen and sodium acetate were utilized in separate batch experiments as the substrate to test hydrogenotrophic and acetoclastic pathways, respectively. The test was performed in duplicate and followed the method described in Chapter 3. All tests were performed in a 38 mL serum glass bottle with 5 mL sludge and 10 mL demineralized water or 10 ml acetate (1 g COD/L), respectively.

5.2.3. H_2S toxicity test

Toxicity assays were performed to determine the resistance of the suspended sludge to H_2S. Suspended sludge samples (5 mL) from the two reactors at the end of stage IV were used as the seed sludge in this test. The sludge samples were added to glass serum bottles (38 mL) and 10 mL of glucose solution (1 g COD/L) was used as the substrate. The test was performed in four groups with sulfide (1 g S^{2-}/L of $Na_2S•9H_2O$) or without sulfide, and with fresh GAC (5 g/L) or with no GAC (Table 5.2). Nitrogen gas was used to flush the headspaces of the bottles and achieve anaerobic conditions. The glass bottles were sealed with rubber stoppers and aluminum caps, and then the samples were shaken at 120 rpm at ambient temperature (20.0 ± 0.5 °C) for 11 days. Biogas was collected through syringes and analyzed by a gas chromatograph (GC-7890B, Agilent Technologies, Santa Clara,

USA). All studies were performed in duplicate. The modified Gompertz model, which is used to describe the microorganism growth, was applied in this test (Zwietering et al., 1990). Biogas production kinetic was modeled and the maximum rate of methane production was analyzed and compared between the sludge from the two reactors.

$$M = P \times exp\left\{-exp\left[\frac{R_m \times e}{P}(\lambda - t) + 1\right]\right\} \qquad \text{(Equation 5.1)}$$

where P is the methane production potential; R_m is the maximum rate of methane production; and λ is duration of the lag phase.

Table 5.2 H_2S toxicity test design

	Sludge (5mL)	Glucose (1 g/L, 10 ml)	$Na_2S \cdot 9H_2O$ (1 g S^{2-}/L)	Fresh GAC (5 g/L)
Group I	+	+	-	-
Group II	+	+	-	+
Group III	+	+	+	-
Group IV	+	+	+	+

Note: '+' represents addition and '-' represents no addition

5.2.4. Analytical methods

The properties of influent and effluent samples were analyzed every two or three days. COD, total suspended solids (TSS), and volatile suspended solids (VSS) were determined according to the Standard Methods of the American Public Health Association (APHA, 2012). A sympHony pH probe (VWR, Radnor, USA) was used to measure pH. The sulfate concentration was measured with sulfate reagent powder pillows (2-70 mg/L SO_4^{2-}, Hach Method 8051, Loveland, USA). The biogas level was determined with a gas chromatograph

(7890B Agilent Technologies, Santa Clara, USA) equipped with Molsieve 5A 2.44 m 2 mm and Hayesep N 1.83 m 2 mm columns. The oven and detector temperatures were 100 ºC and 200 ºC, respectively.

The dissolved methane concentration in the reactor effluent was determined once per week according to the method described by Zhang et al. (2020a). The measurement was conducted in a 38 ml sealed glass serum bottle containing 7 g NaCl. 20 mL of UASB effluent was slowly injected into the bottle with a syringe. The bottle was shaken to mix the UASB effluent and the NaCl, and then the solution was allowed to settle for half an hour. The final gas pressure in the bottle was measured, and the methane content in the headspace was determined by the gas chromatograph. The measurements were performed in duplicate.

5.2.5. DNA extraction, sequencing, and analysis

Microbial community analyses were performed to investigate microbial community structures. Suspended sludge samples (2 mL) were collected from each UASB reactor at the end of stages I, II, and IV; two samples of GAC-biofilm were collected at the end of stage IV. DNA extraction was performed with a DNeasy PowerSoil Kit (QIAGEN, Hilden, Germany), following the manufacturer's protocol. The purity and concentration of the extracted DNA were checked with NanoDrop One (ThermoFisher, Waltham, MA). The DNA sequence was amplified by the polymerase chain reaction (PCR) using primer sets with universal sequencing adaptors 515F and 806R, commonly used for wastewater microbiome research (Caporaso et al., 2011). Sequencing was performed on the Illumina Miseq PE250 platform in Génome Québec (Montréal, Canada) and analyzed using the

Qiime2 DADA pipeline with 99% similarity using the Silva 138 database (Bolyen et al., 2019; Callahan et al., 2016; Yilmaz et al., 2014). The Raw sequence data can be accessed from the National Center for Biotechnology Information (NCBI) GenBank (Bio Project Accession number PRJNA793598. R version 4.0.3 was used for data analysis. R packages "vegan," "pheatmap," "ggplot2," and "ggrepel" were used for microbial community analysis and graphical presentation (Kolde & Kolde, 2015; Oksanen et al., 2017; Slowikowski, 2018; Wickham, 2016). The paired student's t-test was used to analyze reactor performance, and a p-value lower than 0.05 represented a significant difference.

5.3. Results and discussion

5.3.1. COD and SO_4^{2-} removal

The temporal changes of COD are shown in Figure 5.2. Influent COD was controlled at 993 ± 34 mg/L during the operation. The average effluent COD in the non-GAC reactor was 234 ± 61 mg/L in stage I, 204 ± 31 mg/L in stage II, 253 ± 81 mg/L in stage III, and 272 ± 28 mg/L in stage IV. The average effluent COD in the GAC-amended reactor was much lower than the average effluent COD in the non-GAC reactor, with concentrations of 72 ± 17 mg/L, 75 ± 22 mg/L, 49 ± 19 mg/L, and 69 ± 16 mg/L in stages I-IV, respectively. Correspondingly, the efficiencies of COD removal differed significantly between the two reactors ($p < 0.001$). The average COD removal efficiencies (> 92%) of the GAC-amended reactor in all stages were much higher compared to the average COD removal efficiencies (72% to 80%) in the non-GAC reactor.

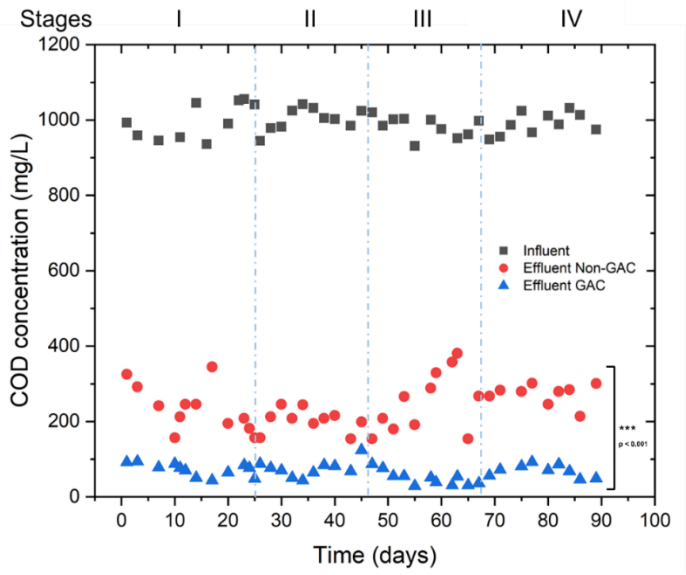

Figure 5.2 Temporal changes of influent and effluent COD concentrations in the non-GAC and the GAC-amended UASBs in the four stages of reactor operation.

The average effluent sulfate concentrations are shown in Figure 5.3. The demineralized water used contained less than 5 mg SO_4^{2-}/L, and therefore was not taken into consideration. In stages II, III, and IV, extra Na_2SO_4 was added to the influent, increasing the sulfate concentrations to 107 ± 6 mg/L, 150 ± 5 mg/L, and 204 ± 8 mg/L, respectively. The average sulfate removal efficiencies were high (> 94%) in both reactors. Although average effluent sulfate concentrations in the non-GAC reactor were slightly higher than those in the GAC-amended reactor, the difference between the two reactors was not statistically significant ($p > 0.05$) in all three stages.

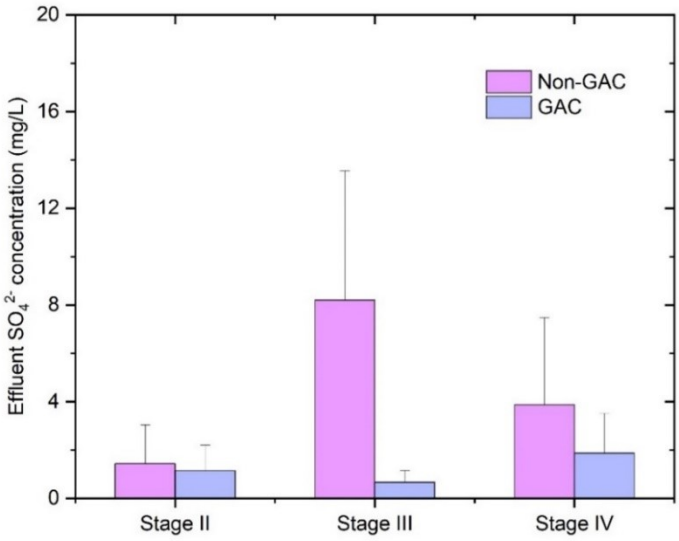

Figure 5.3 The average effluent sulfate concentrations in the non-GAC and the GAC-amended UASB in stages II-IV.

5.3.2. Methane production and specific methanogenic activity

Figure 5.4 shows the daily methane production in gas and liquid phases in the four stages of reactor operation. With the GAC addition, the methane production (gas phase) significantly increased by 33% in stage I and 35% in stage II compared to the non-GAC reactor. With an increase in sulfate concentrations in the influent in stages III and IV, the difference in methane production (gas phase) between the two reactors increased. The methane production (gas phase) in the GAC-amended reactor was 92% higher in stage III and 81% higher in stage IV than the methane production in the non-GAC reactor. The biogas compositions in the two reactors were similar, with average methane contents remaining at ~ 82% during the operation. The observed high methane content in biogas can be attributed to the higher solubility of CO_2 (as compared to CH_4) under low-temperature

conditions (Masse & Masse, 2001).

Figure 5.4B shows the dissolved methane produced in the two reactors. The concentrations of dissolved methane in the non-GAC reactor fluctuated at ~ 75 mg COD/L, equaling 170-200 mg COD/d. In the GAC-amended reactor, the concentrations of dissolved methane fluctuated at ~ 95 mg COD/L, equaling 220-265 mg COD/d. The dissolved methane in the reactors did not decrease significantly with an increase in influent sulfate concentrations because methane dissolves more readily under psychrophilic conditions.

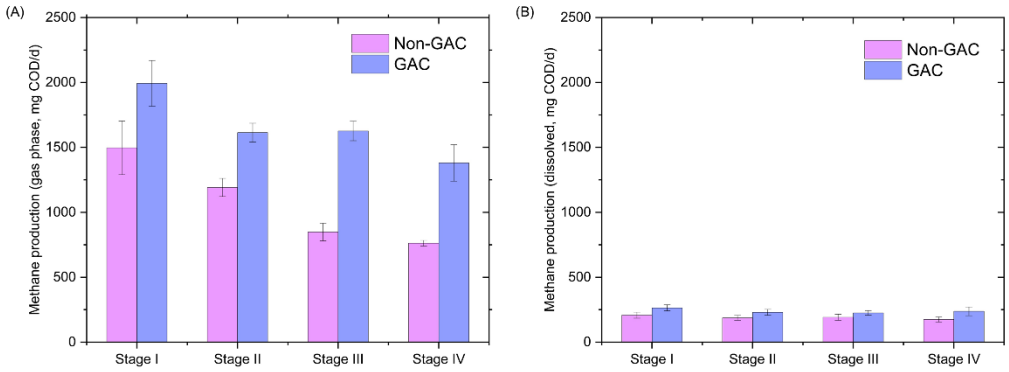

Figure 5.4 (A) Daily methane (gas) production (mg CH_4-COD/d) in the non-GAC and the GAC-amended UASB; (B) Daily methane (dissolved) production (mg CH_4-COD/d) in the non-GAC and the GAC-amended UASB. Error bars represent standard deviations.

As shown in Figure 5.5A, the specific methanogenic activity (SMA) using acetate as the substrate in the two reactors was high in stage I and remained stable in stage II with the sulfate supplement (~ 100 mg CH_4-COD/g VSS/d in the non-GAC reactor and ~ 120 mg CH_4-COD/g VSS/d in the GAC-amended reactor). Hence, an ~ 20% increase in SMA was achieved with the GAC addition. In stages III and IV, the SMA of acetate decreased

in both reactors, but it was still higher in the GAC-amended reactor. The SMA of hydrogen in the two reactors showed a different trend from the SMA of acetate in the two reactors. In the non-GAC reactor, the SMA of hydrogen was stable at about 40 mg CH_4-COD/g VSS/d under various influent sulfate concentrations (stage I – stage IV). In the GAC-amended reactor, the SMA of hydrogen increased during the operation and reached 78 ± 0.6 mg CH_4-COD/g VSS/d in stage IV, a 78% higher SMA of hydrogen compared to the non-GAC reactor in stage IV. These results indicated that hydrogenotrophic methanogens are more robust than acetoclastic methanogens to sulfate stress.

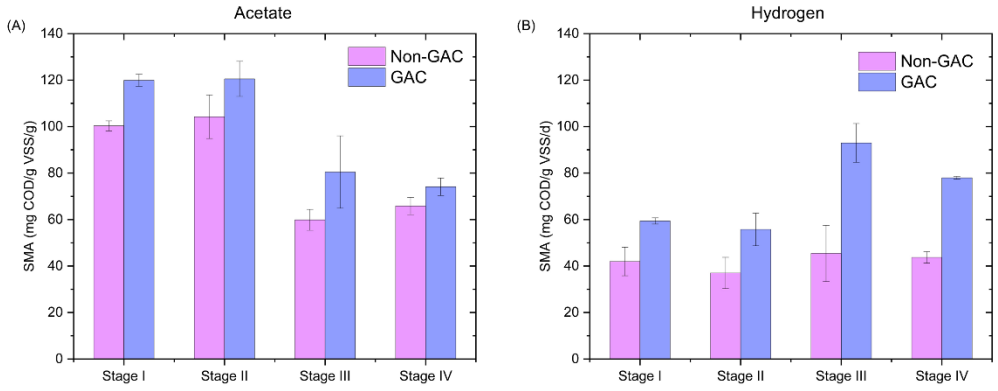

Figure 5.5 (A) SMA of acetate, and (B) SMA of hydrogen in the non-GAC and GAC-amended UASBs in four stages. Error bars represent standard deviations.

5.3.3. Sulfide toxicity test

Table 5.3 shows the maximum methane production rates in the sulfide toxicity test. Without sulfide addition, the maximum CH_4 production rates of sludge from the non-GAC reactor were 55.7 ± 6.7 (sludge without fresh GAC addition) and 61.6 ± 6.8 (sludge with fresh GAC addition) mg CH_4-COD/g VSS/d. As for sludge from the GAC-amended reactor,

these values were 65.7 ± 8.7 and 69.5 ± 7.9 mg CH_4-COD/g VSS/d, respectively. When sulfide was added, the maximum rates of sludge from the non-GAC reactor decreased to 24.3 ± 4.5 mg CH_4-COD/g VSS/d, which was only 43.6% of that without sulfide. However, the maximum rate of the sludge from GAC-amended sludge was 85% of that without sulfide. Fresh GAC addition helped the sludge from the non-GAC reactor resist the toxicity of sulfide and increased the maximum rate by 19%. As for the sludge from the GAC-amended reactor, the effects of fresh GAC addition were not obvious.

Table 5.3 Maximum methane production rate calculated based on the Modified Gompertz model in the sulfide toxicity test

Maximum rate (mg CH_4-COD/gVSS/d)	Without GAC and sulfide	With GAC, without sulfide	Without GAC, with sulfide	With GAC and sulfide
Sludge from the non-GAC reactor	55.7 ± 6.7	61.6 ± 6.8	24.3 ± 4.5	28.8 ± 4.9
Sludge from the GAC-amended reactor	65.7 ± 8.7	69.5 ± 7.9	56.0 ± 2.2	56.8 ± 4.7

5.3.4. COD balance

The chemical oxygen demand (COD) in the two reactors is presented in Figure 5.6. The methane production in the non-GAC reactor was 63 ± 6% of the influent COD in stage I and decreased to 41 ± 1% in stage IV. In the GAC-amended UASB, the methane production was 84 ± 7% of the influent COD in stage I and decreased to 71 ± 6% in stage IV. The sulfate reduction was similar in the two reactors, from around 7% (stage II) to 14% (stage

IV). In total, sulfate reduction and methane production in the non-GAC UASB occupied 63 ± 6% of the total influent COD in stage I and decreased to 55 ± 1% of the total influent COD in stage IV, indicating negative effects of sulfate on reactor performance in the non-GAC reactor. In the GAC-amended UASB, sulfate reduction and methane production occupied 84 ± 7% in stage I and 85 ± 6% of the total influent COD in stage IV. The decrease in methane production (13%) was close to the increase in sulfate reduction (14%), indicating that methanogens did not outcompete SRB in the presence of GAC, and methanogens retained high activities under sulfate-reducing conditions. Effluent COD accounted for 20% to 28% in the non-GAC reactor and 5% to 8% in the GAC-amended reactor. The extracellular substances observed in the non-GAC reactor resulted in a higher COD accumulation compared to the COD accumulation in the GAC-amended reactor. Overall, the differences in methane production between the two reactors were close to the differences in the sum of effluent COD and sludge accumulation.

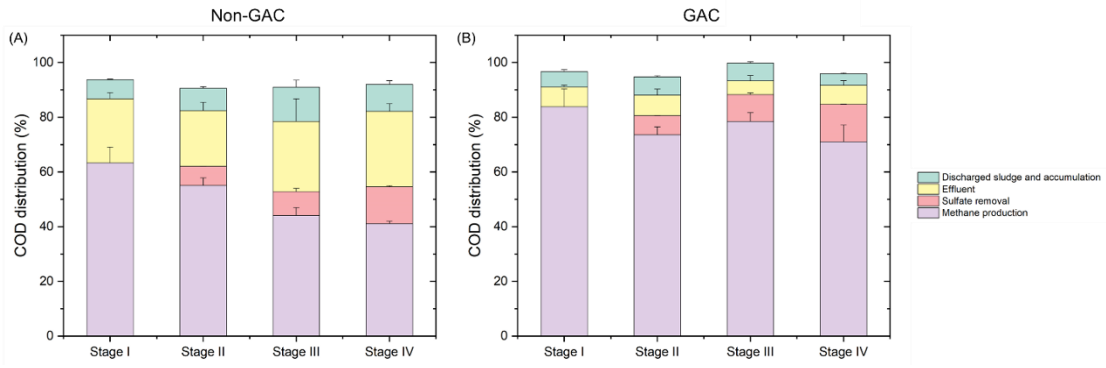

Figure 5.6 COD balance in the non-GAC and the GAC-amended UASB in the four stages of the experiment. Error bars represent standard deviations.

5.3.5. Microbial community analysis

Figure 5.7 shows the principal coordinate analysis (PCoA) results of archaeal communities (A) and bacterial communities (B). In both reactors, the GAC biofilm showed large differences in archaeal and bacterial communities compared to the suspended sludge, indicating the different communities formed on the GAC surface. The archaeal community difference between the reactors decreased during the operation and was not significant ($p > 0.05$) between suspended sludges, indicating the increasing sulfate input led to the increased similarity of archaeal communities in these two reactors (Figure 5.7A). For bacterial communities, the effects of sulfate input were different. At the end of stage IV, there was a large difference between the suspended sludges in the two reactors compared to those in stages I and II.

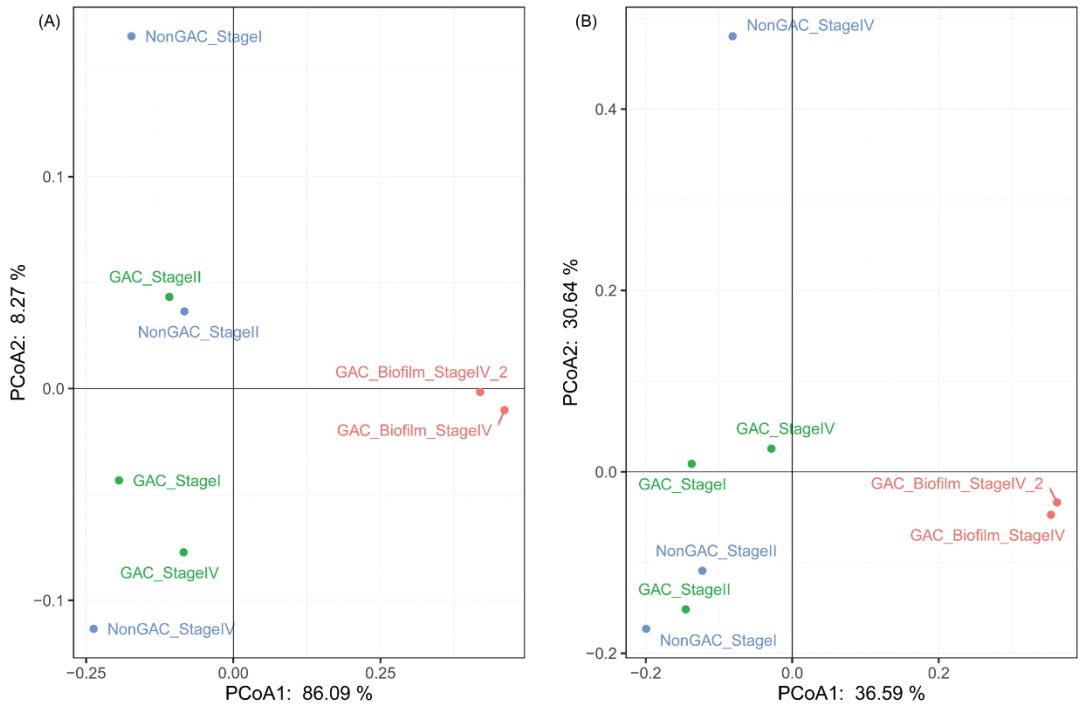

Figure 5.7 Principal Coordinate Analysis (PCoA) of (A) archaea and (B) bacteria.

Figure 5.8 shows the archaeal communities at the genus level in the non-GAC and GAC reactors with a relative abundance > 1% in at least one sample. *Methanosaeta* dominated in both reactors with relative abundances increasing from 33% to 46% in the non-GAC reactor, and fluctuating between 38% and 47% in the GAC-amended reactor. The higher relative abundance of *Methanosaeta* indicated that the acetoclastic pathways played a significant role in both reactors. *Methanobacterium*, which represents hydrogenotrophic methanogens, was the second most dominant genus in the GAC suspended sludge (30%) and the most dominant genus in the GAC-biofilm (> 80%) in stage IV. In the non-GAC suspended sludge, although *Methanobacterium* was also the second most dominant genus in stage IV (14.7%), its relative abundance was significantly lower than that in the GAC reactor and was only slightly higher than the third and fourth most abundant genera in the non-GAC reactor (i.e., *Methanocorpusculum* 11.6% and *Candidatus Methanofastidiosum* 10.7%).

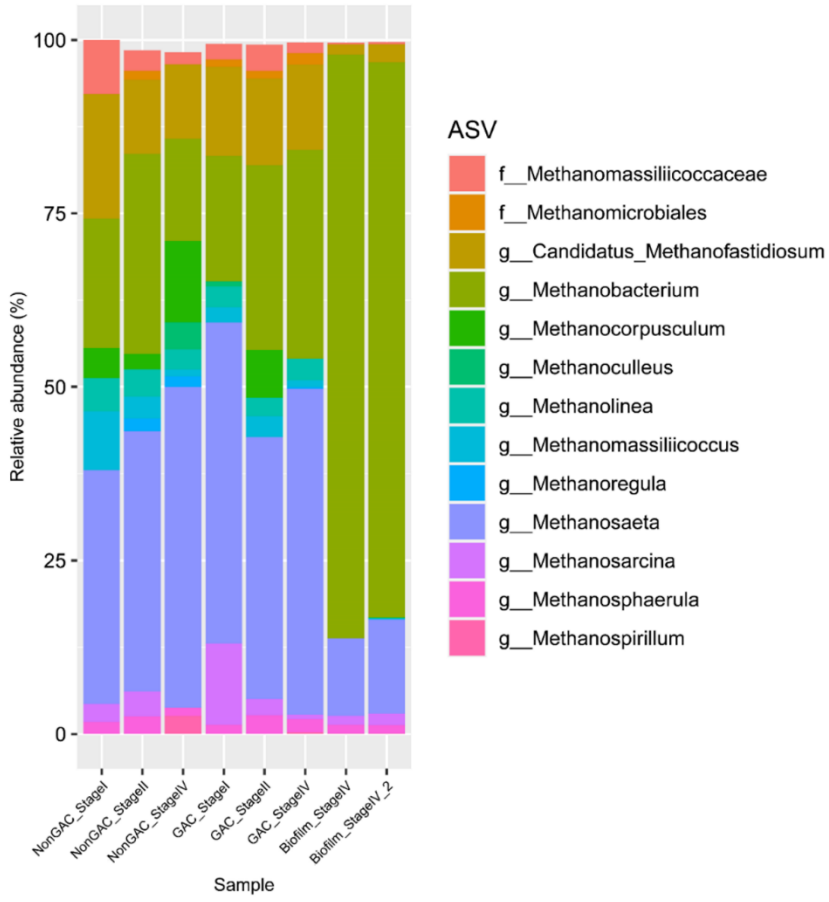

Figure 5.8 Relative abundances of archaeal genera with abundance > 1% in at least one sample in the non-GAC and GAC UASB suspended sludges (stages I, II, and IV) and GAC-biofilm (stage IV). Unidentified genera were named at family (f__).

The most abundant bacterial genera (> 2% in any sample) from each sample were assembled with several unclassified genera (Figure 5.9). Specifically, the relative abundance of *Bacteroidetes_vadinHA17* increased during the operation and became the most abundant genus in the GAC suspended sludge with a relative abundance higher than 30% in stage IV, whereas it decreased during the operation with a relative abundance of only 2.5% in the non-GAC suspended sludge in stage IV. *Trichococcus* fluctuated during the operation and became the second most abundant genus (11% in stage IV) in the GAC

suspended sludge, while it was only 0.8% in the non-GAC suspended sludge in Stage IV. The third most abundant genus in the GAC-amended UASB was *Smithella*, with a stable abundance during the operation (3-3.8%). *Bacteroidetes_vadinHA17* is a facultative bacteria capable of degrading complex carbon organics (Baldwin et al., 2015). *Trichococcus* could produce lactate, formate, acetate, and ethanol from glucose (Vos et al., 2011). *Smithella* is known as a syntrophic propionate oxidizing bacteria (Müller et al., 2010), which was enriched previously in the GAC-amended UASB (Yu et al., 2021). In the non-GAC suspended sludge, the relative abundance of *Lactococcus* and *Tolumonas* increased, and they became the two most abundant genera at the end of the operation, with abundances of 15.8% and 6% in stage IV, respectively. *Lactococcus* are lactic acid bacteria that rapidly ferment sugars and proteins to lactic acid (McAteer et al., 2020), while *Tolumonas* can use glucose to produce acetate, ethanol, and formate (Saia et al., 2016). The different microbial communities enriched in the two reactors may help to explain the different treatment performances of these reactors.

Like the archaeal communities, the GAC-biofilm showed the presence of a different community compared to the suspended sludges in the GAC reactor. *f_Spirochaetaceae*, *Bacteroidetes_vadinHA17*, and *f_Rikenellaceae* were the most abundant genera in the GAC-biofilm in stage IV. *Geobacter*, which is often considered an indicator of direct interspecies electron transfer (DIET) in AD (Rotaru et al., 2014a; Rotaru et al., 2014b), was only enriched in the GAC-biofilm, but not in the suspended sludge in the same reactor and the non-GAC reactor. The enrichment of *Geobacter* in CMs-amended reactors was widely reported (Feng et al., 2021; Florentino et al., 2019a), indicating the possible existence of DIET. In addition, *Desulfobulbus*, a sulfate-reducing bacterium, was also only enriched in

the GAC-biofilm with a relative abundance of ~ 6.7%. Other syntrophic bacteria, such as *Syntrophus*, were not enriched in this study.

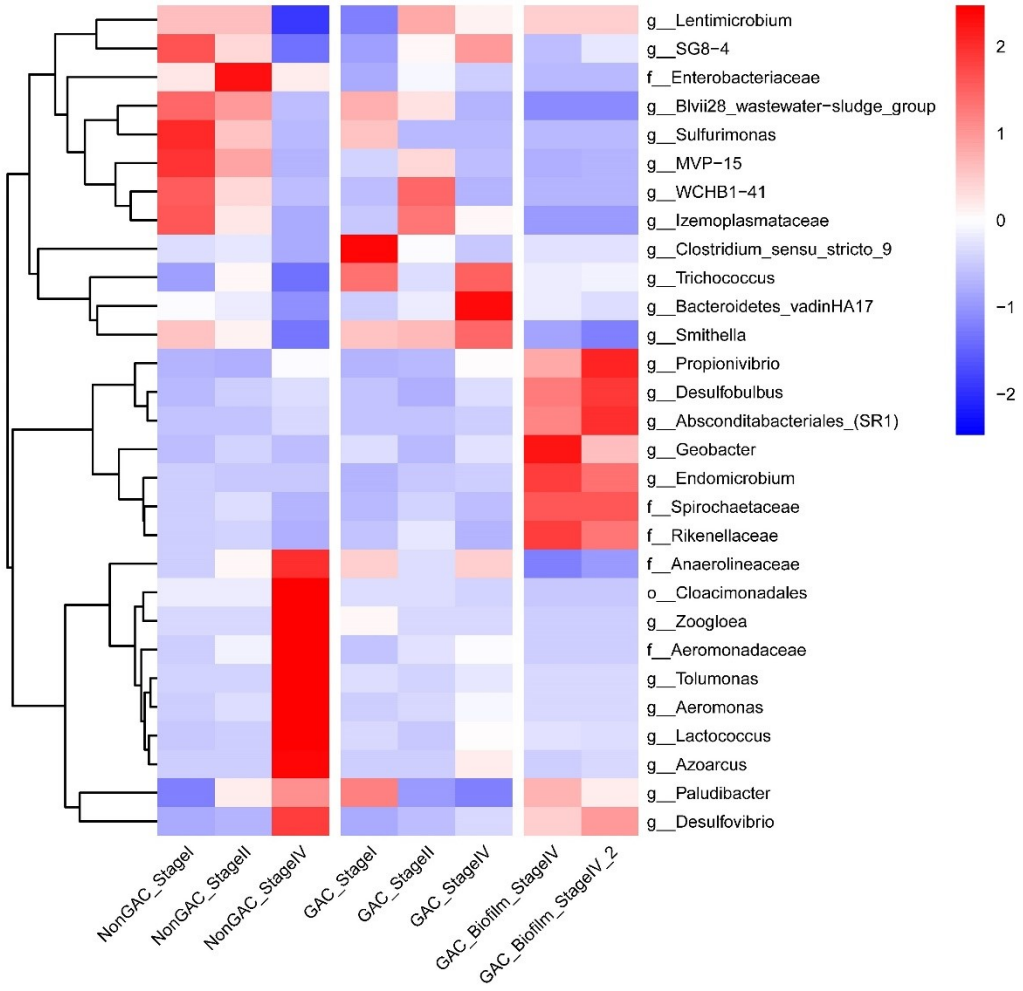

Figure 5.9 Relative abundances of the most abundant bacterial genera with abundance > 2% in at least one sample in the non-GAC and GAC UASB suspended sludge (stages I, II, and IV) and GAC-biofilm (stage IV). Unidentified genera were named at family (f__) or order level (o__).

5.3.6. Discussion

5.3.6.1. The addition of conductive materials increased the presence of methanogens under sulfate-reducing conditions

Table 5.4 Studies that used different conductive materials in continuous anaerobic digestions

Reactor type	Temperature	Conductive materials (CMs)	COD/SO_4^{2-} ratio	COD removal (CMs/non-CMs)	CH_4 production (CMs/non-CMs)	Reference
UASB	20 °C	GAC	10.0 - 5.0	~1.3	~1.7	Present study
UASB	37 °C	Fe_3O_4	5.0 – 2.5	~1.3	~6	(Jin et al., 2019)
UASB	37 °C	Stainless steel	1.2	~1.13	~4.1	(Li et al., 2017)
ASBR	35 °C	Fe_3O_4	6	~1.4	~1.5	(Liu et al., 2019)
Semi-continuous	37 °C	Fe_3O_4	3.4	~1.2	-	(Jin et al., 2021)

A lowering of effluent chemical oxygen demand (COD) and an increase in methane production were achieved with the addition of granular activated carbon (GAC) to anaerobic digestion (AD) of low-strength wastewater under sulfate-reducing conditions. In the presence of GAC, the COD removal increased from 72% to 93%, and the methane production increased from 41% to 71% of the total COD input. These results are consistent with results obtained in previous studies (using the UASB and other reactor types) when sulfate presented in the influent (Jin et al., 2021; Jin et al., 2019; Li et al., 2017; Liu et al., 2019). As shown in Table 5.4, these results indicate that the addition of conductive

materials (CMs) can increase the presence of methanogens when sulfate is present in the reactor influent.

5.3.6.2. GAC addition enhanced AD to resist H_2S toxicity

In this study, the sulfate removed in stage IV correlated to ~70 mg/L H_2S, which is toxic to anaerobic microbes. In the non-GAC reactor, the decrease in methane production (22%) was higher than the COD utilized for sulfate reduction (14%) (Figure 5.6), which can be attributed to the toxic effects of H_2S produced during sulfate reduction. However, in the GAC-amended UASB, the decrease in methane production was close to the COD utilized for sulfate reduction, indicating a reduced toxic effect. In the sulfide toxicity test, 1 g/L S^{2-} added in this experiment was much higher than the reported IC_{50} of H_2S for methanogens (220 mg/L) (Chen et al., 2014). The batch experiments showed that under this condition, the maximum methane production rate of suspended sludge from the GAC-amended UASB (56.0 ± 2.2 mg CH_4-COD/g VSS/d) was significantly higher than that for the suspended sludge from the non-GAC UASB (24.3 ± 4.5 mg CH_4-COD/g VSS/d). These results, together with higher SMA values in the GAC-amended UASB, indicated that the GAC addition enhanced the resistance of methanogens to H_2S. Further, the fresh GAC addition only slightly increased the maximum rates with the sulfide addition, indicating long-term acclimation is required to develop this resistance.

More importantly, the PCoA showed that the bacterial communities in the two reactors were significantly different, which might have influenced the H_2S resistance of the communities. The two enriched bacteria genera in the GAC-amended reactor (*Bacteroidetes_vadinHA17* and *Trichococcus*) have been reported to develop syntrophic

relationships with methanogens. For instance, *Trichococcus* and *Methanosaeta* were enriched together in an AD with the hydrochar addition, and the enriched culture showed 39% higher methane production rates compared to the non-CMs system (Ren et al., 2020). In another study, the authors revealed that activated carbon stimulated the growth of *Trichococcus* and *Bacteroidetes_vadinHA17* in the batch tests (Wang et al., 2021b). The enhanced syntrophic relationship with GAC addition might be the reason for the higher activities and performance enhancement in the GAC-amended UASB under high H_2S conditions.

5.3.6.3. The coexistence of competition and cooperation between SRB and methanogens with the GAC addition

The competition between SRB and methanogens is ubiquitous in traditional AD, where SRB can outcompete methanogens based on their kinetic properties (Hao et al., 2014). In the previous CMs addition related study, the development of active methanogens might help outcompete SRB. In other words, methanogens may obtain electrons more easily than SRB in the presence of CMs (Li et al., 2017). In this study, higher SMAs and better performance of the GAC-amended UASB indicated the enhancement of methanogens with the GAC addition. In comparison, the sulfate removal in the two reactors was similar. Hence, different COD/SO_4^{2-} ratios, substrates, operational conditions, and seed sludge may all significantly impact reactor performance and influence electron competition between methanogens and SRB under CMs-amended conditions. More conditions should be tested in future studies.

More interestingly, although sulfate removal was similar between the two reactors,

SRB (i.e., *Desulfobulbus*) can be enriched in the GAC biofilm (~ 6.7% in biofilm and ~ 1.8% in the two suspended sludges at the end of stage IV, Figure 5.9), indicating that cooperation between SRB and methanogens might exist. *Desulfobulbus* might grow by fermentation of lactate, pyruvate, ethanol (+ CO_2), malate, or fumarate when an external electron acceptor (e.g., SO_4^{2-}) does not exist (Kuever et al., 2015b). Meanwhile, several SRB have been reported to grow syntrophically with hydrogenotrophic methanogens, where the function of the pili structure was crucial (Brileya et al., 2014). Further, active SRB (i.e., *Desulfovibrio*) was identified in the GAC biofilm through RNA communities when SO_4^{2-} was not fed into the reactors (Guo et al., 2020b). These results indicated that SRB might work as a fermenter and cooperate with methanogens, instead of competing with methanogens for electrons. In this study, the high COD/SO_4^{2-} ratios and high sulfate removal revealed that a very low sulfate condition, or even a sulfate-depleting condition, might exist in the reactor's microenvironment. These conditions might prompt SRB to ferment and transfer electrons to other electron acceptors, such as the methanogens in this study. Further, *Desulfobulbus* has been reported to transfer electrons extracellularly to Fe (III) and graphite electrodes (Holmes et al., 2004). This EET ability and bio-electric activity of SRB may also help to explain the enrichment of SRB in the GAC biofilm.

In summary, due to the diversity of SRB species and the ability to utilize various substances, competition and cooperation between SRB and methanogens with the GAC addition might coexist. When sulfate exists in the microenvironment, competition between SRB and methanogens might be dominant. However, when sulfate is depleted, cooperation between SRB and methanogens might take precedence. Further, these suggestions were mainly based on the 16S rRNA microbial community analysis. The direct evidence should

be tested through direct measurements (e.g., isotope-based studies) in the future. It should be noted that sulfate exists in a wide range of wastewater (Liu et al., 2015; Xu et al., 2020a), and the strategy to overcome the H_2S inhibition as applied in this study could be applied in AD treating these wastewaters.

5.4. Conclusion

This chapter demonstrated that the GAC addition enhanced COD removal and methane production during anaerobic digestion of low-strength wastewater under sulfate-reducing conditions. The GAC addition helped and rebuilt a robust relationship between fermenters and methanogens to enhance the resistance to H_2S toxicity. The enrichment of methanogens and SRB in the GAC-amended UASB suggested the coexistence of competition and cooperation between SRB and methanogens with the GAC addition. These results indicated that the addition of CMs is a suitable strategy for enhancing methanogenesis under sulfate-reducing conditions.

Chapter 6. Settled granular activated carbon enhanced syntrophic partnerships during anaerobic digestion of municipal sewage[5]

6.1. Introduction

The mechanisms of granular activated carbon (GAC) addition in anaerobic digestion (AD) treating synthetic wastewater have been discussed in Chapters 3, 4, and 5. However, the impacts of GAC additions to AD systems treating municipal sewage at low temperatures have not yet been investigated. Here, we hypothesize that adding GAC to AD reactors operating at low temperatures can improve the methanogenic activity, result in a higher methanogenic growth rate, and improve the overall AD performance for municipal sewage treatment.

More importantly, the mechanisms behind the effects of conductive materials (CMs) on AD are not well understood in treating actual and complex wastewater. The enrichment of *Geobacter* is considered to be an indicator of direct interspecies electron transfer (DIET) (Rotaru et al., 2014a; Rotaru et al., 2014b). However, some studies have shown that the abundances of *Geobacter* were in low percentages or even absent with CM additions (Dang et al., 2017; Zhao et al., 2017; Zhao et al., 2016c), indicating that other bacteria may have been enriched by CMs and contribute to the enhancement of AD. Thus, the influence of

[5] A version of this chapter has been published: Zhang, Y., Guo, B., Zhang, L. and Liu, Y. (2020). Key syntrophic partnerships identified in a granular activated carbon amended UASB treating municipal sewage under low temperature conditions. *Bioresource Technology*, 312, 123556. https://doi.org/10.1016/j.biortech.2020.123556

CMs on microbial communities is still unclear. Furthermore, the direct comparison of data from 16S ribosomal RNA (rRNA) amplicon sequencing presents challenges to ecological interpretation. Therefore, further statistical analysis is essential to reveal the enriched microorganisms by CMs, especially when treating complex wastewater where both deterministic and stochastic factors may affect the microbial ecology (Kirkegaard et al., 2017; Yuan et al., 2019).

This chapter investigates the effects of the low-cost conductive material GAC on anaerobic reactors for the treatment of municipal sewage at low temperatures (16.5 ± 2.0 °C) and performs a statistical analysis of microbial community differences induced by GAC (Lima et al., 2008). This chapter represents the first study on the development of DIET-active microbiome in UASB through the GAC amendment for municipal sewage treatment under psychrophilic conditions.

6.2. Materials and methods

6.2.1. Reactor operation

Experiments were performed using two laboratory-scale plexiglass up-flow anaerobic sludge blankets (UASB) reactors (height 78 cm, diameter 10 cm, 4.7 L working volume) locating at a pilot plant in a local municipal wastewater treatment plant (WWTP) in Edmonton, Alberta, Canada. Two peristaltic pumps (LongerPump®, BT100-2J, Baoding, China) were used to feed influent from feeding tanks (22 L). Inoculum sludge was collected from a full-scale mesophilic anaerobic digester operated in the same WWTP. Addition of 25 g/L GAC (4-12 mesh, Sigma-Aldrich, St. Louis, USA) to one of the UASBs resulted in

a GAC packing ratio of 7%. The UASBs were acclimatized at ambient temperature (20 °C), initially using glucose as the carbon source, then fed with raw municipal primary effluent at ambient temperature (16.5 ± 2.0 °C) and operated for 120 days at three different hydraulic retention times (HRTs) (36, 24, and 16 h).

6.2.2. Specific methanogenic activity

The SMA of UASB sludge was measured according to the method described by Gao et al. (2019). Sludge samples (5 mL) were collected from each UASB reactor and added with 10 mL acetate solution (1 g COD/L) as a substrate in the SMA acetate test, or 10 mL DI water in the SMA hydrogen test. The mixtures were transferred into a serum bottle (38 mL), flushed with nitrogen gas (for acetate SMA) or hydrogen gas and carbon dioxide gas (mole ratio: 4:1 for hydrogen SMA) to achieve anaerobic conditions, then sealed and placed in a shaker at 120 rpm and 20.0 ± 0.5 °C in the dark. All studies were performed in triplicates.

6.2.3. Analytical methods

Total COD, soluble COD, total suspended solids (TSS), and volatile suspended solids (VSS) were determined according to the Standard Methods (APHA, 2012). A Symphony pH probe (VWR, Radnor, USA) was used to determine the pH values. Biogas was collected in a 0.5 L gas bag (CHROMSPEC™, Brockville, Canada). Sulfate concentration was determined by Sulfate Reagent Powder Pillows (SulfaVer® 4, Hach, Loveland, USA), and Sulfide 2 Reagent (Hach method 8131) was used to determine sulfide concentration.

A gas chromatograph GC-7890B (Agilent Technologies, Santa Clara, USA) was used to determine the biogas concentrations of nitrogen, methane, oxygen, and carbon

dioxide in the headspace of batch bottles and gas bags connected to the UASB reactors. The temperatures of oven and detector in the GC were 100 ºC and 200 ºC, respectively. Helium (99.999% purity) was used as the carrier gas in the system. A hand-held pressure meter (GMH 3151, Regenstauf, Germany) was used to measure the gas pressure in batch tests.

Dissolved methane concentration in the effluent was measured once per week according to the method described in Chapter 3. Firstly, 30 mL of UASB effluent was injected slowly into a 60 mL glass bottle, containing 10.6 g NaCl. Contents of the bottle were then mixed thoroughly by vortexing and settled for 30 min. The final headspace pressure was measured using the pressure meter, and the headspace gas composition was determined by the gas chromatograph.

Biomethane potential (BMP) of municipal primary effluent was determined using methods reported previously (Gao et al., 2019). Briefly, 30 mL fresh digester sludge was mixed with 50 mL municipal primary effluent, flushed with nitrogen gas, and incubated in serum glass bottles (160 mL) for 50 days. The headspace pressure and gas composition were measured by the pressure meter and the gas chromatograph, respectively.

6.2.4. Microbial community analysis

Suspended sludge samples (2 mL) were harvested from each UASB reactor from all stages, on day 30 (Stage I), days 59 and 80 (Stage II), and days 92, 103, 115, and 120 (Stage III). GAC-biofilm was collected from GAC-amended UASB at the end of the operation (day 120). DNA extraction was performed by the DNeasy PowerSoil Kit (QIAGEN, Germany). Polymerase chain reaction (PCR) was performed with primer pair 515F/806R (Caporaso

et al., 2011). The purity and concentration of the extracted DNA were analyzed using NanoDrop One (ThermoFisher, USA). The amplicon samples were sent to Genome Quebec (Montréal, Canada) for sequencing on the Illumina PE250 platform. QIIME2 pipeline DADA2 algorithm was used for sequence reads pairings, quality-filtered, and chimera removal (Callahan et al., 2016). Taxonomy was assigned using 99% similarity in GreenGenes (version 13_8) reference database (McDonald et al., 2012b).

6.2.5. Data analysis

The linear discriminant analysis (LDA) effect size (LEfSe) method was used to perform microbial ecology analysis for biomarker discovery (Segata et al., 2011). This method was used to explain differences between microbial communities in the non-GAC and GAC UASBs for statistical significance with additional tests for encoding biological consistency and effect relevance. Student's t-test, Principal Coordinate Analysis (P Co A) of the Bray-Curtis distance, and Canonical Correlation Analysis (CCA) plot were performed using the software package R (http://cran.r-project.org/).

6.3. Results and discussion

6.3.1. COD and SO_4^{2-} removal efficiency

Total and soluble COD and SO_4^{2-} concentrations of the sewage are shown in Figure 6.1. The removal efficiencies of the non-GAC and GAC reactors are shown in Figure 6.2. The influent total COD (TCOD) concentration in this study fluctuated between 105 and 462 mg/L. The effluent TCOD concentrations and TCOD removal efficiencies of the two UASBs are shown in Figure 6.1A and Figure 6.2A. In stage I (HRT of 36 h), the effluent

TCOD in the non-GAC UASB was 106 ± 38 mg/L with an average removal efficiency of 64.6%. The effluent TCOD in the GAC-amended UASB was 53 ± 23 mg/L, with a significantly higher removal efficiency of 82.6% ($p < 0.01$, Figure 6.2A). When the HRT was reduced to 24 h (stage II), the effluent TCOD was 101 ± 29 mg/L in the non-GAC UASB and 68 ± 16 mg/L in GAC UASB. The TCOD removal efficiencies of the non-GAC and GAC reactors were also significantly different (66.1% and 77.1%, respectively, $p < 0.01$). The TCOD removal efficiency in GAC reactor was lower compared to that of stage I ($p < 0.05$, as shown in Figure 6.2A). In stage III, the HRT was further reduced to 16 h, resulting in reduced total COD removal efficiency of 58.5% and 70.5% for the non-GAC and GAC UASBs, respectively.

Figure 6.1B shows the soluble COD (SCOD) concentrations. The influent SCOD concentration ranged from 80 to 368 mg/L, which accounted for 66 ± 14% of the total COD. The SCOD in the non-GAC UASB effluent varied from 23 to 128 mg/L, and the average removal efficiency was 60.4%. In the GAC UASB, effluent SCOD varied from 18 to 79 mg/L, resulting in a significantly higher average removal efficiency of 71.9%. The GAC reactor had a significantly higher SCOD removal efficiency than the non-GAC reactor in all stages ($p < 0.01$, Figure 6.2B). Similar to the TCOD removal efficiency trend, the highest SCOD removal efficiency was achieved when the HRT was 36 h.

The sewage contains a considerable amount of SO_4^{2-} (varied from 78 to 134 mg/L, and TCOD/SO_4^{2-} ratios were 2.9 ± 0.5 and 2.9 ± 0.6 in stages I and II, respectively, and 1.7 ± 0.5 in stage III. Since SO_4^{2-} is known to impact AD systems (Lens et al., 1998), the influent and effluent SO_4^{2-} concentrations were monitored routinely during this study. Figure 6.1C and Figure 6.2C show the temporal changes of influent and effluent SO_4^{2-} and

their removal efficiencies in the non-GAC and GAC reactors. The SO_4^{2-} removal efficiency of the GAC UASB was higher than that of non-GAC UASB in all stages (with differences of 1.7% - 3.5%). However, the difference was only statistically significant in stage III ($p < 0.05$, Figure 6.2C). The SO_4^{2-} removal efficiency increased with reduced HRT ($p < 0.05$, Figure 6.2C), which may be attributed to the acclimation of the sulfate reducing microbial community, especially in stage III. The total sulfide concentrations fluctuated between 13.3 and 29 mg/L in the non-GAC UASB effluent, and between 14.9 and 31.3 mg/L in the GAC-amended UASB. Sulfide emission from UASB treatment can lead to corrosion and if not contained, may lead to significant health concerns. Sulfide produced during AD can be removed by various methods, such as precipitation with metal ions and various biogas purification approaches (Khan et al., 2012; Krayzelova et al., 2015; Lin et al., 2017), which should be considered for future design and operation of such systems.

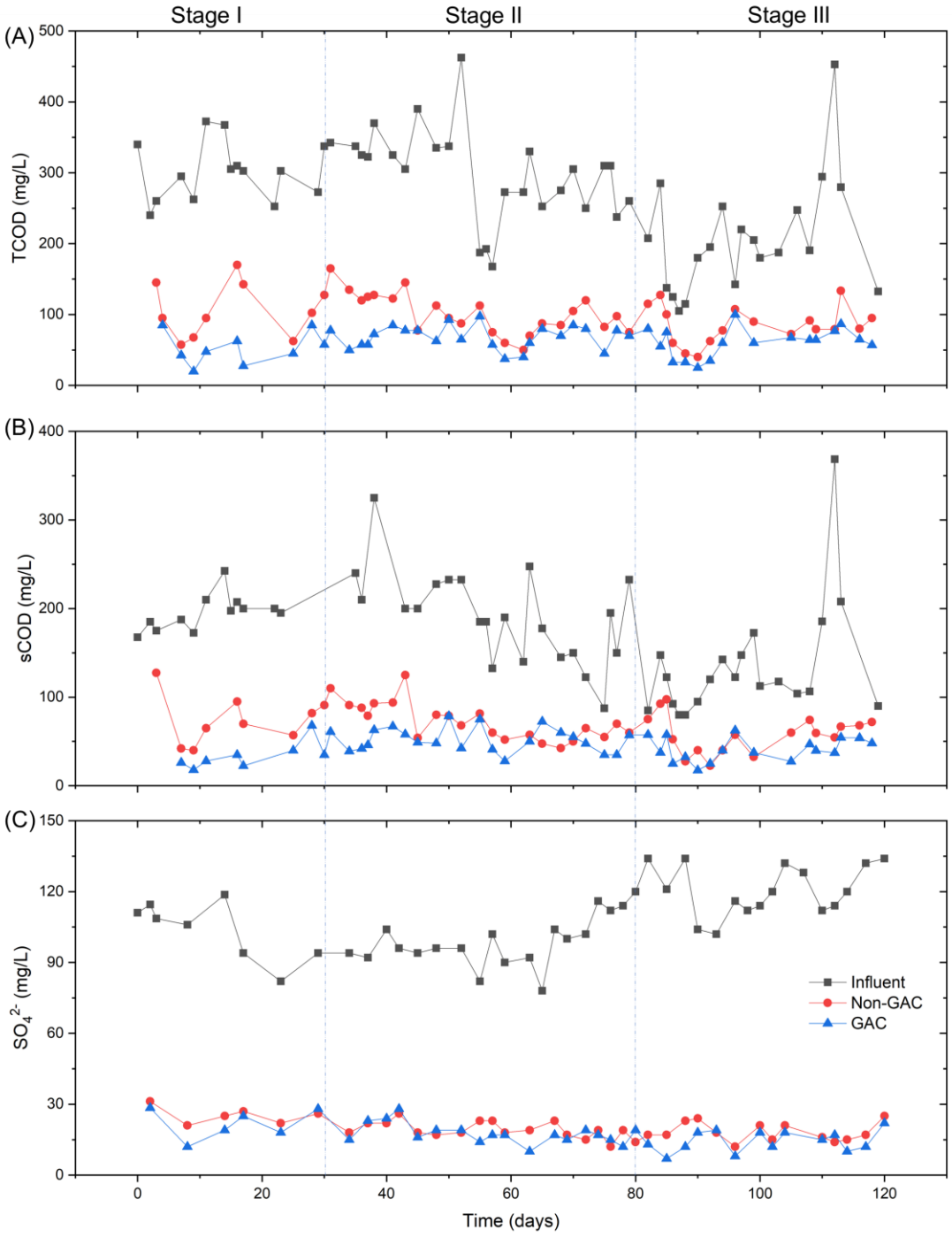

Figure 6.1 (A) Total COD, (B) soluble COD, and (C) SO_4^{2-} concentrations of the non-GAC UASB and GAC UASB treating municipal sewage at three HRTs.

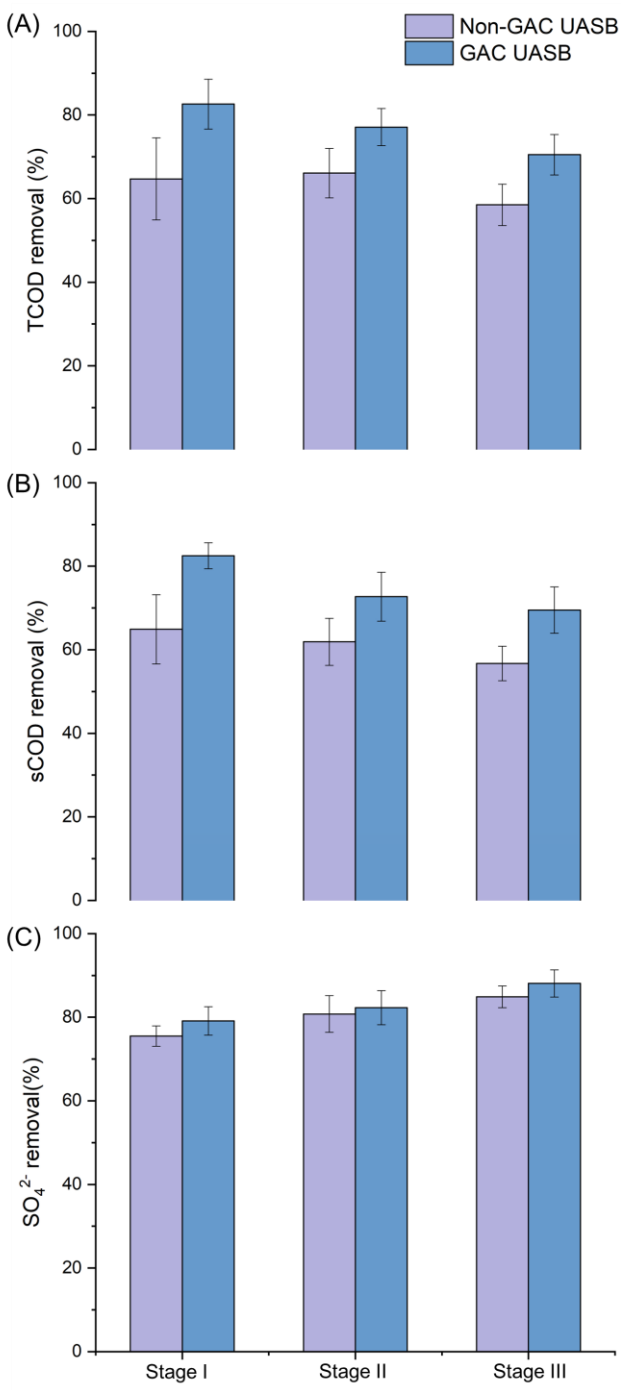

Figure 6.2 Average removal efficiencies of (A) total COD, (B) soluble COD, and (C) SO_4^{2-} for the non-GAC UASB and GAC UASB treating municipal sewage at three HRTs. Error bars represent one standard deviation.

6.3.2. SMA and methane production

Figure 6.3 shows the SMA and total methane production during the operation. With GAC addition, the total methane production of the GAC UASB was 1 to 2.1 times higher than that of non-GAC UASB ($p < 0.05$, Figure 6.3C). With decreased HRTs, the methane production in the GAC reactor did not increase, and in the non-GAC UASB, it increased by 29% from stage I to stage III. The changes in methane production were not proportional to the reduction of HRTs. The explanation is that methane yield (mg CH_4-COD/g influent COD) decreased more than the decrease of HRTs. The observed decrease in methane yield under lower HRT conditions may be attributed to the low COD/SO_4^{2-} ratio in this sewage. Methane has an energy content of approximately 47 MJ/kg based on the Lower Heating Value (LHV) (Crone et al., 2016). Based on the average methane production in the two reactors, the calorific values of CH_4 were 296 kJ/m^3 treated wastewater and 765 kJ/m^3 treated wastewater in the non-GAC and GAC UASB, respectively. It is also important to consider dissolved methane at low temperatures. Dissolved methane was much higher in the GAC UASB from 31 to 68 mg CH_4-COD/L, compared to the 13 to 24 mg CH_4-COD/L in the non-GAC reactor during the operation.

The temporal changes of suspended sludge SMA are shown in Figure 6.3A and Figure 6.3B. Under all conditions, SMAs of acetate and hydrogen were significantly higher in the GAC UASB as compared to the non-GAC UASB ($p < 0.01$). In stages I and II, the GAC UASB suspended sludge had 2.4- and 1.4-times higher acetate SMAs and 0.7- and 1.8-times higher H_2 SMAs respectively, as compared to the non-GAC UASB sludge. In stage II, the GAC UASB microbial community has developed higher hydrogenotrophic

methanogenesis activity, which may be attributed to the development of hydrogenotrophic methanogens, such as *Methanobacterium* (to be further discussed in Sections 6.3.4-6.3.8), in the presence of GAC. When the HRT was reduced to 16 h in stage III, SMAs in both reactors decreased, although SMAs in GAC UASB sludge were still higher than the non-GAC UASB sludge.

Overall, the methane production in the present study (21.7% for GAC reactor, and 8.4% for non-GAC reactor) was significantly lower than that of the feed water BMP (36.4%), which may be attributed to the high SO_4^{2-} and relatively low COD concentrations in the primary effluent. The average TCOD/SO_4^{2-} ratio in stage III was 1.7 ± 0.5, which has been reported to favor the growth of sulfate-reducing bacteria and eliminate the growth of methanogens (Lens et al., 1998). The low TCOD/SO_4^{2-} ratio may also contribute to the low methanogenic activities (SMAs).

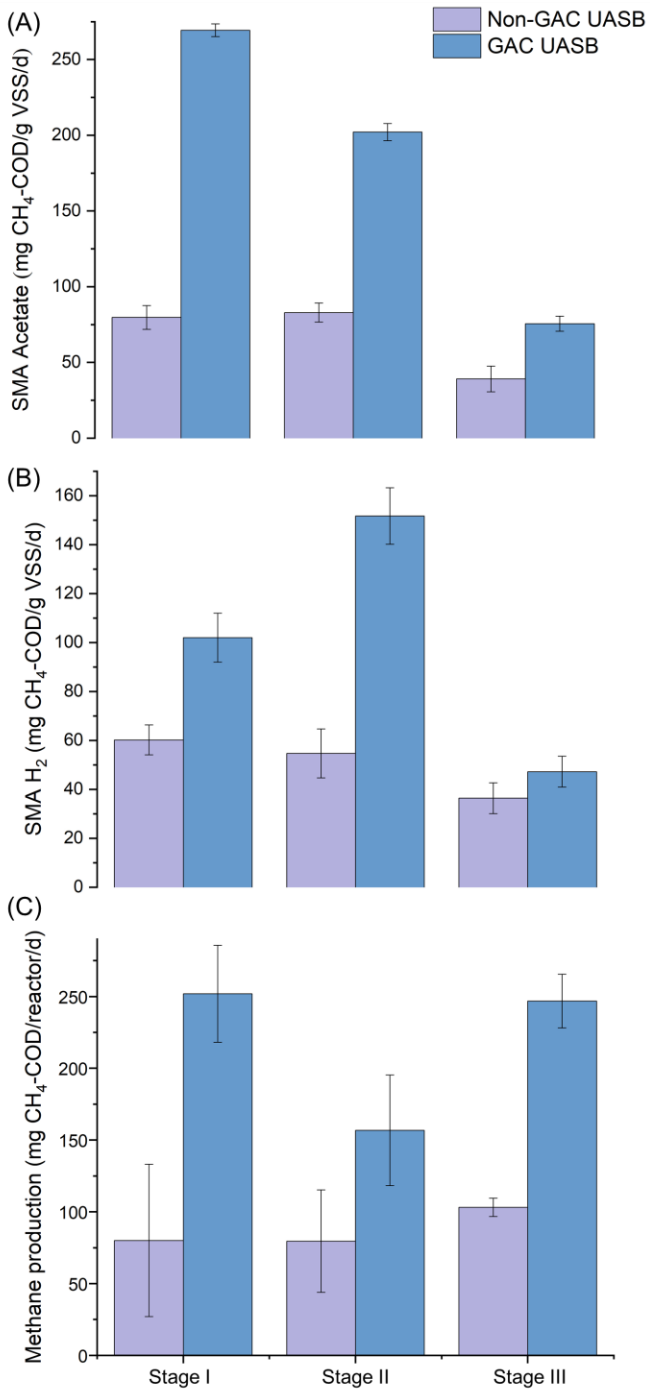

Figure 6.3 (A) SMA acetate, (B) SMA H_2, and (C) methane production of the non-GAC UASB and GAC UASB treating municipal sewage at three HRTs. Error bars represent one standard deviation.

6.3.3. Biomass concentration

The VSS concentrations of suspended sludge at the end of the experiments (Day 120) in the non-GAC UASB and GAC-amended UASB were 7.5 ± 0.5 and 7.9 ± 0.3 g/L, respectively, and the total VSS was similar (average of 10.5 g in the non-GAC UASB and 10.4 g in the GAC-amended UASB, respectively, $p > 0.05$). The total VSS of GAC attached biofilm was 0.55 g, which accounted for 5.3% of the total VSS in the GAC reactor.

6.3.4. Microbial community analysis

6.3.4.1. Archaea

At the genus level (Figure 6.4), the archaeal communities in the non-GAC and GAC reactors were dominated by *Methanosaeta* in stages I (48.4% and 65.6%, respectively) and II (51.8-54.5% and 69.7-64.3%, respectively), indicating acetoclastic methanogens were the main pathway for methane production in both reactors. In stage III, the *Methanosaeta* abundance decreased in both non-GAC and GAC reactors (to 37.8-44.7% in the non-GAC reactor and 28.1-36.2% in the GAC reactor), while the hydrogenotrophic methanogens increased. The hydrogenotrophic methanogen *Methanobacterium* had the highest increase in the GAC reactor sludge, from 10.9% in stage I to 35.7% in stage III. Further, the GAC-biofilm at the end of the third stage was dominated by *Methanobacterium* (75.3%).

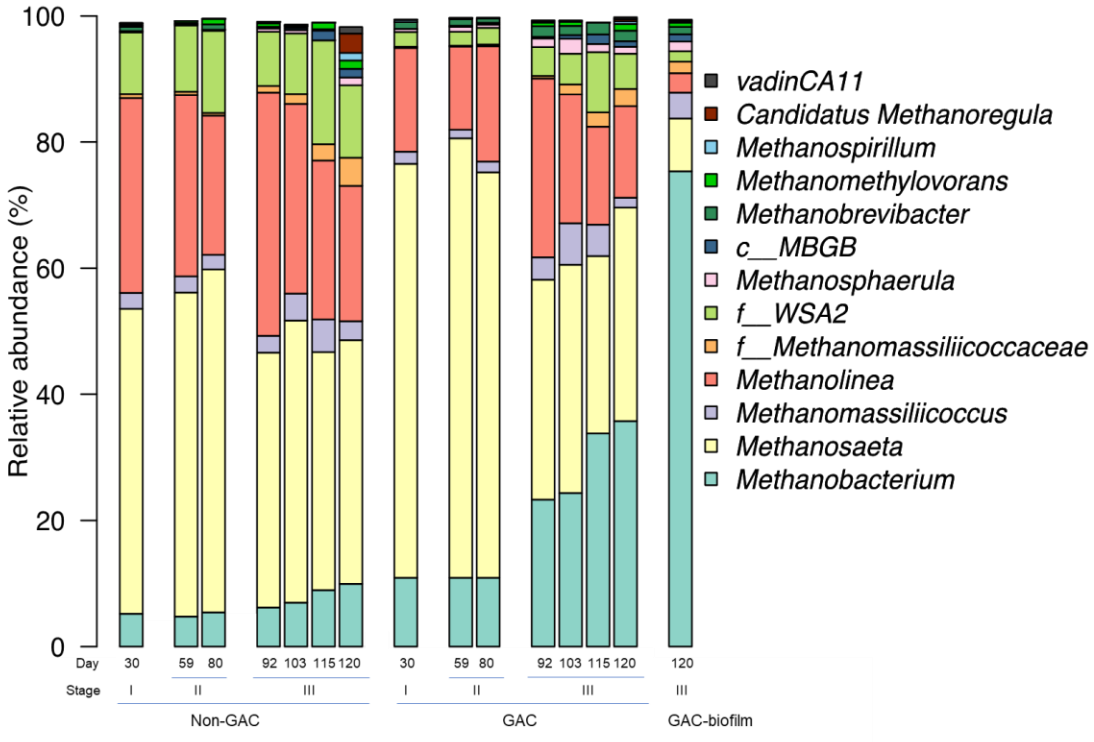

Figure 6.4 Relative abundances of archaeal genera with abundance > 1% in the non-GAC and GAC UASB suspended sludge and GAC-biofilm on day 120. Unidentified genera were named at family (f__) or class level (c__).

6.3.4.2. Bacteria

The bacterial community at the phylum level showed the predominance of *Proteobacteria*, *Bacteroidetes*, and *Firmicutes* (Figure 6.5). A higher abundance of *Chloroflexi* was observed in the non-GAC reactor than in GAC reactor, while the latter had more *Chlorobi*. The most abundant bacterial families from each sample are shown in Figure 6.6. The two reactors shared some abundant families, including *Syntrophaceae*, an unclassified family from the order *Bacteroidales*, *Syntrophorhabdaceae*, *Clostridiaceae*, *Anaerolinaceae*, *Geobacteraceae*, *Spirochaetaceae*, and *Carnobacteriaceae*, which have been reported as

important microorganisms for municipal sewage anaerobic digestion (Petropoulos et al., 2019). Besides these families, the GAC-biofilm also enriched *Desulfobacteraceae*, *Desulfomicrobiaceae*, and *Desulfobulbaceae*, which are sulfate-reducing bacteria (Biswal et al., 2020; Huang et al., 2020) and increased in the GAC reactor suspended sludge during the 120 days of operation. *Thermovirgaceae*, *Cloacamonaceae*, Sediment-4, and SB-1 families were more abundant in the non-GAC reactor than in the GAC reactor.

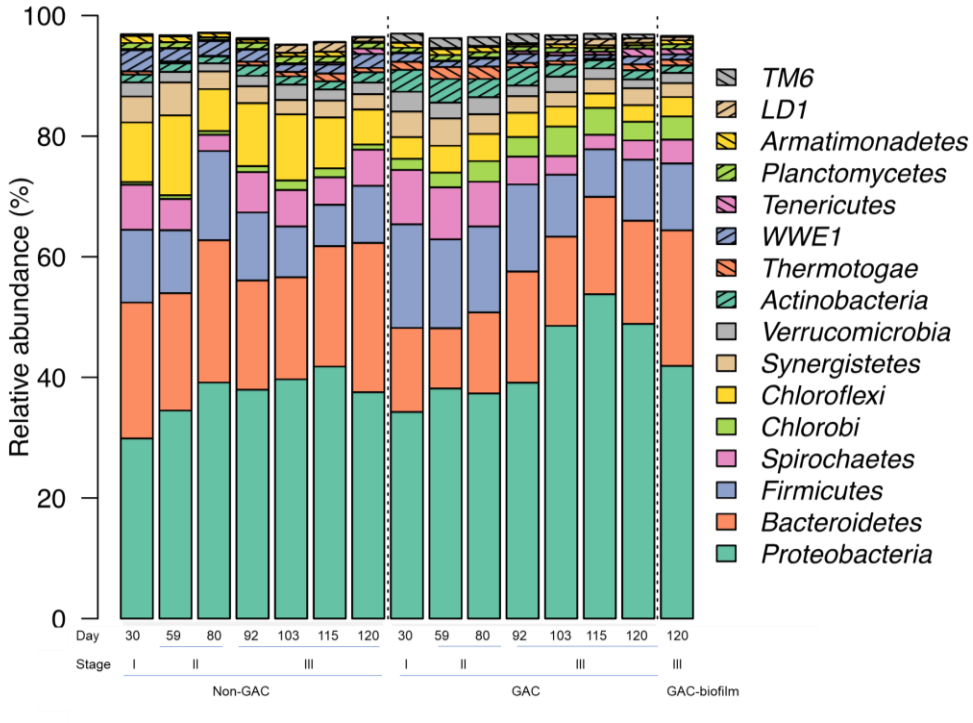

Figure 6.5 Relative abundances of bacteria at phylum level with abundance > 1% in the non-GAC and GAC UASB suspended sludge, and GAC-biofilm on day 120.

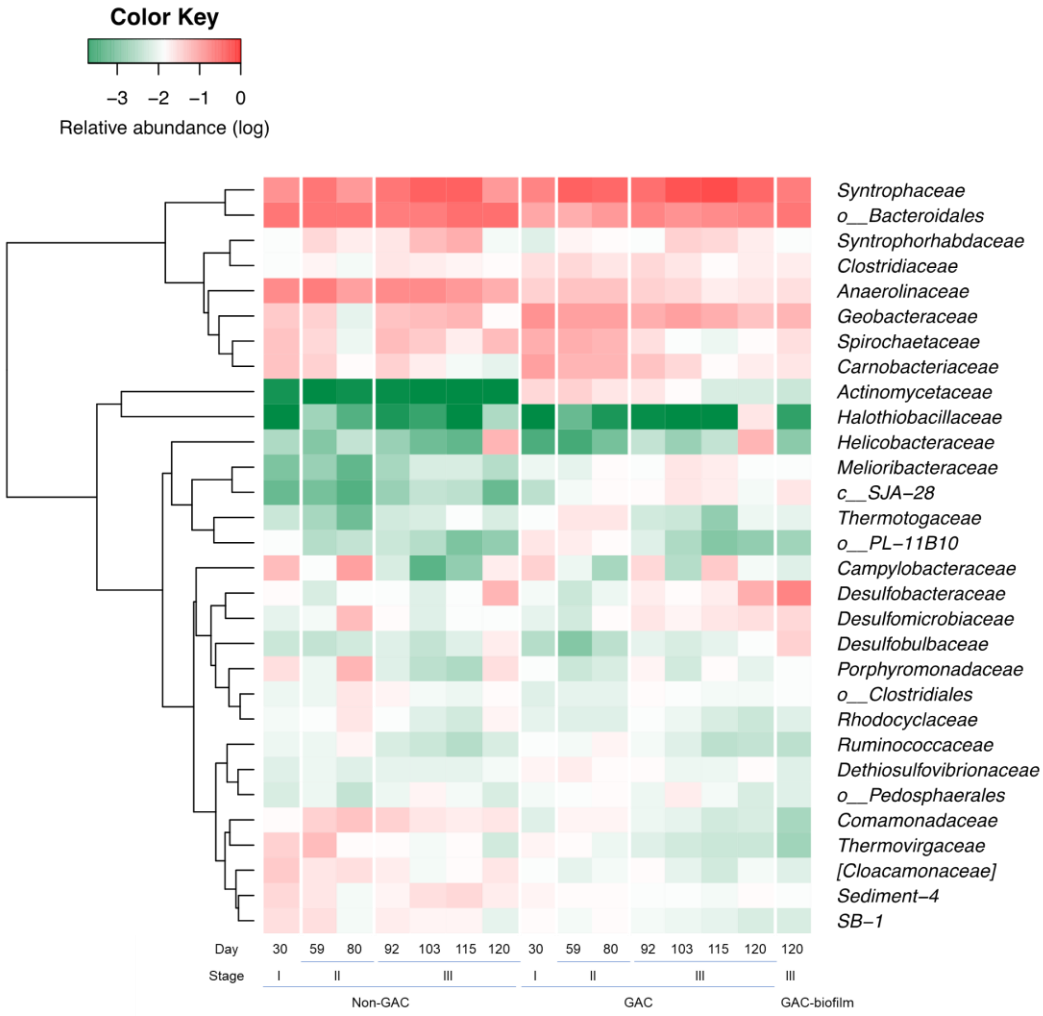

Figure 6.6 Relative abundances of bacteria at family level with abundance > 1% in the non-GAC and GAC UASB suspended sludge, and GAC-biofilm on day 120.

At the genus level, the 10 most abundant genera from each sample were assembled with many unclassified genera (Figure 6.7). *Syntrophus*, *Geobacter*, an unclassified genus from *Bacteroidales*, and *Syntrophaceae* were dominant in both reactors. The GAC-biofilm showed enrichment of SRB (*Desulfobacter* 9.8%, *Desulfobulbus* 2.6% and *Desulfomicrobium* 2.5%). There were a few genera that fluctuated at different stages (*i.e.,*

Arcobacter, *Macellibacteroides*), suggesting these genera can sustain their lives under various operation conditions (Yang et al., 2019).

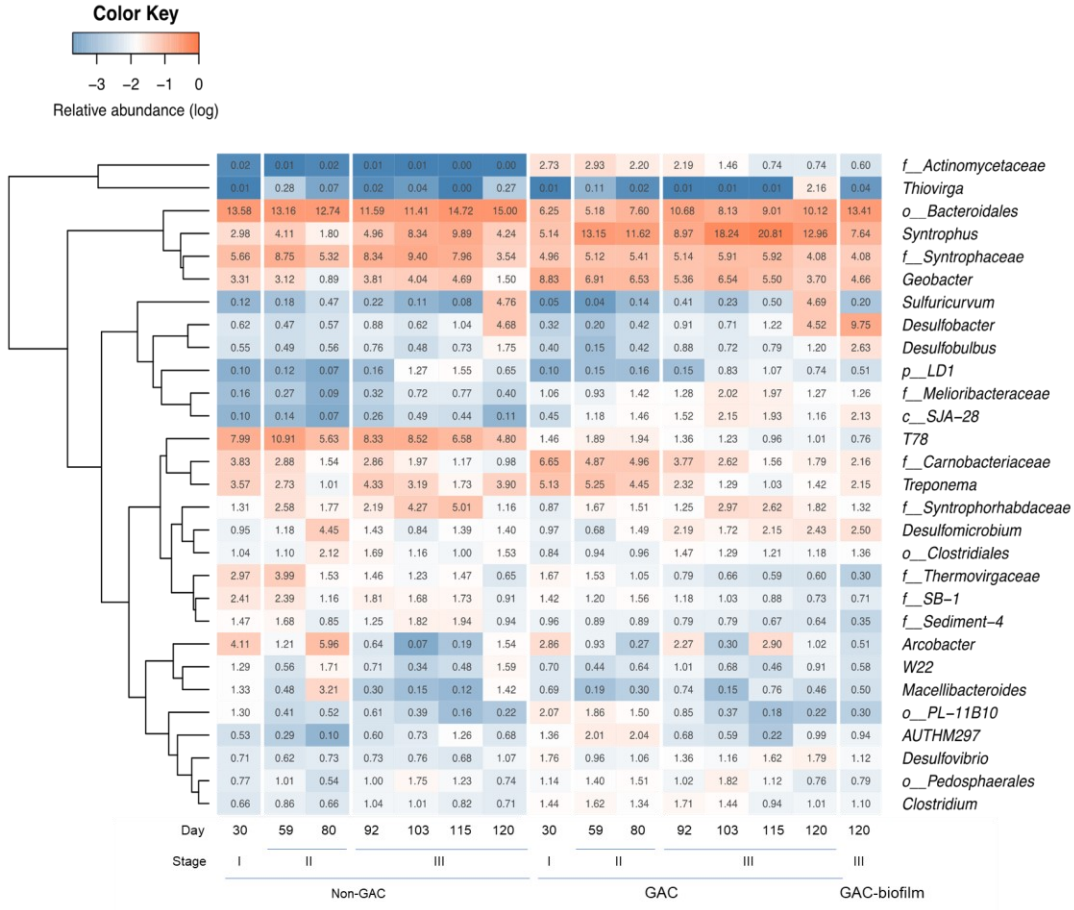

Figure 6.7 Relative abundances of 10 most abundant bacterial genera from each sample in the non-GAC and GAC UASB suspended sludge and GAC-biofilm on day 120. Unidentified genera were named at family (f__), order (o__), class (c__) or phylum (p__) level.

6.3.5. Microbial community diversity

Alpha diversity (Figure 6.8) was not significantly different ($p > 0.05$) between reactors or among different stages. The Beta-diversity was analyzed using Principal Coordinate

Analysis (P Co A) of the Bray-Curtis distance among microbial communities (Figure 6.9). The archaeal community difference (Figure 6.9A) was significant ($p < 0.05$) between reactors and between different stages. Noticeably, the GAC-biofilm at the end of reactor operation showed a large distance from the suspended sludge samples due to the substantial enrichment of *Methanobacterium* (Figure 6.9). For bacterial communities (Figure 6.9B), samples from the non-GAC and GAC reactors were clustered into two groups with significant differences ($p < 0.05$), however, the difference between different stages was less significant ($p = 0.057$). The GAC-biofilm bacterial community was similar to the suspended sludge sample.

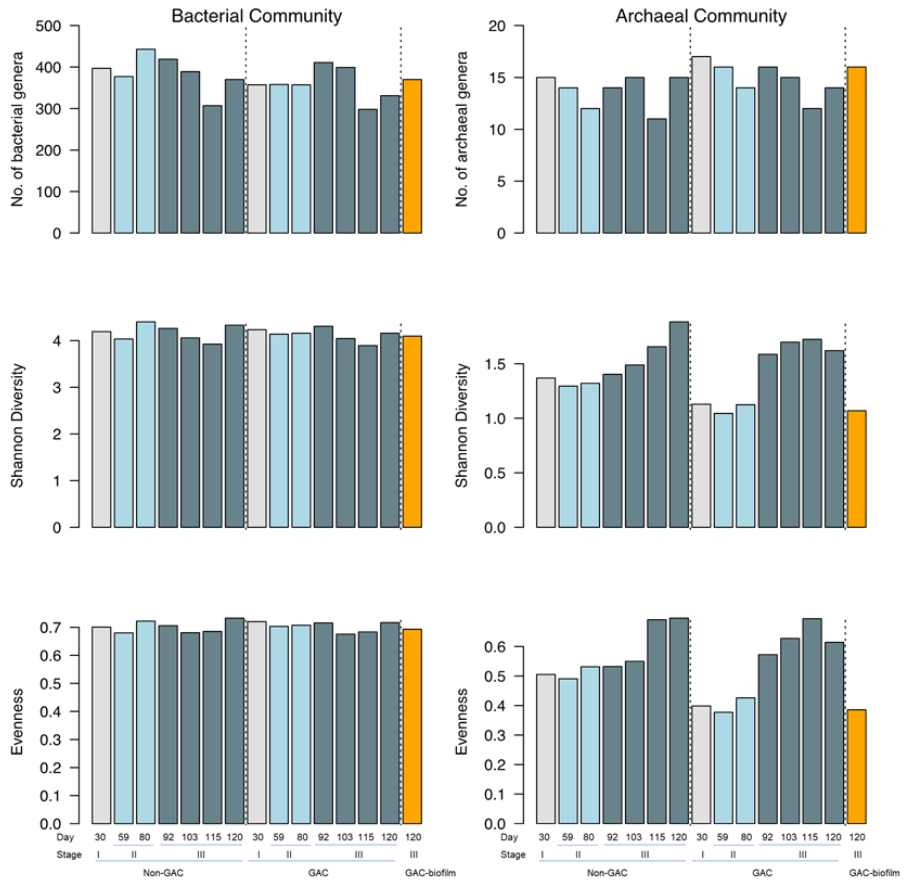

Figure 6.8 Alpha diversity analysis in the non-GAC and GAC UASB suspended sludge,

and GAC-biofilm on day 120.

Reactor influent and effluent characteristics (i.e., TCOD, SCOD, SO_4^{2-}) were used to explain the community variation in a Canonical Correlation Analysis (CCA) plot (Figure 6.9C for archaea, Figure 6.9D for bacteria). These parameters in total can explain 78.7% of archaeal community variance and 68.7% of bacterial community variance. Strong correlations were shown for community variation among operation stages, HRT, and influent TCOD, SCOD, and SO_4^{2-} concentrations for archaea (Figure 6.9C) and bacteria (Figure 6.9D).

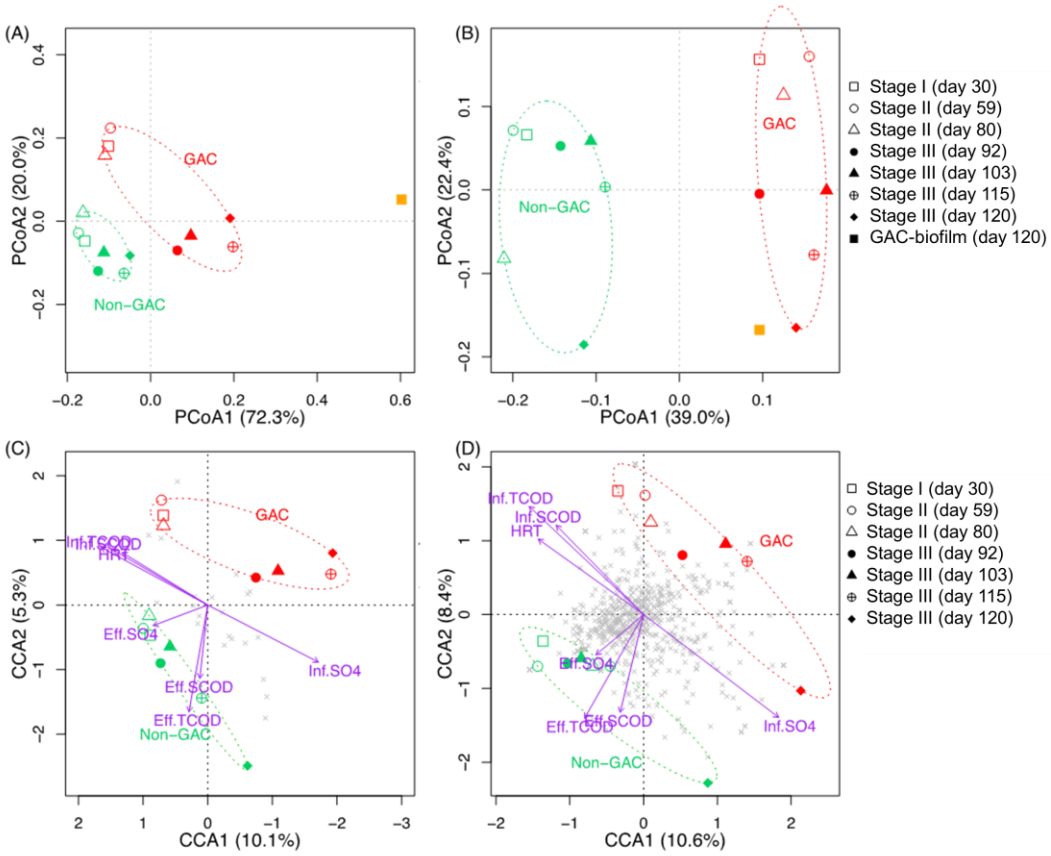

Figure 6.9 Principal Coordinate Analysis (PCoA) of (A) archaea, (B) bacteria. Canonical Correlation Analysis (CCA) of (C) archaea, (D) bacteria.

6.3.6. Community differential analysis

To test the significance of genera variability between the non-GAC and GAC reactors, LEfSe analysis was performed at a threshold level of LDA score of 2, which identifies the community biomarkers. A total of 105 biomarker taxa were identified: 79 in the non-GAC reactor and 26 in the GAC reactor. *Geobacter* had the highest differential LDA score in the GAC reactor sludge community, indicating significantly higher abundance in the GAC reactor (3.7-8.8%) than in the non-GAC reactor (0.9-4.0%). *Chloroflexi* was the most significant biomarker in the non-GAC reactor. The GAC reactor biomarkers are shown in Figure 6.10A. In addition to *Geobacter*, sulfate-metabolism related bacteria, sulfate-reducing bacteria (SRB) (*Desulfovibrio*), and thiosulfate-reducing bacteria (*Dethiosulfovibrionaceae* HA73 and PD-UASB-13) were significantly higher in the GAC reactor than those in the non-GAC reactor. Hydrogenotrophic methanogens (*Methanobacterium*, *Methanobrevibacter*, and *Methanosphaerula*) and *Syntrophomonas* were also enriched in the GAC reactor.

The phylogenetic tree of the significantly different genera is shown in Figure 6.10B. Noticeably, the GAC reactor biomarker genera were phylogenetically related and formed a few clusters, including orders of *Methanobacteriales*, *Synergistales*, and *Desulfuromonadales* and families of *Syntrophomonadaceae* and *Clostridiaceae*.

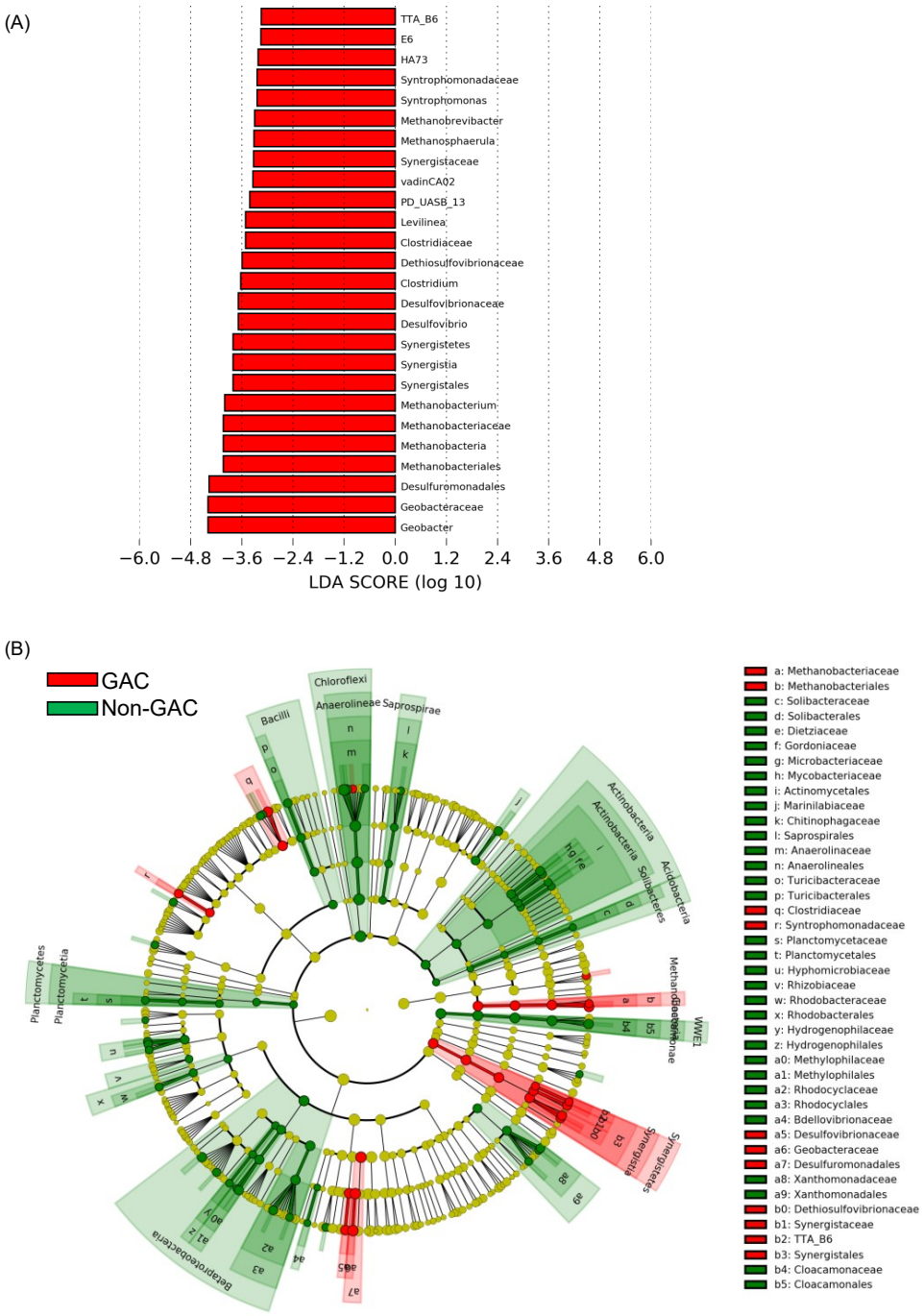

Figure 6.10 LEfSe analysis of non-GAC and GAC reactor communities. (A) Taxa in GAC reactor with LDA score > 2. (B) Phylogenetic distribution of all taxa with LDA score > 2.

6.3.7. SRB and archaea abundances

The SRB abundances were compared between the two reactors at different stages (Figure 6.11A). The SRB total abundances were 3.2-9.6% in the non-GAC reactor suspended sludge, 2.5-11.2% in the GAC reactor suspended sludge, and 17.1% in the GAC-biofilm. Although the relative abundance of SRB fluctuated with time, it maintained stable at the end of stage I (4.3%) and stage II (4.1%), increased and reached the highest value at the end of stage III (11.2%), in the GAC UASB. In comparison, the relative abundance of SRB in the non-GAC reactor increased from 3.7% at the end of stage I to 9.6% at the end of stage III. The increased SRB probably resulted from the continuous feeding of sulfate in the influent and the enrichment of SRB in both reactors (Figure 6.1C).

The enrichment of SRB is associated with the decreasing archaeal abundance (Figure 6.11B) since SRB can compete for electron donors (organic substrates) with methanogens (Lens et al., 1998), which may have contributed to the reduced methane production. Overall, the archaeal fraction of total microbial community accounted for 5.1-7.9% and 12.8-16.5% in the non-GAC and GAC reactors, respectively, from stages I to II, then decreased and fluctuated with time. At the end of stage III, it dropped to 1.9% in the non-GAC reactor and 3.7% in the GAC reactor. In the GAC-biofilm, the archaeal fraction maintained at 9.5% until the end of the operation.

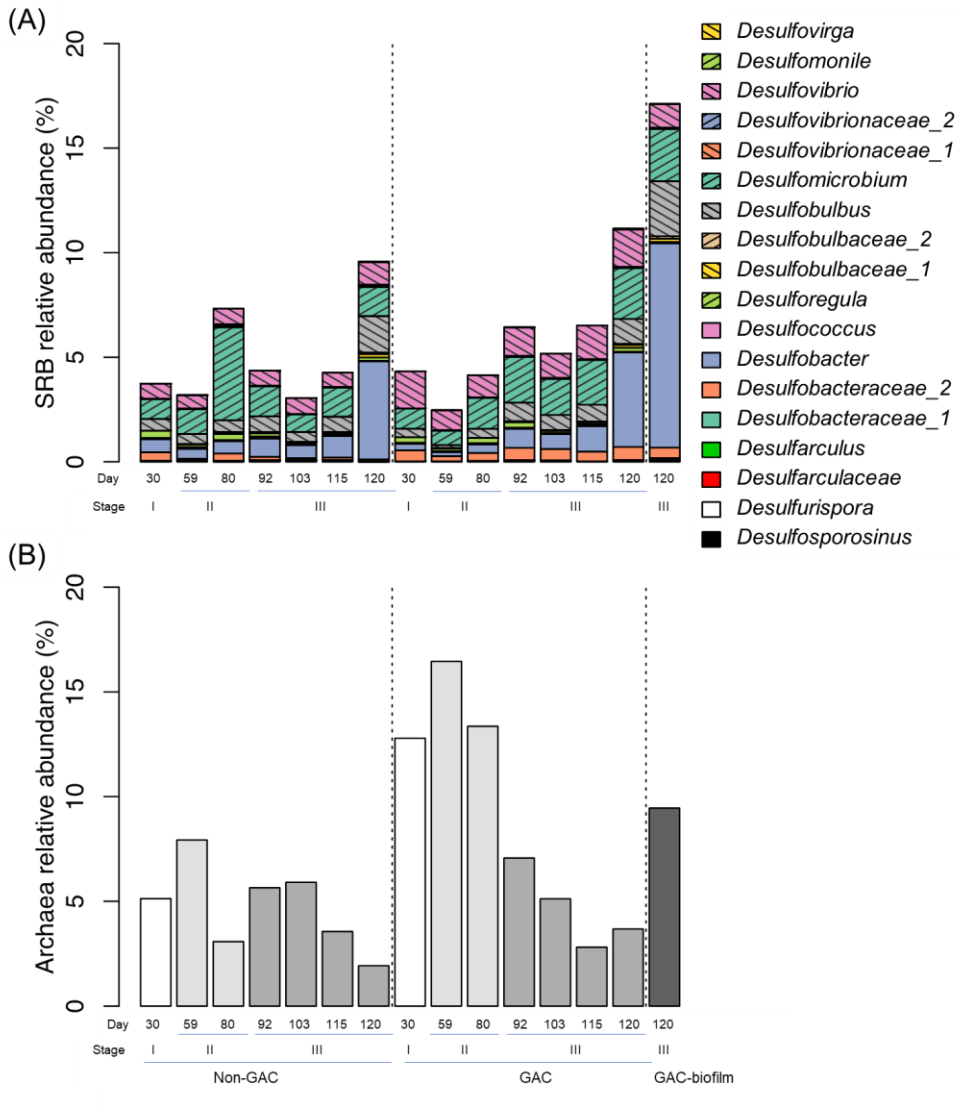

Figure 6.11 Relative abundances of (A) sulfate-reducing bacteria (SRB) and (B) archaea.

6.3.8. GAC enhanced AD performance and electro-active syntrophic microorganisms

The results from this study indicate significant improvements in COD removal efficiency and SMA through the addition of GAC in anaerobic treatment of sewage at low temperatures. GAC mainly functioned as conductive materials that stimulate development of DIET-active microbiome. Biofilms can be developed on GAC surfaces, which can help

to bio-regenerate GAC (Florentino et al., 2019b; Islam et al., 2016). Hence, regeneration and recycling are not needed in this configuration. In regards to the key DIET indicator microorganisms (Rotaru et al., 2014a; Rotaru et al., 2014b; Zhao et al., 2016c), our results showed significantly higher *Geobacter* in the GAC UASB (LEfSe, Figure 6.10); while the commonly reported DIET indicator *Mathanosaeta* did not show improved abundance in GAC reactor than non-GAC reactor (Figure 6.4). As demonstrated recently (Guo et al., 2019), the traditional DIET indicators suggested in the literature may not be sufficient to conclude that the enhancement was mainly caused by GAC-mediated DIET.

Methanobacterium, which has not been proven to directly participate in the DIET process, was the dominant archaea in the GAC-biofilm and in the GAC UASB suspended sludge in stage III. Salvador et al. (2017) found that carbon nanotubes can increase the methane production rates in pure cultures of *Methanobacterium formicicum* by up to 17 times. Our recent studies on the GAC-amended UASB fed with glucose showed a significant increase in the abundance of *Methanobacterium* (Guo et al., 2019). In CM-amended and bioelectrochemical AD systems, *Methanobacterium* has also been enriched in the cathode biofilm and on the surface of GAC (Siegert et al., 2015; Yang et al., 2017). Moreover, the total archaea fractions in the total microbial community were 9.5% on the GAC surface and 1.9-3.7% in the suspended sludge at the end of this study, which implies that GAC may stimulate methanogens growth. These findings may explain that CMs not only function to facilitate the electron transfer between *Geobacter and Mathanosaeta*, but also enrich *Methanobacterium*, which may have electro-activity and should be further investigated.

Syntrophomonas and *Syntrophus* were enriched in the GAC-amended UASB,

which may have also contributed to the improvement of COD removal and methane production. They have been reported as important syntrophic bacteria in AD, with functions of producing hydrogen or formate as electron carriers to methanogens (Jackson et al., 1999; McInerney et al., 1981). Further, *Syntrophomonas* has been found to be highly abundant in other CM-amended reactors (Zhao et al., 2018; Zhao et al., 2016b) and is considered to be a possible player in the DIET process. Moreover, genes for synthesis of type IV pili are present in genome of *Syntrophus,* which may facilitate cell-to-cell attachment and the transfer of hydrogen or formate to its syntrophic partners (McInerney et al., 2007); in a recent study, Walker et al. (2018) found that *Syntrophus aciditrophicus* can produce e-pili and grow *via* the DIET process. These findings demonstrate *Geobacter* and other syntrophic microorganisms, such as *Syntrophomonas* and *Syntrophus,* may all play important roles in the CM-assisted DIET process.

In addition to the previously reported electro-active microorganisms, the GAC reactor showed significant enrichment of SRB in the clusters of *Synergistales*, *Desulfuromonadales*, and *Clostridiaceae* (Figure 6.7). The GAC-biofilm also showed high abundances of SRB (Figure 6.11). Several SRB have been shown to grow syntrophically on various substrates, such as lactate, ethanol, and propionate, and syntrophy with hydrogen- or formate-consuming methanogens in sulfate depleted environments (Raskin et al., 1996). In this study, SRB and the hydrogenotrophic methanogen *Methanobacterium* were enriched in the GAC-biofilm and GAC-suspended sludge in stage III. This finding demonstrates that SRB possibly formed a syntrophy partnership with *Methanobacterium.* Extracellular c-type cytochromes and bacterial type IV pili might play a key role in mediating intercellular electron transfer under direct cell-to-cell contact conditions

(Lovley, 2012). The high expression of several c-type cytochromes and type IV pili in SRB demonstrated that SRB might participate in DIET with methanotrophic archaea in the anaerobic oxidation of methane process (Krukenberg et al., 2018). In this study, the enriched SRB and *Methanobacterium* in GAC UASB illustrate that the DIET process might be stimulated. Metagenomic and metatranscriptomic analyses are needed to elucidate gene abundance and expression associated with c-type cytochromes and type IV pili in further studies (Park et al., 2018).

6.4. Conclusion

This chapter demonstrated that GAC enhanced COD removal and CH_4 production during anaerobic digestion of municipal sewage under low-temperature conditions. Statistical analysis showed that *Geobacter*, one of the most important DIET indicators, was enriched significantly in the GAC-amended UASB, suggesting the possible existence of DIET. The enrichment of *Methanobacterium*, *Syntrophomonas*, *Syntrophus*, and SRB in the GAC-amended UASB suggests that GAC may stimulate the growth of syntrophic partners and help to form a robust relationship in anaerobic digestion.

Chapter 7. Settled granular activated carbon induced methanogenesis during anaerobic digestion of municipal sewage under sulfate-reducing conditions[6]

7.1. Introduction

Sulfate-reducing bacteria (SRB) are common in anaerobic digestion (AD), participating in the conversion of sulfate to sulfide (Lens et al., 1998). In the presence of sulfate, SRB may outcompete methanogens through at least two mechanisms. First, SRB have more advantageous kinetic properties (lower K_s and higher μ_{max}), and sulfate reduction is thermodynamically more favorable than methanogenesis (Dar et al., 2008; Gavala et al., 2003). Second, sulfides — the end products of sulfate reduction— are toxic to methanogens and other AD microorganisms (Gao et al., 2020). Thus, the existence of sulfate in municipal sewage brings more challenges to AD.

SRB have c-type cytochromes genes and type IV pili, indicating their potential to participate in the direct interspecies electron transfer (DIET) process (Krukenberg et al., 2018). A recent study conducted by Krukenberg et al. (2018) demonstrated the presence of DIET in the sulfate-reducing anaerobic oxidation of methane process, through highly expressed genes encoding for the formation of type IV pili and/or c-type cytochromes in SRB. To date, only a few studies have reported the impact of adding conductive materials

[6] A version of this chapter has been published: Zhang, Y., Guo, B., Zhang, L., Zhang, H. and Liu, Y. (2021). Microbial community dynamics in granular activated carbon enhanced up-flow anaerobic sludge blanket (UASB) treating municipal sewage under sulfate reducing and psychrophilic conditions. *Chemical Engineering Journal*, 405, 126957. https://doi.org/10.1016/j.cej.2020.126957

(CMs) to DIET-based methanogenesis processes under sulfate-reducing conditions (Jin et al., 2019; Li et al., 2017), but with conflicting findings.

This chapter assesses the impact of granular activated carbon (GAC, a commonly used CM) on AD reactor treating municipal sewage at ambient temperature (19 ± 1 °C), with a particular focus on the effects on SRB and methanogens. The dynamics of microbial communities and the possible microbial functions within the AD reactors under sulfate-reducing conditions were investigated. The findings of this chapter provide significant insights into microbial communities in DIET-related AD processes treating municipal sewage under psychrophilic and sulfate-reducing conditions.

7.2. Materials and methods

7.2.1. Reactor operation

Two laboratory-scale plexiglass UASB reactors with a working volume of 4.7 L were operated at a full-scale wastewater treatment plant (WWTP) in Alberta, Canada. The reactors were operated for 105 days at ambient temperature (19.0 ± 1 °C), which were divided into three stages (stages I, II and III) with different hydraulic retention times (HRT, 12, 10, and 8 h). Municipal primary effluent was used as influent, feeding by peristaltic pumps (LongerPump®, BT100-2J, Baoding, China). Anaerobic digester sludge, collected from a full-scale anaerobic digester operated at 35 °C in the same WWTP, was used as the inoculum sludge and fed by glucose and municipal primary effluent for 290 days previously. GAC (25 g/L, 4-12 mesh, Sigma-Aldrich, St. Louis, USA) was added to one of the UASBs following a previous study (Zhang et al., 2020a). Due to the gravity, GAC settled and

packed at the bottom of the reactor, occupying 7% of the working volume. Biogas was collected into a 0.5-L gas bag (CHROMSPEC™, Brockville, Canada).

7.2.2. Specific methanogenic activity

The batch assays were performed to determine the specific methanogenic activity of UASB suspended sludge at the end of each HRT, following the method described by Gao et al. (2019). 5 mL suspended sludge samples, which were collected from each UASB reactor, were used as the seed sludge in the batch test. 10 mL acetate solution (1 g COD/L) as the substrate was mixed with sludge samples in the SMA acetate test, while 10 mL demi water was used in the SMA hydrogen test. After mixing well, the 15 mL mixture was transferred into a serum glass bottle (38 mL). To achieve anaerobic conditions, the headspace of the bottles was flushed with nitrogen gas for acetate SMA or hydrogen gas (80%) and carbon dioxide gas (20%) for hydrogen SMA. Lastly, the bottles were sealed with rubber stoppers and aluminum caps, and placed in a shaker at 120 rpm and ambient temperature (20.0 ± 0.5 °C). Biogas was collected through syringes and analyzed by a gas chromatograph GC-7890B (Agilent Technologies, Santa Clara, USA). All studies were performed in duplicate.

7.2.3. Analytical methods

The wastewater characteristics, including total COD (TCOD), soluble COD (SCOD), total suspended solids (TSS), and volatile suspended solids (VSS), were determined following standard methods (APHA, 2012). The pH was measured by a sympHony pH probe (VWR, Radnor, USA). Sulfate and sulfide concentrations were measured using sulfate reagent powder pillows (SulfaVer® 4, Hach, Loveland, USA) and Sulfide 2 Reagent (Hach method

8131), respectively. Biogas contents (nitrogen, methane, oxygen, and carbon dioxide) were analyzed by a gas chromatograph GC-7890B (Agilent Technologies, Santa Clara, USA), which is equipped with a thermal conductivity detector (TCD) and two columns (Molsieve 5A 2.44 m 2 mm and Hayesep N 1.83 m 2 mm). The temperatures of the oven and detector were 100 and 200 °C, respectively. The gas pressure in batch tests was measured through a hand-held pressure meter (GMH 3151, Regenstauf, Germany).

The headspace method was used to determine the dissolved methane in the effluent once per week, following the method by Zhang et al. (2020a). 10.6 g NaCl was added into a 60 mL glass bottle. Then, the bottle was sealed and UASB effluent (30 mL) was slowly injected into the bottle. The bottle was shaken well to fully mix the salts with the effluent. After 30 min of settling, the pressure meter as mentioned above was used to measure the final headspace pressure, and the gas chromatograph was used to analyze the biogas content. The measurement was performed in duplicate.

7.2.4. Microbial community analysis

Sludge samples, including suspended sludge samples and GAC-biofilm samples, were used for genomic deoxyribonucleic acid (DNA) extraction. Suspended sludge samples (2 mL) were collected from each UASB reactor at the end of each stage, on days 35 (stage I), 70 (stage II), and 105 (stage III). GAC-biofilm sample was only collected at the end of stage III (day 105) from the GAC-amended UASB. The DNeasy PowerSoil Kit (QIAGEN, Germany) was used following the manufacturer's protocol for DNA extraction. Polymerase chain reaction (PCR) was performed following the method described by a previous study (Guo et al., 2020b). Primer pair 515F/806R was used in PCR assay. NanoDrop One

(ThermoFisher, USA) was used to analyze the concentration and contamination of the extracted DNA. The amplicon samples were analyzed by Genome Quebec (Montréal, Canada) using the Illumina PE250 platform.

7.2.5. Data analysis

The demultiplexed raw sequences containing forward and reverse sequences were paired, filtered, and chimera-removed through the QIIME2 pipeline DADA2 algorithm (Callahan et al., 2016; Caporaso et al., 2010). GreenGenes (version 13_8) was used as the reference database to assign the taxonomy with 99% similarity (McDonald et al., 2012b; Werner et al., 2012b). The analysis of microbial communities was performed in R software (version 3.5.3) with “pheatmap” packages. The paired student's t-test was performed to determine the significance of differences. A p-value of less than 0.05 was considered significantly different.

7.3. Results

7.3.1. COD removal

Figure 7.1 shows the total and soluble COD concentrations of the sewage. The influent TCOD concentration fluctuated between 96 and 260 mg/L. The effluent TCOD was 87 ± 27 mg/L in the non-GAC UASB in stage I (HRT of 12 h), whereas it was 60 ± 17 mg/L in the GAC-amended UASB. Correspondingly, the average TCOD removal efficiency was increased from 58 ± 11% to 70 ± 8% with GAC addition ($p < 0.01$). In stage II (HRT of 10 h), the average influent TCOD decreased to 154 ± 35 mg/L. The effluent TCOD was 56 ± 18 mg/L in the non-GAC UASB and 45 ± 14 mg/L in the GAC-amended UASB. The

TCOD removal efficiencies were also statistically different in the non-GAC and GAC reactors (62 ± 9% and 70 ± 8%, respectively, $p < 0.01$). In stage III (HRT of 8 h), TCOD removal efficiencies were 64 ± 4% and 69 ± 3% for the non-GAC and GAC-amended UASB, respectively ($p < 0.01$). Figure 7.1B shows the SCOD concentrations. The influent SCOD concentrations ranged from 41 to 219 mg/L, due to the variation of the wastewater quality at the WWTP. The effluent SCOD concentrations in the GAC-amended UASB were 43 ± 11, 30 ± 11, and 51 ± 18 mg/L in each of the three stages, respectively, whereas in the non-GAC UASB, the effluent SCOD measurements were 63 ± 19, 40 ± 13, and 55 ± 16 mg/L. The removal efficiencies of the GAC-amended UASB were significantly higher than those in the non-GAC UASB in stages I (22% higher) and II (32% higher) ($p < 0.01$). In stage III, the SCOD removal efficiencies in both reactors were comparable: 51 ± 11% and 59 ± 11% in the non-GAC and GAC-amended UASBs, respectively ($p < 0.05$). The differences between the two reactors in COD removal efficiency decreased in stage II and stage III. The possible explanation is that low COD concentration and COD/SO_4^{2-} led to the significantly reduced COD removal in the bioreactors, which reduced the positive impacts of GAC amendment.

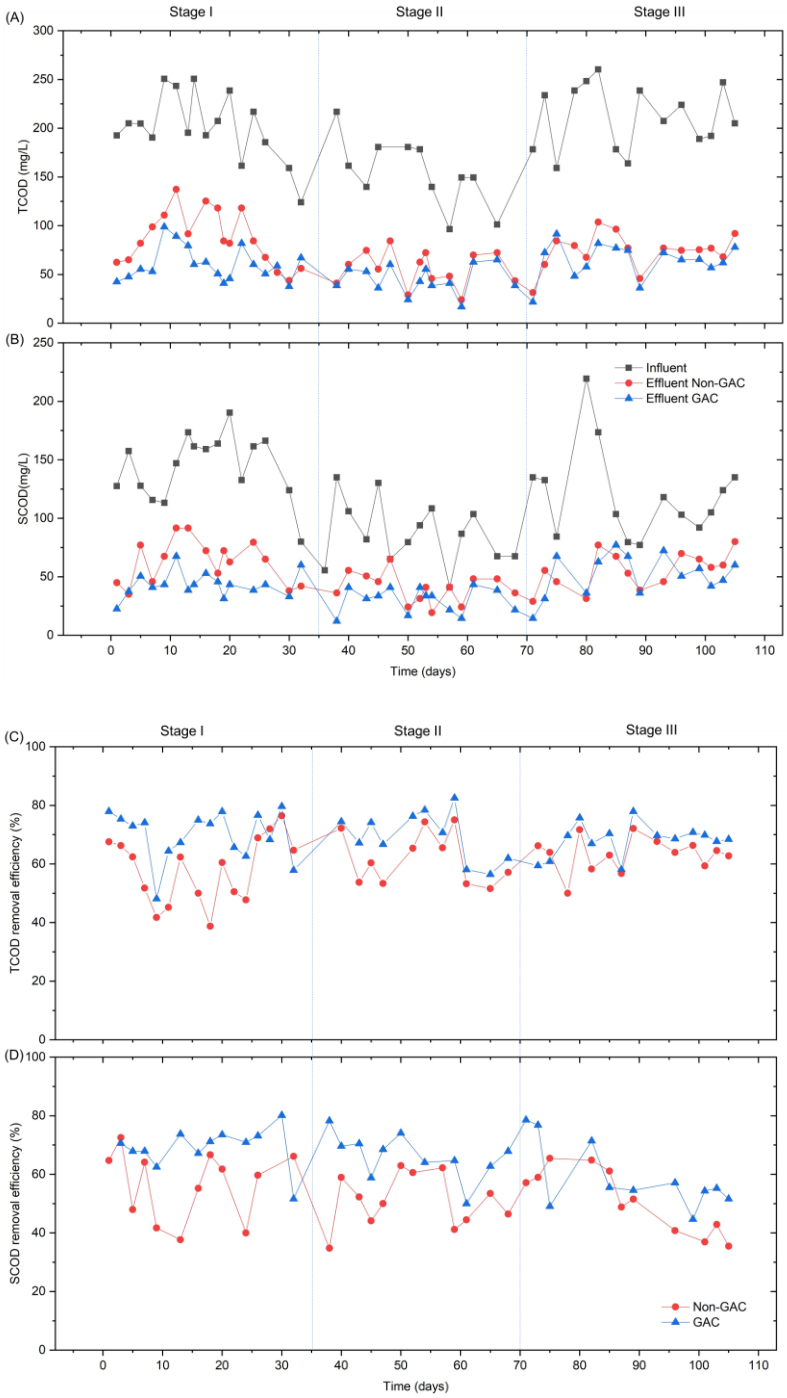

Figure 7.1 (A) Total COD, (B) soluble COD concentrations, (C) total COD removal efficiencies and (D) soluble COD removal efficiencies of the non-GAC and GAC-amended UASBs treating municipal sewage at three stages (HRT 12, 10 and 8 h).

7.3.2. Methane production and SMA

Figure 7.2 shows the total methane production during the operation at three HRTs. With the GAC addition, the total methane production of the GAC UASB significantly increased by 69 to 99%, compared to the non-GAC reactor ($p < 0.05$). At stage II, methane production in both reactors decreased due to a decrease in the influent COD (Figure 7.1A). In biogas, methane and CO_2 occupied 74-80% and 10-15%, respectively. The methane percentage in biogas from the GAC-amended reactor was slightly (1-2%) higher than that obtained from the non-GAC UASB. Determining dissolved methane is necessary at psychrophilic temperatures (< 20°C) because the methane solubility depends on temperature and other factors, such as wastewater salinity (Liu et al., 2014). The dissolved methane was higher in the GAC UASB (ranging from 11 to 30 mg CH_4-COD/L) than that in the non-GAC reactor (ranging from 3 to 17 mg CH_4-COD/L) during the operation, which can be attributed to the higher methane production in the GAC-amended UASB. Dissolved methane represented a substantial fraction (52 - 65%) of the total methane generated, largely due to the high methane dissolution in wastewater under low-temperature conditions studied.

Overall, the average total methane production during the operation in the present study was 19.7 ± 3.1% of the total influent COD in the GAC-amended UASB, and 10.8 ± 0.8% in the non-GAC UASB, respectively. The relatively low COD/SO_4^{2-} ratio in the primary effluent may be the reason for the low methane production. This will be discussed in the next section.

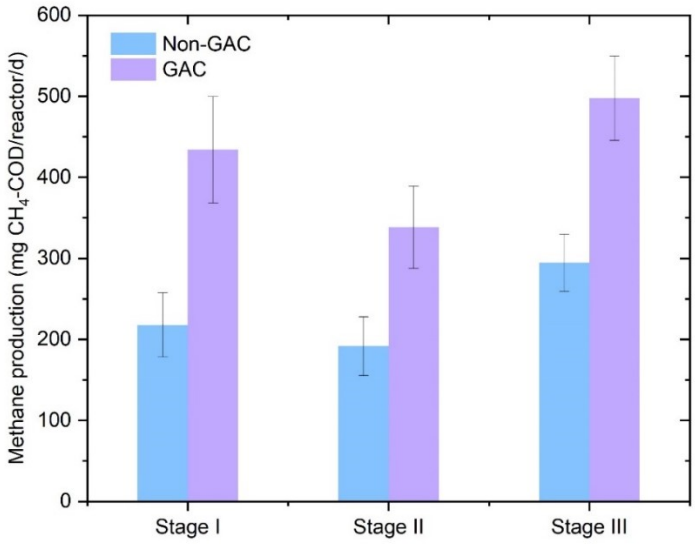

Figure 7.2 Methane production of the non-GAC and GAC-amended UASBs treating municipal sewage at three stages (HRT 12, 10 and 8 h). Error bars represent one standard deviation.

As shown in Figure 7.3, in the non-GAC reactor, the SMA of both acetate and hydrogen decreased during the operation by 22% and 26%, respectively. However, in the GAC-amended UASB, the SMA of acetate decreased by 27%, whereas the SMA of hydrogen increased significantly in stages II and III ($p < 0.05$). SMA in the GAC-amended UASB was significantly higher than that in the non-GAC reactor in all three stages ($p < 0.05$), indicating that the addition of GAC significantly enhanced sludge SMA. The hydrogen SMA enhancement in the GAC-amended UASB can be attributed to the enrichment of bio-electric active hydrogenotrophic methanogens through GAC addition.

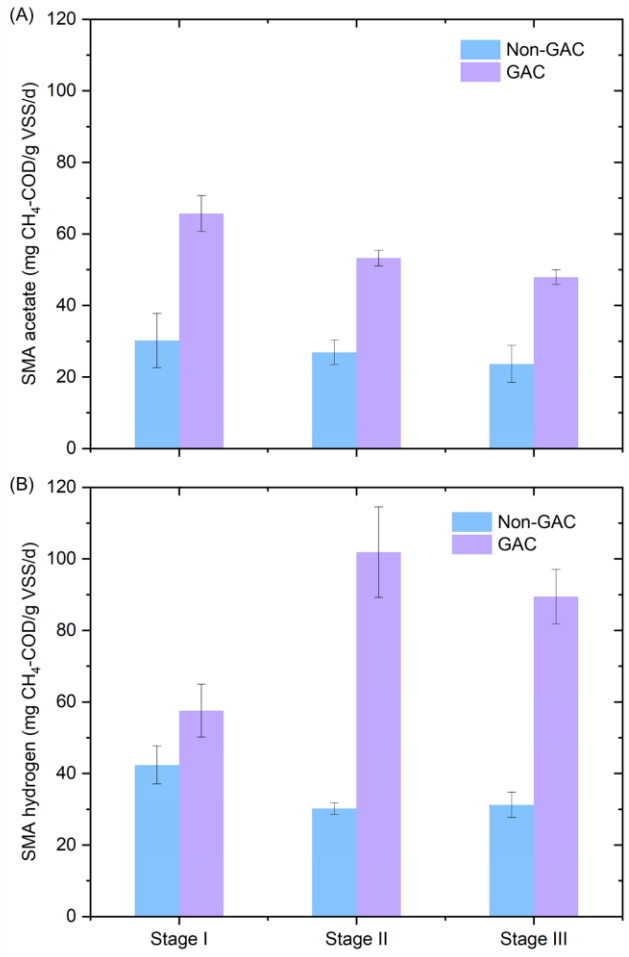

Figure 7.3 (A) SMA acetate and (B) SMA hydrogen of the non-GAC and GAC-amended UASBs treating municipal sewage at three stages (HRT 12, 10 and 8 h). Error bars represent one standard deviation.

7.3.3. SO_4^{2-} removal efficiency

Throughout the operation period, feed water contained a considerable amount of SO_4^{2-}, which ranged between 87 and 160 mg/L during the operation time, resulting in a low COD/SO_4^{2-} ratio (1.8, 1.3 and 1.9 in stages I, II, and III, respectively). Figure 7.4 shows the SO_4^{2-} removal efficiency in the three stages. The average SO_4^{2-} removal efficiency of

the GAC-amended UASB was higher than that of the non-GAC UASB in all stages (84 ± 2%, 80 ± 3%, and 86 ± 3% in the GAC-amended UASB, and 80 ± 3%, 77 ± 4%, and 82 ± 3% in the non-GAC UASB, respectively). Although the differences between reactors were significant in all the stages ($p < 0.05$), the differences were not obvious, which can be attributed to the low SO_4^{2-} loading in the reactors. The total sulfide concentrations in the effluent fluctuated between 19 and 31 mg/L in the non-GAC UASB, whereas in the GAC-amended UASB, the concentrations were between 19 and 37 mg/L. However, the differences between the two reactors were significant in stages I and III ($p < 0.05$) and not in stage II ($p > 0.05$).

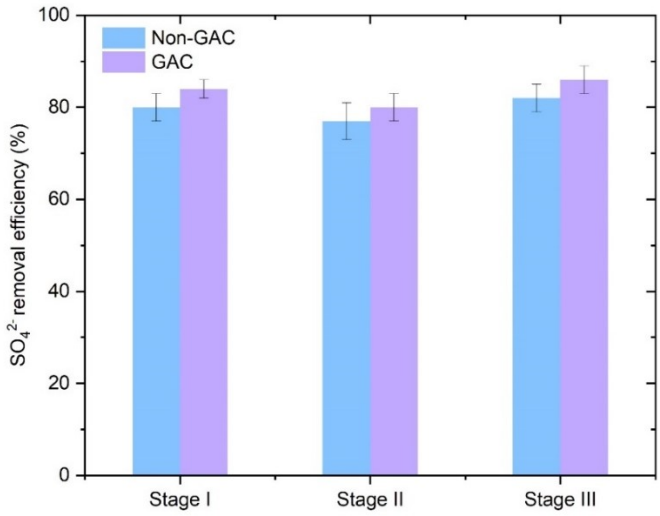

Figure 7.4 SO_4^{2-} removal efficiency of the non-GAC and GAC-amended UASBs treating municipal sewage at three stages (HRT 12, 10 and 8 h). Error bars represent one standard deviation.

7.3.4. COD balance

The overall COD mass balance of the two reactors is shown in Figure 7.5. With the addition

of GAC, methane production and sulfate removal increased by 8.9% and 1.7% in the total COD balance, respectively, while the effluent COD decreased by 8.1%, as compared to the non-GAC reactor. The GAC-amended reactor had 8.6% of influent COD in the discharged sludge and COD accumulation, while in the non-GAC reactor, the value was 10.7%. Around 7% COD was missing in both reactors.

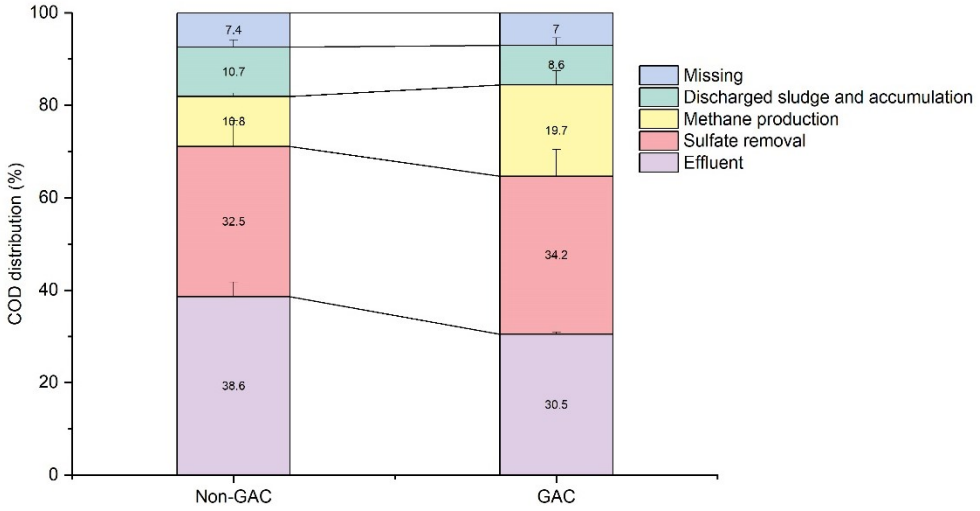

Figure 7.5 Overall COD balance of the non-GAC and GAC-amended UASBs treating municipal sewage. Error bars represent one standard deviation.

7.3.5. Microbial community analysis

7.3.5.1. Archaea

Figure 7.6 shows the relative abundances of archaeal genera. At the genus level, the archaeal communities in the non-GAC reactor during stages I and II were dominated by *Methanosaeta* (29.9% and 26.5%, respectively) and *Methanolinea* (27.1% and 29.5%, respectively). In stage III, *Methanolinea* (27.8%) and an unidentified genus in the family of *Methanomassiliicoccaceae* (19.6%) dominated, followed by *Methanosaeta* (17.6%).

Methanobacterium fluctuated between 7.6% and 12.1%. In the GAC-amended reactor, *Methanobacterium* dominated in all three stages (28.0%, 30.1% and 20.8%, respectively). *Methanosaeta* was the second-most dominant genus in stages I and II, and the third-most in stage III (23.9%, 23.8%, and 16.1%, respectively). *Methanobacterium* (64.8%) dominated in the GAC-biofilm, followed by *Methanomassiliicoccus* (10.5%). The enrichment of *Methanobacterium* in the GAC-biofilm possibly also contributed to the higher abundance of *Methanobacterium* in the suspended sludge in the GAC-amended UASB through biofilm sloughing and inoculation. Further, the development of syntrophic community in the GAC-amended reactor (Figure 7.6) may contribute to the development of the hydrogenotrophic methanogens (e.g., *Methanobacterium*) in both biofilm and suspended sludge. Similar enrichment of *Methanobacterium* has been reported previously (Yang et al., 2017). *Methanosaeta* is considered an important acetoclastic methanogen in anaerobic reactors, while *Methanolinea* and *Methanobacterium* are hydrogenotrophic players (Regueiro et al., 2012; Sakai et al., 2012; Tejerizo et al., 2017). The decreases in relative abundances of *Methanosaeta* in both reactors, as well as the dominated *Methanolinea* and *Methanobacterium,* indicated shifts towards hydrogenotrophic methanogenesis. This is consistent with previous studies, which investigated anaerobic bioreactors under psychrophilic conditions (Bialek et al., 2014; McKeown et al., 2009; O'Reilly et al., 2010). Hydrogenotrophic methanogenesis is less temperature-sensitive than acetoclastic methanogenesis, and is thermodynamically more favorable at low temperatures (Gao et al., 2018; Guo et al., 2020b). Meanwhile, gas solubility increases with reduced temperature, possibly leading to increased levels of hydrogen in reactor liquor (Lettinga et al., 2001a).

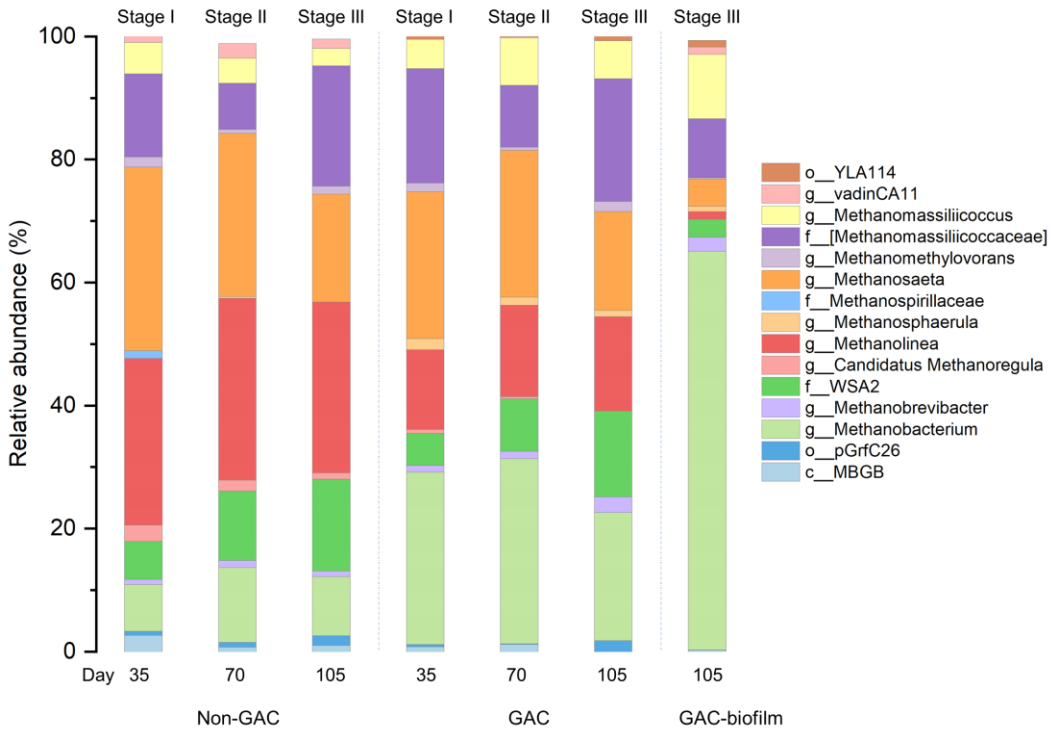

Figure 7.6 Relative abundances of archaeal genera with abundances > 1% in the non-GAC and GAC-amended UASB suspended sludge at the end of three stages (HRT 12, 10 and 8 h) and GAC-biofilm at the end of stage III (HRT 8h). Unidentified genera were named at family (f__), class level (c__), or order level (o__).

7.3.5.2. Bacteria

At the family level, *Syntrophaceae*, an unclassified family from the order *Bacteroidales*, *Desulfobacteraceae*, *Desulfobulbaceae*, *Desulfomicrobiaceae*, and *Desulfovibrionaceae* dominated in both reactors. The addition of GAC enriched *Geobacteraceae*. At the genus level, an unclassified genus from *Bacteroidales*, some SRB (*Desulfobacter*, unclassified genus from *Desulfobulbaceae*, *Desulfomicrobium*, *Desulfovibrio*), *Syntrophus*, and *Syntrophaceae* were dominant in both reactors (Figure 7.7). Although there were fluctuations during the operation, GAC-amended UASB suspended sludge exhibited

higher abundances of SRB and syntrophic bacteria compared to non-GAC UASB suspended sludge. The abundance of *Geobacter*, the key indicator of the DIET process, ranged from 0.3 to 0.7% in the non-GAC reactor and 1.2 to 1.7% in the GAC-amended UASB. The GAC-biofilm showed a higher enrichment of *Geobacter* (4.9%).

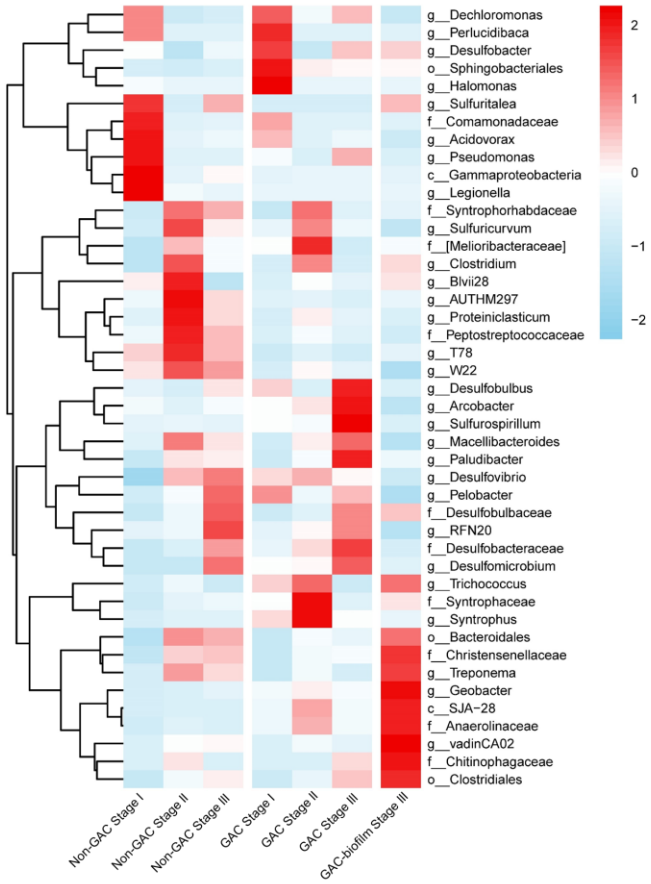

Figure 7.7 Relative abundances of bacteria at the genus level (> 1% in any sample) in the non-GAC and GAC-amended UASB suspended sludge at the end of three stages (HRT 12, 10 and 8 h), and GAC-biofilm at the end of stage III (HRT 8h). Unidentified genera were named at family (f__), class level (c__) or order level (o__).

7.4. Discussion

7.4.1. Microbial community shifted with GAC addition

The results of this study showed that the anaerobic digestion of municipal sewage could be enhanced with GAC addition, likely caused by the development of a more robust and active microbial community, resulting in the enhanced COD removal and CH_4 production. *Geobacter* has been demonstrated to be highly correlated with bio-conductivity in methanogenic digesters and has been considered the DIET-indicator, and the enrichment of *Geobacter* might be one of the important reasons for the enhancement of AD process (Shrestha et al., 2014; Zhao et al., 2016c). In this study, *Geobacter* was highly enriched in the GAC-biofilm (4.9%) and suspended sludge (1.2-1.7%) in the GAC-amended UASB compared to suspended sludge in the non-GAC UASB (< 0.7%) (Figure 7.7). Furthermore, previous studies on the treatment of simple substrates, such as ethanol, demonstrated enrichment of *Geobacter* in CMs-amended AD (Yin & Wu, 2019). However, when treating complex substrates, the addition of CMs to AD reactors may not necessarily enrich the *Geobacter*. For instance, a recent study demonstrated that adding GAC to AD enriched *Geobacter* in a batch reactor (Florentino et al., 2019a). However, when food waste and fresh leachate were used as the substrates, *Geobacter* was low (< 0.1%) or even undetectable with the addition of CMs (Dang et al., 2017; Lei et al., 2016). Different substrates and operational conditions result in different intermediates. Previous studies demonstrated that the presence of alcohol might benefit the enrichment of *Geobacter*, whereas propionate and butyrate cannot stimulate their growth (Zhao et al., 2016c). Thus, different intermediates from complex substrates can affect the growth of *Geobacter*.

Syntrophus, a well-studied model microorganism for interspecies H_2 or formate transfer, was the most abundant syntrophic bacteria in this study. A previous study demonstrated that *S. aciditrophicus* can produce e-pili, and has been shown to grow with *G. sulfurreducens* through the DIET pathway (Walker et al., 2020). Although the syntrophic bacteria have not been proven to participate in DIET with methanogens, the growth with *G. sulfurreducens* demonstrated that common hydrogen-donating syntrophs have the function of direct electron transfer (Walker et al., 2020). In our study, *Syntrophus* was the second-most dominated bacteria in the GAC-amended UASB with a higher abundance in the suspended sludge (4.4-11.0% and 2.2-2.8% in the GAC-amended and non-GAC UASB, respectively, Figure 7.7). The enrichment of *Syntrophus* in this study was similar to a previous study treating propionate with biochar addition, which is helpful to metabolize organic acids to acetate and H_2 (Zhao et al., 2016a). Moreover, our previous study suggested *Syntrophus* was electro-active and associated with DIET through RNA community analysis (Guo et al., 2020b). These results demonstrated that *Syntrophus* might accelerate the conversion of organic acids and contribute to the better performance for COD removal and methane production.

Further, although hydrogenotrophic methanogenesis dominated in both reactors, the abundant genera were different. *Methanobacterium* dominated in the GAC-amended UASB, both in the suspended sludge (20.8-30.1%) and GAC-biofilm (64.8%), which is consistent with our previous study (Guo et al., 2020b). In the non-GAC UASB, *Methanobacterium* only accounted for 7.6 to 12.1%. These results might correlate with higher SMA and methane production in the GAC-amended UASB. Interestingly, *Methanobacterium* can be enriched in the cathode biofilm in bioelectrochemical AD

systems and might participate in the direct electron acceptance for methane production (Cheng et al., 2009; Pozo et al., 2015; Siegert et al., 2015). Salvador et al. (2017) found that the methane production rates in pure cultures of *M. formicicum* can be enhanced by up to 17 times with the addition of carbon nanotubes. The authors attributed the improvement to negative redox potentials in the anaerobic microcosms with the addition of CMs, which was independent of other possible mechanisms that may enhance methane production, such as DIET. In another batch treating wasted activated sludge, the relative abundance of *Methanobacterium* in the GAC-biofilm increased by 7-folds compared to suspended sludge in the non-GAC reactor (Yang et al., 2017). These findings help to explain the observed enrichment of *Methanobacterium* by GAC in our study that *Methanobacterium* probably has electro-activity and can be stimulated by GAC-induced DIET environment.

7.4.2. GAC enhanced methanogens in sulfate reduction communities

In our study, we observed that SMAs of acetate and hydrogen in GAC-amended UASB were higher than those in non-GAC UASB. It was also noted that, with the establishment of sulfate reduction communities in stages II and III, both acetate and hydrogen SMAs were reduced in the non-GAC reactor, but only the acetate SMA reduced in the GAC-amended UASB. The hydrogen SMA in the GAC-amended UASB increased in stages II and III, which may be attributed to the enrichment of highly DIET-active microbes through GAC. Similarly, recent studies have demonstrated that without the presence of SO_4^{2-}, both acetate and hydrogen SMAs can be improved in UASB with the addition of GAC (Guo et al., 2020b). The stimulated hydrogenotrophic methanogen activities even under the sulfate

reduction environment in the current study indicate that hydrogenotrophic methanogens are more robust than acetoclastic methanogens to compete for electrons in the AD process.

The current study also showed a slightly 5% higher in sulfate removal and a higher abundance of SRB (31% higher) in the GAC-amended UASB compared to the non-GAC UASB, which suggested GAC possibly affected SRB and may shift their pathways. SRB have been confirmed to have an electroactive nature with the ability to generate electricity and perform extracellular electron transfer in microbial fuel cells (Kang et al., 2014; Miran et al., 2017). The encoding and expression of e-pili and c-type cytochromes genes implied the possibility of SRB participating in DIET (Fritz et al., 2001; Krukenberg et al., 2018). Currently, SRB have only been considered to enable DIET in a co-culture system with a methanotrophic archaeon (Krukenberg et al., 2018; Lovley, 2017). However, because various substrates can be utilized by SRB, diverse syntrophic metabolisms occur in sulfate-reducing environments (Sieber et al., 2012). DIET is a likely option for common hydrogen-donating syntrophic metabolisms (Walker et al., 2020). Hence, DIET may occur in these diverse SRB syntrophic metabolisms and be stimulated through GAC, leading to a greater efficiency of sulfate reduction and the enrichment of SRB.

Compared to the suspended sludge in both reactors (1.0-3.7%), GAC-biofilm showed a much higher abundance of methanogens (10.4%) in the total microbial community. This may demonstrate that GAC stimulates more methanogens over SRB, even though SRB can also possess genes of e-pili and transcribe as well, resulting in a protective effect on methanogens under sulfate-reducing conditions.

7.5. Conclusion

This chapter demonstrated that COD and CH_4 production were simultaneously enhanced by the addition of GAC in the anaerobic treatment of municipal sewage under sulfate-reducing and psychrophilic conditions. GAC shifted the microbial community and enriched DIET/potential DIET syntrophic partners, i.e. *Geobacter*, *Syntrophus*, *Methanobacterium*, and SRB. Furthermore, GAC showed a protective effect on methanogens and enhanced methanogenic activity. Our results suggest that GAC may stimulate potential bio-electric activities to enhance the AD process under sulfate-reducing and psychrophilic conditions.

Chapter 8. Granular activated carbon and operational factors influenced active microbiome development during anaerobic digestion of municipal sewage[7]

8.1. Introduction

The enhancement of granular activated carbon (GAC) addition on anaerobic digestion (AD) of municipal sewage has been reported in Chapters 6 and 7. However, the differences between the non-GAC and GAC-amended reactors decreased during the operation. Similar to other treatment options, conductive materials (CMs) addition cannot guarantee enhanced methane recovery; understanding the limitations of CMs amended AD is critical for future process design and control. For instance, Florentino et al. (2019b) reported that when treating 5 L and 9 L water-flushed blackwater, CMs addition did not improve methane production in the tests of biochemical methane production (BMP). Unfortunately, in comparison to the number of reported studies on the successful implementation of CMs in AD for methane recovery, information on the limited or marginal impacts of CMs amendment on AD performance is scarce and is often eliminated in the literature; the potential reactor design and extrinsic engineering operational factors that may interfere with the DIET mechanisms in AD have not been described.

In addition, the understanding of active microorganisms involved in the CMs

[7] A version of this chapter has been published: Zhang, Y., Guo, B., Dang, H., Zhang, L., Sun, H., Yu, N., Tang, Y. and Liu, Y. (2022). Roles of granular activated carbon (GAC) and operational factors on active microbiome development in anaerobic reactors. *Bioresource Technology*, 343, 126104. https://doi.org/10.1016/j.biortech.2021.126104

amended AD reactors is still limited. Previous studies on mixed microbial communities largely focused on the most abundant microorganisms and microbial community diversity identified based on the 16S rRNA gene amplicon sequencing. However, high abundance cannot infer functional significance, and microbial population diversity does not directly correlate to the process performance and stability (Li et al., 2015b), underlining the importance of assessing active and functionally important microorganisms. The mass balance model has been used to identify active microbes and explain microbial population dynamics by growth, sludge input, and output (Guo et al., 2021; Mei et al., 2016). In this model, the specific growth rate (μ) of microbes would be calculated. Positive and negative μ represent active or inactive during a period, respectively. The identification of active microbes and related function analysis can be further used to understand DIET in AD.

This chapter identifies active microbes using the mass balance model in continuously operated UASBs with or without GAC treating municipal sewage at ambient temperature (14.5-20 °C). The impacts of GAC addition on AD were described under different operational conditions, which were further linked to the active microbes and functions in AD, and their response to extrinsic operational factors, including GAC addition, as well as concentrations and loadings of chemical oxygen demand (COD) and sulfate. The understanding of microbial evolution in DIET may help to elucidate underlying microbial driving forces and to guide engineered DIET-related reactor design and operation.

8.2. Materials and methods

8.2.1. Reactor operation

Two laboratory-scale up-flow anaerobic sludge blankets (UASB) reactors were operated at ambient temperature (14.5-20 °C) in a reactor operation facility residing in a full-scale centralized municipal wastewater treatment plant (WWTP) in Alberta, Canada. Primary effluent (PE) from the full-scale municipal wastewater treatment plant was used as the reactor influent without storage and was pumped into the UASBs with peristaltic pumps (LongerPump®, BT100-2J, Baoding, China). The working volume of each UASB was 4.7 L. GAC (4-12 mesh, Sigma-Aldrich, St. Louis, USA) was added into one of the UASBs with a concentration of 25 g/L of reactor volume at the beginning. GAC settled down to the bottom of the reactor due to the gravity, which occupies ~ 7% of the UASB reactor volume. GAC was not disturbed or regenerated during the operation. Inoculum sludge for both UASBs was collected from a laboratory-scale UASB sludge fed with glucose (Zhang et al., 2020b). Both UASBs were operated for 225 days under six hydraulic retention times (HRTs) (36, 24, 16, 12, 10, and 8 h, stage I, II, III, IV, V, and VI, accordingly).

8.2.2. Sample collection, DNA extraction, and 16S rRNA gene sequencing

Suspended sludge samples (2 mL) were harvested from each UASB reactor on day 30 (stage I), days 59 and 80 (stage II), days 92, 103, 115, and 120 (stage III), day 155 (stage IV), day 190 (stage V), and day 225 (stage VI). The samples at the end of each stage were considered in the steady state. The DNeasy Power-Soil Kit (QIAGEN, Hilden, Germany) was used to extract genomic DNA following the manufacturer's protocol. The polymerase

chain reaction (PCR) was performed with primer pair 515F/806R following the procedure in the previous study (Guo et al., 2020b). The concentration and quality of extracted DNA were checked using NanoDrop One (ThermoFisher, Waltham, MA). All samples were sent to Genome Quebec (Montréal, Canada) to be analyzed on the Illumina Miseq PE250 platform.

8.2.3. Bioinformatics analysis

The QIIME2 pipeline DADA2 algorithm was used to pair forward and reverse sequences, and to filter and remove low-quality sequences and chimeras (Bolyen et al., 2019; Callahan et al., 2016). The reference database (GreenGenes, version 13_8) was used to assign the taxonomy using 99% similarity (McDonald et al., 2012b; Werner et al., 2012b). Microbial communities were analyzed in R software (version 4.0.2). The heatmap was produced using "pheatmap" package (Kolde & Kolde, 2015). The correlation between active microbes/function annotations and reactor performance was analyzed using the "corrplot" package (Wei et al., 2017). Bray-Curtis distance and the Mantel test were performed through "vegan" package (Oksanen et al., 2017). Functional annotation was used "Functional Annotation of Prokaryotic Taxa" (FAPROTAX) (Louca et al., 2016). Generalized linear models (GLM) were performed using R (Hardin et al., 2007). R packages "ggplot2" and "ggrepel" were used to prepare figures presented in this manuscript (Slowikowski, 2018; Wickham, 2016). A p-value of less than 0.05 was considered to be significant.

8.2.4. Mass balance analysis

The approximate mass balance model was used to identify active microbes in reactors (Guo et al., 2021; Mei et al., 2016). In this study, the mass balance equation was used as follows:

$$\frac{dN_{x,AD}}{dt} = \mu_x N_{x,AD} + n_{x,PE} - n_{x,waste\ sludge} \qquad \text{(Equation 8.1)}$$

where

$N_{x,AD}$ number of microorganism x in AD

μ_x specific growth rate for microorganism x [d^{-1}]

$n_{x,PE}$ number of microorganism x in primary effluent entering AD per day [d^{-1}]

$n_{x,waste\ sludge}$ number of microorganism x in wasted sludge leaving per day [d^{-1}]

When the calculated μ_x is greater than zero, the microorganism x is considered active in the reactor.

8.3. Results and discussion

8.3.1. COD removal efficiencies and CH_4 production

During the 225 days' operation, COD and SO_4^{2-} concentrations in wastewater fluctuated, with the notable changes in the COD/SO_4^{2-} ratios in stages I to VI, which were 2.9, 2.9, 1.7, 1.8, 1.3, and 1.9, respectively. The COD removal efficiencies and CH_4 production of the UASBs are shown in Table 8.1. It can be observed that the average COD removal efficiencies ranged from 69 to 83 for GAC-amended UASB and ranged from 58 to 66 for UASB without GAC addition. The corresponding average methane production ranged

from 157 to 498 mg CH_4-COD/d in the GAC-amended reactor and from 80 to 295 mg CH_4-COD/d in the non-GAC reactor. GAC addition enhanced reactor performance in all stages ($p < 0.05$). The dramatic enhancement was consistent with previous studies (Liu et al., 2021b; Yu et al., 2020; Zhang et al., 2021a). For instance, Yu et al. (2020) found that methane production can be more than doubled with GAC addition in UASBs. Zhang et al. (2021a) found that GAC addition can enhance the co-digestion of blackwater and kitchen waste. When treating butanol octanol wastewater, GAC addition promoted DIET and increased methane production by ~ 100% (Liu et al., 2021b). These observations indicated that CMs addition is a promising strategy for the enhancement of AD performance.

Table 8.1 Average total COD removal efficiencies and methane production of the non-GAC UASB and the GAC-amended UASB treating municipal sewage in six stages with different HRTs

	Stage I	Stage II	Stage III	Stage IV	Stage V	Stage VI
HRT(h)	36	24	16	12	10	8
COD removal (%)						
GAC-amended UASB	83±6	77±4	71±5	70±8	70±8	69±3
Non-GAC UASB	65±10	66±6	59±5	58±11	62±9	64±4
Methane production (mg CH_4-COD/d)						
GAC-amended UASB	252±34	157±39	247±18	434±65	338±51	498±52
Non-GAC UASB	80±53	80±35	103±6	218±40	192±36	295±35

However, the extent of enhancement decreased during the operation. As an example,

the average methane yield in the GAC-amended reactor was 2.14 times greater than that in the non-GAC reactor in stage I; but was only 0.69 times higher than that in the non-GAC reactor in stage VI. The details of operational conditions and performance of the UASBs have been presented in Chapter 6 and Chapter 7.

8.3.2. Abundant microbial community structures

The most abundant (relative abundance >1% in all stages) amplicon sequence variants (ASVs) in microbial communities of the two reactors revealed five ASVs in each reactor (Figure 8.1). Hence, they are the most abundant genera and appear to be the functionally significant genera. Three ASVs were shared by the two reactors, i.e., o_Bacteroidales, *f_Syntrophaceae*, and *Syntrophus*. *T78* and *W22* were the most abundant genus only in the non-GAC reactor, while *Geobacter* and *Treponema* were abundant only in the GAC-amended reactor.

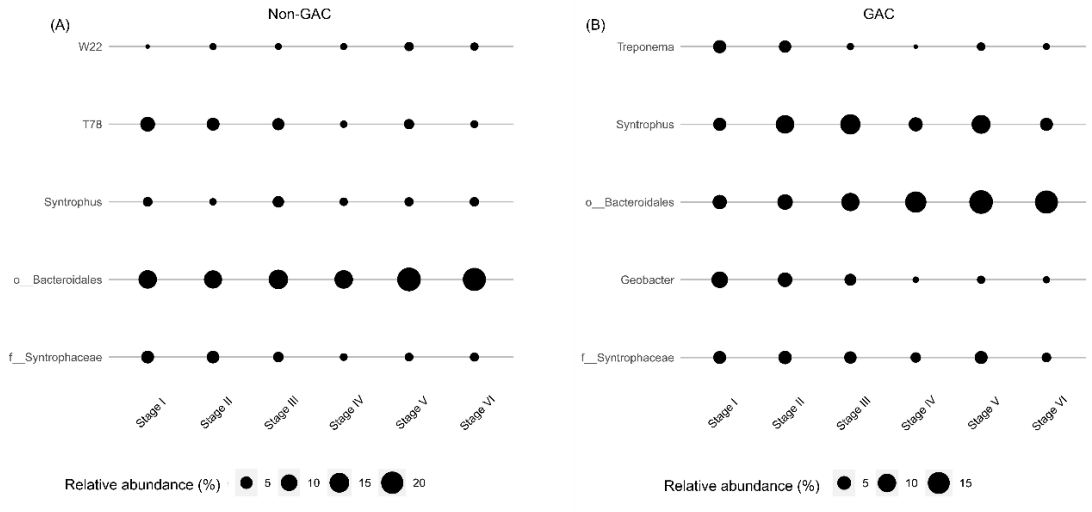

Figure 8.1 Temporal changes in the relative abundance of ASVs (> 1% in all stages, genus level) in the UASBs, (A) non-GAC, and (B) GAC-amended. Unidentified genera were

named at family (f__) or order level (o__).

ASVs belonging to the most abundant genera (> 1%) at least in one of the stages were identified (Figure 8.2). In total, 52 ASVs were identified in the non-GAC UASB and 53 ASVs were identified in the GAC-amended UASB. 41 ASVs were shared by the two reactors. These quantities of ASVs were much higher than the quantities of ASVs belonging to the most abundant genera in all stages, indicating that the microbial community is highly dynamic, and microbes grow instantly and opportunistically under different operation conditions.

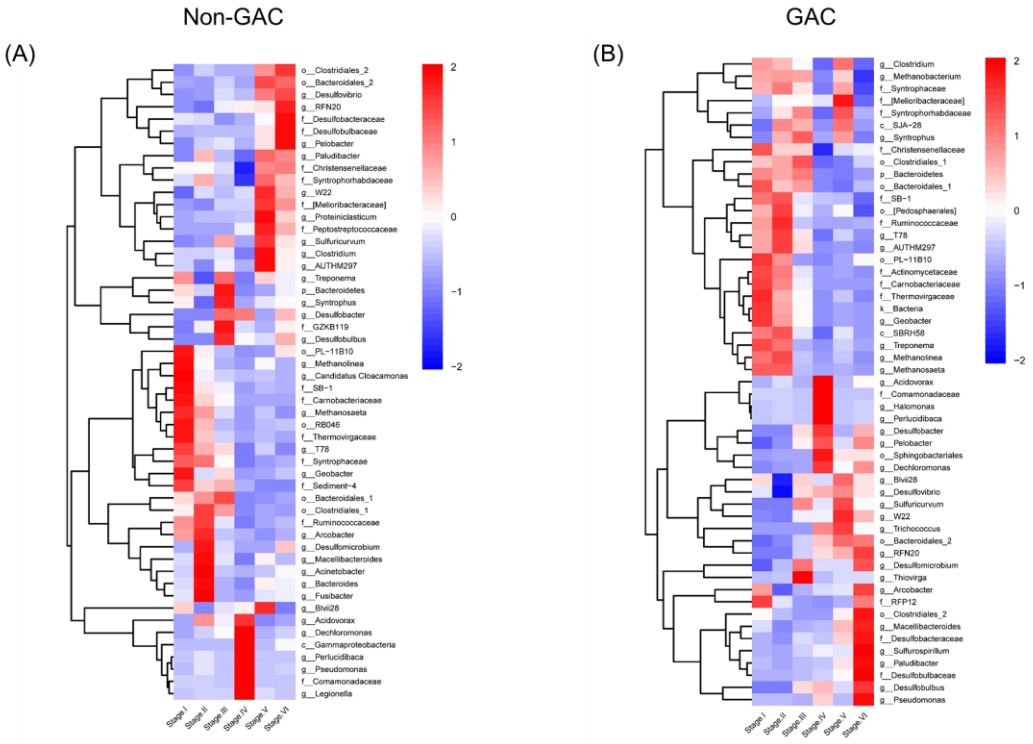

Figure 8.2 Temporal changes in the relative abundance of ASVs belonging to the most dominant genera (> 1% in relative abundance) at least in one of the stages, (A) non-GAC UASB, (B) GAC-amended UASB. Unidentified genera were named at family (f__), order

(o__), class (c__), phylum (p__) and kingdom (k__) level.

8.3.3. Active microbial community structures

Figure 8.3 shows the frequency distribution of active ASVs identified through the mass balance model at the genus level in the total community in the six stages. In total, 635 and 592 ASVs existed at the end of six stages in the non-GAC and GAC-amended UASB, respectively. Overall, the two reactors had similar frequency distributions. The active ASV frequencies with 0% (the ASV was inactive in all stages), 16.7% (the ASV was active only in one stage), 100% (the ASV was active in all stages) were accounted as the most three frequencies, and each was around 20% of the total numbers of ASVs. The rest accounted for around 40%.

The active ASVs with 100% frequency might play the most important roles in the reactors during the operation. In total, 129 and 112 ASVs were identified to be active in all stages in the non-GAC and GAC-amended UASBs, respectively, and 92 ASVs were shared by the two reactors. Although the numbers of these active ASVs only can be accounted for 20.3% and 18.9% of the total numbers of ASVs in the non-GAC and GAC-amended reactors, respectively (Figure 8.3), their relative abundance can be accounted for between 43.4% and 75.3% in the non-GAC UASB, 58.7% and 77.9% in the GAC-amended UASB, indicating they appeared to be more abundant in the total microbial community.

However, the most abundant ASVs did not represent active ASVs completely. For instance, *W22* was one of the most abundant microbes in the non-GAC reactor in all stages (Figure 8.1). However, it was inactive in all stages, indicating that other factors (e.g., influent accumulation) functioned on this ASV. Other abundant microbes in the two

reactors (> 1% in relative abundance in all stages, Figure 8.1) were active in all stages. Meanwhile, the numbers of active ASVs with relative abundance > 1% at least in one stage were 30 and 29 in the non-GAC and GAC-amended UASBs, respectively, which were much less than the numbers of the most abundant ASVs with relative abundance > 1% at least in one stage (52 and 53, respectively). These results indicated that ASVs with relatively high abundance might be inactive during the reactor operation.

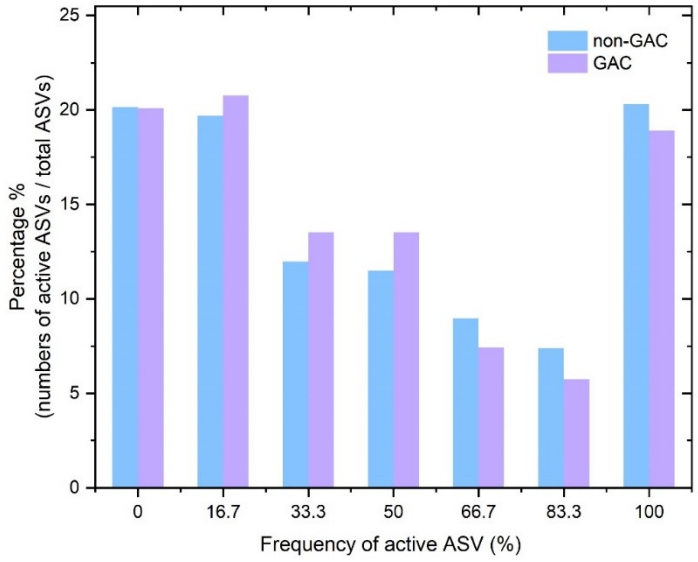

Figure 8.3 Frequency distribution of active ASVs in the total community during the six stages.

Figure 8.4 shows the active ASVs with relative abundance higher than 0.1% of the two reactors in all stages. According to previous studies, the ASVs with low relative abundance (< 1%) might play important roles in anaerobic digestion (e.g., syntrophic bacteria) (Yin et al., 2019; Yin & Wu, 2019), and should be considered. Meanwhile, the transient abundant ASVs might be important under certain conditions; and the active and consistent ASVs might be more important to the whole operation. In total, 38 and 33 ASVs

were identified from the non-GAC and GAC-amended UASBs, respectively. Although these numbers only can account for 29.5% of the total numbers of active ASVs in all stages, their relative abundance can account for 78.5% to 86.2% of the active ASVs in all stages. Nearly 70% of active ASVs in the two reactors represented less than 0.1% relative abundance at least in one of the stages. In addition, 29.5% (non-GAC UASB) and 25% (GAC-amended UASB) of active ASVs were less than 0.1% in relative abundance in all stages. The functions of these active ASVs were neglected frequently, requiring further study.

Specifically, the active ASVs (> 0.1% in relative abundance) in the two reactors were divided into several subgroups according to temporal changes in their relative abundance (Figure 8.4). *Methanosaeta* and *Geobacter* were enriched with higher relative abundances in stages I and II and decreased since stage III. Sulfate-reducing bacteria (SRB, e.g., *Desulfobacter*) were enriched in both reactors. *Methanobacterium*, which has been recently shown the ability to participate in DIET (Zheng et al., 2020), was only identified in the GAC-amended UASB. Although it was active in all stages in the non-GAC UASB, the maximum relative abundance was only 0.27% and the minimum was below 0.1% in the total microbial community.

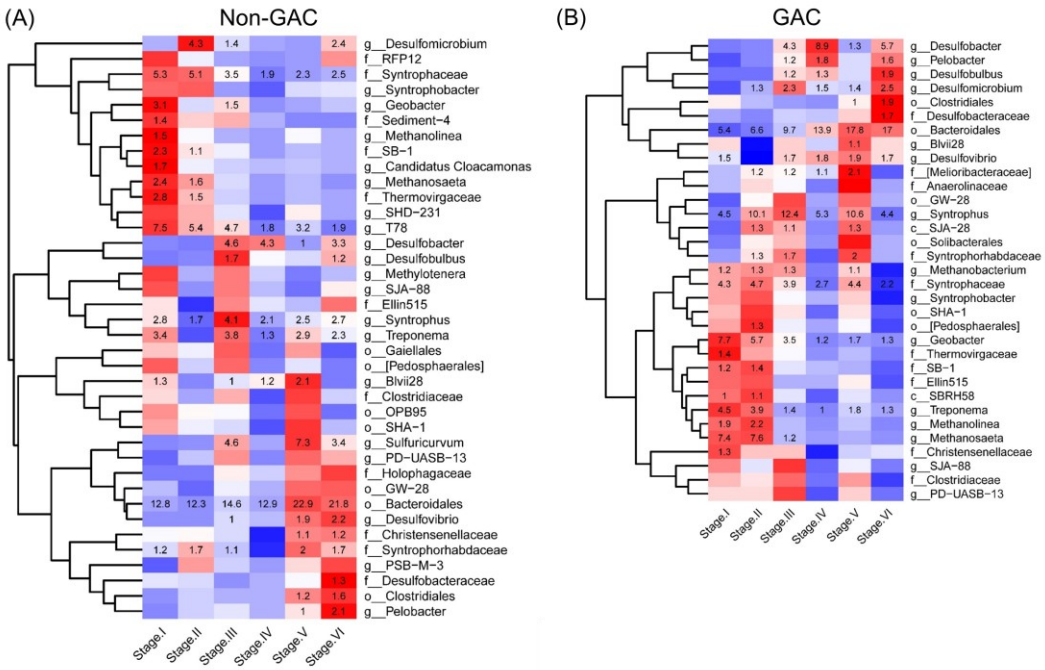

Figure 8.4 The relative abundance (> 0.1% in all stages) of active ASVs with 100% frequency at genus level, (A) non-GAC UASB, (B) GAC-amended UASB. Unidentified genera were named at family (f__), order (o__), and class (c__) levels. The numbers of relative abundances (> 1%) were presented in the figure.

8.3.4. Function annotation and correlations with reactor performance

To further explore the functional characteristics of active ASVs during the operational period, Functional Annotation of Prokaryotic Taxa (FAPROTAX) was applied to annotate the putative function of the active ASVs (Louca et al., 2016). In total, 27 functions were annotated in the two reactors. Sulfate respiration, methanogenesis, iron respiration (only *Geobacter* were identified in this category), fermentation, and chemoheterotrophy are considered important to the anaerobic process, and the changes in relative abundance are

shown in Figure 8.5A. The functions (e.g., human pathogens) with less importance in this study were not shown. Although there were fluctuations during the operation, these functions in the GAC-amended UASB were higher than those in the non-GAC UASB in most stages (Figure 8.5A), indicating the enhancement of GAC addition. Furthermore, methanogenesis function was clustered with iron respiration function, revealing the tight relationship between methanogens and *Geobacter*. Sulfate respiration was not clustered with other functions directly, revealing the low significance of sulfate respiration in the microbial functions in the present systems.

Several parameters, such as methane production and COD removal efficiency, might be used to evaluate the performance of AD reactors. As methane production was low in this study due to the low COD/SO_4^{2-} ratios, the COD removal efficiency was considered to be the most relevant parameter to evaluate reactor performance. As shown in Figure 8.5B, methanogenesis, iron respiration, and chemoheterotrophy were positively correlated with COD removal ($r > 0.7$, $p < 0.01$), implying their importance in reactor performance. Fermentation was also positively correlated with COD removal ($r = 0.4$), but not significant ($p > 0.05$). The function of sulfate respiration was negatively correlated with COD removal ($r = -0.2$, $p > 0.05$). In addition, methanogenesis, iron respiration, fermentation, and chemoheterotrophy were positively correlated with each other, implying the cooperation among the microbes with these functions. Sulfate respiration was negatively and significantly correlated with methanogenesis ($r = -0.6$, $p < 0.05$), which indicated the intense competition between methanogens and SRB, although syntrophic partnerships between these two microbes have been reported in DIET-related reactors and SRB can be enriched in the CMs-amended UASB (Xing et al., 2020). The correlation between iron

respiration and methanogenesis was strongly positive (r = 0.9, $p < 0.001$). These results illustrate that the development of *Geobacter* might be the key that correlated with the best performance in this system.

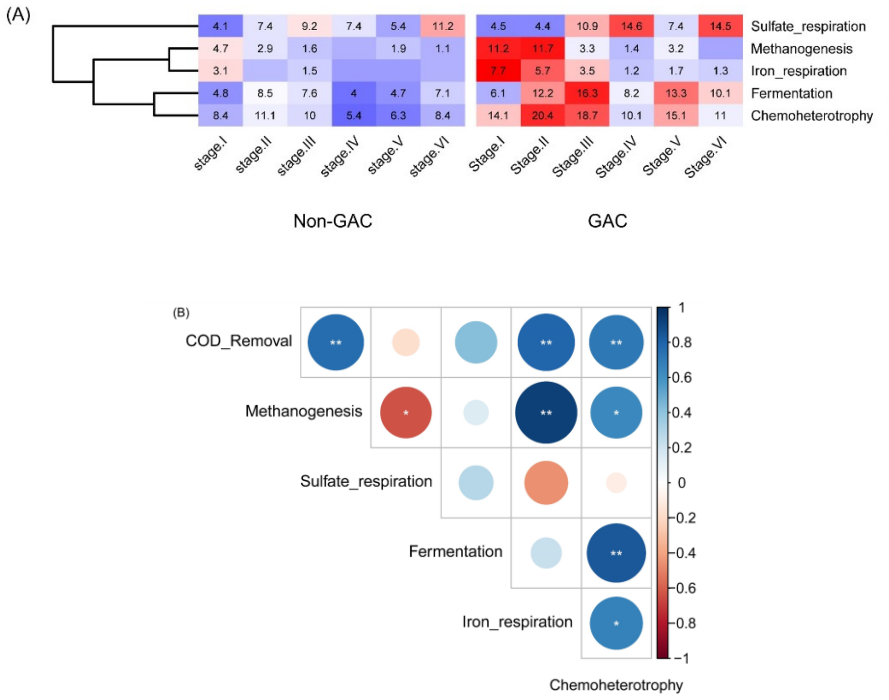

Figure 8.5 (A) Function annotation using FAPROTAX (Functional Annotation of Prokaryotic Taxa) based on the active microbes in all stages in the non-GAC and GAC-amended UASBs. The numbers of relative abundances (> 1%) were presented. (B) the correlations of function annotations with reactor performance.

8.3.5. Correlations of microbial community compositions with operational factors

To further explore the driving forces for the changes in microbial communities and functions, the Mantel test was conducted to identify important extrinsic engineering operational factors in shaping community variations in the two reactors (Table 8.2). The

concentrations of influent total COD (TCOD), soluble COD (SCOD), and SO_4^{2-}, HRT, sludge retention time (SRT), COD and SO_4^{2-} loading, and influent COD/SO_4^{2-} ratio were used. Overall, these factors were positively correlated to the microbial community variations in the two reactors ($r = 0.47$, $p < 0.01$). Specifically, SO_4^{2-} loading and influent TCOD were correlated to microbial community variations significantly with higher r values ($r > 0.5$, $p < 0.01$), indicating these two factors might play more important roles in the shaping of microbial communities. Other factors (i.e., influent SCOD, HRT, COD/ SO_4^{2-} ratio, and SRT) were also positively correlated well to the microbial community variations ($r > 0.4$).

Table 8.2 Mantel correlations highlight the relationships between operational factors and microbial community compositions in the UASBs

Operational factors	Mantel score (r)	P-value
All the factors	0.47	0.001
Influent TCOD	0.5335	0.001
Influent SCOD	0.4582	0.002
Influent SO_4^{2-}	0.3463	0.003
COD loading	0.2921	0.046
SO_4^{2-} loading	0.5496	0.001
HRT	0.4958	0.002
Influent COD/SO_4^{2-} ratio	0.4093	0.01
SRT	0.4181	0.008

Relative abundances of the shared active 92 ASVs presented in both reactors in all stages and these operational factors of the bioreactors were processed with GLM to investigate the extent of those operational factors affecting the active ASVs (Figure 8.6). The impact of GAC addition on the shared active 92 ASVs was not the most important factor according to the response beta values (Figure 8.6). In total, GAC addition was the most important factor for only 11 ASVs (12%), and the second factor for 32 ASVs (35%), indicating other operational factors played more important roles than GAC addition during the operation. The COD/SO_4^{2-} ratio was the most important parameter for 81.5% of shared active ASVs (e.g., *Methanosaeta*, *Methanobacterium*, and *Geobacter*), revealing its importance in controlling the active microbial communities during the long operation. SO_4^{2-} loading also played an important role in controlling these active ASVs, which was the second important factor for more than half of these ASVs.

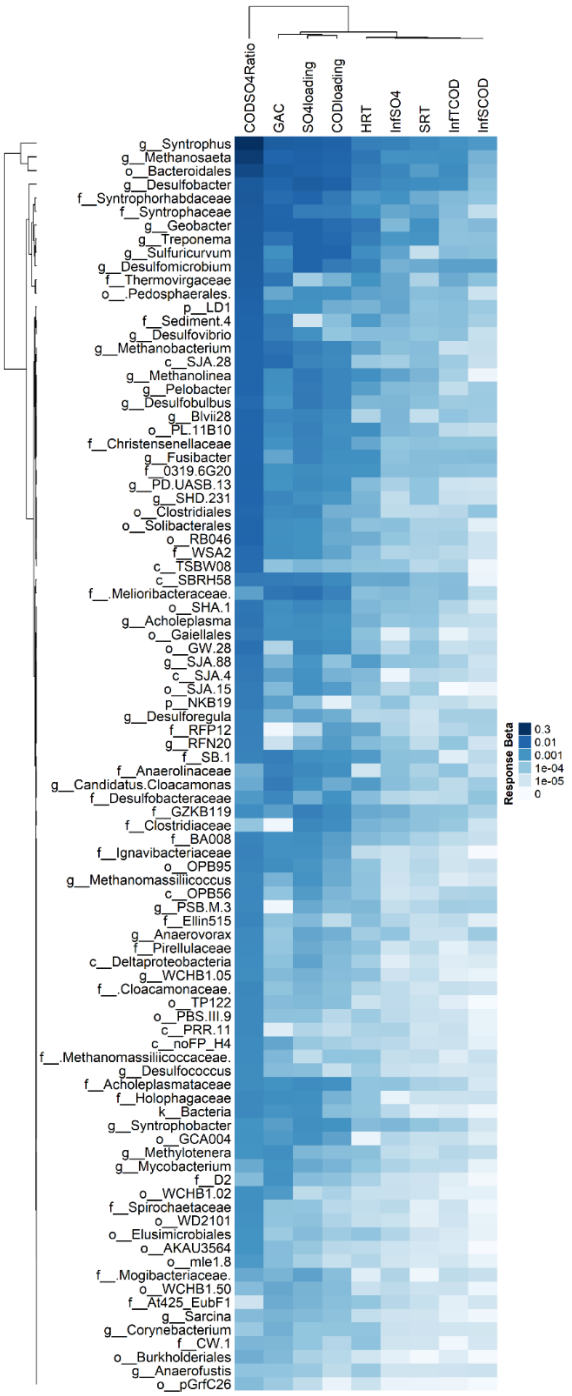

Figure 8.6 The response beta of active ASVs on the operational parameters based on the GLM analysis.

8.3.6. Discussion

8.3.6.1. The importance of active microbe identification

The results of this study highlight the importance of identifying active microbes when evaluating the microbiome community in bioreactors, which could take more responsibility for reactor performance compared to inactive microbes (Mei et al., 2016). *W22*, which frequently exists in various anaerobic digesters (Wang et al., 2018a), was abundant in the non-GAC UASB. However, it was inactive in all stages, indicating its function might not be as important as the dominance in the relative abundance. Meanwhile, the presence of numbers of transient abundant ASVs in the system (Figure 8.2) increased the complexity of the analysis. In total, 42.3% of ASVs in the non-GAC UASB and 45.3% of ASVs in the GAC-amended UASB identified as the most abundant as least in one of the stages were not active in all stages. These results indicate although these transient abundant ASVs may be functionality important under a particular operational condition, they were less important during the whole operation compared to the active and abundant ASVs.

In addition, if the analysis only focuses on ASVs with high relative abundance (> 1%), certain functionally significant ASVs will be missed. For instance, the archaeal (methanogenic) community often accounts for less than 5% of total reads (Sundberg et al., 2013). However, their actual contribution of total transcripts or proteins in the total community could be up to 30%, based on metatranscriptomics or metaproteomics analysis (Hanreich et al., 2013; Zakrzewski et al., 2012). In this study, only 2 and 3 archaea were identified in the non-GAC and GAC-amended UASB as the most abundant at least in one of the stages. However, 8 and 9 archaea were active in all stages in the two reactors,

respectively. These disproportionate data suggest the importance to analyze ASVs with less relative abundance in the active state.

8.3.6.2. Roles of GAC addition in UASBs

Although GAC has long been applied as an adsorbent and biofilm support media in bioreactors, the function of GAC addition as an electron conduit to promote syntrophic relationships in AD has only been observed in recent years (Liu et al., 2012; Tan et al., 2021). This function is determined by the intrinsic nature, i.e., conductivity, and does not diminish over the operational time when water quality is stable (Yu et al., 2020; Zhao et al., 2020a). In the present study, the impact of GAC addition on reactor performance varied when reactor feed water quality varied. Further, more than 70% of species of active microbes were the same between two reactors, all indicating that GAC was not the only important driving force in shaping microbial communities. GAC addition induced the increase of specific growth rates of several microbes to shape the microbial community structure in quantity. The increased growth rate was similar to the previous observation that *Methanosaeta* could grow faster through DIET compared to the acetate uptake (Holmes et al., 2017). However, the majority of microbes were not affected directly by GAC addition. These results are consistent with the previous DIET-related study that only several microbes can be stimulated by GAC addition (Yin & Wu, 2019). It was clear that these stimulated microbes are active and are very important to reactor performance (Figure 8.5). Although it is still a challenge to link the reactor performance to specific microbes directly due to the complexity and inherent variation of wastewater microbiome, mathematic analysis together with the analysis of microbial functions can reveal the

importance of key microbes and functions. Further studies to directly link specific microbes with DIET should be considered in future studies.

8.3.6.3. Roles of operational parameters in shaping the microbial community

In this study, although the COD removal efficiencies in the GAC-amended UASB were higher than those in the non-GAC UASB, the differences between the two reactors decreased during the operational periods (Table 8.1), indicating the reduced effects of GAC addition. These reduced effects of GAC addition were significantly affected by operational parameters, especially SO_4^{2-} input. A stable influent SO_4^{2-} and a decreased influent TCOD led to the low COD/SO_4^{2-} ratios during the operation, together with the increased SO_4^{2-} loading, affecting the microbial communities in the reactors and leading to the decreased relative abundances of key functions (Figure 8.5A). COD/SO_4^{2-} ratio and SO_4^{2-} loading rate might be the most important parameters in controlling the whole microbial community and active microbial community (Table 8.2 and Figure 8.6). As a result, more active SRB were enriched during the operation and might compete with methanogens for electrons. Although CMs addition can enhance methanogenesis under sulfate-reducing conditions (Jin et al., 2019; Li et al., 2017), in this study, the effects of GAC addition on methanogenesis were weakened under intense conditions. Further, higher influent TCOD and COD loading were correlated to better performance of DIET by several researchers (Dang et al., 2016; Florentino et al., 2019b). In this study, the influent TCOD concentrations decreased since stage III and kept low in the last three stages. Although COD loading increased during the operation, the effects of SO_4^{2-} input and influent TCOD might be more important compared to the COD loading in this study. The high correlation

between the COD/SO_4^{2-} ratio and the whole microbial community (Table 8.2), together with the largest response beta values from GLM, indicated that the COD/SO_4^{2-} ratio is more important compared to the COD loading. HRT and SRT also affected anaerobic processes and microbial communities (Gao et al., 2019). In this study, the decreased HRT and SRT were also highly correlated with the changes in microbial communities (Table 8.2).

In summary, similar microbial communities in the two reactors were developed (Bray-Curtis distance < 0.3 at the end of stage VI), and key functions were weakened in the GAC-amended UASB during the operation, indicating that adjusting operational factors appropriately (e.g., increase COD/SO_4^{2-} ratio in this study) to maintain key microbes over long-term applications is necessary for the DIET processes. Furthermore, more operational conditions should be tested in the future for complex raw wastewater to get insight into the understanding of the working conditions for DIET.

8.4. Conclusion

This chapter evaluated the evolution of active microbial communities in UASBs treating municipal sewage under psychrophilic conditions with or without GAC addition. GAC addition had positive effects on several active microbes, e.g., methanogens and *Geobacter*, which might play the most important roles in reactor performance. Extrinsic engineering operational factors, instead of GAC addition, controlled the microbial community variations and further affected reactor performance. This study underlines the importance of evaluating the relative significance of extrinsic factors on reactor performance during anaerobic digestion when designing DIET-based AD reactors.

Chapter 9. Fluidized granular activated carbon enhanced anaerobic treatment of municipal sewage[8]

9.1. Introduction

Anaerobic biofilm systems (e.g., anaerobic fluidized bed reactor) have been studied widely (Cayetano et al., 2022). Biofilm carriers can enrich slow-growing microorganisms (e.g., methanogens) and maintain active methanogens from hydraulic disturbance and washout events. These integrated biofilm systems enhance biomethane recovery, chemical oxygen demand (COD) removal, and process stability (Cayetano et al., 2022). The physicochemical characteristics of carriers play vital roles in biofilm formation and immobilization (Cayetano et al., 2022). To date, various materials (e.g., polyurethane, polypropylene, polyester, and polyamide) have been tested in AD to support the growth of microorganisms (de Aquino et al., 2017; Liu et al., 2017). Different biofilm carriers can select different microbial communities, leading to different reactor performances (Shi et al., 2019). Conductive materials (CMs), such as granular activated carbon (GAC), can provide solid surfaces for microorganism growth and biofilm development and can serve as an electrical bridge to facilitate electron transfer between

[8] A version of this chapter has been published: Zhang, Y., Yu, N., Guo, B., Mohammed, A., Zhang, L., & Liu, Y. (2022). Conductive biofilms in up-flow anaerobic sludge blanket enhanced biomethane recovery from municipal sewage under ambient temperatures. *Bioresource Technology*, 361, 127658. https://doi.org/10.1016/j.biortech.2022.127658

microorganisms (Lovley, 2017). Compared to plastic carriers, conductive carriers might enable the growth of microorganisms that have faster growth rates than those using the conventional AD pathways (Holmes et al., 2017; Zhang et al., 2022a). However, the roles of GAC biofilm have not been well clarified so far. Furthermore, GAC settled at the bottom of the reactor in Chapters 6 and 7, which may limit the contact between GAC and suspended sludge and result in clogging when municipal sewage contains high suspended solids. New designs of CMs-amended reactors are required to overcome these drawbacks for practical applications.

This chapter explores the effects of the biofilms integrated up-flow anaerobic sludge blanket (UASB) reactors treating municipal sewage at temperatures of 18 ± 0.8 °C. The GAC or polyethylene sponge was added into hollow plastic balls and suspended in the middle and upper layers of the UASB. The chemical oxygen demand (COD), CH_4 generation, and microbial activities were measured at different hydraulic retention times (HRTs). Further, the microbial community structures in the biofilms and sludge beds were analyzed, and the effects of the biofilms on the sludge bed were discussed. Understanding the effects of conductive and non-conductive biofilms in UASB on microbial communities and reactor performance will benefit future engineering design and applications.

9.2. Materials and methods

9.2.1. Experimental setup and reactor operation

Two UASBs were operated continuously at ambient temperatures (18 ± 0.8 °C) for 100 days. The height and the diameter of each UASB were 78 cm and 10 cm, respectively. The

total working volume of each UASB was 4.7 L. Inoculum sludge was obtained from laboratory-scale UASBs treating primary effluent (Chapter 7). Thirty-five polyethylene hollow plastic balls were added to each UASB (Figure 9.1). The diameter of the plastic ball was 1 inch, and the total volume of plastic balls was ~ 0.3 L. The plastic ball contained a cubic sponge with no GAC and worked as the control carrier in the reactor (R_s); the plastic ball contained GAC (4-12 mesh, Sigma-Aldrich, St. Louis, USA) and worked as the test carrier in the reactor (R_g). The pore size on the surface of balls was smaller than the size of GAC. Thus, GAC can be maintained inside the plastic balls. GAC occupied around 50% of ball volume in each ball. 50% of the void ratio led to the expanded space for GAC inside the balls under the agitation of up-flow liquid and biogas. The plastic balls were packed in the middle and upper layers of the UASB (Figure 9.1). Fresh primary effluent was collected from a local sewage treatment plant using as the influent. Peristaltic pumps (LongerPump®, BT100-2J, Baoding, China) were used to pump primary effluent into the UASBs continuously. Four hydraulic retention times (HRT) of 24 h (stage I), 16 h (stage II), 12 h (stage III), and 8 h (stage IV) were tested. Each stage lasted 25 days. The sludge retention time for suspended sludge in sludge bed was controlled at ~ 120 days in both reactors.

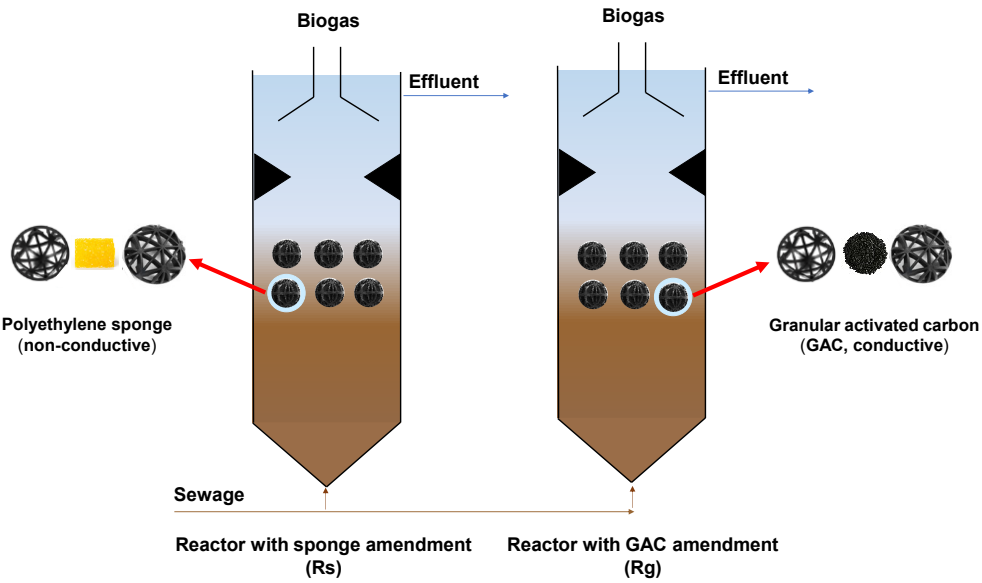

Figure 9.1 The schematic layout of the up-flow anaerobic sludge blanket (UASB) system with sponge bio-carriers (R_s) or with granular activated carbon (GAC) bio-carriers (R_g).

9.2.2. Specific methanogenic activity

The methanogenic activity was measured for suspended sludge from the sludge bed in the two reactors when stages II, III, and IV were completed. 5 mL reactor sludge was taken and mixed with 10 mL deionized water (SMA of hydrogen) or 10 mL sodium acetate solution with the concentration of 1 COD g/L (SMA of acetate) for each SMA test. The 15 mL mixture was transferred to 38 mL serum bottles. H_2/CO_2 (molar ratio 4:1, SMA of hydrogen) and N_2 gas (SMA of acetate) were used for flushing the headspace of the bottles, respectively. Aluminum caps, as well as rubber stoppers, were used to seal these bottles. After that, these bottles were shaken at 120 rpm and ambient temperature. Foil paper was used to cover bottles to avoid light effects. A gas chromatograph (GC-7890B, Agilent Technologies, Santa Clara, USA) was used to determine the biogas composition (N_2, CO_2,

O_2, and CH_4).

9.2.3. Analytical methods

Every two or three days, influent and effluent samples taken from the R_s and R_g were evaluated. The concentrations of total COD and soluble COD were measured following the standard methods (APHA, 2012). The pH values were determined with a benchtop meter (VWR, USA). When each stage was completed, the sludge samples were taken from the R_s and R_g. The total and volatile suspended solids (TSS and VSS) of sludge samples were measured following the standard methods (APHA, 2012). The concentrations of sulfate were determined through sulfate reagent powder pillows (SulfaVer® 4). Gases produced by the reactors were collected in the foil gasbag with a volume of 1 L (CHROMSPEC™, Brockville, Canada). Gas volumes were measured with a 300 mL syringe, and the biogas composition (N_2, O_2, CO_2, and CH_4) was measured through a gas chromatograph (columns: Molsieve 5A 2.44 m 2 mm and Hayesep N 1.83 m 2 mm; detector temperature: 200 °C). The amount of dissolved CH_4 in the UASB effluent was measured through a sodium salt saturation method (Zhang et al., 2020a).

9.2.4. Microbial community analysis

Biomass samples from sludge beds and GAC/sponge biofilms were collected when stage IV was completed. The samples were extracted using the DNeasy PowerSoil® DNA Isolation Kits (QIAGEN, Hilden, Germany). The polymerase chain reaction (PCR) was used to amplify 16S rRNA genes through the universal primer pair 515F and 806R. The samples were sent to the Génome Québec Innovation Centre (Montréal, QC, Canada) and

analyzed on the Illumina Miseq PE250 platform. Raw sequences were paired and quality-controlled through the Qiime2 DADA pipeline (Bolyen et al., 2019; Callahan et al., 2016). 99% similarity and Silva 138 database were used to identify microorganisms (Yilmaz et al., 2014). Microbial community analysis was performed in R with version 4.0.3. Tax4fun2 and the Kyoto Encyclopedia of Genes and Genomes (KEGG) database were used to predict the functional profiles of microbial communities (Wemheuer et al., 2020). The raw sequencing data analyzed in this study are available from the NCBI database (BioProject accession number: PRJNA855970).

9.2.5. Statistical analysis

The level of significance between means of reactor performance was determined through a paired student's t-test, with a p-value of less than 0.05 considered a significant difference.

9.3. Results and discussion

9.3.1. COD removal, methane production, and COD balance

Figure 9.2 shows the sewage and reactor effluent total chemical oxygen demand (TCOD) concentrations and CH_4 production in the two reactors during the operation. Influent TCOD fluctuated between 216 and 654 mg/L and increased gradually during the reactor operation due to variations in wastewater quality (Figure 9.2A). The average influent TCOD changed from 331 ± 26 mg/L in stage I to 353 ± 42 mg/L, 513 ± 54 mg/L, and 465 ± 17 mg/L in the last three stages, respectively. Soluble COD (SCOD) accounted for ~ 45% of the TCOD in the influent, on average. Effluent TCOD values fluctuated between 58 and 262 mg/L in stages I to IV in the R_s with sponge carriers; effluent TCOD values in the R_g with GAC

carriers fluctuated between 55 and 226 mg/L in the four stages. Specifically, the average R_s effluent TCOD concentrations in the four stages were 76 ± 4 mg/L, 102 ± 12 mg/L, 157 ± 16 mg/L, and 207 ± 26 mg/L, respectively. The average R_g effluent TCOD concentrations were 67 ± 11 mg/L, 80 ± 11 mg/L, 129 ± 18 mg/L, and 155 ± 29 mg/L, respectively. Average effluent TCOD values were always lower in the R_g. Accordingly, higher COD removal efficiencies were observed in the R_g. Overall, the R_g removed ~ 74% of the TCOD and the R_s removed ~ 68% of the TCOD; the difference was significant ($p < 0.01$). Effluent SCOD accounted for > 80% of the effluent TCOD in the two reactors; effluent SCOD was ~ 20% lower in the R_g. Further, reactor performance (COD removal) showed a strong correlation with the changes of HRTs during the operation ($r = 0.84$, $p < 0.01$), which was higher than the correlation with the changes of influent COD ($r = -0.55$, $p > 0.05$), indicating that the impacts of HRTs were greater than influent CODs.

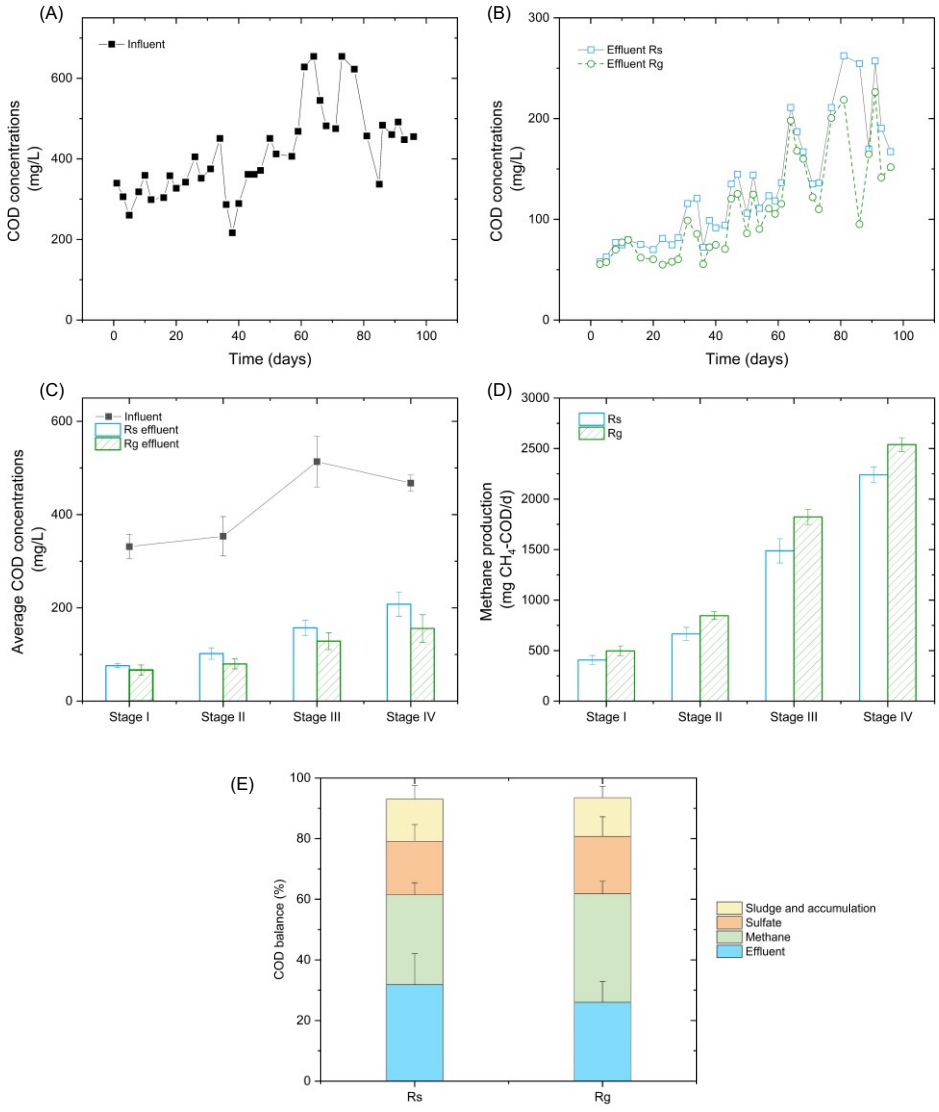

Figure 9.2 (A) Influent COD concentrations during the operation (sample numbers = 38), (B) effluent COD concentrations in the two reactors (R_g with GAC amendment and R_s with sponge amendment, sample numbers = 36), (C) average influent COD concentrations (top line) and average effluent COD concentrations (bottom bar graphs) in the R_g and R_s in stages I-IV, (D) average daily total CH_4 production in the two reactors in stages I-IV, and (E) overall COD balance in the R_g and R_s. Error bars represent standard deviations.

Average daily total CH_4 (gas and dissolved in effluent) production in stages I to IV are shown in Figure 9.2D. During reactor operation, the total CH_4 production increased with the increase of influent COD concentrations and the decrease of HRTs in both reactors. The daily total CH_4 production increased from 407 ± 45 mg CH_4-COD in the first stage to 2240 ± 78 mg CH_4-COD in the last stage in the R_s. The CH_4 production was higher in the R_g ($p = 0.011$) and increased from 498 ± 50 mg CH_4-COD in stage I to 2539 ± 68 mg CH_4-COD in the last stage. Overall, CH_4 production increased by 21% in the R_g in comparison to the R_s. The dissolved CH_4 occupied 30% to 40% of the total CH_4 production, which was lower compared to the results reported in a previous study (Zhang et al., 2021b). The higher COD input might have contributed to the higher CH_4 production in the gas phase.

The COD mass balance is presented in Figure 9.2E. The R_g (with GAC amendment) showed a low COD percentage (26%) in the effluent than the COD percentage in the R_s (with sponge amendment, 32%) ($p < 0.05$). The total CH_4 production accounted for ~ 30% of the TCOD input in the R_s and ~ 36% in the R_g ($p < 0.05$). The difference in effluent COD percentages in the two reactors was close to the difference in CH_4 production. The CH_4 production was similar to a previous study (31.5%) using a UASB-digester system treating municipal sewage at around 10 °C (Xu et al., 2018). In the present study, substantial sulfate concentrations in the influent changed between 80 and 120 mg/L, leading to around 18% COD consumption. The difference in sulfate reduction between R_s and R_g was not significant ($p > 0.05$). COD accumulation and discharged sludge were similar in both reactors.

The enhancement of COD removal efficiencies and the increase in CH_4 production

with GAC amendment than with sponge amendment are consistent with the results of previous studies. Zhang et al. (2021a) found that a biomethane production potential (BMP) increased from 76% to 81% of the TCOD input when GAC was added to a thermophilic anaerobic treatment of blackwater and kitchen waste. An anaerobic dynamic membrane bioreactor with carbon cloth worked well under high COD concentration (> 5000 mg/L) conditions, whereas COD removal dropped significantly in a control reactor with non-conductive polyester cloth (Jia et al., 2020). GAC addition enhanced the consumption of volatile fatty acids and long-chain fatty acids (particularly palmitate) in the treatment of wastewater rich in lipids (Tan et al., 2021). All the results suggest that introducing carbon materials to anaerobic digestion can enhance reactor performance.

9.3.2. Biomass amount, specific methanogenic activity, and reactor capacity

The VSS concentrations and sludge volumes in sludge beds were similar between the two reactors throughout the reactor operation period. When stage IV was complete, the concentrations of VSS in the sludge beds were 21.1 ± 0.2 g/L in the R_s and 19.6 ± 1.3 g/L in the R_g. The total amounts of VSS in sludge beds were 46.4 ± 0.4 g (R_s) and 45.1 ± 3.1 g (R_g), respectively. Biofilm colonization on biofilm carriers was observed within ten days after carrier introduction (via microscopic observation). At the end of the operation, biofilm densities were 4.4 ± 1.0 g (accounting for ~ 8.6% of the total biomass) and 2.0 ± 0.6 g (accounting for ~ 4.3% of the total biomass) in the R_s and R_g reactors, respectively.

Figure 9.3 shows the specific methanogenic activity (SMA) in suspended sludge from the sludge beds in the two reactors in the last three stages. Figure 9.3A shows that the SMA of acetate increased during reactor operation, indicating that the methanogens using

acetate performed a vital function in each reactor. Specifically, the SMA of acetate in the R_g (with GAC amendment) was larger than the SMA of acetate in the R_s (with sponge amendment) in stages II and III, with an increase of 18% and 25%. The two reactors had similar SMA values in stage IV. The SMA of hydrogen is shown in Figure 9.3B. R_g showed a higher SMA of hydrogen in all three stages, increasing by 33%, 22%, and 62% over stages II, III, and IV, respectively. In both reactors, the SMA of hydrogen was higher than the SMA of acetate in stages II and III, and lower than the SMA of acetate in stage IV. The SMA results implied that conductive (GAC) biofilms have more positive impacts than non-conductive (sponge) biofilms on the sludge bed.

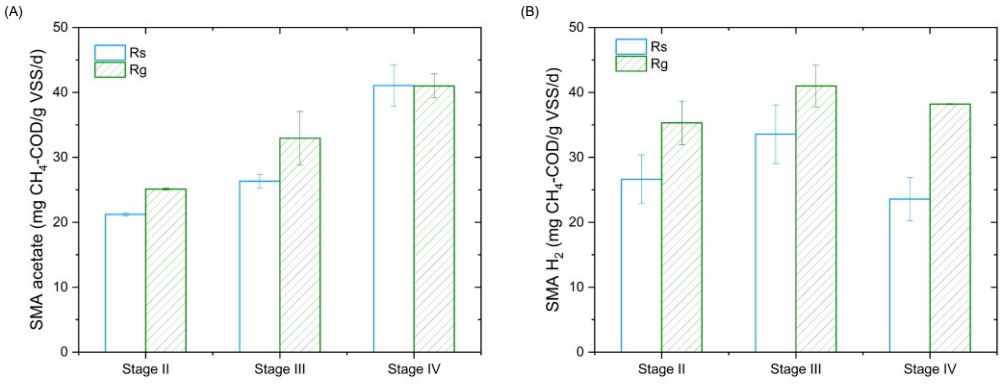

Figure 9.3 Specific methanogenic activity of acetate (A) and hydrogen (B) in the R_g (granular activated carbon amendment) and R_s (sponge amendment). Error bars represent standard deviations (n=2).

The methanogenic capacities of the sludge beds were estimated according to the sludge SMA values and the sludge amounts (Zhang et al., 2013). The sludge beds accounted for 70% - 85% of the total CH_4 production in the two reactors. Substrates other than acetate and H_2 (e.g., butyrate) could provide a higher methanogenic capacity (Collins

et al., 2003). The real capacity of sludge beds could be larger than 70% - 85%. Thus, the impact of biofilms on sludge activity in sludge beds was important in the UASBs.

9.3.3. Microbial community analysis

9.3.3.1. Microbial community diversity

The Bray-Curtis dissimilarity among microbial communities in the sludge beds and biofilms was studied through Principal Coordinate Analysis (PCoA) (BC index, Figure 9.4). Archaeal communities (Figure 9.4A) between the sludge beds of the two reactors had a low BC index of 0.21 suggesting high similarity. The BC index of 0.35 between the biofilm and sludge bed in the R_g indicated a higher similarity than the biofilm and sludge bed in the R_s (BC index 0.51) (Figure 9.4A). For bacterial communities (Figure 9.4B), similar results to archaeal communities were observed. The bacterial communities in the sludge beds of the two reactors had a high similarity (BC index 0.22) after the completion of operations. Meanwhile, the conductive (GAC) biofilm and the R_g sludge bed sludge were more similar (BC index 0.40) than the non-conductive (sponge) biofilm and the R_s sludge bed sludge (BC index 0.76) at the end of the operation. In summary, in comparison to the R_s, the R_g showed similar microbial communities in the sludge bed and the biofilm, indicating that the effects of conductive (GAC) biofilm on the sludge bed might be greater than the effects of the non-conductive (sponge) biofilm.

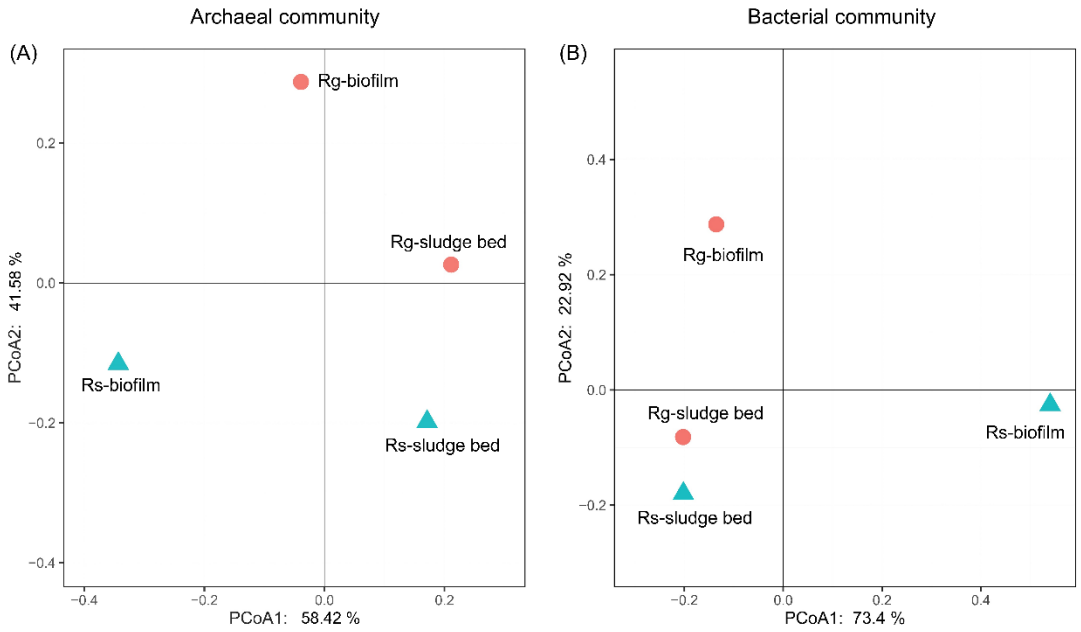

Figure 9.4 Principal Coordinates Analysis (PCoA) of the biofilms and sludge beds of the two reactors at the end of stage IV (R_g with granular activated carbon amendment and R_s with sponge amendment): (A) the archaeal community, and (B) the bacterial community.

9.3.3.2. Archaeal community

Figure 9.5A shows the archaeal communities in the two reactors. An acetoclastic methanogen, *Methanosaeta*, with a relative abundance of 32%, dominated the sludge bed in the R_s. Meanwhile, *Methanosaeta* was the genus with the second-highest population in the non-conductive biofilm (28%). In the R_g sludge bed and conductive biofilm, the relative abundances of *Methanosaeta* were the same (23%). The enrichment of *Methanosaeta* in all the samples indicated that it might be controlled by the influent conditions. Further, the enrichment of *Methanosaeta* and the increased SMA values (Figure 9.3A) indicated that the methanogenic pathway using acetate might play a vital role in the two reactors. These results differed from a previous study in which a lower relative abundance of *Methanosaeta*

(< 18%) was observed (Zhang et al., 2021b). Possibly, *Methanosaeta* is sensitive to environmental pressures. In the previous study, a low COD/SO_4^{2-} ratio led to a lower *Methanosaeta* population. In the present study, the dominance of *Methanosaeta* might be related to the high influent COD concentrations. When stage IV was completed, *Candidatus Methanofastidiosum* was the genus with the second-highest population (30%) in the R_s sludge bed; it dominated the R_g sludge bed (30%). However, *Candidatus Methanofastidiosum* was only 6% and 7%, respectively, in non-conductive and conductive biofilms. Therefore, biofilm might not be suitable for the growth of *Candidatus Methanofastidiosum*. *Candidatus Methanofastidiosum* is thought to perform methanogenesis through methylated thiol reduction (Nobu et al., 2016), suggesting that sulfur and methyl-carbon might play important roles in methane production in this study. *Methanobacterium* was the genus with the third-highest relative abundance in the R_g sludge bed (22%). Meanwhile, *Methanobacterium* dominated the conductive biofilm in the same reactor (39%). However, in the R_s, only less than 4% *Methanobacterium* was detected in the sludge bed and biofilm. An enrichment of *Methanobacterium* with GAC amendment was reported in a previous study (Zhang et al., 2020a), suggesting that GAC was the cause of *Methanobacterium* enrichment. *Methanobacterium* has been enriched in bioelectrochemical anaerobic digestions and has been shown to participate in direct interspecies electron transfer (DIET) (Huang et al., 2022; Zheng et al., 2020). The possible bioelectric activities of *Methanobacterium* could be the reason for the enrichment in the R_g. *Methanoregula* (33%) dominated the non-conductive biofilm but was not detected in the R_s sludge bed. Only about 1% of *Methanoregula* was detected in the R_g. *Methanobacterium* dominated the conductive biofilm and was also enriched in the R_g

sludge bed, whereas *Methanoregula*, the most dominant genus in the non-conductive biofilm, was not detected in the R_s sludge bed. Thus, there were fewer effects of biofilms on archaeal communities of sludge beds with sponge amendment compared with GAC amendment.

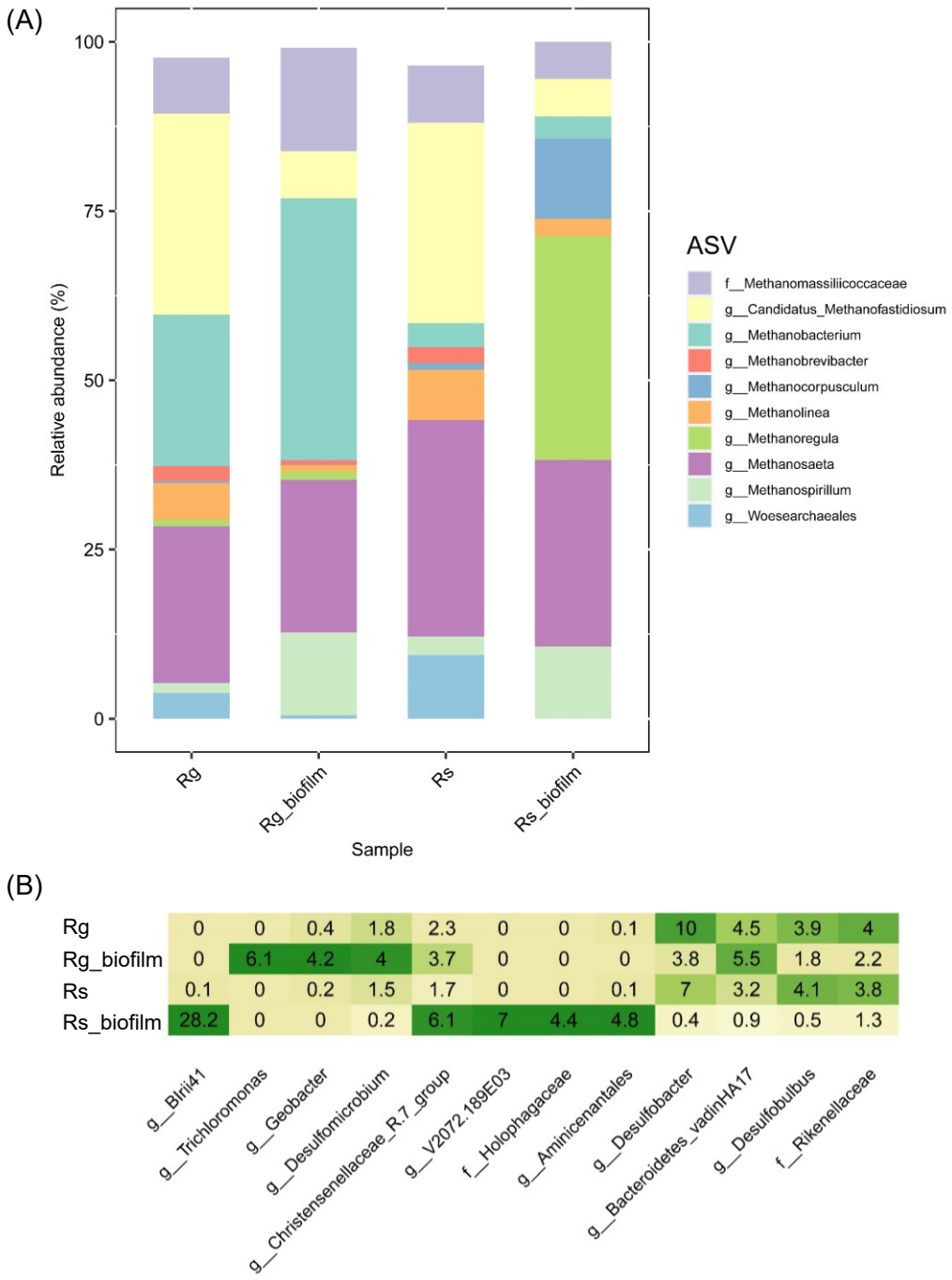

Figure 9.5 Microbial communities in the R_s sludge bed, the R_s non-conductive (sponge) biofilm, the R_g sludge bed, and the R_g conductive (GAC) biofilm in stage IV, (A) relative abundances of dominant archaeal communities, and (B) relative abundances of dominant

bacterial communities. The taxonomic names refer to genus level (g__) or higher level (family: f_) if not identified at the genus level.

9.3.3.3. Bacterial community

The most abundant bacterial genera are shown in Figure 9.5B. *Desulfobacter* is a sulfate-reducing bacteria (SRB) that can use various substrates, such as acetate, H_2, and ethanol (Kuever et al., 2015a). It can oxidize organic substrates completely to CO_2. *Desulfobacter* dominated the two sludge beds (7% and 10% in the R_s and R_g sludge beds, respectively) and was ~ 3.8% in the conductive biofilm and 0.4% in the non-conductive biofilm. Another SRB, *Desulfobulbus* (Kuever et al., 2015b), was the genus with the second-highest population in the R_s sludge bed. Meanwhile, *Desulfobulbus* was the genus with the fourth-highest population in the R_g sludge bed. The relative abundances were ~ 4% in both sludge beds. The enrichment of SRB in both reactors indicated that sulfate reduction was one of the most important pathways in this study. *Bacteroidetes vadinHA17* was the genus with the second-highest population in the R_g sludge bed (4.5%) and in the conductive biofilm (5.5%). In the R_s, it was the genus with the fourth-highest population in the sludge bed (3.2%), and its relative abundance was low in the biofilm (< 1%). *Bacteroidetes_vadinHA17* might be a facultative metabolism bacteria involved in the degradation of complex carbon organics (Baldwin et al., 2015). *Bacteroidetes_vadinHA17* can be enriched by activated carbon addition and has been demonstrated to participate in the production of propionic and lactic acids (Wang et al., 2021b). *Geobacter*, the indicator of DIET, was enriched (4.2%) only in the conductive biofilm. It was below 0.5% in the two sludge beds and was not detected in the non-conductive biofilm. *BIrii41* was abundant

with a relative abundance of 28% in the non-conductive biofilm. However, it was below 0.1% in the R_s sludge bed and was not detected in the conductive biofilm and R_g sludge bed. Other genera abundant in the non-conductive biofilm (e.g., *Christensenellaceae_R-7_group* and *V2072-189E03*) were less abundant in the sludge beds of the two reactors and in the conductive biofilm. Similar to archaeal communities, bacterial genera were more similar in the R_g than bacterial genera in the R_s.

9.3.4. Predictions of functional genes

Functional gene profiles in biofilm and sludge bed were predicted based on 16S rRNA data to evaluate how biofilm affected microbial functions and interactions. The most abundant 15 functional profiles in any samples were divided into two groups (> 4% and < 4%), as shown in Figure 9.6. In functional profiles with a relative abundance higher than 4%, the biofilm and sludge bed had similar abundances of ko02010 (ABC transporters), ko01110 (biosynthesis of secondary metabolites), ko01130 (biosynthesis of antibiotics), ko01100 (metabolic pathways), and ko01120 (microbial metabolism in diverse environments). The relative abundance of ko02020 (two-component system) in biofilm was 15% higher than that in the sludge bed. In two biofilms, the relative abundance of ko02020 in the conductive (GAC) biofilm was 17% higher in comparison to that in the non-conductive (sponge) biofilm. The two-component system is the signal transduction mechanism mediating responses to environmental stimuli (Wösten et al., 2000), and it is also responsible for quorum sensing and pili synthesis (Huang et al., 2019), which are important in interspecies electron transfer. The higher relative abundance of ko02020 in biofilms indicated that biofilms might be more active to the environmental stimuli and to interactions between

microorganisms. As shown in Figure 9.6B, although there are fluctuations in the relative abundance of different pathways between biofilm and sludge bed, biofilm showed a 27% higher relative abundance in methane metabolism (ko00680) compared to the relative abundance in sludge bed, indicating that biofilm can remain low growth methanogenic archaea.

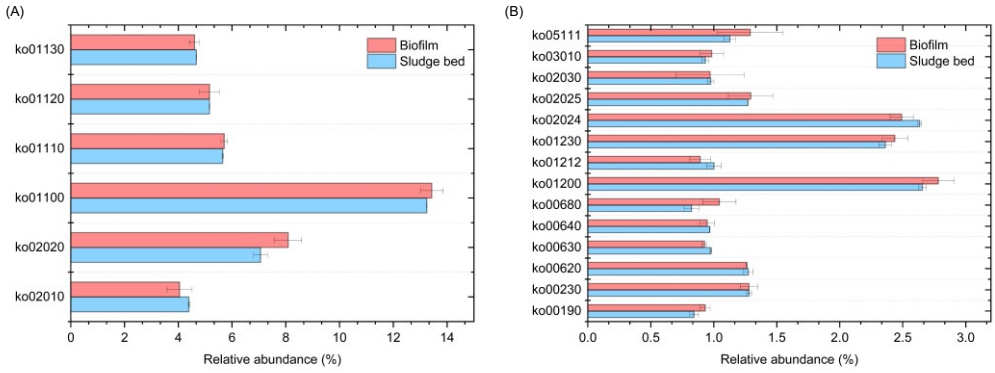

Figure 9.6 The most abundant 15 predicted pathways (in any samples) based on the KEGG database; (A) relative abundance higher than 4%, (B) relative abundance less than 4%. Error bars represent standard deviations (n=2).

9.3.5. The roles of biofilm in UASBs

Biofilm plays a crucial role in enriching microorganisms that have low growth rates (e.g., methanogens) and improving biogas production (Liu et al., 2017). In the present work, the higher methane metabolism in biofilms indicated that carriers kept methanogens in reactors (Figure 9.6B). Further, different carriers may have different effects on microorganisms (Liu et al., 2017). In comparison with the non-conductive (sponge) biofilm, conductive (GAC) biofilm might stimulate the syntrophic relationship and DIET among anaerobic microorganisms, leading to the enhanced short-chain fatty acid conversion and CH_4

production (Guo et al., 2020a). A higher growth rate could be achieved in the conductive biofilm compared to in the non-conductive biofilm, as the latter uses conventional anaerobic pathways (Zhang et al., 2022a). These could be used to explain that better performance (higher COD removal and greater CH_4 production) was achieved in the UASB containing GAC carriers.

More importantly, suspended sludge from the sludge bed can account for the majority of the sludge in the reactor. As a result, suspended sludge possibly takes responsibility for the majority of CH_4 generation based on SMA values (section 9.3.2). The effects of biofilm on the suspended sludge would be expected to enhance reactor performance. Biofilm can affect the sludge bed via (i) biofilm detachment and (ii) interspecies communication. The fast growth rate of microorganisms in the conductive biofilm (compared to growth rate of microorganisms in the non-conductive biofilm) might lead to more natural biofilm shedding into the sludge bed, directly affecting the microbial communities in the sludge bed. This could be the reason that less distance between the conductive biofilm and R_g sludge bed was observed compared to the distance between non-conductive biofilm and R_s sludge (Figure 9.4). That is, microorganisms enriched with higher activities fell into the sludge beds, resulting in a higher SMA in the R_g sludge bed (Figure 9.3B). Further, the higher relative abundance of ko02020 (Two-component system) pathway indicated that biofilm may secret signal molecules that could be used by microbes to control their population behavior (Du et al., 2021; Yin & Wu, 2019). It has been reported that GAC addition can increase the concentrations of signal molecules (i.e., acyl-homoserine lactones) (Yu et al., 2020), and the abundant signal genes in CMs-amended reactors were coupled with higher CH_4 production (Du et al., 2021). In this study,

conductive biofilms may secret more signal molecules than non-conductive biofilms, leading to the high activities of the sludge in the R_g sludge bed.

Furthermore, these suggestions in the present study were primarily based on the activities of suspended sludge and the analysis of microbial communities using 16S rRNA sequencing. Future studies might estimate biogas production from biofilms and sludge beds separately by adjusting amounts of suspended sludge and carriers. The direct evidence might further deepen the understanding of the roles of biofilms and sludge beds in the integrated biofilm UASB.

9.4. Conclusion

This chapter explored the effects of integrated biofilm UASBs treating municipal sewage. Reactor performance was enhanced in the reactor containing conductive biofilm compared to the reactor containing non-conductive biofilm. Different dominant genera (e.g., *Methanobacterium* in the conductive biofilm; *Methanoregula* in the non-conductive biofilm) were enriched in the two reactors. The positive impacts of conductive biofilm on the sludge bed could be the key to reactor performance. These findings provide insight into the roles of biofilms and sludge beds and suggest an efficient reactor configuration for future reactor design.

Chapter 10. Conclusions and recommendations[9]

The findings of the current study comprehensively revealed the roles of granular activated carbon (GAC) in anaerobic digestion (AD) (Objective 1) and demonstrated that adding GAC to AD is an effective way for biomethane recovery from municipal sewage under psychrophilic conditions (Objective 2), providing essential theoretical and practical guidance for future research and applications.

10.1. GAC stimulates anaerobic microorganisms through multiple mechanisms

The results in Chapter 3 demonstrated that GAC addition to AD changes electron transfer pathways to direct interspecies electron transfer (DIET). The systematic examination of the sludge activity, physiological property, and DIET pathway revealed that GAC addition in AD can shift electron transfer from using H_2 as carriers to DIET. In addition, rather than shifting the microbial community, the physiological changes played a more critical role in enhancing microbial activities for treating synthetic municipal sewage under psychrophilic conditions.

The results in Chapter 4 showed that GAC addition to AD enhances the biosynthesis of growth factors (e.g., vitamins and amino acids), further stimulating suspended anaerobic sludge that does not contact GAC directly. More growth factors in the effluent from the GAC-amended reactor changed microbial kinetics and enhanced reactor performance in the downstream treatment, rather than dramatically shifting the

[9] A version of this chapter has been submitted for journal publication in August 2022.

microbial community. These results explained that a few grams of GAC addition in laboratory reactors (25 g/L) can induce up to hundreds of percent increase in methane production and increase the methanogenic activities in the suspended sludge, which does not contact GAC and cannot perform DIET. These results demonstrated that the impact of GAC on AD does not only rely on the direct contact of microorganisms and GAC materials. The GAC-stimulated secretion of microbial extracellular products represents an important mechanism in conductive material amended AD.

The enrichment of methanogens and sulfate-reducing bacteria (SRB) simultaneously in the GAC biofilm suggested the coexistence of competition and cooperation between SRB and methanogens (Chapter 5). The sulfate concentrations in the microenvironment might be the key to the relationship. More importantly, a robust relationship between fermenters and methanogens was built to enhance the resistance to H_2S toxicity under sulfate-reducing conditions with GAC addition. These results demonstrated that adding GAC is a suitable strategy for enhancing methanogenesis under sulfate-reducing conditions.

10.2. GAC addition to AD is an effective way for biomethane recovery from municipal sewage under psychrophilic conditions

In the long-term operation, GAC addition enhanced COD removal and methane production during AD of actual municipal sewage under psychrophilic conditions (Chapters 6–9). Statistical analysis showed that *Geobacter*, one of the most important DIET indicators, was enriched significantly in the GAC-amended UASB, suggesting the possible existence of DIET. Other microbes, such as *Methanobacterium*, *Syntrophomonas*, *Syntrophus*, and SRB,

were also enriched in the GAC-amended UASB. This result suggests that GAC may stimulate the growth of syntrophic partners and help to form a robust relationship (Chapter 6). GAC showed a protective effect on methanogens and enhanced methanogenic activity under sulfate-reducing conditions (Chapter 7). The variations of influent and operational factors can influence the roles of GAC in AD significantly (Chapter 8). Overcoming the negative effects of influent variations is the key to long-term stable performance improvement. Conductive biofilms showed positive effects on reactor performance and suspended sludge. Suspended sludge was responsible for most methane production (Chapter 9), demonstrating that the mechanism proposed in Chapter 4 is important and might be the key to reactor enhancement. In summary, GAC addition to AD is an effective way for biomethane recovery from municipal sewage under psychrophilic conditions.

10.3. Recommendations

This thesis comprehensively explored the roles of GAC in AD. However, the electron transfer identification was performed indirectly (H_2 inhibition test in batch mode). Direct methods, such as H_2 inhibition in continuous feeding reactors, can further demonstrate the shift of electron transfer. Molecular analyses, such as metatranscriptomics, are likely the best approach to validate metabolic pathways for the degradation of organic carbon, methanogenesis and DIET. The changes in gene expression and statistical correlations might be used to identify pathways, electron transfer and the effects of microbial secretions. Furthermore, diverse anaerobic microorganisms represent diverse genetic systems and bring more challenges to understanding anaerobic microorganisms. More fundamental research on the genetic level in anaerobic microorganisms is necessary to deeply

comprehend the diverse metabolic pathways and electron transfer in AD. These insights might result in more new concepts to enhance AD.

Although carbon-based materials (CBMs) have been widely tested on laboratory scales, the way of adding CBMs and recycling materials is less discussed. Suspended and packed carriers of CBMs can enhance anaerobic digestion, but with different drawbacks. The separation of CBMs from the digestate could be problematic when used as suspended carriers in continuously stirred systems. Continuous adding materials might be required, resulting in considerable increases in cost. Packed carriers, with less issue in separation, are only suitable for wastewater with fewer solids, similar to the municipal sewage in this study. The clogging of reactors is expected when treating wastewater with high solids contents, increasing the operational cost. Fluidized GAC has been tested in Chapter 9, and more new designs (e.g., plastic bio-carriers coated with GAC) are required in the future. Furthermore, variations in influent and operational parameters in a reactor performing AD can reduce the effects of CBMs (Chapter 8). Therefore, based on the practical application of CBMs in AD systems, long-term case studies should be highly concerned with evaluating the effects of variations in practice.

Overall, the addition of carbon-based materials provides new opportunities and developments in AD. Fast-developing microbial and engineered technologies promise to promote the understanding of this ancient technology, improve its effectiveness, overcome its challenges, and extend its application. In the future, more insights into anaerobic microorganisms and modifications of bioreactors are essential to resolve constraints and further improve the sustainability of the technology.

Bibliography

Aller, M.F. 2016. Biochar properties: Transport, fate, and impact. *Critical reviews in environmental science and technology*, **46**(14-15), 1183-1296.

Alvarez, L.H., Arvizu, I.C., García-Reyes, R.B., Martinez, C.M., Olivo-Alanis, D., Del Angel, Y.A. 2017. Quinone-functionalized activated carbon improves the reduction of congo red coupled to the removal of p-cresol in a UASB reactor. *Journal of hazardous materials*, **338**, 233-240.

Angelakis, A.N., Snyder, S.A. 2015. Wastewater treatment and reuse: Past, present, and future, Vol. 7, Multidisciplinary Digital Publishing Institute, pp. 4887-4895.

APHA. 2012. Standard methods for the examination of water and wastewater. *American Public Health Association, Washington, DC*.

Baghoth, S., Sharma, S., Amy, G. 2011. Tracking natural organic matter (NOM) in a drinking water treatment plant using fluorescence excitation–emission matrices and PARAFAC. *Water research*, **45**(2), 797-809.

Balch, W., Fox, G., Magrum, L., Woese, C., Wolfe, R. 1979. Methanogens: reevaluation of a unique biological group. *Microbiological reviews*, **43**(2), 260-296.

Baldwin, S.A., Khoshnoodi, M., Rezadehbashi, M., Taupp, M., Hallam, S., Mattes, A., Sanei, H. 2015. The microbial community of a passive biochemical reactor treating arsenic, zinc, and sulfate-rich seepage. *Frontiers in bioengineering and biotechnology*, **3**, 27.

Bandara, W.M., Kindaichi, T., Satoh, H., Sasakawa, M., Nakahara, Y., Takahashi, M.,

Okabe, S. 2012. Anaerobic treatment of municipal wastewater at ambient temperature: Analysis of archaeal community structure and recovery of dissolved methane. *Water research*, **46**(17), 5756-5764.

Batstone, D.J., Keller, J., Angelidaki, I., Kalyuzhnyi, S., Pavlostathis, S., Rozzi, A., Sanders, W., Siegrist, H., Vavilin, V. 2002. The IWA anaerobic digestion model no 1 (ADM1). *Water Science and technology*, **45**(10), 65-73.

Bhatnagar, A., Hogland, W., Marques, M., Sillanpää, M. 2013. An overview of the modification methods of activated carbon for its water treatment applications. *Chemical Engineering Journal*, **219**, 499-511.

Bialek, K., Cysneiros, D., O'Flaherty, V. 2014. Hydrolysis, acidification and methanogenesis during low-temperature anaerobic digestion of dilute dairy wastewater in an inverted fluidised bioreactor. *Applied microbiology and biotechnology*, **98**(20), 8737-8750.

Biswal, B.K., Wang, B., Tang, C.J., Chen, G.H., Wu, D. 2020. Elucidating the effect of mixing technologies on dynamics of microbial communities and their correlations with granular sludge properties in a high-rate sulfidogenic anaerobic bioreactor for saline wastewater treatment. *Bioresour Technol*, **297**, 122397.

Bolyen, E., Rideout, J.R., Dillon, M.R., Bokulich, N.A., Abnet, C.C., Al-Ghalith, G.A., Alexander, H., Alm, E.J., Arumugam, M., Asnicar, F. 2019. Reproducible, interactive, scalable and extensible microbiome data science using QIIME 2. *Nature biotechnology*, **37**(8), 852-857.

Boone, D.R. 2015. Methanobacterium. *Bergey's manual of systematics of archaea and*

bacteria, 1-8.

Brileya, K.A., Camilleri, L.B., Zane, G.M., Wall, J.D., Fields, M.W. 2014. Biofilm growth mode promotes maximum carrying capacity and community stability during product inhibition syntrophy. *Frontiers in microbiology*, **5**, 693.

Cadoret, A., Conrad, A., Block, J.-C. 2002. Availability of low and high molecular weight substrates to extracellular enzymes in whole and dispersed activated sludges. *Enzyme and Microbial Technology*, **31**(1-2), 179-186.

Callahan, B.J., McMurdie, P.J., Rosen, M.J., Han, A.W., Johnson, A.J.A., Holmes, S.P. 2016. DADA2: high-resolution sample inference from Illumina amplicon data. *Nature methods*, **13**(7), 581.

Caporaso, J.G., Kuczynski, J., Stombaugh, J., Bittinger, K., Bushman, F.D., Costello, E.K., Fierer, N., Pena, A.G., Goodrich, J.K., Gordon, J.I. 2010. QIIME allows analysis of high-throughput community sequencing data. *Nature methods*, **7**(5), 335.

Caporaso, J.G., Lauber, C.L., Walters, W.A., Berg-Lyons, D., Lozupone, C.A., Turnbaugh, P.J., Fierer, N., Knight, R. 2011. Global patterns of 16S rRNA diversity at a depth of millions of sequences per sample. *Proceedings of the national academy of sciences*, **108**(Supplement 1), 4516-4522.

Cayetano, R.D.A., Kim, G.-B., Park, J., Yang, Y.-H., Jeon, B.-H., Jang, M., Kim, S.-H. 2022. Biofilm formation as a method of improved treatment during anaerobic digestion of organic matter for biogas recovery. *Bioresource technology*, **344**, 126309.

Chen, J.L., Ortiz, R., Steele, T.W., Stuckey, D.C. 2014. Toxicants inhibiting anaerobic digestion: a review. *Biotechnology advances*, **32**(8), 1523-1534.

Chen, W., Westerhoff, P., Leenheer, J.A., Booksh, K. 2003. Fluorescence excitation− emission matrix regional integration to quantify spectra for dissolved organic matter. *Environmental science & technology*, **37**(24), 5701-5710.

Cheng, S., Xing, D., Call, D.F., Logan, B.E. 2009. Direct biological conversion of electrical current into methane by electromethanogenesis. *Environmental science & technology*, **43**(10), 3953-3958.

Chernicharo, C., Van Lier, J., Noyola, A., Ribeiro, T.B. 2015. Anaerobic sewage treatment: state of the art, constraints and challenges. *Reviews in Environmental Science and Bio/Technology*, **14**(4), 649-679.

Chernicharo, C.d. 2006. Post-treatment options for the anaerobic treatment of domestic wastewater. *Reviews in Environmental Science and Bio/Technology*, **5**(1), 73-92.

Colleran, E., Concannon, F., Golden, T., Geoghegan, F., Crumlish, B., Killilea, E., Henry, M., Coates, J. 1992. Use of methanogenic activity tests to characterize anaerobic sludges, screen for anaerobic biodegradability and determine toxicity thresholds against individual anaerobic trophic groups and species. *Water Science and Technology*, **25**(7), 31-40.

Collins, G., Woods, A., McHugh, S., Carton, M.W., O'Flaherty, V. 2003. Microbial community structure and methanogenic activity during start-up of psychrophilic anaerobic digesters treating synthetic industrial wastewaters. *FEMS microbiology ecology*, **46**(2), 159-170.

Costa, K.C., Leigh, J.A. 2014. Metabolic versatility in methanogens. *Current opinion in biotechnology*, **29**, 70-75.

Crone, B.C., Garland, J.L., Sorial, G.A., Vane, L.M. 2016. Significance of dissolved methane in effluents of anaerobically treated low strength wastewater and potential for recovery as an energy product: A review. *Water Res*, **104**, 520-531.

Cruz Viggi, C., Rossetti, S., Fazi, S., Paiano, P., Majone, M., Aulenta, F. 2014. Magnetite particles triggering a faster and more robust syntrophic pathway of methanogenic propionate degradation. *Environmental science & technology*, **48**(13), 7536-7543.

Cydzik-Kwiatkowska, A., Zielińska, M. 2016. Bacterial communities in full-scale wastewater treatment systems. *World Journal of Microbiology and Biotechnology*, **32**(4), 66.

Dang, H., Yu, N., Mou, A., Zhang, L., Guo, B., Liu, Y. 2022. Metagenomic Insights into Direct Interspecies Electron Transfer and Quorum Sensing in Blackwater Anaerobic Digestion Reactors Supplemented with Granular Activated Carbon. *Bioresource Technology*, 127113.

Dang, Y., Holmes, D.E., Zhao, Z., Woodard, T.L., Zhang, Y., Sun, D., Wang, L.Y., Nevin, K.P., Lovley, D.R. 2016. Enhancing anaerobic digestion of complex organic waste with carbon-based conductive materials. *Bioresour Technol*, **220**, 516-522.

Dang, Y., Sun, D., Woodard, T.L., Wang, L.Y., Nevin, K.P., Holmes, D.E. 2017. Stimulation of the anaerobic digestion of the dry organic fraction of municipal solid waste (OFMSW) with carbon-based conductive materials. *Bioresour Technol*, **238**, 30-38.

Dar, S.A., Kleerebezem, R., Stams, A.J., Kuenen, J.G., Muyzer, G. 2008. Competition and coexistence of sulfate-reducing bacteria, acetogens and methanogens in a lab-scale anaerobic bioreactor as affected by changing substrate to sulfate ratio. *Applied microbiology and biotechnology*, **78**(6), 1045-1055.

de Aquino, S., Fuess, L.T., Pires, E.C. 2017. Media arrangement impacts cell growth in anaerobic fixed-bed reactors treating sugarcane vinasse: Structured vs. randomic biomass immobilization. *Bioresource technology*, **235**, 219-228.

De Bok, F., Plugge, C., Stams, A. 2004. Interspecies electron transfer in methanogenic propionate degrading consortia. *Water Research*, **38**(6), 1368-1375.

Deng, C., Lin, R., Kang, X., Wu, B., Wall, D.M., Murphy, J.D. 2021. What physicochemical properties of biochar facilitate interspecies electron transfer in anaerobic digestion: A case study of digestion of whiskey by-products. *Fuel*, **306**, 121736.

Drewnowski, J., Remiszewska-Skwarek, A., Duda, S., Łagód, G. 2019. Aeration process in bioreactors as the main energy consumer in a wastewater treatment plant. Review of solutions and methods of process optimization. *Processes*, **7**(5), 311.

Dryden, L., Hartman, A., Bryant, M., Robinson, I., Moore, L. 1962. Production of vitamin B12 and vitamin B12 analogues by pure cultures of ruminal bacteria. *Nature*, **195**(4837), 201-202.

Du, Q., Mu, Q., Wu, G. 2021. Metagenomic and bioanalytical insights into quorum sensing of methanogens in anaerobic digestion systems with or without the addition of conductive filter. *Science of the Total Environment*, **763**, 144509.

El-Naggar, M.Y., Wanger, G., Leung, K.M., Yuzvinsky, T.D., Southam, G., Yang, J., Lau, W.M., Nealson, K.H., Gorby, Y.A. 2010. Electrical transport along bacterial nanowires from Shewanella oneidensis MR-1. *Proceedings of the National Academy of Sciences*, **107**(42), 18127-18131.

Enzmann, F., Mayer, F., Rother, M., Holtmann, D. 2018. Methanogens: biochemical background and biotechnological applications. *Amb Express*, **8**(1), 1-22.

Facchin, S., Alves, P.D.D., de Faria Siqueira, F., Barroca, T.M., Victória, J.M.N., Kalapothakis, E. 2013. Biodiversity and secretion of enzymes with potential utility in wastewater treatment.

Farajzadehha, S., Mirbagheri, S., Farajzadehha, S., Shayegan, J. 2012. Lab scale study of HRT and OLR optimization in UASB reactor for pretreating fortified wastewater in various operational temperatures. *APCBEE Procedia*, **1**, 90-95.

Feng, D., Xia, A., Liao, Q., Nizami, A.-S., Sun, C., Huang, Y., Zhu, X., Zhu, X. 2021. Carbon cloth facilitates semi-continuous anaerobic digestion of organic wastewater rich in volatile fatty acids from dark fermentation. *Environmental Pollution*, **272**, 116030.

Florentino, A.P., Sharaf, A., Zhang, L., Liu, Y. 2019a. Overcoming ammonia inhibition in anaerobic blackwater treatment with granular activated carbon: the role of electroactive microorganisms. *Environmental Science: Water Research & Technology*.

Florentino, A.P., Xu, R., Zhang, L., Liu, Y. 2019b. Anaerobic digestion of blackwater assisted by granular activated carbon: From digestion inhibition to methanogenesis

enhancement. *Chemosphere*, **233**, 462-471.

Fritz, G., Griesshaber, D., Seth, O., Kroneck, P.M. 2001. Nonaheme cytochrome c, a new physiological electron acceptor for [Ni, Fe] hydrogenase in the sulfate-reducing bacterium Desulfovibrio desulfuricans Essex: primary sequence, molecular parameters, and redox properties. *Biochemistry*, **40**(5), 1317-1324.

Gali, V., Thakur, M., Gupta, A.K., Ganguly, R. 2018. Role of UASBs in river water quality conservation in India. *E3S Web of Conferences*. EDP Sciences. pp. 02046.

Gao, M., Guo, B., Zhang, L., Zhang, Y., Yu, N., Liu, Y. 2020. Biomethane recovery from source-diverted household blackwater: Impacts from feed sulfate. *Process Safety and Environmental Protection*, **136**, 28-38.

Gao, M., Zhang, L., Guo, B., Zhang, Y., Liu, Y. 2019. Enhancing biomethane recovery from source-diverted blackwater through hydrogenotrophic methanogenesis dominant pathway. *Chemical Engineering Journal*, **378**, 122258.

Gao, M., Zhang, L., Zhang, H., Florentino, A.P., Liu, Y. 2018. Energy recovery from municipal wastewater: impacts of temperature and collection systems. *Journal of Environmental Engineering and Science*, **14**(1), 24-31.

Gavala, H.N., Angelidaki, I., Ahring, B.K. 2003. Kinetics and modeling of anaerobic digestion process. *Biomethanation I*, 57-93.

Gonzalez-Estrella, J., Asato, C.M., Jerke, A.C., Stone, J.J., Gilcrease, P.C. 2017. Effect of structural carbohydrates and lignin content on the anaerobic digestion of paper and paper board materials by anaerobic granular sludge. *Biotechnology and*

bioengineering, **114**(5), 951-960.

Guo, B., Sheng, Z., Liu, Y. 2021. Evaluation of influent microbial immigration to activated sludge is affected by different-sized community segregation. *npj Clean Water*, **4**(1), 20.

Guo, B., Zhang, Y., Yu, N., Liu, Y. 2020a. Impacts of Conductive Materials on Microbial Community during Syntrophic Propionate Oxidization for Biomethane Recovery. *Water environment research: a research publication of the Water Environment Federation*.

Guo, B., Zhang, Y., Zhang, L., Zhou, Y., Liu, Y. 2020b. RNA-based spatial community analysis revealed intra-reactor variation and expanded collection of direct interspecies electron transfer microorganisms in anaerobic digestion. *Bioresource Technology*, **298**, 122534.

Guo, B., Zhang, Y., Zhang, L., Zhou, Y., Liu, Y. 2019. RNA-Based Spatial Community Analysis Revealed Intra-Reactor Variation and Expanded Collection of Direct Interspecies Electron Transfer Microorganisms in Anaerobic Digestion. *Bioresource Technology*

Hagemann, N., Spokas, K., Schmidt, H.-P., Kägi, R., Böhler, M.A., Bucheli, T.D. 2018. Activated carbon, biochar and charcoal: linkages and synergies across pyrogenic carbon's ABCs. *Water*, **10**(2), 182.

Hanreich, A., Schimpf, U., Zakrzewski, M., Schlüter, A., Benndorf, D., Heyer, R., Rapp, E., Pühler, A., Reichl, U., Klocke, M. 2013. Metagenome and metaproteome analyses of microbial communities in mesophilic biogas-producing anaerobic batch

fermentations indicate concerted plant carbohydrate degradation. *Systematic and applied microbiology*, **36**(5), 330-338.

Hao, T.-w., Xiang, P.-y., Mackey, H.R., Chi, K., Lu, H., Chui, H.-k., van Loosdrecht, M.C., Chen, G.-H. 2014. A review of biological sulfate conversions in wastewater treatment. *Water research*, **65**, 1-21.

Hao, Y., Winans, S.C., Glick, B.R., Charles, T.C. 2010. Identification and characterization of new LuxR/LuxI - type quorum sensing systems from metagenomic libraries. *Environmental Microbiology*, **12**(1), 105-117.

Hardin, J.W., Hardin, J.W., Hilbe, J.M., Hilbe, J. 2007. *Generalized linear models and extensions*. Stata press.

Hassan, M.M. 2018. Role of biological electron mediators in microbial extracellular electron transfer, Murdoch University.

He, C., Liu, T., Ou, H., Yuan, S., Hu, Z., Wang, W. 2021. Coupling granular activated carbon and exogenous hydrogen to enhance anaerobic digestion of phenol via predominant syntrophic acetate oxidation and hydrogenotrophic methanogenesis pathway. *Bioresource Technology*, **323**, 124576.

Heizer Jr, E.M., Raiford, D.W., Raymer, M.L., Doom, T.E., Miller, R.V., Krane, D.E. 2006. Amino acid cost and codon-usage biases in 6 prokaryotic genomes: a whole-genome analysis. *Molecular biology and evolution*, **23**(9), 1670-1680.

Hernández-Eligio, A., Pat-Espadas, A.M., Vega-Alvarado, L., Huerta-Amparán, M., Cervantes, F.J., Juárez, K. 2020. Global transcriptional analysis of Geobacter

sulfurreducens under palladium reducing conditions reveals new key cytochromes involved. *Applied Microbiology and Biotechnology*, 1-11.

Holmes, D.E., Bond, D.R., Lovley, D.R. 2004. Electron transfer by Desulfobulbus propionicus to Fe (III) and graphite electrodes. *Applied and environmental microbiology*, **70**(2), 1234-1237.

Holmes, D.E., Shrestha, P.M., Walker, D.J., Dang, Y., Nevin, K.P., Woodard, T.L., Lovley, D.R. 2017. Metatranscriptomic evidence for direct interspecies electron transfer between Geobacter and Methanothrix species in methanogenic rice paddy soils. *Applied and environmental microbiology*, **83**(9), e00223-17.

Huang, F., Liu, H., Wen, J., Zhao, C., Dong, L., Liu, H. 2021. Underestimated humic acids release and influence on anaerobic digestion during sludge thermal hydrolysis. *Water Research*, **201**, 117310.

Huang, H., Biswal, B.K., Chen, G.H., Wu, D. 2020. Sulfidogenic anaerobic digestion of sulfate-laden waste activated sludge: Evaluation on reactor performance and dynamics of microbial community. *Bioresour Technol*, **297**, 122396.

Huang, H., Chen, Y., Yang, S., Zheng, X. 2019. CuO and ZnO nanoparticles drive the propagation of antibiotic resistance genes during sludge anaerobic digestion: possible role of stimulated signal transduction. *Environmental Science: Nano*, **6**(2), 528-539.

Huang, Q., Liu, Y., Dhar, B.R. 2022. A critical review of microbial electrolysis cells coupled with anaerobic digester for enhanced biomethane recovery from high-strength feedstocks. *Critical Reviews in Environmental Science and Technology*,

52(1), 50-89.

Hubalek, V., Buck, M., Tan, B., Foght, J., Wendeberg, A., Berry, D., Bertilsson, S., Eiler, A. 2017. Vitamin and amino acid auxotrophy in anaerobic consortia operating under methanogenic conditions. *Msystems*, **2**(5), e00038-17.

Islam, M.S., Zhang, Y., McPhedran, K.N., Liu, Y., El-Din, M.G. 2016. Mechanistic investigation of industrial wastewater naphthenic acids removal using granular activated carbon (GAC) biofilm based processes. *Science of the Total Environment*, **541**, 238-246.

Jackson, B.E., Bhupathiraju, V.K., Tanner, R.S., Woese, C.R., McInerney, M.J. 1999. Syntrophus aciditrophicus sp. nov., a new anaerobic bacterium that degrades fatty acids and benzoate in syntrophic association with hydrogen-using microorganisms. *Archives of microbiology*, **171**(2), 107-114.

Jari Oksanen, F.G.B., Michael Friendly, Roeland Kindt,, Pierre Legendre, D.M., Peter R. Minchin, R. B. O'Hara, Gavin L., Simpson, P.S., M. Henry H. Stevens, Eduard Szoecs and Helene, Wagner. 2017. vegan: Community Ecology Package.

Ji, B., Zhang, M., Gu, J., Ma, Y., Liu, Y. 2020. A self-sustaining synergetic microalgal-bacterial granular sludge process towards energy-efficient and environmentally sustainable municipal wastewater treatment. *Water research*, **179**, 115884.

Jia, R., Sun, D., Dang, Y., Meier, D., Holmes, D.E., Smith, J.A. 2020. Carbon cloth enhances treatment of high-strength brewery wastewater in anaerobic dynamic membrane bioreactors. *Bioresource technology*, **298**, 122547.

Jin, Z., Zhao, Z., Liang, L., Zhang, Y. 2021. Effects of ferroferric oxide on azo dye degradation in a sulfate-containing anaerobic reactor: From electron transfer capacity and microbial community. *Chemosphere*, 131779.

Jin, Z., Zhao, Z., Zhang, Y. 2019. Potential of direct interspecies electron transfer in synergetic enhancement of methanogenesis and sulfate removal in an up-flow anaerobic sludge blanket reactor with magnetite. *Science of The Total Environment*, **677**, 299-306.

Kang, C.S., Eaktasang, N., Kwon, D.Y., Kim, H.S. 2014. Enhanced current production by Desulfovibrio desulfuricans biofilm in a mediator-less microbial fuel cell. *Bioresour Technol*, **165**, 27-30.

Kato, S. 2015. Biotechnological aspects of microbial extracellular electron transfer. *Microbes and environments*, ME15028.

Khan, A.A., Gaur, R.Z., Lew, B., Diamantis, V., Mehrotra, I., Kazmi, A. 2012. UASB/Flash aeration enable complete treatment of municipal wastewater for reuse. *Bioprocess and biosystems engineering*, **35**(6), 907-913.

King, S., Courvoisier, P., Guiot, S., Barrington, S. 2012. In-storage psychrophilic anaerobic digestion: acclimated microbial kinetics. *Environmental technology*, **33**(15), 1763-1772.

Kirkegaard, R.H., McIlroy, S.J., Kristensen, J.M., Nierychlo, M., Karst, S.M., Dueholm, M.S., Albertsen, M., Nielsen, P.H. 2017. The impact of immigration on microbial community composition in full-scale anaerobic digesters. *Scientific reports*, **7**(1), 9343.

Kolde, R., Kolde, M.R. 2015. Package 'pheatmap'. *R Package*, **1**(7), 790.

Krayzelova, L., Bartacek, J., Díaz, I., Jeison, D., Volcke, E.I., Jenicek, P. 2015. Microaeration for hydrogen sulfide removal during anaerobic treatment: a review. *Reviews in Environmental Science and Bio/Technology*, **14**(4), 703-725.

Krukenberg, V., Riedel, D., Gruber-Vodicka, H.R., Buttigieg, P.L., Tegetmeyer, H.E., Boetius, A., Wegener, G. 2018. Gene expression and ultrastructure of meso- and thermophilic methanotrophic consortia. *Environ Microbiol*, **20**(5), 1651-1666.

Kuever, J., Rainey, F.A., Widdel, F. 2015a. Desulfobacter. *Bergey's Manual of Systematics of Archaea and Bacteria*, 1-7.

Kuever, J., Rainey, F.A., Widdel, F. 2015b. Desulfobulbus. *Bergey's Manual of Systematics of Archaea and Bacteria*, 1-6.

Leang, C., Malvankar, N.S., Franks, A.E., Nevin, K.P., Lovley, D.R. 2013. Engineering Geobacter sulfurreducens to produce a highly cohesive conductive matrix with enhanced capacity for current production. *Energy & Environmental Science*, **6**(6), 1901-1908.

Lee, J.Y., Lee, S.H., Park, H.D. 2016. Enrichment of specific electro-active microorganisms and enhancement of methane production by adding granular activated carbon in anaerobic reactors. *Bioresour Technol*, **205**, 205-12.

Lei, Y., Sun, D., Dang, Y., Chen, H., Zhao, Z., Zhang, Y., Holmes, D.E. 2016. Stimulation of methanogenesis in anaerobic digesters treating leachate from a municipal solid waste incineration plant with carbon cloth. *Bioresour Technol*, **222**, 270-276.

Lei, Y., Sun, D., Dang, Y., Feng, X., Huo, D., Liu, C., Zheng, K., Holmes, D.E. 2019. Metagenomic analysis reveals that activated carbon aids anaerobic digestion of raw incineration leachate by promoting direct interspecies electron transfer. *Water research*, **161**, 570-580.

Lens, P.N.L., Visser, A., Janssen, A.J.H., Pol, L.W.H., Lettinga, G. 1998. Biotechnological Treatment of Sulfate-Rich Wastewaters. *Critical Reviews in Environmental Science and Technology*, **28**(1), 41-88.

Lettinga, G., Rebac, S., Zeeman, G. 2001a. Challenge of psychrophilic anaerobic wastewater treatment. *TRENDS in Biotechnology*, **19**(9), 363-370.

Lettinga, G., Van Lier, J., Van Buuren, J., Zeeman, G. 2001b. Sustainable development in pollution control and the role of anaerobic treatment. *Water science and technology*, **44**(6), 181-188.

Lew, B., Tarre, S., Belavski, M., Green, M. 2004. UASB reactor for domestic wastewater treatment at low temperatures: a comparison between a classical UASB and hybrid UASB-filter reactor. *Water Science and Technology*, **49**(11-12), 295-301.

Li, L.-L., Tong, Z.-H., Fang, C.-Y., Chu, J., Yu, H.-Q. 2015a. Response of anaerobic granular sludge to single-wall carbon nanotube exposure. *Water research*, **70**, 1-8.

Li, L., He, Q., Ma, Y., Wang, X., Peng, X. 2015b. Dynamics of microbial community in a mesophilic anaerobic digester treating food waste: relationship between community structure and process stability. *Bioresource Technology*, **189**, 113-120.

Li, S.-W., Sheng, G.-P., Cheng, Y.-Y., Yu, H.-Q. 2016. Redox properties of extracellular

polymeric substances (EPS) from electroactive bacteria. *Scientific reports*, **6**(1), 1-7.

Li, Y., Zhang, Y., Yang, Y., Quan, X., Zhao, Z. 2017. Potentially direct interspecies electron transfer of methanogenesis for syntrophic metabolism under sulfate reducing conditions with stainless steel. *Bioresour Technol*, **234**, 303-309.

Lima, I.M., McAloon, A., Boateng, A.A. 2008. Activated carbon from broiler litter: process description and cost of production. *Biomass and bioenergy*, **32**(6), 568-572.

Lin, H., King, A., Williams, N., Hu, B. 2017. Hydrogen sulfide removal via appropriate metal ions dosing in anaerobic digestion. *Environmental Progress & Sustainable Energy*, **36**(5), 1405-1416.

Lin, R., Deng, C., Cheng, J., Xia, A., Lens, P.N., Jackson, S.A., Dobson, A.D., Murphy, J.D. 2018. Graphene facilitates biomethane production from protein-derived glycine in anaerobic digestion. *Iscience*, **10**, 158-170.

Liu, F., Rotaru, A.-E., Shrestha, P.M., Malvankar, N.S., Nevin, K.P., Lovley, D.R. 2012. Promoting direct interspecies electron transfer with activated carbon. *Energy & Environmental Science*, **5**(10), 8982.

Liu, H., Xu, Y., Li, L., Dai, X., Dai, L. 2021a. A review on application of single and composite conductive additives for anaerobic digestion: Advances, challenges and prospects. *Resources, Conservation and Recycling*, **174**, 105844.

Liu, H., Yu, T., Liu, Y. 2015. Sulfate reducing bacteria and their activities in oil sands process-affected water biofilm. *Science of the Total Environment*, **536**, 116-122.

Liu, T., Ou, H., Su, K., Hu, Z., He, C., Wang, W. 2021b. Promoting direct interspecies electron transfer and acetoclastic methanogenesis for enhancing anaerobic digestion of butanol octanol wastewater by coupling granular activated carbon and exogenous hydrogen. *Bioresource Technology*, 125417.

Liu, Y., Gu, M., Yin, Q., Wu, G. 2019. Inhibition mitigation and ecological mechanism of mesophilic methanogenesis triggered by supplement of ferroferric oxide in sulfate-containing systems. *Bioresource technology*, **288**, 121546.

Liu, Y., Zhu, Y., Jia, H., Yong, X., Zhang, L., Zhou, J., Cao, Z., Kruse, A., Wei, P. 2017. Effects of different biofilm carriers on biogas production during anaerobic digestion of corn straw. *Bioresource technology*, **244**, 445-451.

Liu, Z.-h., Yin, H., Dang, Z., Liu, Y. 2014. Dissolved methane: a hurdle for anaerobic treatment of municipal wastewater, ACS Publications.

Louca, S., Parfrey, L.W., Doebeli, M. 2016. Decoupling function and taxonomy in the global ocean microbiome. *Science*, **353**(6305), 1272-1277.

Lovley, D.R. 2012. Electromicrobiology. *Annual review of microbiology*, **66**, 391-409.

Lovley, D.R. 2011. Reach out and touch someone: potential impact of DIET (direct interspecies energy transfer) on anaerobic biogeochemistry, bioremediation, and bioenergy. *Reviews in Environmental Science and Bio/Technology*, **10**(2), 101-105.

Lovley, D.R. 2017. Syntrophy goes electric: direct interspecies electron transfer. *Annual review of microbiology*, **71**, 643-664.

Lovley, D.R., Holmes, D.E. 2022. Electromicrobiology: the ecophysiology of

phylogenetically diverse electroactive microorganisms. *Nature Reviews Microbiology*, **20**(1), 5-19.

Lu, J.-S., Chang, J.-S., Lee, D.-J. 2019a. Adding carbon-based materials on anaerobic digestion performance: A mini-review. *Bioresource Technology*, 122696.

Lu, J.-Y., Wang, X.-M., Liu, H.-Q., Yu, H.-Q., Li, W.-W. 2019b. Optimizing operation of municipal wastewater treatment plants in China: the remaining barriers and future implications. *Environment international*, **129**, 273-278.

Müller, N., Worm, P., Schink, B., Stams, A.J., Plugge, C.M. 2010. Syntrophic butyrate and propionate oxidation processes: from genomes to reaction mechanisms. *Environmental microbiology reports*, **2**(4), 489-499.

Mahmoud, N., Zeeman, G., Gijzen, H., Lettinga, G. 2004. Anaerobic sewage treatment in a one-stage UASB reactor and a combined UASB-Digester system. *Water Research*, **38**(9), 2348-2358.

Malvankar, N.S., Lovley, D.R. 2014. Microbial nanowires for bioenergy applications. *Current Opinion in Biotechnology*, **27**, 88-95.

Marsili, E., Baron, D.B., Shikhare, I.D., Coursolle, D., Gralnick, J.A., Bond, D.R. 2008. Shewanella secretes flavins that mediate extracellular electron transfer. *Proceedings of the National Academy of Sciences*, **105**(10), 3968-3973.

Martins, G., Salvador, A.F., Pereira, L., Alves, M.M. 2018. Methane Production and Conductive Materials: A Critical Review. *Environ Sci Technol*, **52**(18), 10241-10253.

Masse, D.I., Masse, L. 2001. The effect of temperature on slaughterhouse wastewater treatment in anaerobic sequencing batch reactors. *Bioresource technology*, **76**(2), 91-98.

McAteer, P.G., Trego, A.C., Thorn, C., Mahony, T., Abram, F., O'Flaherty, V. 2020. Reactor configuration influences microbial community structure during high-rate, low-temperature anaerobic treatment of dairy wastewater. *Bioresource technology*, **307**, 123221.

McCarty, P.L., Bae, J., Kim, J. 2011. Domestic wastewater treatment as a net energy producer--can this be achieved? *Environ Sci Technol*, **45**(17), 7100-6.

McDonald, D., Price, M.N., Goodrich, J., Nawrocki, E.P., DeSantis, T.Z., Probst, A., Andersen, G.L., Knight, R., Hugenholtz, P. 2012a. An improved Greengenes taxonomy with explicit ranks for ecological and evolutionary analyses of bacteria and archaea. *ISME J*, **6**(3), 610-8.

McDonald, D., Price, M.N., Goodrich, J., Nawrocki, E.P., DeSantis, T.Z., Probst, A., Andersen, G.L., Knight, R., Hugenholtz, P. 2012b. An improved Greengenes taxonomy with explicit ranks for ecological and evolutionary analyses of bacteria and archaea. *The ISME journal*, **6**(3), 610-618.

McInerney, M., Bryant, M., Hespell, R., Costerton, J. 1981. Syntrophomonas wolfei gen. nov. sp. nov., an anaerobic, syntrophic, fatty acid-oxidizing bacterium. *Appl. Environ. Microbiol.*, **41**(4), 1029-1039.

McInerney, M.J., Rohlin, L., Mouttaki, H., Kim, U., Krupp, R.S., Rios-Hernandez, L., Sieber, J., Struchtemeyer, C.G., Bhattacharyya, A., Campbell, J.W. 2007. The

genome of Syntrophus aciditrophicus: life at the thermodynamic limit of microbial growth. *Proceedings of the National Academy of Sciences*, **104**(18), 7600-7605.

McKeown, R.M., Hughes, D., Collins, G., Mahony, T., O'Flaherty, V. 2012. Low-temperature anaerobic digestion for wastewater treatment. *Current opinion in biotechnology*, **23**(3), 444-451.

McKeown, R.M., Scully, C., Mahony, T., Collins, G., O'Flaherty, V. 2009. Long-term (1,243 days), low-temperature (4-15 degrees C), anaerobic biotreatment of acidified wastewaters: bioprocess performance and physiological characteristics. *Water Res*, **43**(6), 1611-20.

Mee, M.T., Collins, J.J., Church, G.M., Wang, H.H. 2014. Syntrophic exchange in synthetic microbial communities. *Proceedings of the National Academy of Sciences*, **111**(20), E2149-E2156.

Mehta-Kolte, M.G., Bond, D.R. 2012. Geothrix fermentans secretes two different redox-active compounds to utilize electron acceptors across a wide range of redox potentials. *Applied and environmental microbiology*, **78**(19), 6987-6995.

Mei, R., Narihiro, T., Nobu, M.K., Kuroda, K., Liu, W.T. 2016. Evaluating digestion efficiency in full-scale anaerobic digesters by identifying active microbial populations through the lens of microbial activity. *Sci Rep*, **6**, 34090.

Miran, W., Jang, J., Nawaz, M., Shahzad, A., Jeong, S.E., Jeon, C.O., Lee, D.S. 2017. Mixed sulfate-reducing bacteria-enriched microbial fuel cells for the treatment of wastewater containing copper. *Chemosphere*, **189**, 134-142.

Morris, J.J., Lenski, R.E., Zinser, E.R. 2012. The Black Queen Hypothesis: evolution of dependencies through adaptive gene loss. *MBio*, **3**(2), e00036-12.

Naeem, S., Baheti, V., Tunakova, V., Militky, J., Karthik, D., Tomkova, B. 2017. Development of porous and electrically conductive activated carbon web for effective EMI shielding applications. *Carbon*, **111**, 439-447.

Nobu, M.K., Narihiro, T., Kuroda, K., Mei, R., Liu, W.-T. 2016. Chasing the elusive Euryarchaeota class WSA2: genomes reveal a uniquely fastidious methyl-reducing methanogen. *The ISME journal*.

Noyola, A., Padilla-Rivera, A., Morgan-Sagastume, J.M., Güereca, L.P., Hernández-Padilla, F. 2012. Typology of municipal wastewater treatment technologies in Latin America. *Clean–Soil, Air, Water*, **40**(9), 926-932.

O'Reilly, J., Lee, C., Chinalia, F., Collins, G., Mahony, T., O'Flaherty, V. 2010. Microbial community dynamics associated with biomass granulation in low-temperature (15 C) anaerobic wastewater treatment bioreactors. *Bioresource technology*, **101**(16), 6336-6344.

Oksanen, J., Blanchet, F., Friendly, M., Kindt, R., Legendre, P., McGlinn, D., Minchin, P., O'Hara, R., Simpson, G., Solymos, P. 2017. Vegan: community ecology package. 2017. R package version 2.4–5.

Park, J.H., Park, J.H., Je Seong, H., Sul, W.J., Jin, K.H., Park, H.D. 2018. Metagenomic insight into methanogenic reactors promoting direct interspecies electron transfer via granular activated carbon. *Bioresour Technol*, **259**, 414-422.

Patel, G.B. 2015. Methanosaeta. *Bergey's Manual of Systematics of Archaea and Bacteria*, 1-8.

Patel, G.B., Sprott, G.D. 1990. Methanosaeta concilii gen. nov., sp. nov.("Methanothrix concilii") and Methanosaeta thermoacetophila nom. rev., comb. nov. *International Journal of Systematic and Evolutionary Microbiology*, **40**(1), 79-82.

Petropoulos, E., Yu, Y., Tabraiz, S., Yakubu, A., Curtis, T.P., Dolfing, J. 2019. High rate domestic wastewater treatment at 15 °C using anaerobic reactors inoculated with cold-adapted sediments/soils – shaping robust methanogenic communities. *Environmental Science: Water Research & Technology*, **5**(1), 70-82.

Pozo, G., Jourdin, L., Lu, Y., Ledezma, P., Keller, J., Freguia, S. 2015. Methanobacterium enables high rate electricity-driven autotrophic sulfate reduction. *RSC Advances*, **5**(109), 89368-89374.

Raskin, L., Nielsen, P.H. 2019. Editorial overview: Integrating biotechnology and microbial ecology in urban water infrastructure through a microbiome continuum viewpoint. *Current opinion in biotechnology*, **57**, iii.

Raskin, L., Rittmann, B.E., Stahl, D.A. 1996. Competition and coexistence of sulfate-reducing and methanogenic populations in anaerobic biofilms. *Appl. Environ. Microbiol.*, **62**(10), 3847-3857.

Regueiro, L., Veiga, P., Figueroa, M., Alonso-Gutierrez, J., Stams, A.J., Lema, J.M., Carballa, M. 2012. Relationship between microbial activity and microbial community structure in six full-scale anaerobic digesters. *Microbiol Res*, **167**(10), 581-9.

Ren, S., Usman, M., Tsang, D.C., O-Thong, S., Angelidaki, I., Zhu, X., Zhang, S., Luo, G. 2020. Hydrochar-facilitated anaerobic digestion: evidence for direct interspecies electron transfer mediated through surface oxygen-containing functional groups. *Environmental science & technology*, **54**(9), 5755-5766.

Rizvi, H., Ahmad, N., Abbas, F., Bukhari, I.H., Yasar, A., Ali, S., Yasmeen, T., Riaz, M. 2015. Start-up of UASB reactors treating municipal wastewater and effect of temperature/sludge age and hydraulic retention time (HRT) on its performance. *Arabian Journal of Chemistry*, **8**(6), 780-786.

Rotaru, A.-E., Shrestha, P.M., Liu, F., Markovaite, B., Chen, S., Nevin, K.P., Lovley, D.R. 2014a. Direct interspecies electron transfer between Geobacter metallireducens and Methanosarcina barkeri. *Appl. Environ. Microbiol.*, **80**(15), 4599-4605.

Rotaru, A.-E., Shrestha, P.M., Liu, F., Shrestha, M., Shrestha, D., Embree, M., Zengler, K., Wardman, C., Nevin, K.P., Lovley, D.R. 2014b. A new model for electron flow during anaerobic digestion: direct interspecies electron transfer to Methanosaeta for the reduction of carbon dioxide to methane. *Energy Environ. Sci.*, **7**(1), 408-415.

Saia, F.T., Souza, T.S., Duarte, R.T.D., Pozzi, E., Fonseca, D., Foresti, E. 2016. Microbial community in a pilot-scale bioreactor promoting anaerobic digestion and sulfur-driven denitrification for domestic sewage treatment. *Bioprocess and biosystems engineering*, **39**(2), 341-352.

Sakai, S., Ehara, M., Tseng, I.-C., Yamaguchi, T., Bräuer, S.L., Cadillo-Quiroz, H., Zinder, S.H., Imachi, H. 2012. Methanolinea mesophila sp. nov., a hydrogenotrophic methanogen isolated from rice field soil, and proposal of the archaeal family

Methanoregulaceae fam. nov. within the order Methanomicrobiales. *International journal of systematic and evolutionary microbiology*, **62**(6), 1389-1395.

Salvador, A.F., Martins, G., Melle-Franco, M., Serpa, R., Stams, A.J.M., Cavaleiro, A.J., Pereira, M.A., Alves, M.M. 2017. Carbon nanotubes accelerate methane production in pure cultures of methanogens and in a syntrophic coculture. *Environ Microbiol*, **19**(7), 2727-2739.

Scholten, J.C., Culley, D.E., Brockman, F.J., Wu, G., Zhang, W. 2007. Evolution of the syntrophic interaction between Desulfovibrio vulgaris and Methanosarcina barkeri: involvement of an ancient horizontal gene transfer. *Biochemical and biophysical research communications*, **352**(1), 48-54.

Schröder, U., Harnisch, F., Angenent, L.T. 2015. Microbial electrochemistry and technology: terminology and classification. *Energy & Environmental Science*, **8**(2), 513-519.

Segata, N., Izard, J., Waldron, L., Gevers, D., Miropolsky, L., Garrett, W.S., Huttenhower, C. 2011. Metagenomic biomarker discovery and explanation. *Genome biology*, **12**(6), R60.

Seghezzo, L., Guerra, R., González, S., Trupiano, A., Figueroa, M., Cuevas, C., Zeeman, G., Lettinga, G. 2002. Removal efficiency and methanogenic activity profiles in a pilot-scale UASB reactor treating settled sewage at moderate temperatures. *Water Science and Technology*, **45**(10), 243.

Shen, Y., Yu, Y., Zhang, Y., Urgun-Demirtas, M., Yuan, H., Zhu, N., Dai, X. 2021. Role of redox-active biochar with distinctive electrochemical properties to promote

methane production in anaerobic digestion of waste activated sludge. *Journal of Cleaner Production*, **278**, 123212.

Sheng, G.-P., Yu, H.-Q., Li, X.-Y. 2010. Extracellular polymeric substances (EPS) of microbial aggregates in biological wastewater treatment systems: a review. *Biotechnology advances*, **28**(6), 882-894.

Sheng, Z., Van Nostrand, J.D., Zhou, J., Liu, Y. 2018. Contradictory effects of silver nanoparticles on activated sludge wastewater treatment. *J Hazard Mater*, **341**, 448-456.

Shi, J., Han, Y., Xu, C., Han, H. 2019. Enhanced biodegradation of coal gasification wastewater with anaerobic biofilm on polyurethane (PU), powdered activated carbon (PAC), and biochar. *Bioresource technology*, **289**, 121487.

Shi, L., Dong, H., Reguera, G., Beyenal, H., Lu, A., Liu, J., Yu, H.-Q., Fredrickson, J.K. 2016. Extracellular electron transfer mechanisms between microorganisms and minerals. *Nature Reviews Microbiology*, **14**(10), 651-662.

Shrestha, P.M., Malvankar, N.S., Werner, J.J., Franks, A.E., Elena-Rotaru, A., Shrestha, M., Liu, F., Nevin, K.P., Angenent, L.T., Lovley, D.R. 2014. Correlation between microbial community and granule conductivity in anaerobic bioreactors for brewery wastewater treatment. *Bioresource technology*, **174**, 306-310.

Sieber, J.R., McInerney, M.J., Gunsalus, R.P. 2012. Genomic insights into syntrophy: the paradigm for anaerobic metabolic cooperation. *Annu Rev Microbiol*, **66**, 429-52.

Siegert, M., Yates, M.D., Spormann, A.M., Logan, B.E. 2015. Methanobacterium

dominates biocathodic archaeal communities in methanogenic microbial electrolysis cells. *ACS Sustainable Chemistry & Engineering*, **3**(7), 1668-1676.

Slowikowski, K. 2018. ggrepel: Automatically position non-overlapping text labels with 'ggplot2'. R package version 0.8. 0.

Song, X., Liu, J., Jiang, Q., Zhang, P., Shao, Y., He, W., Feng, Y. 2019. Enhanced electron transfer and methane production from low-strength wastewater using a new granular activated carbon modified with nano-Fe3O4. *Chemical Engineering Journal*, **374**, 1344-1352.

Stams, A.J., De Bok, F.A., Plugge, C.M., Van Eekert, M.H., Dolfing, J., Schraa, G. 2006. Exocellular electron transfer in anaerobic microbial communities. *Environmental microbiology*, **8**(3), 371-382.

Stams, A.J., Plugge, C.M. 2009. Electron transfer in syntrophic communities of anaerobic bacteria and archaea. *Nature Reviews Microbiology*, **7**(8), 568-577.

Storck, T., Virdis, B., Batstone, D.J. 2016. Modelling extracellular limitations for mediated versus direct interspecies electron transfer. *The ISME journal*, **10**(3), 621.

Summers, Z.M., Fogarty, H.E., Leang, C., Franks, A.E., Malvankar, N.S., Lovley, D.R. 2010. Direct exchange of electrons within aggregates of an evolved syntrophic coculture of anaerobic bacteria. *Science*, **330**(6009), 1413-1415.

Sundberg, C., Al-Soud, W.A., Larsson, M., Alm, E., Yekta, S.S., Svensson, B.H., Sørensen, S.J., Karlsson, A. 2013. 454 pyrosequencing analyses of bacterial and archaeal richness in 21 full-scale biogas digesters. *FEMS microbiology ecology*, **85**(3), 612-

626.

Tan, L.C., Lin, R., Murphy, J.D., Lens, P.N. 2021. Granular activated carbon supplementation enhances anaerobic digestion of lipid-rich wastewaters. *Renewable Energy*.

Tan, Y., Adhikari, R.Y., Malvankar, N.S., Pi, S., Ward, J.E., Woodard, T.L., Nevin, K.P., Xia, Q., Tuominen, M.T., Lovley, D.R. 2016. Synthetic biological protein nanowires with high conductivity. *small*, **12**(33), 4481-4485.

Tejerizo, G.T., Kim, Y.S., Maus, I., Wibberg, D., Winkler, A., Off, S., Pühler, A., Scherer, P., Schlüter, A. 2017. Genome sequence of Methanobacterium congolense strain Buetzberg, a hydrogenotrophic, methanogenic archaeon, isolated from a mesophilic industrial-scale biogas plant utilizing bio-waste. *Journal of biotechnology*, **247**, 1-5.

Tian, T., Qiao, S., Li, X., Zhang, M., Zhou, J. 2017. Nano-graphene induced positive effects on methanogenesis in anaerobic digestion. *Bioresour Technol*, **224**, 41-47.

Tobi, A.R., Dennis, J., Zaid, H., Adekoya, A., Yar, A., Fahad, U. 2019. Comparative analysis of physiochemical properties of physically activated carbon from palm bio-waste. *Journal of Materials Research and Technology*, **8**(5), 3688-3695.

Tremblay, P.-L., Angenent, L.T., Zhang, T. 2017. Extracellular electron uptake: among autotrophs and mediated by surfaces. *Trends in biotechnology*, **35**(4), 360-371.

Tsui, T.-H., Wu, H., Song, B., Liu, S.-S., Bhardwaj, A., Wong, J.W. 2020. Food waste leachate treatment using an Upflow Anaerobic Sludge Bed (UASB): Effect of

conductive material dosage under low and high organic loads. *Bioresource Technology*, **304**, 122738.

Uemura, S., Harada, H. 2000. Treatment of sewage by a UASB reactor under moderate to low temperature conditions. *Bioresource Technology*, **72**(3), 275-282.

Van Den Brand, T.P., Roest, K., Chen, G., Brdjanovic, D., Van Loosdrecht, M. 2015. Potential for beneficial application of sulfate reducing bacteria in sulfate containing domestic wastewater treatment. *World Journal of Microbiology and Biotechnology*, **31**(11), 1675-1681.

Van Der Zee, F.P., Bisschops, I.A., Lettinga, G., Field, J.A. 2003. Activated carbon as an electron acceptor and redox mediator during the anaerobic biotransformation of azo dyes. *Environmental science & technology*, **37**(2), 402-408.

Van, D.P., Fujiwara, T., Tho, B.L., Toan, P.P.S., Minh, G.H. 2020. A review of anaerobic digestion systems for biodegradable waste: Configurations, operating parameters, and current trends. *Environmental Engineering Research*, **25**(1), 1-17.

van Loosdrecht, M.C., Brdjanovic, D. 2014. Anticipating the next century of wastewater treatment. *Science*, **344**(6191), 1452-1453.

Van Steendam, C., Smets, I., Skerlos, S., Raskin, L. 2019. Improving anaerobic digestion via direct interspecies electron transfer requires development of suitable characterization methods. *Curr Opin Biotechnol*, **57**, 183-190.

Vos, P., Garrity, G., Jones, D., Krieg, N.R., Ludwig, W., Rainey, F.A., Schleifer, K.-H., Whitman, W.B. 2011. *Bergey's manual of systematic bacteriology: Volume 3: The*

Firmicutes. Springer Science & Business Media.

Wösten, M.M., Kox, L.F., Chamnongpol, S., Soncini, F.C., Groisman, E.A. 2000. A signal transduction system that responds to extracellular iron. *Cell*, **103**(1), 113-125.

Walker, D.J., Nevin, K.P., Holmes, D.E., Rotaru, A.-E., Ward, J.E., Woodard, T.L., Zhu, J., Ueki, T., Nonnenmann, S.S., McInerney, M.J. 2018. Syntrophus conductive pili demonstrate that common hydrogen-donating syntrophs can have a direct electron transfer option. *Biorxiv*, 479683.

Walker, D.J.F., Nevin, K.P., Holmes, D.E., Rotaru, A.E., Ward, J.E., Woodard, T.L., Zhu, J., Ueki, T., Nonnenmann, S.S., McInerney, M.J., Lovley, D.R. 2020. Syntrophus conductive pili demonstrate that common hydrogen-donating syntrophs can have a direct electron transfer option. *ISME J*, **14**(3), 837-846.

Wang, J., Zhao, Z., Zhang, Y. 2021a. Enhancing anaerobic digestion of kitchen wastes with biochar: Link between different properties and critical mechanisms of promoting interspecies electron transfer. *Renewable Energy*, **167**, 791-799.

Wang, P., Yu, Z., Zhao, J., Zhang, H. 2018a. Do microbial communities in an anaerobic bioreactor change with continuous feeding sludge into a full-scale anaerobic digestion system? *Bioresource technology*, **249**, 89-98.

Wang, R., Li, C., Lv, N., Pan, X., Cai, G., Ning, J., Zhu, G. 2021b. Deeper insights into effect of activated carbon and nano-zero-valent iron addition on acidogenesis and whole anaerobic digestion. *Bioresource Technology*, **324**, 124671.

Wang, X., Daigger, G., Lee, D.-J., Liu, J., Ren, N.-Q., Qu, J., Liu, G., Butler, D. 2018b.

Evolving wastewater infrastructure paradigm to enhance harmony with nature. *Science advances*, **4**(8), eaaq0210.

Wasserfallen, A., Nölling, J., Pfister, P., Reeve, J., De Macario, E.C. 2000. Phylogenetic analysis of 18 thermophilic Methanobacterium isolates supports the proposals to create a new genus, Methanothermobacter gen. nov., and to reclassify several isolates in three species, Methanothermobacter thermautotrophicus comb. nov., Methanothermobacter wolfeii comb. nov., and Methanothermobacter marburgensis sp. nov. *International Journal of Systematic and Evolutionary Microbiology*, **50**(1), 43-53.

Watanabe, K., Manefield, M., Lee, M., Kouzuma, A. 2009. Electron shuttles in biotechnology. *Current Opinion in Biotechnology*, **20**(6), 633-641.

Wei, T., Simko, V., Levy, M., Xie, Y., Jin, Y., Zemla, J. 2017. Package 'corrplot'. *Statistician*, **56**(316), e24.

Wemheuer, F., Taylor, J.A., Daniel, R., Johnston, E., Meinicke, P., Thomas, T., Wemheuer, B. 2020. Tax4Fun2: prediction of habitat-specific functional profiles and functional redundancy based on 16S rRNA gene sequences. *Environmental Microbiome*, **15**, 1-12.

Werner, J.J., Koren, O., Hugenholtz, P., DeSantis, T.Z., Walters, W.A., Caporaso, J.G., Angenent, L.T., Knight, R., Ley, R.E. 2012a. Impact of training sets on classification of high-throughput bacterial 16s rRNA gene surveys. *ISME J*, **6**(1), 94-103.

Werner, J.J., Koren, O., Hugenholtz, P., DeSantis, T.Z., Walters, W.A., Caporaso, J.G.,

Angenent, L.T., Knight, R., Ley, R.E. 2012b. Impact of training sets on classification of high-throughput bacterial 16s rRNA gene surveys. *The ISME journal*, **6**(1), 94-103.

Wickham, H. 2016. *ggplot2: elegant graphics for data analysis*. springer.

Widdel, F. 1986. Growth of methanogenic bacteria in pure culture with 2-propanol and other alcohols as hydrogen donors. *Applied and Environmental Microbiology*, **51**(5), 1056-1062.

Xiao, L., Zheng, S., Lichtfouse, E., Luo, M., Tan, Y., Liu, F. 2020. Carbon nanotubes accelerate acetoclastic methanogenesis: From pure cultures to anaerobic soils. *Soil Biology and Biochemistry*, **150**, 107938.

Xiao, R., Zheng, Y. 2016. Overview of microalgal extracellular polymeric substances (EPS) and their applications. *Biotechnology Advances*, **34**(7), 1225-1244.

Xing, L., Zhang, W., Gu, M., Yin, Q., Wu, G. 2020. Microbial interactions regulated by the dosage of ferroferric oxide in the co-metabolism of organic carbon and sulfate. *Bioresource technology*, **296**, 122317.

Xu, R., Li, B., Xiao, E., Young, L.Y., Sun, X., Kong, T., Dong, Y., Wang, Q., Yang, Z., Chen, L. 2020a. Uncovering microbial responses to sharp geochemical gradients in a terrace contaminated by acid mine drainage. *Environmental Pollution*, **261**, 114226.

Xu, S., Zhang, L., Huang, S., Zeeman, G., Rijnaarts, H., Liu, Y. 2018. Improving the energy efficiency of a pilot-scale UASB-digester for low temperature domestic

wastewater treatment. *Biochemical Engineering Journal*, **135**, 71-78.

Xu, Y., Wang, M., Yu, Q., Zhang, Y. 2020b. Enhancing methanogenesis from anaerobic digestion of propionate with addition of Fe oxides supported on conductive carbon cloth. *Bioresource Technology*, **302**, 122796.

Yamaguchi, T., Harada, H., Hisano, T., Yamazaki, S., Tseng, I.-C. 1999. Process behavior of UASB reactor treating a wastewater containing high strength sulfate. *Water Research*, **33**(14), 3182-3190.

Yan, W., Shen, N., Xiao, Y., Chen, Y., Sun, F., Kumar Tyagi, V., Zhou, Y. 2017. The role of conductive materials in the start-up period of thermophilic anaerobic system. *Bioresour Technol*, **239**, 336-344.

Yan, W., Sun, F., Liu, J., Zhou, Y. 2018. Enhanced anaerobic phenol degradation by conductive materials via EPS and microbial community alteration. *Chemical Engineering Journal*, **352**, 1-9.

Yang, B., Xu, H., Liu, Y., Li, F., Song, X., Wang, Z., Sand, W. 2020. Role of GAC-MnO2 catalyst for triggering the extracellular electron transfer and boosting CH4 production in syntrophic methanogenesis. *Chemical Engineering Journal*, **383**, 123211.

Yang, K., Li, L., Wang, Y., Xue, S., Han, Y., Liu, J. 2019. Airborne bacteria in a wastewater treatment plant: Emission characterization, source analysis and health risk assessment. *Water research*, **149**, 596-606.

Yang, Y., Zhang, Y., Li, Z., Zhao, Z., Quan, X., Zhao, Z. 2017. Adding granular activated

carbon into anaerobic sludge digestion to promote methane production and sludge decomposition. *Journal of Cleaner Production*, **149**, 1101-1108.

Yao, J., Zeng, Y., Wang, M., Tang, Y.-Q. 2021. Energy Availability Determines Strategy of Microbial Amino Acid Synthesis in Volatile Fatty Acid–Fed Anaerobic Methanogenic Chemostats. *Frontiers in microbiology*, **12**.

Yilmaz, P., Parfrey, L.W., Yarza, P., Gerken, J., Pruesse, E., Quast, C., Schweer, T., Peplies, J., Ludwig, W., Glöckner, F.O. 2014. The SILVA and "all-species living tree project (LTP)" taxonomic frameworks. *Nucleic acids research*, **42**(D1), D643-D648.

Yin, Q., Gu, M., Hermanowicz, S.W., Hu, H., Wu, G. 2020a. Potential interactions between syntrophic bacteria and methanogens via type IV pili and quorum-sensing systems. *Environment International*, **138**, 105650.

Yin, Q., Gu, M., Wu, G. 2020b. Inhibition mitigation of methanogenesis processes by conductive materials: A critical review. *Bioresource Technology*, **317**, 123977.

Yin, Q., He, K., Echigo, S., Wu, G., Zhan, X., Hu, H. 2018. Ferroferric oxide significantly affected production of soluble microbial products and extracellular polymeric substances in anaerobic methanogenesis reactors. *Frontiers in microbiology*, 2376.

Yin, Q., Wang, Z., Wu, G. 2019. Impacts of environmental factors on microbial diversity, distribution patterns and syntrophic correlation in anaerobic processes. *Archives of microbiology*, **201**(5), 603-614.

Yin, Q., Wu, G. 2019. Advances in direct interspecies electron transfer and conductive

materials: Electron flux, organic degradation and microbial interaction. *Biotechnol Adv*, **37**(8), 107443.

Yu, N., Guo, B., Liu, Y. 2021. Shaping biofilm microbiomes by changing GAC location during wastewater anaerobic digestion. *Science of The Total Environment*, **780**, 146488.

Yu, N., Guo, B., Zhang, Y., Zhang, L., Zhou, Y., Liu, Y. 2020. Self-fluidized GAC-amended UASB Reactor for Enhanced Methane Production. *Chemical Engineering Journal*, 127652.

Yuan, H., Mei, R., Liao, J., Liu, W.-T. 2019. Nexus of stochastic and deterministic processes on microbial community assembly in biological systems. *Frontiers in microbiology*, **10**, 1536.

Zabranska, J., Pokorna, D. 2018. Bioconversion of carbon dioxide to methane using hydrogen and hydrogenotrophic methanogens. *Biotechnology advances*, **36**(3), 707-720.

Zakrzewski, M., Goesmann, A., Jaenicke, S., Jünemann, S., Eikmeyer, F., Szczepanowski, R., Al-Soud, W.A., Sørensen, S., Pühler, A., Schlüter, A. 2012. Profiling of the metabolically active community from a production-scale biogas plant by means of high-throughput metatranscriptome sequencing. *Journal of biotechnology*, **158**(4), 248-258.

Zhang, G., Jiang, N., Liu, X., Dong, X. 2008. Methanogenesis from methanol at low temperatures by a novel psychrophilic methanogen,“Methanolobus psychrophilus” sp. nov., prevalent in Zoige wetland of the Tibetan plateau. *Applied and*

environmental microbiology, **74**(19), 6114-6120.

Zhang, G., Zhang, F., Ding, G., Li, J., Guo, X., Zhu, J., Zhou, L., Cai, S., Liu, X., Luo, Y. 2012a. Acyl homoserine lactone-based quorum sensing in a methanogenic archaeon. *The ISME journal*, **6**(7), 1336-1344.

Zhang, L. 2016. Anaerobic treatment of municipal wastewater in a UASB-Digester system: temperature effect on system performance, hydrolysis and methanogenesis, Wageningen University and Research.

Zhang, L., De Vrieze, J., Hendrickx, T.L., Wei, W., Temmink, H., Rijnaarts, H., Zeeman, G. 2018. Anaerobic treatment of raw domestic wastewater in a UASB-digester at 10 C and microbial community dynamics. *Chemical Engineering Journal*, **334**, 2088-2097.

Zhang, L., Hendrickx, T.L., Kampman, C., Temmink, H., Zeeman, G. 2013. Co-digestion to support low temperature anaerobic pretreatment of municipal sewage in a UASB-digester. *Bioresour Technol*, **148**, 560-6.

Zhang, L., Hendrickx, T.L., Kampman, C., Zeeman, G., Temmink, H., Li, W., Buisman, C.J. 2012b. The effect of sludge recirculation rate on a UASB-digester treating domestic sewage at 15° C. *Water Science and Technology*, **66**(12), 2597-2603.

Zhang, Q., Li, R., Guo, B., Zhang, L., Liu, Y. 2021a. Thermophilic co-digestion of blackwater and organic kitchen waste: Impacts of granular activated carbon and different mixing ratios. *Waste Management*, **131**, 453-461.

Zhang, Y., Guo, B., Dang, H., Zhang, L., Sun, H., Yu, N., Tang, Y., Liu, Y. 2022a. Roles

of granular activated carbon (GAC) and operational factors on active microbiome development in anaerobic reactors. *Bioresource technology*, **343**, 126104.

Zhang, Y., Guo, B., Zhang, L., Liu, Y. 2020a. Key syntrophic partnerships identified in a granular activated carbon amended UASB treating municipal sewage under low temperature conditions. *Bioresource Technology*, **312**, 123556.

Zhang, Y., Guo, B., Zhang, L., Zhang, H., Liu, Y. 2021b. Microbial community dynamics in granular activated carbon enhanced up-flow anaerobic sludge blanket (UASB) treating municipal sewage under sulfate reducing and psychrophilic conditions. *Chemical Engineering Journal*, **405**, 126957.

Zhang, Y., Zhang, L., Guo, B., Zhou, Y., Gao, M., Sharaf, A., Liu, Y. 2020b. Granular Activated Carbon Stimulated Microbial Physiological Changes for Enhanced Anaerobic Digestion of Municipal Sewage. *Chemical Engineering Journal*, 125838.

Zhang, Y., Zhang, L., Yu, N., Guo, B., Liu, Y. 2022b. Enhancing the resistance to H2S toxicity during anaerobic digestion of low-strength wastewater through granular activated carbon (GAC) addition. *Journal of Hazardous Materials*, 128473.

Zhao, J., Li, F., Cao, Y., Zhang, X., Chen, T., Song, H., Wang, Z. 2021. Microbial extracellular electron transfer and strategies for engineering electroactive microorganisms. *Biotechnology Advances*, **53**, 107682.

Zhao, Z., Li, Y., Yu, Q., Zhang, Y. 2018. Ferroferric oxide triggered possible direct interspecies electron transfer between Syntrophomonas and Methanosaeta to enhance waste activated sludge anaerobic digestion. *Bioresource technology*, **250**, 79-85.

Zhao, Z., Li, Y., Zhang, Y., Lovley, D.R. 2020a. Sparking Anaerobic Digestion: Promoting Direct Interspecies Electron Transfer to Enhance Methane Production. *Iscience*, 101794.

Zhao, Z., Wang, J., Li, Y., Zhu, T., Yu, Q., Wang, T., Liang, S., Zhang, Y. 2020b. Why do DIETers like drinking: Metagenomic analysis for methane and energy metabolism during anaerobic digestion with ethanol. *Water Research*, **171**, 115425.

Zhao, Z., Zhang, Y., Holmes, D.E., Dang, Y., Woodard, T.L., Nevin, K.P., Lovley, D.R. 2016a. Potential enhancement of direct interspecies electron transfer for syntrophic metabolism of propionate and butyrate with biochar in up-flow anaerobic sludge blanket reactors. *Bioresour Technol*, **209**, 148-56.

Zhao, Z., Zhang, Y., Li, Y., Dang, Y., Zhu, T., Quan, X. 2017. Potentially shifting from interspecies hydrogen transfer to direct interspecies electron transfer for syntrophic metabolism to resist acidic impact with conductive carbon cloth. *Chemical Engineering Journal*, **313**, 10-18.

Zhao, Z., Zhang, Y., Quan, X., Zhao, H. 2016b. Evaluation on direct interspecies electron transfer in anaerobic sludge digestion of microbial electrolysis cell. *Bioresource technology*, **200**, 235-244.

Zhao, Z., Zhang, Y., Yu, Q., Dang, Y., Li, Y., Quan, X. 2016c. Communities stimulated with ethanol to perform direct interspecies electron transfer for syntrophic metabolism of propionate and butyrate. *Water Res*, **102**, 475-484.

Zhen, G., Kobayashi, T., Lu, X., Xu, K. 2015. Understanding methane bioelectrosynthesis from carbon dioxide in a two-chamber microbial electrolysis cells (MECs)

containing a carbon biocathode. *Bioresource technology*, **186**, 141-148.

Zheng, S., Liu, F., Wang, B., Zhang, Y., Lovley, D.R. 2020. Methanobacterium Capable of Direct Interspecies Electron Transfer. *Environmental Science & Technology*.

Zhou, Y., Li, R., Guo, B., Xia, S., Liu, Y., Rittmann, B.E. 2022. The influent COD/N ratio controlled the linear alkylbenzene sulfonate biodegradation and extracellular polymeric substances accumulation in an oxygen-based membrane biofilm reactor. *Journal of hazardous materials*, **422**, 126862.

Zhu, X., Campanaro, S., Treu, L., Seshadri, R., Ivanova, N., Kougias, P.G., Kyrpides, N., Angelidaki, I. 2020. Metabolic dependencies govern microbial syntrophies during methanogenesis in an anaerobic digestion ecosystem. *Microbiome*, **8**(1), 1-14.

Zhuang, H., Zhu, H., Shan, S., Zhang, L., Fang, C., Shi, Y. 2018. Potential enhancement of direct interspecies electron transfer for anaerobic degradation of coal gasification wastewater using up-flow anaerobic sludge blanket (UASB) with nitrogen doped sewage sludge carbon assisted. *Bioresource technology*, **270**, 230-235.

Ziels, R.M., Svensson, B.H., Sundberg, C., Larsson, M., Karlsson, A., Yekta, S.S. 2018. Microbial rRNA gene expression and co‐occurrence profiles associate with biokinetics and elemental composition in full‐scale anaerobic digesters. *Microbial biotechnology*, **11**(4), 694-709.

Zwietering, M., Jongenburger, I., Rombouts, F., Van't Riet, K. 1990. Modeling of the bacterial growth curve. *Applied and environmental microbiology*, **56**(6), 1875-1881.